Engineering of the Secretory Pathway of CHO Cells for Recombinant Protein Production: Manipulation of SNARE Proteins

2018

Théo Mozzanino

A thesis submitted to the University of Kent for the degree of Doctor of Biochemistry

University of Kent

Faculty of Science

Declaration

No part of this Thesis has been submitted in support of an application for any degree or other qualification of the University of Kent or any other University or Institute of learning.

Théo Mozzanino Date December 2018

Acknowledgment

Firstly, I would like to thank Professor Mark Smales for his guidance and support throughout this project. I am grateful to have had the opportunity to perform my PhD project in such a thriving lab. I would also like to thank Fay Saunders for her knowledge and support. Working at Fuji was an amazing opportunity, I enjoyed every moment.

Thank you to Marie Skłodowska-Curie actions for founding this project and made possible the fantastic adventure that was the eCHO consortium.

I would like to thank my colleagues both at the University of Kent and Fujifilm for making the lab such a lovely place to work.

Finally, I would like to thanks my family and my friends for their support during this crazy period that was my PhD.

Abstract

The production of recombinant biotherapeutic proteins is usually achieved at an industrial scale using cultured cell systems with a number of host systems used including bacteria, yeast, insect cells and mammalian cells, depending on the needs of the protein to be produced. In the last 2-3 decades, the market for recombinant protein production has been dominated by monoclonal antibodies (mAbs), glycoproteins with complex post-translational modifications necessary for their therapeutic function. For the production of such molecules, mammalian cells and particularly Chinese hamster ovary (CHO) cells are often the host expression system of choice for their ability to correctly fold and assemble such complex molecules and to perform human-like glycosylation. The ability of CHO host cells to generate high levels (>5 g/L) of mAbs in particular has been enhanced and attained over the years via the implementation of different strategies including the design of media and feeding strategies, use of high throughput screening approaches to identify high producing cell lines, redesign of processes during bioprocessing, manipulation of genetic constructs to drive recombinant gene expression and protein engineering to improve CHO host cell productivity and product quality. Despite these approaches, there remains a desire to further improve the ability of CHO and other host cell systems to be improved to enhance their ability even further with regard to production and quality of biopharmaceuticals, particular more difficult to express molecules than 'standard' mAbs. One strategy that has been undertaken to enhance the cellular capacity for recombinant protein expression is cell line engineering, where a desired phenotype of the host is achieved by genetic manipulation. In this study, the secretory pathway of the CHO cell has been manipulated to investigate whether its engineering can improve the secretory capacity of two different CHO host cell lines under batch and fed-batch conditions. Specifically, members of the SNARE family, a family of proteins involved in the fusion machinery of vesicles which have been suggested to be a bottleneck in the secretory pathway, were ectopically over-expressed and the effect(s) of the overexpression on growth, culture viability and recombinant protein productivity of the CHO hosts determined. In a CHO-S cell line, overexpression of specific levels of syntaxin 17 (STX17) and SNAP29 fused to eGFP increased culture longevity and late culture viability, possibly through an impact on the autophagy pathway. Assessment of the impact of the ectopic expression of these SNAREs in CHO-S during transient expression of model proteins under batch culture conditions, IgG1 Adalimumab and the fusion protein Etanercept, showed an increase in titre up to 5-fold (STX17) and 2.4-fold (SNAP29) respectively. Specific levels of SNARE expression were required to observe a titre increase. Indeed, only cell lines overexpressing to a lower level of SNAP29 demonstrated an increased titre whereas a more linear effect was observed for cell lines expressing STX17, with higher STX17 expressing cell lines having a greater increase in titre than low STX17 overexpressers. Cells expressing STX18 also revealed an increase, up to 3-fold, in yield when producing Adalimumab, but not Etanercept, suggesting a molecule specific effect. Transferability of this approach to a second CHO host in the industrial environment was then investigated by engineering of an industrial host cell line, "Clone 27", a CHO-DG44 derived cell line. No increase in product titre was observed when the SNAREs were over-expressed in already high expressing recombinant mAb cell lines. The differences in the approaches and environment, as well as the intrinsic differences in the CHO host cell lines, might explain the divergence of observed effects between the cell lines. Nonetheless, a positive impact upon the overexpression of target SNAREs at specific levels was observed with regard to growth and productivity in CHO-S host cells suggesting SNARE manipulation was successful for the engineering of CHO-S cells. Moreover, the mechanisms by which the overexpressed SNAREs potentially elicit their changes in secretory phenotypes in the CHO-S host offers up new areas of interest for future cell line engineering strategies such as autophagy and mitophagy.

List of Figures 1
List of Tables 6
List of Abbreviations 7
CHAPTER 1: Introduction 10
1.1. The biopharmaceutical market 10
1.2. Cultured host cell systems for the expression of recombinant proteins 11
1.2.1. Bacteria cell expression systems 11
1.2.2. Yeast cell expression systems 12
1.2.3. Insect cell expression systems 13
1.2.4. Mammalian cell expression systems 13
1.3. Approaches undertaken to increase growth and recombinant protein yields from CHO host cell systems in industrial processes 14
1.3.1. Development of Media and feeding strategies 15
1.3.2. Different CHO host cells and selection systems 16
1.3.3. Design of expression vectors for enhanced recombinant gene and protein expression from CHO cells 17
1.3.4. Cell engineering for enhance cell growth and secretory recombinant protein production 18
1.3.4.1. Approaches applied to date for mammalian cell line engineering 18
1.3.4.2. Cell line engineering strategies 19
1.3.4.2.1. Enhancement of cell proliferation 19
1.3.4.2.2. Apoptosis engineering 20
1.3.4.2.3. Engineering to enhance the protein folding capacity of the cell 22
1.3.4.2.4. Glycosylation modifications and tuning via cell engineering approaches 23
1.3.4.2.5. Metabolic engineering of CHO cells 23
1.3.4.2.6. Engineering to increase the secretion capacities of CHO cells 24
1.4. The mammalian secretory pathway 26
1.4.1. Translocation of nascent polypeptides into the endoplasmic reticulum 26
1.4.2. Protein folding and quality control in the endoplasmic reticulum 27
1.4.3. Transit from the endoplasmic reticulum to the Golgi apparatus and protein maturation in the different cistern of the Golgi apparatus 29
1.4.4. *Trans*-Golgi traffic and exocytosis through the plasma membrane 30
1.5. Engineering strategies to enhance the capacity of the secretory pathway 31

1.5.1. Improving the efficiency of translocation of nascent polypeptide into the endoplasmic reticulum 31
1.5.2. Endoplasmic reticulum and unfolded protein response cell engineering 32
1.5.3. Engineering of vesicle formation and trafficking 33
1.6. The SNARE protein family 34
1.6.1. Vesicle associated membrane proteins or VAMPs 38
1.6.1.1. VAMP3 38
1.6.1.2. VAMP4 39
1.6.1.3. VAMP7 39
1.6.1.4. VAMP8 40
1.6.2. Syntaxins and synaptosome associated proteins (SNAPs) 41
1.6.2.1. Syntaxin7 or STX7 41
1.6.2.2. Syntaxin17 or STX17 41
1.6.2.3. Syntaxin18 or STX18 42
1.6.2.4. SNAP29 43
1.7. Aims of this study 44
CHAPTER 2: Materials and Methods 45
2.1. DNA manipulation and cloning 45
2.1.1. DNA plasmid sources 45
2.1.2. Polymerase chain reaction for fragment amplification 45
2.1.3. Enzymatic digest of plasmid DNA 45
2.1.4. Agarose gel electrophoresis for DNA observation and analysis 45
2.1.5. DNA purification 46
2.1.6. Ligation of DNA fragments 46
2.1.7. Generation of DH5α *Escherichia coli* competent cells 46
2.1.8. Transformation of DNA into competent cells 47
2.1.9. Plasmid DNA amplification 47
2.1.10. DNA sequencing 47
2.1.11. Plasmid linearization and DNA precipitation 47
2.1.11.1. University of Kent procedure 47
2.1.11.2. Fujifilm Diosynth Biotechnologies procedure 48
2.2. Cell culture 48
2.2.1. Suspension cell lines 48
2.2.1.1. CHO-S cells 48

2.2.1.2. Clone 27 (Fujifilm Diosynth Biotechnologies) CHO cells 49
2.2.2. Adherent cell lines 49
2.2.2.1. Flp-In ™ CHO cells 49
2.2.3. Cell maintenance 50
2.2.3.1. Suspension cells 50
2.2.3.2. Adherent cells 50
2.2.4. Antibiotic kill curve 50
2.2.4.1. University of Kent procedure 50
2.2.4.2. Fujifilm Diosynth Biotechnologies procedure 50
2.2.5. Stably expressing cell line generation 51
2.2.5.1. University of Kent procedure 51
2.2.5.2. Fujifilm Diosynth Biotechnologies procedure 51
2.2.6. Transient transfection experiments 51
2.2.6.1. University of Kent procedures 51
2.2.6.1.1. Lipofectamine 2000 51
2.2.6.1.2. Novachoice 52
2.2.6.1.3. Electroporation 52
2.2.6.2. Fujifilm Diosynth Biotechnologies procedures 52
2.2.6.2.1. Novachoice 52
2.2.6.2.2. Electroporation 52
2.2.7. Limiting dilution cloning 52
2.2.8. Cell line revival after cryopreservation 53
2.2.8.1. University of Kent procedure 53
2.2.8.2. Fujifilm Diosynth Biotechnologies procedure 54
2.2.9. Cryopreservation of cell lines 54
2.2.9.1. University of Kent procedure 54
2.2.9.2. Fujifilm Diosynth Biotechnologies procedure 54
2.2.10. Mini-pool cell line generation procedure 54
2.2.11. Fed-batch over grow or FOG cultures 55
2.2.12. Tissue culture in 96 Deep Well Plates (DWP) 55
2.3. Protein analysis 56
2.3.1. Total protein extraction from cell pellets 56
2.3.2. SDS-PAGE 56
2.3.2.1. Sample preparation procedure 56

2.3.2.2. Gel preparation and electrophoresis 57
2.3.3. Western blot analysis 57
2.3.4. Densitometry 58
2.3.5. Flow cytometry 58
2.3.6. Bradford assay 58
2.3.7. Octet measurements 58
2.3.8. Cellometer analysis 59
2.4. Microscopy techniques 59
2.4.1. Coverslip treatment with poly-L-lysine 59
2.4.2. Cell culture for microscopy 59
2.4.3. Coverslip preparation 59
2.5. Statistical analysis 60
CHAPTER 3: Molecular Cloning of Target SNARE Proteins and Subsequent SNARE CHO Cell Line Engineering 61
3.1. Introduction 61
3.2. Generation of mammalian expression vectors for the expression of the SNARE genes of interest 63
3.2.1. VAMP expressing vectors 63
3.2.2. Syntaxin (STX) and SNAP expressing vectors 68
3.3. Generation of stably expressing CHO-S cell lines 70
3.3.1. Initial confirmation of expression of the eGFP tag of the fused proteins 70
3.3.2. Titration of hygromycin B and puromycin to determine the appropriate amount that kills the host CHO-S cell in the absence of the selection marker for use in stable cell line generation 72
3.3.3. Stable CHO-S cell line generation and selection 74
3.3.4. Analysis of target eGFP-SNARE fusion protein expression in stable CHO-S cell pools 75
3.4. Monoclonal CHO-S eGFP-SNARE expressing cell line generation 78
3.4.1. Limiting dilution cloning for generation of monoclonal cell lines from the CHO-S SNARE engineered cell pools 78
3.4.2. Monoclonal cell line selection for further study 80
3.4.3. Evaluation of the stability of EGFP-SNARE expression in CHO-S monoclonal cell lines over time 87
3.5. Discussion 91
3.6. Summary of the main findings from the work in this chapter 96

CHAPTER 4: Assessment of the Impact of Over-expression of Target SNAREs in CHO-S Cells on the Cell and Recombinant Protein Expression 98

4.1. Introduction 98

4.2. Characterisation of different selected syntaxin/SNAP expressing cell lines 100

4.2.1. Microscopy studies confirm the presence of a correctly processed eGFP tag in the different eGFP-syntaxin/SNAP fusion protein engineered CHO-S cells 100

4.2.2. Western blot relative expression analysis of the eGFP-syntaxin/SNAP fused protein in the different CHO-S engineered monoclonal populations 103

4.2.3. Analysis of growth profiles during batch culture of the different eGFP-syntaxin/SNAP CHO-S engineered cell lines 105

4.2.3.1. Growth assessment of SNARE engineered CHO-S cells in shake flasks 105

4.2.3.2. Growth assessment of SNARE engineered CHO-S cells in spin tubes .. 116

4.3. Characterisation of the impact of engineering over-expression of syntaxins and SNAP in CHO-S cells on recombinant protein productivity 118

4.3.1. Rapid screening of the eGFP-syntaxin/SNAP engineered CHO-S monoclonal populations for any impact on the secretory productivity of a recombinant protein at small scale 118

4.3.1.1. Determination of the expression of the recombinant protein Etanercept 119

4.3.1.2. Determination of the expression of the recombinant protein Adalimumab 124

4.3.2. Investigating the impact of syntaxin/SNAP engineering of CHO-S cells on secretory productivity under fed-batch culture conditions 128

4.3.2.1. Fed-batch analysis of Adalumimab expression from syntaxin/SNAP engineered CHO-S cells 128

4.3.2.2. Fed-batch analysis of Etanercept expression from syntaxin/SNAP engineered CHO-S cells 132

4.3.3. Larger scale transient expression of Etanercept and Adalimumab from the syntaxin/SNAP engineered CHO-S cells 137

4.3.3.1. Larger scale transient expression of Etanercept from the syntaxin/SNAP engineered CHO-S cells 138

4.3.3.1.1. Impact on secreted Etanercept productivity of syntaxin/SNAP engineering of CHO-S cells 138

4.3.3.1.2. Evaluation of the performance of the different syntaxin/SNAP engineered CHO-S cell lines at two different scales, 96-DWP and 125 mL Erlenmeyer flasks, for scalability purposes 142

4.3.3.2. Larger scale transient expression of Adalimumab from the syntaxin/SNAP engineered CHO-S cells 143

4.3.3.2.1. Impact on secreted adalimumab productivity of syntaxin/SNAP engineering of CHO-S cells 143

4.3.3.2.2. Evaluation of the performance of the different syntaxin/SNAP engineered CHO-S cell lines at two different scales, 96-DWP and 125 mL Erlenmeyer flasks, for scalability purposes 148

4.4. Discussion 149

4.5. Conclusions 158

CHAPTER 5: Industrial Scale Investigation and Validation of SNARE Engineering of CHO Cells on Secretory Recombinant Protein Production 160

5.1. Introduction 160

5.2. Generation of vectors for the engineering of syntaxin/SNAP and expression of model recombinant proteins in the FDB CHO-DG44 host cell line 161

5.3. Generation of CHO-DG44 cell pools stably expressing the SNAREs and target model recombinant proteins 175

5.3.1. Generation of stably expressing mini-pools 175

5.3.2. Generation of stably expressing antibody and syntaxin/SNAP pools using the DG44 Clone 27 host cell line 179

5.4. Transient transfection experiments to evaluate the impact of the use of different promoters and presence of the fluorescent tag on the expression of model recombinant protein 179

5.5. Generation of stably expressing CHO-DG44 cell pools co-expressing a model protein and a syntaxin/SNAP protein by transfection of stably expressing recombinant biotherapeutic protein expressing cell pools with the different SNAREs 184

5.5.1. Titration of puromycin to determine the appropriate amount that kills the mini-pools expressing Adalimumab or Blosozumab for use in stable cell line generation 185

5.5.2. Transfection of mini-pools expressing model IgGs with pMRXIP plasmids for the generation of stably expressing cell lines expressing a model IgG recombinant protein and a target SNARE protein 186

5.5.3. Determination of IgG titre and expression of the eGFP fused proteins in the SNARE engineered IgG expressing mini-pools 187

5.5.4. Fed-batch over grow (FOG) assessment of the cell pools co-expressing a model IgG protein and a target eGFP-SNARE 193

5.5.5. Analysis of the expression of the syntaxin/SNAP fused proteins in the DG44 cell pools co-expressing a model IgG recombinant protein 197

5.6. Comparison of the endogenous amounts of the target SNAREs in the two CHO host cell lines, Clone 27 and CHO-S 198

5.7. Discussion 201

5.8. Conclusions 209

CHAPTER 6: Overall Discussion, Conclusions and Future Work 211
References 222
Appendices 240

List of Figures

Figure 1.1. Intrinsic or Bcl-2 pathways controlling apoptosis from Ashkenazi et al. (2017). 21

Figure 1.2. Representation of the secretory pathway of mammalian cells (from Lodish et al., 2000) 25

Figure 1.3. Protein translocation into the ER (from Wickner and Schekman, 2005). 27

Figure 1.4. Steps of vesicle formation and budding (from Bonifacino and Glick, 2004). 30

Figure 1.5. Formation of the *trans*-SNARE complex of SNAP-25, syntaxin1 and Synaptobrevin (VAMP2). 35

Figure 1.6. Structure of the different subfamilies of SNAREs 37

Figure 2.1. Graphical representation of the dilution performed for limiting dilution cloning in 96 well plates. 53

Figure 2.2. Equipment for 96-DWP tissue culture. 56

Figure 3.1. Agarose gel electrophoresis analysis of digested DNA 65

Figure 3.2. Agarose gel electrophoresis analysis of digested DNA 67

Figure 3.3. Agarose gel electrophoresis analysis of DNA digestion 69

Figure 3.4. Fluorescent image analysis of transiently transfected cells 71

Figure 3.5. Viable cell number and culture viability of CHO-S cells cultivated with different concentration of selection agents (A) Hygromycin B and (B) Puromycin 73

Figure 3.6. Expression profiling of the different eGFP-SNARE stably expressing CHO-S cell lines for the different SNARE candidates 77

Figure 3.7. Graphical representation of the process used in this project for the generation and selection of monoclonal CHO-S cell lines expressing the target eGFP-SNARE proteins from the initial cell pools 79

Figure 3.8. GFP signal analysis of the different clones after limiting dilution by flow cytometry 82

Figure 3.9. GFP signal analysis of the different clones after limiting dilution by flow cytometry 85

Figure 3.10. GFP signal of the selected clones after subculture in spin tubes to determine stability of expression over time 88

Figure 4.1. Fluorescent image analysis of the different monoclonal populations of eGFP-syntaxin/SNAP engineered CHO-S cells 102

Figure 4.2. Expression analysis by western blot of eGFP-syntaxin/SNAP fusion protein expression in the different monoclonal cell lines 104

Figure 4.3. Quantification of the relative expression levels of the eGFP-syntaxin/SNAP fusion proteins in the different cell lines using densitometry from the images in Figure 4.2 (n=1) 105

Figure 4.4. Cell growth and culture viability profiles of the different control cell lines CHO/MRXIP-GFP H, L (engineered to express eGFP alone) and the original host cell line (CHO-S) during batch cultivation in shake flasks 107

Figure 4.5. Growth and culture viability profiles of the different eGFP-STX7 engineered cell lines CHO/STX7 A, B, C, and the control CHO/MRXIP-GFP H and host CHO-S cell line in shake flask batch culture 109

Figure 4.6. Growth and culture viability profiles of the different CHO/STX17 K, J engineered cells, CHO/MRXIP-GFP H eGFP control and original host CHO-S cell line under batch culture conditions in shake flasks 111

Figure 4.7. Growth and culture viability profiles of the different CHO/STX18 C, F, H, and CHO/MRXIP-GFP H and CHO-S host cell lines during batch culture in shake flasks 113

Figure 4.8. Growth and culture viability profiles of the different engineered cell lines CHO/SNAP29 A, B, and eGFP control CHO/MRXIP-GFP H and original CHO-S host cell line under batch culture in shake flasks 115

Figure 4.9. Growth and culture viability profiles of different eGFP-syntaxin/SNAP engineered and control cell lines when cultured in batch culture in spin tubes 117

Figure 4.10. Western blot analysis of supernatant from day 5 after transient transfection of the different syntaxin/SNAP engineered cell lines with the plasmid pEtanercept in 96-DWPs 120

Figure 4.11. Etanercept concentrations in the supernatants of the different syntaxin/SNAP engineered CHO-S cell lines as determined using an Octet instrument on day 5 of batch culture following transient transfection with pEtanercept in 96-DWPs 121

Figure 4.12. Viable cell concentration and culture viability of the different eGFP-syntaxin/SNAP engineered CHO-S and control cell lines monitored at day 5 after transient transfection with pEtanercept in 96-DWP batch culture 123

Figure 4.13. Western blot analysis of supernatant samples from day 5 batch cultures after transient transfection of the different syntaxin/SNAP engineered CHO-S cell lines with the plasmid pAdalimumab in 96-DWPs 125

Figure 4.14. IgG titre results obtained by Octet measurement of supernatants from day 5 following the transient transfection with pAdalimumab in 96-DWPs of the different syntaxin/SNAP engineered and control cell lines 126

Figure 4.15. Viable cell concentration and culture viability monitored at day 5 after transient transfection with pEtanercept of the different clonal cell lines in 96-DWPs..... 127

Figure 4.16. Western blot analysis of supernatant samples from day 5 post-transfection fed-batch cultures of the different syntaxin/SNAP engineered cell lines with the plasmid pAdalimumab..... 129

Figure 4.17. IgG titre results as determined by Octet measurements on supernatants from day 3 and 5 after transient transfection with pAdalimumab in fed-batch cultures of the control and syntaxin/SNAP engineered CHO-S cell lines..... 130

Figure 4.18. Viable cell concentration and culture viability monitoring of the different cell lines transiently transfected with pAdalimumab in fed-batch cultures 131

Figure 4.19. Calculated cell specific productivity for the different syntaxin/SNAP engineered CHO-S cell lines transiently transfected with pAdalimumab during fed-batch culture..... 132

Figure 4.20. Western blot analysis of supernatant samples from day 5 of a fed-batch culture after transient transfection of the different syntaxin/SNAP engineered cell lines with the plasmid pEtanercept..... 133

Figure 4.21. Assessment of Etanercept titre by Octet analysis on supernatants from day 3 and 5 after the transient transfection of the different syntaxin/SNAP engineered CHO-S cell lines with pEtanercept in fed-batch cultures..... 134

Figure 4.22. Viable cell concentration and culture viability of the different syntaxin/SNAP CHO-S engineered cell lines transiently transfected with pEtanercept in fed-batch cultures 136

Figure 4.23. Calculated specific productivity for the different syntaxin/SNAP engineered CHO-S cell lines transiently transfected with pEtanercept in fed-batch culture..... 137

Figure 4.24. Western blot analysis of supernatant samples on day 8 of batch culture after transient transfection of the syntaxin/SNAP engineered CHO-S cells with pEtanercept in 125 mL Erlenmeyer flasks..... 139

Figure 4.25. Assessment of product titre across different days of batch culture for the different syntaxin/SNAP engineered CHO-S cell lines when transiently expressing Etanercept..... 140

Figure 4.26. Viable cell concentration and culture viabilities on the different sampling days across batch culture after transient transfection of the different syntaxin/SNAP engineered cells with pEtanercept..... 141

Figure 4.27. Calculated specific productivity for the different syntaxin/SNAP CHO-S engineered monoclonal populations after transient transfection of pEtanercept in 125 mL flasks under batch culture conditions 142

Figure 4.28. Comparison of the Etanercept product titre in supernatants from days 2 and 4 from 96-DWP and 125 mL flask experiments 143

Figure 4.29. Western blot analysis of supernatant samples at day 8 of batch culture after transient transfection of the syntaxin/SNAP engineered CHO-S cell lines with pAdalimumab in 125 mL Erlenmeyer flasks 144

Figure 4.30. Product titre analysis across the different days of batch culture for the different syntaxin/SNAP engineered CHO-S cell lines when transiently expressing Adalimumab 145

Figure 4.31. Viable cell concentration and culture viability profiles for the different sampling days after transient transfection of the syntaxin/SNAP engineered CHO-S cells with pAdalimumab 147

Figure 4.32. Calculated specific productivity for the different syntaxin/SNAP CHO-S engineered monoclonal populations after transient transfection of pAdalimumab in 125 mL flasks under batch culture conditions 148

Figure 4.33. Comparison of the product titre of supernatants from day 4 between 96-DWP and 125 mL flasks under batch culture conditions 149

Figure 5.1. Agarose gel electrophoresis analysis of digested DNA 164

Figure 5.2. Agarose gel electrophoresis analysis of digested DNA 166

Figure 5.3. Analyses of digested DNA by agarose gel electrophoresis 168

Figure 5.4. Agarose gel electrophoresis analysis of digested DNA 170

Figure 5.5. Agarose gel electrophoresis analysis of digested DNA 172

Figure 5.6. Graphical representation of the process to establish mini-pools at Fujifilm Dyosinth Biotechnologies 176

Figure 5.7. Output data obtained using the Solentim plate reader to check confluency and monoclonality of 96-well plates 177

Figure 5.8. Blosozumab and Adalimumab titres in cell culture supernatant 6 days after transient transfection with the different plasmids using NovaCHOice reagent as described in the text 181

Figure 5.9. Transient transfection experiment to determine improved conditions for transfection of the clone 27 host cell using the NovaCHOice reagent in 24-well plates 182

Figure 5.10. Determination of transient transfection efficiency using NovaCHOice reagent with different media's..... 184

Figure 5.11. Viable cell concentration and culture viability of mpDG44/ADA 7 cell pools after 5 days of incubation using media with various concentration of puromycin..... 186

Figure 5.12. Titre and transfection efficiency measurement of pools generated by the transfection of pMRXIP plasmids into mpDG44/ADA 7 and mpDG44/Bloso 6 mini pools. 188

Figure 5.13. Titre and fluorescence measurement of pools generated by the transfection of pMRXIP plasmids into mpDG44/ADA 7 and mpDG44/Bloso 6 after recovery and 2-3 passages in Erlenmeyer flasks..... 191

Figure 5.14. Growth curve characteristics of the different cell pools engineered with a syntaxin/SNAP target and expressing a model IgG molecule assessed during the FOG experiment..... 194

Figure 5.15. IgG titre and specific productivity measurement of the different cell pools engineered with a syntaxin/SNAP target and expressing a model IgG molecule assessed during the FOG experiment 196

Figure 5.16. Western blot analysis for eGFP-syntaxin/SNAP fusion protein expression on protein extracts from the different cell pools assessed during the FOG experiment at day 4 and 8 198

Figure 5.17. Western blot and densitometry analysis on protein extracts from Clone 27 and CHO-s host cells using syntaxin/SNAP specific antibodies..... 200

Figure 5.18. Physical position and orientation of the gene coding for the heavy chain of Adalumimab and the gene coding for syntaxin 17 showing the back-to-back bGH polyA tails. 204

List of Tables

Table 1.1. Exemple of cell line engineering strategies with their target genes and resulting phenotypes 19

Table 1.2. Known members of the SNARE family in mammalian cells (Hong 2005). 36

Table 2.1. List of the antibodies used and sources for western blot analysis during this work. 58

Table 3.1. List of vectors described in Chapter 3. 68

Table 3.2. Results of nucleotide sequence alignment using BLASTn between the Human and the Chinese Hamster candidate genes. 92

Table 4.1. Summary of the results of the different experiments for the characterisation of the monoclonal populations 157

Table 5.1. List of the vectors generated and used in Chapter 5. 174

Table 5.2. Titre measurement using an Octet instrument of the mini-pool and cell pools transfected with pAVE vectors expressing a model recombinant protein and a syntaxin/SNAP gene. 178

List of Abbreviations

ADA, Adalimumab

ANOVA, Analysis of variance

ATP, Adenosine triphosphate

Bcl, B-cell lymphoma

BH, Bcl-2 homology

BHK, Baby Hamster Kidney

BiP, Binding immunoglobulin protein

BLASTn, Basic local alignment search tool nucleotides

Bloso, Blosozumab

CHO, Chinese hamster ovary

CMV, Cytomegalovirus

COP, Coat protein

CPS I, Carbamoyl phosphate synthetase I

CRISPR, Clustered regularly interspaced short palindromic repeats

Dam, DNA adenine methylase

Dcm, DNA cytosine methyltransferase

DGV, Double gene vector

DHFR, Dihydrofolate reductase,

DMSO, Dimethyl sulfoxide

DNA, Deoxyribonucleic acid

DWP, Deep well plate

ECL, Electrochemiluminescence

EDTA, Ethylenediaminetetraacetic acid

eGFP, Enhanced green fluorescent protein

EPO, Erythropoietin

ER, Endoplasmic reticulum

ERAD, ER associated degradation

ERES, ER exit sites

Fc, Fragment crystallisable

FDA, Food and Drug Administration

FDB, Fujifilm Diosynth Biotechnologies

FOG, fed-batch over growth

FUT8, α-1,6-fucosyltransferase

Glc, Glucose

GlcNAc, N-acetylglucosamine

GPI, Glycosylphosphatidylinositol

GRAS, Generally recognised as safe

GRP78, Glucose regulated protein 78

GS, Glutamine synthetase

GT, UDP-glucose: glycoprotein glucosyltransferase ()

GTP, Guanosine-5'-triphosphate

HC, Heavy chain

HEK, Human embryonic kidney

Hsp, Heat shock protein

IgG, Immunoglobulin G

LB, Lysogeny broth

LC, Light chain

LDHA, Lactate dehydrogenase A

mAbs, Monoclonal antibody

Man, Mannose

MOMP, Mitochondrial outer membrane permeabilization

MSX, Methionine Sulfoximine

MTX, Methotrexate

NADH, Reduced nicotinamide adenine dinucleotide

NSF, N-ethylmaleimide-sensitive factor

OTC, Ornithine transcarbamoylase

PBS, Phosphate-buffered saline

PCD, Programmed cell death

PCR, Polymerase chain reaction

PDI, Protein disulphide isomerase

PolyA, Polyadenylation

PPi, Peptidyl-prolyl isomerases

PTFE, Polytetrafluoroethylene

PTM, Post translational modifications

RNA, Ribonucleic acid

ROS, Reactive oxygen species

SDS-PAGE, Sodium dodecyl sulphate–polyacrylamide gel electrophoresis

SM, Sec1/Munc18

SMAC, Second mitochondria-derived activator of caspase

SNAP, Soluble NSF attachment protein

SNARE, Soluble NSF attachment protein receptor

SOB, Super optimal broth

SRP, Signal recognition particle

SRPR, signal recognition particle receptor

STX, Syntaxin

TAE, Tris-acetate-EDTA

TCA, Tricarboxylic acid cycle

TGN, Trans-Golgi network

TK, Tyrosine kinase

Tm, Melting temperature

TNF, Tumour necrosis factor

TNFR, TNF receptor

UPR, Unfolded protein response

UPRE, UPR response elements

UTR, Untranslated region

UV, Ultraviolet

VAMP, Vesicle associated membrane proteins

XIAP, X-linked inhibitor of apoptosis protein

CHAPTER 1: Introduction

1.1. The biopharmaceutical market

With the development and improvement of our ability to manipulate recombinant DNA in the 1970s, the protein biopharmaceutical market also developed and expanded rapidly. The first drug produced from recombinant DNA approved by the FDA was Humulin in 1982 (Walsh 2014). This drug developed by Eli Lilly was produced in *Escherichia coli* to provide recombinant insulin. In 2017, the biopharmaceutical market was worth $160 billion (Morrison and Lähteenmäki 2018) and composed of a variety of products of differing complexity from recombinant insulin to therapeutic antibodies. The first FDA approved antibody was OKT3 or muronomab a murine IgG2 α CD3 used as a transplant rejection drug in 1983 (Hooks, Wade, and Millikan 1991). In the past 10-15 years, monoclonal antibodies have emerged as the prominent class of protein based drug in terms of sales, with 6 of the top 10 drugs in 2014 by value being monoclonal antibodies worth a staggering $70 billion (Walsh 2014). By 2020, 70 monoclonal antibodies are expected to be on the market with combined world-wide sales of $125 billion (Ecker, Jones, and Levine 2015). Antibodies being more complex to produce than other proteins that might consist of just one polypeptide with few or no post-translational modifications, antibody production necessitates a host with the cellular machinery able to undertake complex post translational modifications (PTM), notably glycosylation and disulphide bond formation. For example, mammalian cells are able to undertake such human-like glycosylation.

Cultured mammalian cells have been used for recombinant protein production since 1986 when they were used for the production of tissue plasminogen activator, and now around 60% of biotherapeutic protein products are manufactured in mammalian cells (Walsh 2014). Different mammalian cell hosts are available, but the most commonly used mammalian cell host is the Chinese hamster ovary (CHO) cell. This is discussed in more detail below. The commercially viable production of monoclonal antibodies and other complex protein based drugs is possible due to constant improvement in the ability to generate cell biomass rapidly and of the productivity from mammalian cells, particularly in chemically defined, protein free media. All of the combined improvements has allowed improvements in titres from around 50 mg/L in 1986 to 4.7 g/L in 2004 (Wurm 2004). Since 2004, titres in excess of 5 g/L (Handlogten et al. 2018; Reinhart et al. 2015) and even greater than 10 g/L have now been reported (Huang et al. 2010). Such improvements are

the results of overall efforts in the development of host selection, media and feed improvement, process engineering, enhancement of vectors and cell lines engineering.

1.2. Cultured host cell systems for the expression of recombinant proteins

1.2.1. Bacteria cell expression systems

One of the most common hosts for the production of proteins at the laboratory scale and for protein biopharmaceuticals are bacterial strains, and particularly *E. coli* strains. *E. coli* strains have been used for decades, not only for protein biopharmaceutical production, but also for basic research, resulting in accumulation of a profound knowledge about the host giving significant advantage for their utilisation. *E. coli* expression systems have been used to produce principally non-glycosylated molecules such as somatostatin, insulin, bovine growth hormone for veterinary applications, α-1 antitrypsin, interleukin-2, tumor necrosis factor, β-interferon, and γ-interferon (Fernández and Vega 2016), constituting a large segment of the biopharmaceutic products market. Advantages of protein expression in *E. coli* are its fast growth rate, ability to generate high viable cell concentrations, high titre, its simplicity to manipulate and engineer, and its affordability. Often, expression analysis of a target molecule is performed in *E. coli* with the product of interest if it does not require human-like post-translational modifications or complex folding and assembly to assess the compatibility of production with the system.

Nonetheless, this system is not perfect, bacteria being prokaryotes organisms they are unable to perform human like glycosylation or complex folding and assembly processes vital for the production of antibodies and other molecules. Those proteins that require disulphide bonding or complex folding and assembly tend to form inclusion bodies in the cytoplasm of the cell and need supplementary processing (e.g. refolding) and this can cause a large loss of product (Singh et al. 2015). The presence of endotoxins (notably lipopolysaccharides, an essential component of the bacteria external membrane) can also be a problem if the product is targeted for a biopharmaceutical usage and need to be safe for use in humans (Raetz and Whitfield 2002). *E. coli,* being a gram negative strain, the outer membrane impacts on the secretion of the recombinant product which, if targeted into the periplasm is retained here and hence extra steps are required in downstream processing to recover the product from within the cell (Mergulhão, Summers, and

Monteiro 2005). The reducing environment in *E coli* in the cytoplasm is not optimal for the formation of disulphide bonds although proteins may be directed to the periplasm where the environment can facilitate disulphide bond formation. As many proteins require disulphide bond formation as a PTM for correct folding and activity, some strains have been specifically developed (e.g. overexpression of oxydoreductases such as PDI or exportation of protein of interest into the periplasm (de Marco 2009)) to address this issue (Ke and Berkmen 2014). Nonetheless, 20% of drugs approved since 1984 are produced in *E. coli* (Walsh 2014). Other bacteria strains than *E. coli* are also used for protein production, such as some *Bacillus* strains that are mainly favoured for production of proteases (detergent industry) and amylases (food industry) (Westers, Westers, and Quax 2004).

1.2.2. Yeast cell expression systems

Yeast organisms have been developed as cell factories for the recombinant production of proteins over many years. The main yeast strain used in industry is *Saccharomyces cerevisiae* although *Pichia pastoris* is also used. Like bacteria hosts, yeasts have been used and studied for decades, giving a large amount of genetic tools and history around there use compared to other hosts. Yeasts are generally considered GRAS hosts (generally recognised as safe) due to the long history of their use in the food industry for brewing and baking purposes. As for bacteria hosts, yeast strains are able to reach high viable cell concentrations rapidly, and as a eukaryotic host have the required organelles and cellular machinery to undertake complex PTMs and glycosylation. Specifically with regard to glycosylation, there are 2 types known as *N*- and *O*-linked glycosylation. It has been demonstrated that *N*-glycosylation is often important for protein function and immunogenicity while less is known about *O*-glycosylation. In this regard, *S. cerevisiae N*-glycosylation processing in the early Golgi is limited to addition of mannoses and mannosylphosphate sugars often resulting in hyperglycosylation (abundance of mannoses residues) which are immunogenic (Teh, Fong, and Mohamed 2011) and hence limit the use of this system for making proteins destined for human use. *Pichia pastoris* is sometimes preferred to *S. cerevisiae* because it does not have a α-1,3-mannosyltransferase in the Golgi leading to a reduced mannose pattern (Wildt and Gerngross 2005). A strain of *P. pastoris* has also been engineered to give human glycosylation patterns (Irani et al. 2016), although this has not seen wide up as of yet in industry. *S. cerevisiae* and other yeast can secrete proteins into the media when using an appropriate ER peptide signal facilitating entry into the secretory pathway and presenting an advantage compared to bacteria hosts (Demain and Vaishnav 2009).

Yeast strains other than *S. cerevisiae* are therefore used for recombinant protein production, notably methylotrophic yeasts such as *P. pastoris*. Methylotrophic yeasts have the ability to grow using only one source of carbon, methanol. Compare to *S. cerevisiae*, *P pastoris* have advantages such as a higher protein production, the ability to grow on high concentrations of methanol able to kill most of microorganisms and less hyperglycosylation (Demain and Vaishnav 2009).

1.2.3. Insect cell expression systems

The first use of the baculovirus expression system in insect cells was in 1983 (Pennock, Shoemaker, and Miller 1984) and since then this has been used as an alternative system for the production of recombinant proteins. The main host used with baculovirus is the fall armyworm (*Spodoptera frugiperda*) in suspension culture. Insect cells, compared to bacterial and yeast systems, can perform more complex PTMs, notably glycosylation closer to human cells as a result of the activity of glycosylation enzymes in the Golgi. The main vector used to engineer insect cells is the baculovirus, that naturally targets invertebrate cells (Agathos 1991) assuring high levels of biosafety. Insect cells cultures are cheap, easy to scale up and can reach high cell concentration cultures. Since their first utilisation, more than 200 different recombinant proteins have been produced successfully in insect cells demonstrating their wide adaptability (Demain and Vaishnav 2009). One drawback of insect cell systems is that unexpected PTMs specific to insect cells might apply to the recombinant protein used and the glycosylation profiles are similar to, but not exactly the same as, that from mammalian cells. Some engineering has been undertaken in this area to obtain similar glycosylation (Jarvis 2003; Mabashi-Asazuma and Jarvis 2017). The yields from insect cell expression systems are also much lower than those that can be achieved from cultured mammalian cells.

1.2.4. Mammalian cell expression systems

Culture mammalian cells, compared to the other hosts described above, have traditionally been much more labour intensive and time consuming. Mammalian cells traditionally generate less biomass, reaching lower maximum viable cell concentrations and achieve lower product titres, but have become the host of choice for many commercial biotherapeutic recombinant proteins due to their ability to undertake complex folding and assembly process and to give human-like PTMs, particularly *N*-glycosylation. Glycosylation has been demonstrated to impact on different characteristics of recombinant proteins such as their immunogenicity, stability, biological activity and *in vivo* half-life (Walsh and Jefferis

2006). Different types of cultured mammalian cells are used, for example HEK (Human embryonic kidney), BHK (baby hamster kidney) and NS0 cells (Dumont et al. 2016; Lalonde and Durocher 2017; Mead et al. 2012), but the main host cell line currently used for the commercial production of biotherapeutic recombinant proteins is the Chinese hamster ovary (CHO) cell line. Compared to the other potential mammalian cell hosts, CHO cells display good growth in suspension culture in chemically defined, protein free media, are less susceptible to various pathogenic viruses (Berting, Farcet, and Kreil 2010) and are easier to manipulate. Moreover, CHO cells have been approved by the FDA and other authorities as a safe host for the production of recombinant proteins. CHO cells also give 'human-like' glycosylation profiles and have a history of more than 30 years of producing biotherapeutic recombinant proteins that have been safely administered to humans. Nonetheless, CHO cells are not perfect; they don't perform identical glycosylation to human cells and can generate glycol forms that result in immunogenic recombinant products (Butler and Spearman 2014) and, although these can produce large quantities (>5 g/L) of IgG monoclonal antibodies (Reinhart et al. 2015), the yields of many other proteins remain much lower. Approaches to improve the CHO cell expression platform as discussed in more detail below.

The different host cell systems described above therefore all have their specific dis/advantages and choosing one for the production of recombinant protein is a considered process. This includes the protein folding and assembly requirements of the target protein, the complexity of the target protein and the required PTMs. Since the production of the first recombinant proteins, improvements of the different hosts, but also of the processes used to generate recombinant expressing strains or cell lines and approaches to the culturing of these have been performed to enhance the ability of the different systems to commercially manufacture target biopharmaceuticals. Here, a general review of the approaches and improvements to enhance the productivity of mammalian cells, and particularly CHO cells, is provided as the host cell line of investigation in this thesis.

1.3. Approaches undertaken to increase growth and recombinant protein yields from CHO host cell systems in industrial processes

The development of a CHO cell expression systems involves the assessment of the impact of a number of elements including the isolation/development of the host cell line itself, the media and fed used to grow the cells during manufacturing, and elements of the expression

vectors used to select for integration of the gene(s) of interest into the host genome and drive transcription and translation of the target recombinant genes and mRNAs. There have been huge amounts of work undertaken in each of these areas and below a general review of these is provided.

1.3.1. Development of Media and feeding strategies

As well as manipulating the CHO cell host or the vectors integrated in the host for protein production, process and media improvement have been performed to increase productivity and growth. This is often specific to an individual host cell line and will reflect the metabolism of the specific CHO host cell and its requirements for growth and that of the recombinant protein. When mammalian cells were initially cultured *in vitro*, the cultivation media contained animal serum which was a source of nutrients, hormones, growth factors and protease inhibitors. This also provided protection against shear stress, a common problem in bioreactors when growing mammalian cells in suspension culture (Hesse and Wagner 2000). Serum-free media was developed to solve the issue of using undefined serum which could be a source of contamination/viruses, was not consistent in its nature from batch-to-batch and could have undesired effects on the performance of the cells.

Media optimisation has been a large part of process optimisation taken over the years in order to at best the needs of the cells during the culture and brings all the nutrients necessary. For example, early reports showed maximum viable cell numbers achievable to be 2 x 10^6 cells/mL, however now viable cell numbers in excess of 30 x 10^6 cells/mL are reported (Westoby et al. 2011). As product titre is the sum of the number of cells, their cell specific productivity and the length of the culture, higher cell numbers, maintained for longer underpin increased product yields. As such, much work has been undertaken to develop chemically defined media and the improvement of the feeding strategies in fed-batch cultures. Fed-batch culture is a culture mode with addition of nutrients to the media (feed) at various times through culture to replace depleted nutrients. Feed is added into the media to address the limit in nutrient encountered in batch processes and obtain extended and more viable cultures. Fed-batch processes are easier to work with and to optimise than continuous processes, although continuous processes are now being developed that allow smaller culture sizes to be run. Continuous or perfusion processes involve replacement of media at constant rates with cell retention. This process enables to reach high cell concentrations (>20 x 10^7 cells/mL) for extended periods of time (>40 days) (Clincke et al. 2013; Ritacco, Wu, and Khetan 2018).

Culture process improvements have also been an important part of increases in productivity of different cell lines, with notably induction systems or application of cold shock to increase the production of recombinant protein by slowing down transcription and translation during the process (Kaufmann et al. 1999). Improvements to the design of the equipment have also been reported such as more friendly methods of agitation or optimised controls of different parameters in the vessels (pH, temperature, and oxygenation).

1.3.2. Different CHO host cells and selection systems

The CHO cell host cell lines used for the commercial production of biopharmaceutical products are different from the original CHO cell line isolated by Puck in the 1950's (Puck 1958). Indeed, through years of selection, CHO host cell lines have evolved and being chosen for specific characteristics making them desirable for commercial manufacturing of recombinant biotherapeutic proteins. In particular, different metabolic selection markers have been developed to give different CHO cell hosts in order to introduce genetic material for the expression of a gene(s) of interest. The CHO cell line was established for the first time in 1956 in the laboratory of Theodorus Puck (Puck 1958). From this original cell line, different cell lines have been derived such as the CHO-K1 subclone of the original CHO cell line; CHO-DG44, a depleted cell line for *dhfr* generated in 1981 by Urlaub et al.; and CHO-S another cell line derived from the original source in 1991 (Reinhart et al. 2018). For the selection of cells expressing exogenous DNA in CHO cells, two systems are popular in industry, the glutamine synthetase (GS) system and the dihydrofolate reductase (DHFR) system using the CHO-DG44 cell line.

The glutamine synthetase (GS) system is widely used for the selection of host cells containing the desired genetic material. The GS system is based on a metabolic selection around the conversion of glutamate and ammonia into glutamine by glutamine synthetase. The chemical methionine sulfoximine (MSX) is an irreversible inhibitor of the glutamine synthetase enzyme (Noh, Shin, and Lee 2018) although it is not specific for GS. In media without glutamine, only cells expressing GS at high enough levels to generate their own glutamine in the presence of the GS inhibitor MSX are able to grow and proliferate, selecting for those cells where the integration of genetic vectors containing a GS expressing gene has occurred. Addition of MSX helps to obtain high levels of stringency for the cells in order to obtain cells with the genetic construct of interest whereby the GS gene is on the same piece of DNA (usually a plasmid vector) as the gene(s) of interest. Thus, expression of

exogenous GS and selection of this helps to select for those cells also expressing the recombinant protein genes of interest too. The system has now been optimised with the use of CHO cells depleted of GS (GS knockout) (Fan et al. 2012).

The dihydrofolate reductase (DHFR) system is used complementarily with CHO-DG44 cell lines. Established in 1981 by Urlaub et al., this cell line is DHFR deficient, an important enzyme for the synthesis of purines and amino acids (Chen et al. 1984). Cells deficient in DHFR can be grown without this enzyme by the addition of a supplement to the media. Methotrexate (MTX) is an inhibitor of DHFR. DHFR deficiency can be overcome by expression of exogenous DHFR in cells by integration of a genetic construct expressing a *dhfr* gene (Goodsell 1999). Selection of highly expressing *dhfr* cells is undertaken by culturing in the presence of MTX which also simultaneously selects for the expression of cells with the recombinant product gene(s) of interest on the genetic construct securing the integration into the cell line genome. Increasing concentrations of MTX are sometimes used to amplify the number of gene copy numbers in the genome of selected cells (Hausmann et al. 2018).

More classic systems for the selection of recombinant gene expressing cells are through the use of antibiotics and the expression of a rescue gene (e.g. hygromycin, puromycin). These are usually eluted for commercial manufacturing as the use of antibiotics is best avoided and hence the metabolic selection systems described above tend to be used.

1.3.3. Design of expression vectors for enhanced recombinant gene and protein expression from CHO cells

For the production of a recombinant protein from a mammalian cell line, a method of introducing the gene and of controlling its expression is required and this is usually achieved using a plasmid based expression vector. The expression vector contains basic elements necessary for metabolic (or antibiotic) selection of integration of the DNA into the host and for the expression of the recombinant gene, including an appropriate promoter(s), and the 5’ and 3’ untranslated regions, including a polyA tail. Much optimisation work has been performed over the years on the different elements of genetic vectors to generate vectors that support high expression of the product with long term genetic stability. Promoters are sequences needed to recruit polymerases in order to generate RNA via a process known as transcription with the resulting RNA further processed to generate a mature mRNA in the nucleus. Common promoters are often derived from viruses such as the cytomegalovirus immediate early promotor (CMV) (Xia et al. 2006), but more recently

endogenous mammalian cell promoters have been used to drive constitutive expression of recombinant genes such as the EF-1 α promoter in CHO cells (RunningDeer and Allison 2004). Promoters can be coupled to enhancer sequences able to increase a promoters activity by facilitating recruitment of transcription factors (Riethoven 2010). Genes for selection markers or antibiotics are often present on expression vectors for cell selection. Common selection systems in CHO are the DHFR/MTX or the GS/MSX selection described in section 1.3.2 above (Kingston et al. 2002). A polyadenylation (PolyA) sequence or tail are present at the 3' end of the sequence of the gene of interest as this is required for transport out of the nucleus and impacts mRNA stability (Makrides 1999). Addition of other elements such as introns or untranslated regions (UTRs) are also known to improve translation in some cases (Makrides 1999). A further area that has received much attention is that of codon optimisation whereby the gene sequence is optimised to use codons that are thought to improve the rate of polypeptide elongation and improve mRNA stability (Chung et al. 2013). Optimisation of each individual component of the vector of expression has the potential to improve transcription and subsequent translation and hence impact upon product production.

1.3.4. Cell engineering for enhance cell growth and secretory recombinant protein production

1.3.4.1. Approaches applied to date for mammalian cell line engineering

Improvements to the media used for culturing of cells, feed or process, host cell line selection and enhancement of vectors for gene expression have all been extensively investigated to improve recombinant protein yields from cultured cell systems as they are easier to perform than targeted cell line engineering and have a controlled impact on the performance of the process. Modification of the host by cell line engineering is a more complex approach due to the intricacy of the host and wide genetic variability within a host cell line population of cells. Cell line engineering of a host sets out to have a direct impact on the phenotype of the host by adding, increasing or removing a specific characteristic. Two approaches to cell line engineering are typically used, overexpression or knockout/down of genes of interest. Overexpressing a gene gives the opportunity to amplify or add a new characteristic to the cell line phenotype. Multiple genes can be (over)expressed and entire pathways can be redesigned in some cases. With regard to gene knockout or down, the expression of targeted genes can be abolished/reduced using techniques such as CRISPR. There are important differences between knockdown and knockout. Knockout can only be used where genes are not essential otherwise this

approach is lethal whereas knockdown can be used to target essential genes but reduce their expression. Table 1.1 summarises the different approaches presented in section 1.3.4.2 and 1.5.

Table 1.1. Exemple of cell line engineering strategies with their target genes and resulting phenotypes

Celular pathway	strategy	target gene	Engineered phenotype	reference
apoptosis	Overexpression	E2F-1	Increased culture times and 20% higher viable cell concentration	Majors et al. (2008)
apoptosis	Overexpression	Bcl-xL	Increase of 88% in cell viability and >2 fold in titre	Chiang and Sisk (2005)
apoptosis	Overexpression	Bcl-2	Increase of 75% in maximum viable cell concentration	Tey et al. (2000)
apoptosis	Knockout	Bak/Bax	Increase of 5-fold in titre	Cost et al. (2010)
apoptosis	Overexpression	XIAP	Increased resistance to apoptosis and culture times, decreased proliferation	Liew et al. (2010)
apoptosis	Knockdown	caspase-3/caspase-7	Increase of 55% in titre and extension of culture time	Sung et al. (2007)
apoptosis	Knockdown	caspase-8/caspase-9	Increased the viability in both batch and fed-batch suspension cultures	Yun et al. (2007)
cell cycle	Overexpression	c-Myc	Increase >70% in maximal cell concentration without additional supply of nutrients	Kuystermans and Al-Rubeai (2009)
glycosylation	Knockout	FUT8	Production of completely non-fucosylated antibodies resulting in 100-fold enhanced antibody-dependent cellular cytotoxicity	Yamane-Ohnuki et al. (2004)
glycosylation	Overexpression	α2,6-sialyltransferase	Production of α2,6-linked sialic acid and increased total sialic acid conten	Lin et al. (2015)
glycosylation	Knockout	β-1,4-galactosyltransferase isoform genes	Reduced galactosylated N-glycans levels to 1%	Amann et al. (2018)
metabolism	Overexpression	malate dehydrogenase II	Increase in intracellular ATP and NADH, and up to 1.9-fold improvement in integral viable cell number	Chong et al. (2010)
metabolism	Overexpression	CPS I and OTC	Reduction of ammonium ion levels by 33% and increase of 30% in growth rate	Park et al. (2000)
metabolism	Knockdown	LDHA	Reduction of glucose consumption rates up to 87% and specific lactate production ratesup to 79%	Kim and Lee (2007)
proliferation	Overexpression	cyclin-dependent kinase like 3	Increase of 9% in specific growth rate and 5% in maximum viable cell concentration	Jaluria et al. (2007)
proliferation	Overexpression	valosin-containing protein	Increase up to 30% in viable cell concentration	Doolan et al. (2010)
protein folding	Overexpression	calreticulin/calnexin	Increase of 1.9-fold productivity	Chung et al. (2004)
protein folding	Overexpression	ERp57	Increase of 2.1-fold in productivity	Hwang, Chung, and Lee (2003)
secretion	Overexpression	SRP14	Increase up to 6-fold in titre	Le Fourn et al (2014)
UPR	Overexpression	XBP-1 spliced	Increase of 4-fold in productivity	Gulis et al. (2014)
protein folding	Overexpression	PDI	Increase of 1.37-fold in productivity	Borth et al. (2005)
			Decrease in productivity up to 1.6-fold	Hansen et al. (2015)
			No effect	Hayes, Smales, and Klappa (2010)

1.3.4.2. Cell line engineering strategies

1.3.4.2.1. Enhancement of cell proliferation

Mammalian cells have slower growth kinetics compared to bacteria or yeast (typically cell doubling times are in the region of 24-48 h for cultured mammalian cells) and obtain lower

maximum viable cell concentrations (or total biomass) and as such improving growth kinetics has been an aspect of interest. Faster growth and therefore time to obtain higher maximum viable cell concentrations can help deliver more cost effective and faster processes. To impact on these parameters, engineering targets investigated have been proteins involved in control of the cell cycle. To deliver faster growth and high cell concentrations, overexpression of the c-Myc protein has resulted in improvements in these key phenotypic cell characteristics (Kuystermans and Al-Rubeai 2009). Protein c-Myc is a nuclear localised phosphoprotein involved in cell cycle progression and apoptosis. Other proteins impacting the cell cycle such as cyclin-dependent kinase like 3 and E2F-1 resulted in improved cellular growth rates and increased maximum viable cell concentrations when engineered in mammalian cells (Jaluria et al. 2007; Majors et al. 2008). Strategies involving proteins in pathways other than the cell cycle have also been successfully investigated, such as the overexpression of the malate dehydrogenase II portion of the tricarboxylic acid cycle (TCA) cycle for energy production in the mitochondria or valosin-containing protein involved in invasion, metastasis and cell proliferation but its function are not fully elucidated (Chong et al. 2010; Doolan et al. 2010).

1.3.4.2.2. Apoptosis engineering

Apoptosis is a programmed cell death mechanism triggered by stresses such as nutrient depletion, accumulation of toxic metabolites, and shear stress (Krampe and Al-Rubeai 2010). It has been widely studied because it impacts on culture viability and longevity (Arden and Betenbaugh 2004) but also can impact upon product concentration and quality by the effect of proteases realised in media when cells burst (Kaneko, Sato, and Aoyagi 2010). Apoptosis is mainly controlled by the Bcl-2 family which contains proteins conveying anti- and pro-apoptotic signals sensed by the cell and is subdivided into three sub-families: (i) anti-apoptotic Bcl-2 homologs containing Bcl-2 homology (BH) domains 1, 2, 3 and 4; (ii) pro-apoptotic members containing BH1, 2, and 3 homology domains; and (iii) BH3 only pro-apoptotic members (Adams and Cory 2001). The Bcl-2 pathway is detailed in Figure 1.1 (Ashkenazi et al. 2017). By the manipulation of the expression of members of the Bcl-2 family, it has been shown that it is possible to impact the onset of apoptosis and increase culture viability and longevity (Fischer, Handrick, and Otte 2015; Kim and Park 2003). In CHO cells, overexpression of Bcl-xL or Bcl-2, both anti-apoptotic proteins, increased culture viability (Chiang and Sisk 2005; Kim and Lee 2000; Tey et al. 2000) whilst knockout of pro-apoptotic proteins from the Bcl-2 family such as Bak and Bax also resulted in improved culture viability (Cost et al. 2010).

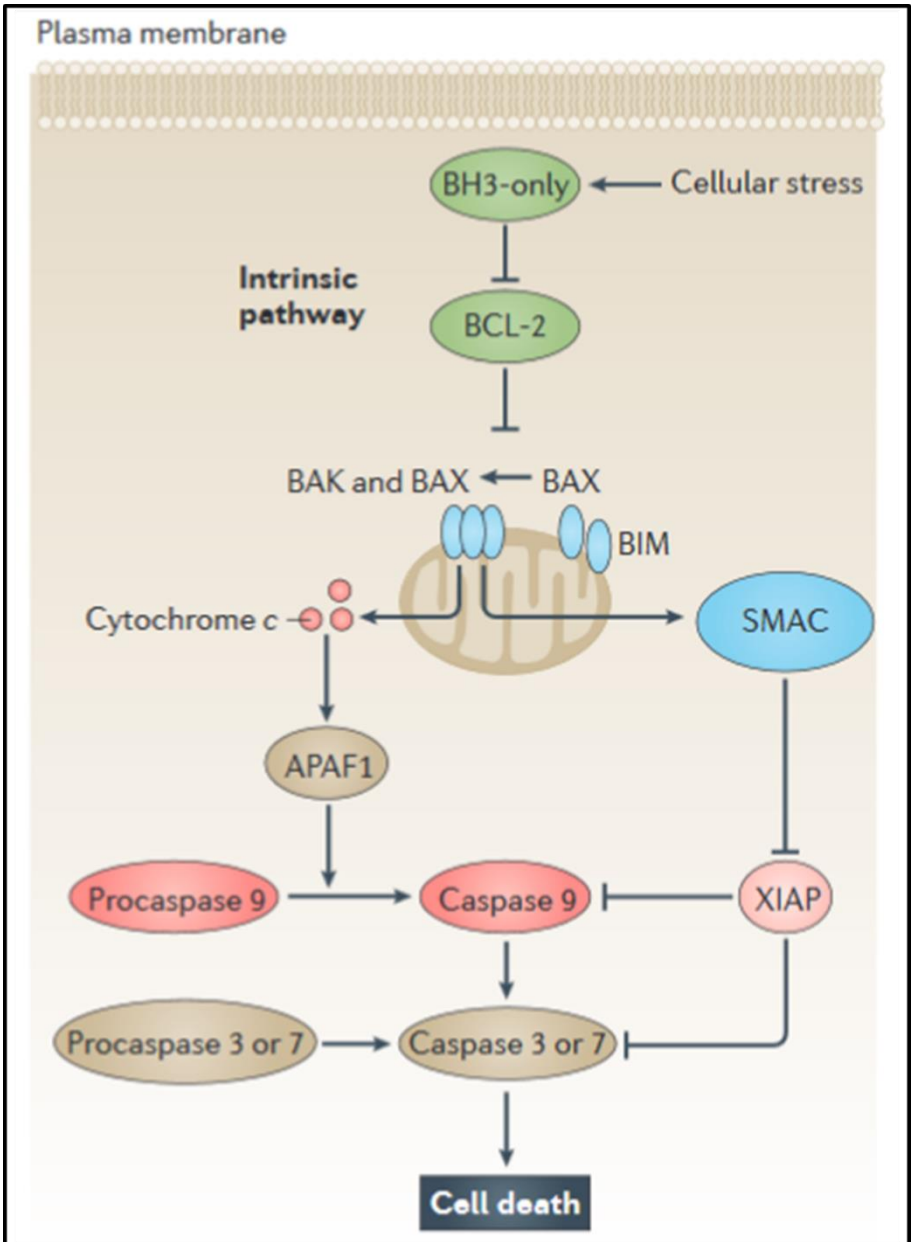

Figure 1.1. Intrinsic or Bcl-2 mediated pathways controlling apoptosis from Ashkenazi et al. (2017). After activation of the intrinsic/Bcl-2 pathway by cellular stress, pro-apoptotic BH3-only proteins inhibit the anti-apoptotic Bcl-2 and homologs such as Bcl-xL. This allows the activation and oligomerisation of the pro-apoptotic proteins BAK and BAX resulting in mitochondrial outer membrane permeabilization (MOMP). Following permeabilization, cytochrome c and second mitochondria-derived activator of caspase (SMAC) are realised from the mitochondria. Cytochrome c forms a complex with procaspase 9 and apoptotic APAF1, which leads to the activation of caspase-9 whereas SMAC interacts with XIAP to stop its inhibitory effect on caspases-3, -7 and -9. Caspase-9 then activates procaspase 3 and procaspase 7, resulting in cell death.

Caspases are proteins that also play a central role in apoptosis and are activated by a proteolytic cascade of cleaved caspases (Parrish, Freel, and Kornbluth 2013). Thus, suppression of their activation or disruption of their proteolytic effect on cells has become a promising strategy to prevent or delay apoptosis. Caspases can be divided in two groups: initiator caspases involved in interaction with upstream molecules and

activating/processing effector caspases and effector caspases responsible for cleaving cellular components (Li and Yuan 2008). Overexpression of intracellular caspase inhibitors such as X-linked inhibitor of apoptosis protein (XIAP) has been a strategy investigated and showed in the case of XIAP an inhibition of caspase-3 activity leading into reduced apoptosis, prolonged cultures times and decreased proliferation (Liew et al. 2010). Knockdown of caspase-3 and -7, and overexpression of double negative mutants of caspase-8/caspase-9 (Sung et al. 2007; Yun et al. 2007) were also successful approaches for caspase engineering. The result of these strategies was an increase in viability of culture in batch and fed-batch conditions when overexpressing double negative mutants of caspase-8/-9 while knockdown of caspase-3 and -7 not only increased culture times and culture viability but also raised productivity by 55%.

1.3.4.2.3. Engineering to enhance the protein folding capacity of the cell

When using strong promoters to drive gene expression or with the insertion of multiple copies of a gene, it has been observed that the amount of protein product generated is not proportional between the amount of transcript (mRNA) and protein. It was therefore suggested that there is a bottleneck or limitation in mRNA translation instead of transcription once a mRNA threshold is exceeded. For secretory recombinant proteins, the nascent polypeptide is translated on ribosomes on the ER where the polypeptide is fed co-translationally into the ER where the polypeptides are folded and assembled in the case of multi-chain proteins such as antibodies. ER localised chaperones and foldases are involved in the protein folding in the ER and a number of these have been investigated as possible limiting factors via cell engineering approaches (Mohan et al. 2008). Overexpression of ER chaperones such as calreticulin, calnexin or ERp57 have been shown to increase by approximatively 2 fold the recombinant protein productivity of some cell lines (Chung et al. 2004; Hwang, Chung, and Lee 2003) but more varied results have been reported for over-expression of PDI (Borth et al. 2005; Hansen et al. 2017; Mohan and Lee 2010). PDI through its ability to form and reduce disulphide bonds of nascent proteins and also to inhibit aggravation of folding intermediates through its chaperone function (Appenzeller-Herzog and Ellgaard 2008) have been a target of interest to increase productivity. For example, while Borth et al. (2005) observed an increase of 1.37 fold in productivity when overexpressing PDI, null or even decrease in productivity have been observed (Hansen et al. 2015; Hayes, Smales, and Klappa 2010) suggesting that overexpression of an effector gene can be a limited strategy and depend on parameters such as the nature of the recombinant product.

1.3.4.2.4. Glycosylation modifications and tuning via cell engineering approaches

Despite CHO cells being mammalian and generating proteins with 'human-like' glycosylation patterns, glycosylation between CHO and human cells is not identical. Moreover, glycosylation is an important biological modification that can impact immunogenicity, protein stability, biological activity and half-life of a protein molecule (Walsh and Jefferis 2006). Thus, ensuring a particular glycosylation pattern window is important when manufacturing a glycoprotein and the ability to tailor and control glycosylation is an important aspect. For example, it has been demonstrate that monoclonal antibodies lacking a core fucose residue have a stronger antibody-dependent cell-mediated cytotoxicity at lower doses (Yamane-Ohnuki and Satoh 2009). In this regard, strategies to generate CHO cells not capable of performing fucosylation have been implemented successfully, notably by knockout of the alpha-1,6-fucosyltransferase (FUT8) enzyme (Malphettes et al. 2010; Yamane-Ohnuki et al. 2004). Yang et al. (2015) have taken the process further and studied the knockout of 19 glycosyltransferase genes enabling the generation of host able to process only desired glycosylation. The advent of CRISPR technology has simplified the knockout of genes in cells and is an adapted and successful strategy for tailored glycosylation. For example, successful work has been undertaken to generate CHO cells producing agalactosylated antibodies using a CRISPR approach (Amann et al. 2018). Work has also been focused on the sialic acid modulation important for therapeutic molecule half-life and efficacy (Bhide and Colley 2017). Indeed, due to the absence of α2,6-sialyltransferase expression CHO cells are not able to perform α2,6-linked terminal sialic acid. Lin et al. (2015) demonstrated that overexpression of α2,6-sialyltransferase was sufficient to improve sialylation and perform α2,6-linked terminal sialic acid in CHO cells.

1.3.4.2.5. Metabolic engineering of CHO cells

During the culture of CHO cells, nutrients required to support cellular properties including growth, and their consumption can be inefficient and generate toxic by-products of which some are released into the media. The main by-products that are produced by *in vitro* cultured CHO cells that have been well studied are lactate and ammonia, known to impact upon the growth and productivity of cells at particular concentrations in the media (Lao and Toth 1997). They are generated from the breakdown or metabolism of glutamine and glucose present in the media. Different approaches have been taken to limit or remove the production of by-products or increase the energy efficiency of cells. In order to reduce

ammonia production, carbamoyl phosphate synthetase I (CPS I) and ornithine transcarbamoylase (OTC), both enzymes involved in the urea cycle (Park et al. 2000) were overexpressed in CHO cells and resulted in ammonia media reduction by generation of carbomoyl phosphate by CPS I necessitating ammonium cations. Because carbomoyl phosphate is unstable, it is converted into citrulline by the OCT. Another strategy taken for the reduction of ammonia was the introduction of glutamate into the media instead of glutamine. Glutamate is a less ammoniagenic substrate and when coupled with overexpression of glutamine synthetase which requires glutamate and ammonia as substrates to generate glutamine, ammonia generation was reduced (Zhang et al. 2006).

The main source of lactate during *in vitro* culture of mammalian cells, which causes acidification of the media as a result of lactic acid formation, is the conversion of pyruvate via lactate dehydrogenase A (LDHA) to lactate. Knockout of the LDHA gene has been shown to be lethal (Yip et al. 2014), whereas knockdown of LDHA by siRNA has been shown to decrease the production of lactate by up to 89% compared to control cell lines without affecting growth or recombinant protein production (Kim and Lee 2007) proving to be a successful strategy to reduce lactate formation and the effects of this.

Other strategies to manipulate cell metabolism have also been undertaken successfully, such as the overexpression of malate dehydrogenase II involved in the TCA cycle leading to increased amounts of ATP, NADH and higher maximum viable cell numbers (Chong et al. 2010). A further successful example is that of the overexpression of the taurine transporter involved in transport of nutrients leading to improved culture viability and higher recombinant protein titres (Tabuchi et al. 2010) .

1.3.4.2.6. Engineering to increase the secretion capacities of CHO cells

When therapeutic recombinant proteins are made using mammalian cell expression systems, they are targeted to the secretory pathway which results ultimately in their secretion out of the cell into the culture media initially via an ER signal sequence. The secretory pathway starts with the translocation of nascent proteins into the ER directed by an ER signal peptide and finishes with the secretion of the fully folded, assembled and post-translationally modified (when required) protein into the external environment at the plasma membrane (Figure 1.2). As highly efficient transcriptional control of recombinant genes is achievable associated with efficient mRNA translation, the capacity of the secretory pathway is potentially limiting in terms of the recombinant protein load that a cell can process. This work described in this thesis focusses upon trafficking within the

secretory pathway and the manipulation of this important component of the secretory pathway, and thus the different steps within this are discussed in detail below, as well as potential strategies to improve the capacity of this pathway.

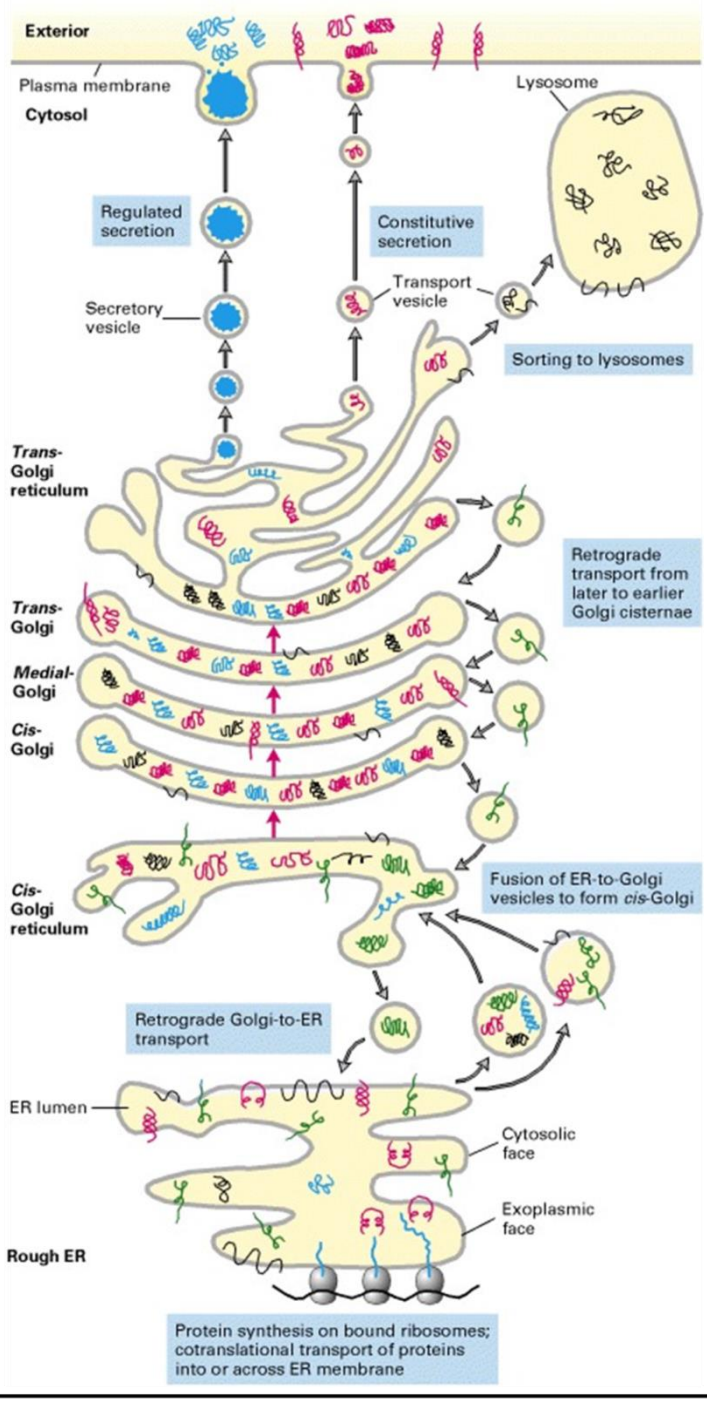

Figure 1.2. Representation of the secretory pathway of mammalian cells (from Lodish et al., 2000). The secretory pathway starts with the translocation of the nascent polypeptide into the ER. The ER provides the appopriate environment for protein folding and to undertake specific PTMs (e.g. disulphide bond formation, adds initial N-glycan structures). Folded and assembled proteins transit from the ER to the Golgi compartment via vesicles. PTMs are refined or added in the Golgi where proteins mature as they travel through the different cistern. Once at the *trans*-Golgi, proteins destined for secretion out of the cell are directed to the plasma membrane via vesicle traffic to be released into the external environment.

1.4. The mammalian secretory pathway

1.4.1. Translocation of nascent polypeptides into the endoplasmic reticulum

The first step in the secretory pathway is the targeting of the nascent polypeptide to the endoplasmic reticulum (ER)(Figure 1.3) (Wickner and Schekman 2005). Recognition of polypeptides to be targeted to the secretory pathway or requiring to transit through the ER is achieved by recognition of an ER signal sequence as it emerges from the ribosome entry tunnel by the signal recognition particle (SRP) composed of 6 protein subunits and the 7S RNA (Walter and Blobel 1982). ER targeting signal sequences are N-terminal motifs of 15 to 50 amino acids and comprise 3 distinct regions; a positively charged N-terminus, a central hydrophobic region and a more polar C-terminal region that defines the cleaving site. ER signal sequences contain a huge diversity in terms of variation in length and composition. Signal sequences, by their variety, are able to provide different efficiencies of recognition by the SRP and therefore of targeting to the ER. Different protein families have different ER sequences and SRP recognition is thought to be a more structural basis rather than sequence specific (von Heijne 1985; Von Heijne 1983; Martoglio and Dobberstein 1998). The recognition of the signal sequence by the SRP is achieved as soon as the nascent peptide is translated and a key step is that interaction between the SRP and the ribosome complex, through the SRP54 subunit, results in the attenuation of mRNA translation. The SRP-nascent-polypeptide-ribosome complex is targeted to the rough ER membrane by the binding of the SRP to the signal recognition particle receptor (SRPR) that is present on the rough ER. The SRPR is a heterodimer, consisting of α and β subunits, localised at the ER through its β subunit. Interaction between the SRPR and the complex formed by the SRP and the ribosomes is GTPase regulated and causes dissociation of SRP54 from the signal sequence and hence dissociation of the SRP and the ribosome (Connolly, Rapiejko, and Gilmore 1991). This also causes attachment of the nascent protein to the Sec translocon complex. The nascent polypeptide is translocated into the ER through the channel formed by the Sec61 heterotrimeric complex composed of Sec61α1, Sec61β and Sec61γ. Additional elements are necessary to ensure the polypeptide is fed through the channel such as the chaperone BiP. BiP has roles in closing the sec61 channel (Hamman, Hendershot, and Johnson 1998), helping the insertion of the nascent polypeptide into the channel (Dierks et al. 1996) and having a “pull” effect on the polypeptide in the translocon complex (Nicchitta and Blobel 1993). Other proteins are involved in forming the translocon complex such as TRAM, TRAP complex and PAT-10 protein (Zimmermann et al. 2011).

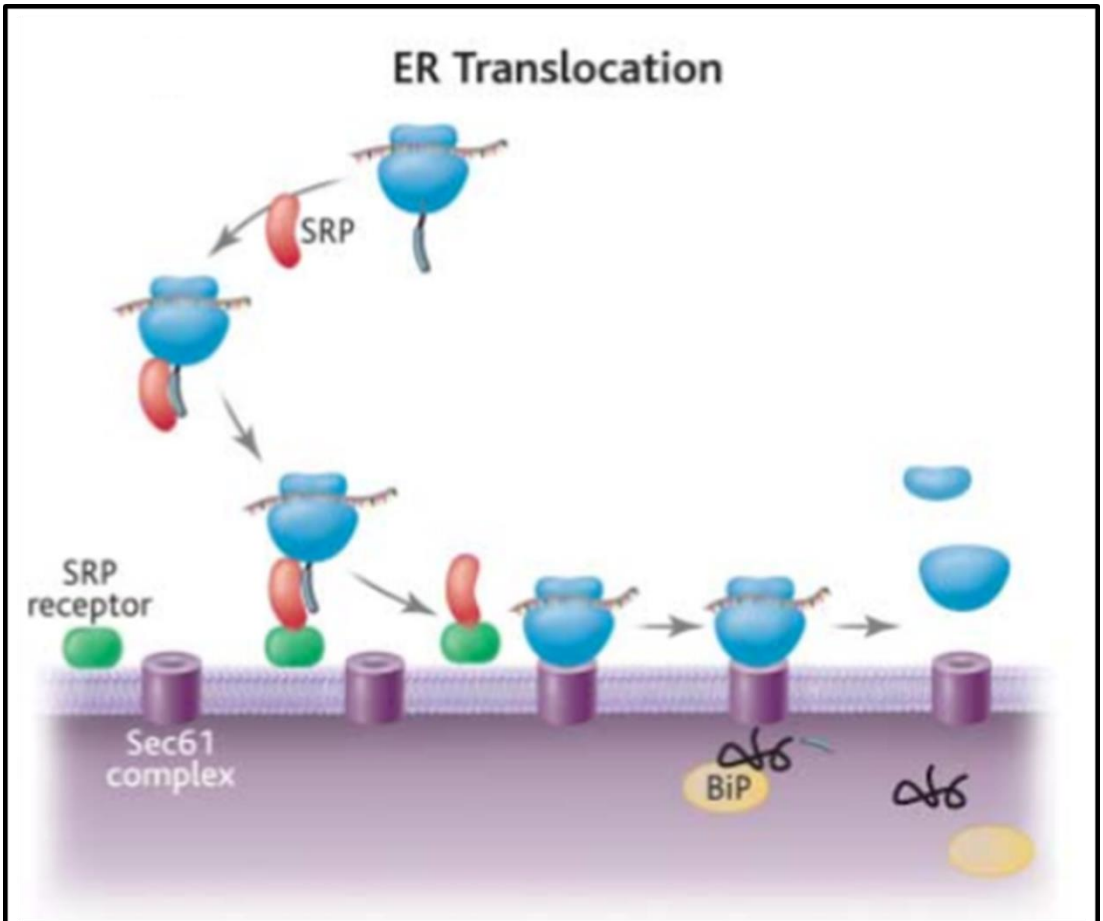

Figure 1.3. Protein translocation into the ER (from Wickner and Schekman, 2005). SRP recognises the signal peptide of the nascent polypeptide and interacts with the ribosomal complex attenuating mRNA translation. The SRP-nascent-polypeptide-ribosome complex is targeted to the translocon/Sec61 complex by its interaction with the SRP receptor. Attachment of the nascent polypeptide to the translocon complex induces release of SRP and SRPR and resumption of mRNA translation. Translocation of the nascent polypeptide through the translocon channel is helped by diverse elements, notably BiP.

1.4.2. Protein folding and quality control in the endoplasmic reticulum

Once polypeptides are directed into the ER, several steps occur to fold the protein and check the correct folding. The signal peptide is cleaved from the polypeptide to release this from the ER lumen membrane by specific signal sequence peptidases (Martoglio and Dobberstein 1998). The initial N-linked glycan structure is also added to N-glycosylation sequences as the polypeptide is delivered into the ER (Koenig and Ploegh 2014). To be functional, proteins need to achieve correct folding and for this purposes some proteins have a role to help folding and assure the quality control within the ER. They are termed chaperones proteins and belong to the Hsp (heat shock protein) family (Hartl 1996). Chaperone proteins are joined by foldases such as protein disulfide isomerase (PDI) and

peptidyl-prolyl isomerases (PPi) which accelerates reactions otherwise too slow such as disulphide bond generation or isomerisation of peptidylprolyl bonds. The ER also possess unique oxidising conditions compared to other compartment to aid folding (Hwang, Sinskey, and Lodish 1992).

BiP (also known as GRP78 or glucose regulated protein 78), a member of the Hsp70 family, is an important chaperone in the ER. Peptides contain a BiP binding domain approximately every 36 amino acids (Rüdiger, Buchberger, and Bukau 1997). The binding of BiP prevents mis-folding of the polypeptide before it can be correctly folded and BiP is removed during folding in an ATP dependent manner. BiP is also a master regulator in the signalling of accumulation of unfolded protein in the ER and hence of the unfolded protein response (UPR) (Lewy, Grabowski, and Bloom 2017). BiP binds to the UPR sensing ATF6, PERK and IRE1 ER transmembrane transducing proteins in the ER lumen and prevents the activation of the signalling pathways these elicit. However, as BiP is removed from these as it binds polypeptides in the ER, these sensors can sense and activate the UPR as BiP is released from them and they dimerise (Hetz 2012). Thus, an overload of recombinant polypeptide in the ER can activate the UPR as BiP is required to bind the unfolded recombinant material in the ER. Activation of the UPR initially upregulates expression of the folding and processing chaperones in the ER to try and alleviate the load of unfolded protein, but if this cannot be achieved the UPR ultimately activates apoptosis (Hetz and Papa 2018). BiP functions alongside a number of co-factors (Hsp40 family) and other proteins associating with it to aid in the folding and assembly of proteins in the ER.

Quality control of protein folding in ER is achieved through the calreticulin/calnexin cycle. When entering the ER, nascent polypeptides get preassembled *N*-glycan (Glc3Man9GlcNAc2) structures attached to them by the oligosaccharide transferase complex where N-glycan sequences are present (Parodi et al. 1972). Addition of the *N*-linked glycans occurs co-translationally as polypeptides enter the ER. The initial donor sugar complex contains 3 glucose residues and 2 of these glucoses are removed from the *N*-glycans by sequential action of the glucosidase I and II to yield a Glc1Man9GlcNAc2 structure. The monoglucosylated structures are binding sites for calreticulin and calnexin (Kapoor et al. 2003). Calreticulin and calnexin slow down folding events which improves folding efficiency and also recruit ERp57 to aid in disulphide bond generation (Kapoor et al. 2003).

When correct protein folding is achieved, the last glucose is removed from the glycan structure by glucosidase II which inhibits rebinding to the chaperones (Araki and Nagata 2012). Unfolded/misfolded proteins can go through the calreticulin/calnexin cycle by the addition of a glucose by UDP-glucose:glycoprotein glucosyltransferase (GT). GT ignores folded protein that is targeted for transport to the Golgi in a COPII dependent process (Caramelo and Parodi 2015). Proteins are able to be subjected to several cycles in the calnexin/calreticulin cycle to obtain correct folding of the proteins but if this is not achieved, proteins are directed to the ER-associated degradation (ERAD) pathway (Hebert and Molinari 2007).

1.4.3. Transit from the endoplasmic reticulum to the Golgi apparatus and protein maturation in the different cistern of the Golgi apparatus

Folded proteins gather at ER exit sites to be exported from the ER to the Golgi. The sorting of the proteins to be exported is done via the COPII coat protein and a GTPase, Sar1-GTP. The coat binds and concentrates proteins into secretory vesicles (Barlowe 2002). The recruitment of the different elements of COPII complex is via the small GTPase SarI. The minimal components of a COPII complex are the Sec23/Sec24 heterodimer, the Sec13/Sec31 heterotetramer and SarI (Matsuoka et al. 1998). Sorting of the transmembrane cargo proteins is achieved through Sec24 and its several binding sites (Mancias and Goldberg 2008). For soluble cargo proteins, cargo receptors are from the ERGIC-53 family, the p24 family, or the Erv family (Szul and Sztul 2011). Membrane invagination is performed by Sar1 and the Sec23/24 complex while the Sec13/31 complex stabilises the vesicle.

Once the vesicle is formed, the COPII coat is shed and targeting and fusion to specific destination compartment, here the *cis*-Golgi, is mediated through the interaction of SNARE proteins. SNAREs are proteins with targeting and fusion properties (Bonifacino and Glick 2004). Promotion of fusion by SNAREs is helped by the action of tethering factors activated by Rab proteins. Figure 1.4 details the different stages of vesicle formation and budding between two compartments. The content of the vesicle is realised into the Golgi where PTM modifications such as glycosylation undergo further processing. As previously stated, glycosylation is an important PTM for recombinant glycol-proteins and glycosylation has effects on folding, function, immunogenicity, stability and/or half-life (Walsh and Jefferis 2006). The Golgi apparatus has a major role in secretion as it is a crossroad for the secretion, lysosome and endosome routes (Mellman and Warren 2000). Traffic in the

different cistern of the Golgi is not fully understood and several models have been proposed. For a full review of the different models refer to Glick and Luini (2011).

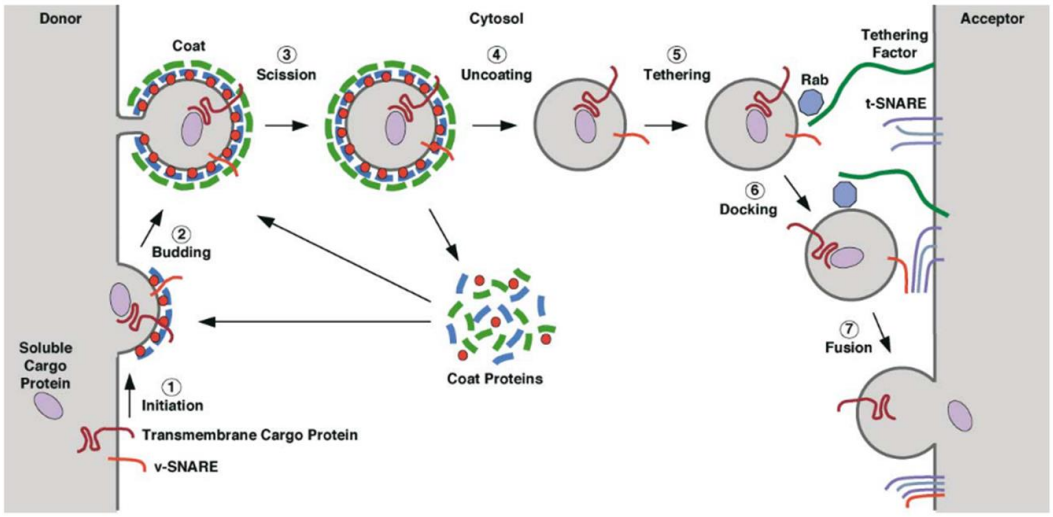

Figure 1.4. Steps of vesicle formation and budding (from Bonifacino and Glick, 2004). (*1*) Initiation of coat assembly. The first layer of coat components (blue, Sec23/24 in COPII transport) is recruited to the donor compartment by binding to a membrane-associated GTPase (red, Sar1 in COPII vesicles). Transmembrane cargo proteins and SNAREs begin to gather at the assembling coat. (*2*) Budding. The missing coat components (green, Sec13/31 in COPII complexes) are added and cargo proteins become concentrated and membrane curvature increases. (*3*) Scission. The neck between the vesicle and the donor compartment is severed either by direct action of the coat or by accessory proteins. (*4*) Uncoating. The vesicle sheds its coat due to various events including inactivation of the small GTPase and/or the action of uncoating enzymes. Cytosolic coat proteins are then recycled for additional rounds of vesicle budding. (*5*) Tethering. The uncoated vesicle travels towards the acceptor compartment and helped by the combination of a GTP bound Rab and a tethering factor, is taken in close proximity to the acceptor compartment. (*6*) Docking. The v- and t-SNAREs assemble into a four-helix bundle and form the *trans*-SNARE complex. (*7*) Fusion. This *trans*-SNARE promotes fusion of the vesicle, cargo proteins are released into the target compartment and SNAREs and other effectors are recycled for future vesicle transport.

1.4.4. *Trans*-Golgi traffic and exocytosis through the plasma membrane

After maturation and travel through the different compartment of the Golgi apparatus, secretory proteins arrive at the *trans*-Golgi network (TGN) where final PTM processing occurs and proteins are sorted for their final destination. The TGN is an important hub for protein secretion and sorting, directing proteins to their final destination such as the plasma membrane, the early endosome or the lysosome. It is believed that export to the plasma membrane or other destinations from the TGN is completed by the tubular export of domains acting as export carriers (De Matteis and Luini 2008). The sorting of cargo

proteins is processed by the recognition of specific domain motifs by cargo receptors and coat proteins. PTMs also play a key role in the recognition of cargo proteins, for example glycosylation (Yeaman et al. 1997) and phosphorylation (Hinners 2003). Once cargos are sorted, they are segregated to different TGN domains using sorting motifs or microenvironment conditions for which cargo have a specific selectivity. The main players in these functions are protein from the ERF and Rab family, adaptors, GRIP-golgins and lipids. When the different cargo proteins are segregated into TGN domains, tubular domains are generated. A number of mechanisms are thought to be involved in the bending of the membrane to form tubular domain including action of the BAR Family (Neubrand et al. 2005) or the GRIP-golgins (Gleeson et al. 2004). Enzymes linked to lipid metabolism are also proposed to play a role, for example CERT and FAPP2 (Godi et al. 2004; De Matteis and Luini 2008). Extrusions of the tubular domain from the TGN are observed after interaction with a motor. During extrusion of the mature domain from the TGN compartment, fission is observed at the thinnest section of the tubular domains (Polishchuk et al. 2003). Different fission machineries can be involved with perhaps the best studied being dynamin (McNiven et al. 2000). Targeting and fusion of the tubular domain with the plasma membrane, exocytosis, is performed using SNARE proteins and SM associated proteins such as Munc18c (Rizo and Südhof 2002).

1.5. Engineering strategies to enhance the capacity of the secretory pathway

1.5.1. Improving the efficiency of translocation of nascent polypeptide into the endoplasmic reticulum

The secretory pathway is complex and integrates several steps, the first being the translocation of the nascent polypeptide into the ER. Translocation is thought to be a rate limiting step so different strategies have been investigated to improve the efficiency of this step and increase the production of secreted recombinant proteins with some success. Le Fourn et al (2014) engineered CHO cells to overexpressed one component of the SRP, SRP14. Overexpression of SRP14 in cell lines expressing difficult-to-express and more easy-to-express products improved the secretory productivity of the cells by up to 6 fold suggesting this was indeed a rate limiting step in the secretory pathway. SRP14, along with SRP9 is responsible for the arrest of translation of the nascent peptide once the ER signal sequence has emerged from the ribosome exit tunnel (Akopian et al. 2013). It is supposed

that overexpression of SRP14 allows a more stringent control of mRNA translation arrest, leading to improved and more efficient targeting to the ER and the SRP receptor, resumption of mRNA translation and cleavage of the peptide signal.

Another strategy that has been investigated to enhance the translocation step is to manipulate the signal sequence so that the nascent peptide is more efficiently recognised by the SRP. Several reports have demonstrated that production of a secreted protein can be altered by using different ER targeting peptide signals (Knappskog et al. 2007; L. Zhang, Leng, and Mixson 2005). Kober et al (2013) screened 16 different ER signal peptides from different origins and investigated the impact these had on the expression of a light and heavy chain of an antibody. The different signal peptides gave a range of HC and LC secretory productivities and the productivity of the cells could be increased by 50-100% from the lowest expression with different signal peptides.

1.5.2. Endoplasmic reticulum and unfolded protein response cell engineering

The ER is an important organelle which is the first destination of secretory proteins and is where folding and assembly of secretory proteins and quality control checks for correct folding is undertaken. Attempts to improve the folding of secretory polypeptides in the ER through the overexpression of different chaperone proteins has been undertaken and is discussed in section 1.3.4.2.3. Successful strategies where overexpression has enhanced secretory productivity includes BiP(GRP78), PDI, Calreticulin/Calnexin, and ERp57 proteins which are all ER resident proteins that are chaperones or foldases with a number involved in formation or isomerisation of disulphide bonds.

A specific stress response pathway that senses and responds to stress in the ER has also being engineered, the unfolded protein response pathway (UPR). The UPR is a mechanism triggered by the cell in the presence of abnormal levels of unfolded proteins. When expressing a recombinant polypeptide, the ER can become overwhelmed with polypeptides to fold and the amount of unfolded protein is elevated. To cope with the situation, the UPR is triggered and through ER stress sensors and the responses this elicits, tries to alleviate this bottleneck of unfolded protein in the ER of the secretory pathway. When the stress is too intense, the UPR eventually activates signals that triggers ER mediated apoptosis. An important response of the UPR that is mediated in response to unfolded protein is the XBP-1 protein which is a transcription factor. The UPR has 3 stress sensors, PERK, ATF6 and IRE1α which have their activation regulated by BiP. In the presence of high amounts of unfolded protein, BiP disassociates from the stress sensors and binds the unfolded proteins

allowing activation of the different stress sensors. IRE1α activates XBP-1 using its exonuclease activity to generate XBP-1 mRNA that is spliced to generate a powerful transcription factor that binds to UPR response elements (UPRE) upstream of chaperone and foldase genes (Yoshida et al. 2001). Spliced XBP-1, as a transcription factor, activates the transcription of a number of genes in the secretory pathway (Shaffer et al. 2004) such as chaperones and foldases but also pro-apoptotic proteins. Different reports have successfully demonstrated that the overexpression of the active form of spliced XBP-1 can improve secretory recombinant protein production up to 4-fold increase(Becker et al. 2008; Gulis et al. 2014; Ku et al. 2008; Tigges and Fussenegger 2006).

1.5.3. Engineering of vesicle formation and trafficking

Another strategy implemented to improve the secretory pathway is the manipulation of vesicle formation and trafficking. The ER and Golgi apparatus are important in protein folding and PTMs that are thought to be rate limiting steps in the secretory pathway, however another essential step in the secretory pathway is the trafficking of cargo (proteins) to/from the different organelles and out of the cell. The traffic is mediated through vesicles formed and regulated by different protein complexes. As such, Peng and Fussenegger (2009) overexpressed two proteins of the Sec1/Munc18 (SM) family, Sly1 and Munc18c. The SM family is suggested to be involved in catalysing the fusion of the membranes after docking of the vesicle on the target membrane (Jahn, Lang, and Südhof 2003). Sly1 modulates fusion of the vesicle from the ER with the Golgi (Peng and Gallwitz 2002) whereas Munc18c modulates fusion between *trans*-Golgi vesicles and the plasma membrane (Rizo and Südhof 2002). Overexpression of Sly1 or Munc18c in CHO-K1 cells increased productivity of the cells up to five-fold, demonstrating that vesicle fusion could be a limiting step in at least CHO-K1 cells.

Another approach reported with regard to engineering of vesicle traffic is the manipulation of SNARE proteins. SNARE proteins are involved in the fusion of vesicles but also the sorting of the different vesicles. Peng et al (2011) reported on the overexpression of several SNAREs to investigate the impact on mammalian cell secretory productivity. These authors investigated the overexpression of STX2, STX3, SNAP23, SNAP25, VAMP2 and VAMP8 proteins that are principally involved in traffic between the ER and the Golgi and the Golgi and the plasma membrane. It was observed that only the overexpression of SNAP23 and VAMP8 increased the secretory productivity of the different cell lines used (HeLa, CHO and HEK293). The authors suggested that enhanced secretory productivity was the result of an

increase in membrane turnover and dynamics as SNAP23 and VAMP8 are located at the secretory vesicle and the plasma membrane. Collectively, such studies suggest that engineering of vesicle traffic and formation is a good strategy for increased secretory productivity of mammalian host cell lines. The work presented in this thesis is based on the manipulation of the SNARE family to improve the secretory capacity of CHO cells.

1.6. The SNARE protein family

Soluble N-ethylmaleimide-sensible factor attachment protein receptor or SNARE is a family of proteins involved in the promotion of vesicle fusion and in determining the specificity of the fusion. SNAREs are proteins with a size between 100 to 300 amino acids that can functionally be divided in two, the v-SNAREs and the t-SNAREs (Jahn and Scheller 2006). The v-SNAREs for vesicle-SNARE are present on the surface of the vesicle and the t-SNAREs for target-SNARE are present on the surface of the targeted compartment to which the vesicle will fuse. Recognition of a v-SNARE, a tail-anchored SNARE containing a single SNARE motif, with a t-SNARE, composed of two or three polypeptides, generates a complex termed a *trans*-SNARE (or SNAREpin) composed of a four SNARE motif organised as a twisted parallel four helical bundle (Figure 1.5A). The action of the four-motif facilitates the fusion of the two opposed membranes. Table 1.2 reports the 36 SNAREs known in mammalian cells (Bonifacino and Glick 2004; Hong 2005). All the family members present at least one SNARE motif that is evolutionary conserved. SNARE proteins can also be classified structurally as Q or R type which is a more accurate definition because it takes in account homotypic fusion. During the formation of *trans*-SNARE complex, the four helixes form an interaction surface of 16 layers. The central layer, defined as the layer 0, has a hydrophobic interaction between 3 arginine residues (Q) and one glutamine residue (R) (Figure 1.5B). According to what residue of the SNARE participates in the central layer of the bundle, SNARE proteins are qualified as Q or R-SNARE (Figure 1.5C). Q-SNAREs can be subdivided into 3 types Qa, Qb and Qc. A particular subfamily of SNARE, the SNAP25 family, is classified as Qbc due to the presence of a Qb and Qc motif. Proteins are classified as Qb and Qc depending on the homology of their SNARE motif to the N-term (Qb) or C-term motif (Qc) of SNAP25.

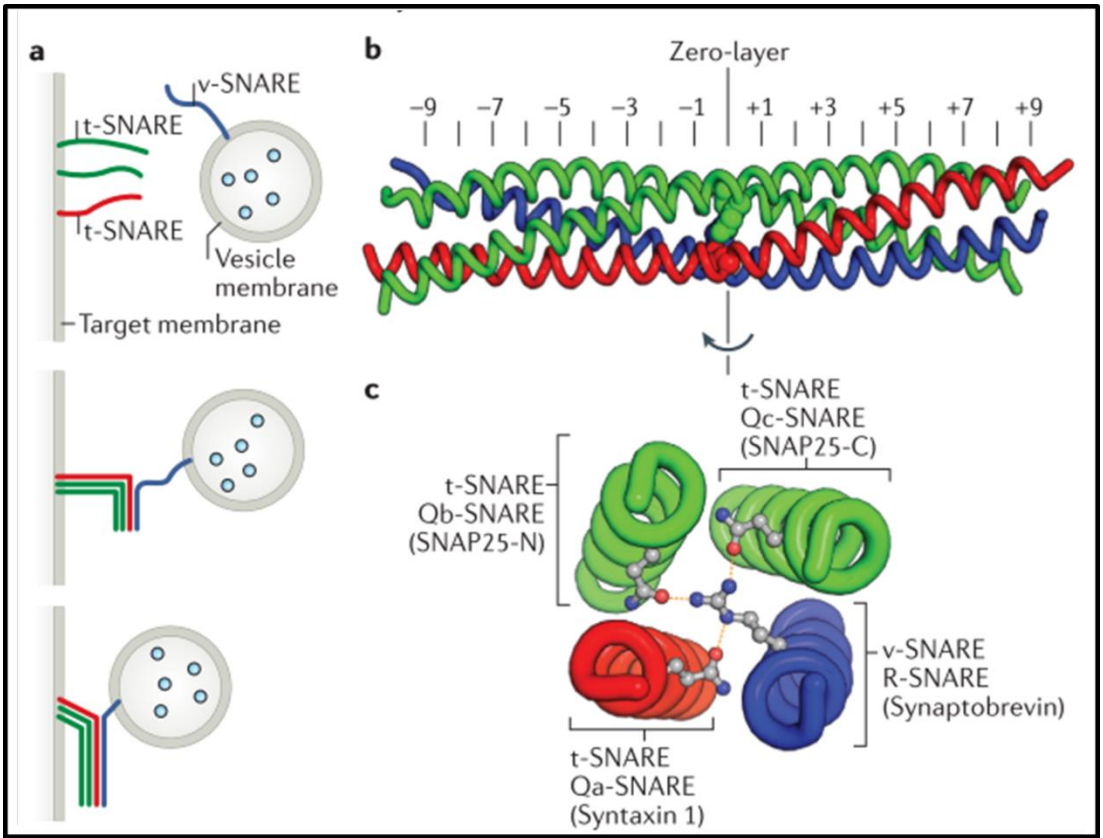

Figure 1.5. Formation of the *trans*-SNARE complex of SNAP25, syntaxin1 and Synaptobrevin (VAMP2). **A**, a v-SNARE (blue, synaptobrevin) recognises t-SNAREs (green, SNAP25; red, synxtaxin1) to form the *trans*-SNARE complex promoting membrane fusion. **B**, *trans*-SNARE complex, the four helixes form an interaction surface of 16 layers. The central layer or zero layer is generally composed of 4 hydrophilic residues, usually arginine and glutamine. **C**, The residue of the SNARE motif participating in the central layer defines if the SNARE is a Q-SNARE (for glutamine) or R-SNARE (for arginine). The SNAP25 family are exotic SNAREs possessing two SNARE motif taking part in the *trans*-SNARE complex.

Table 1.2. Known members of the SNARE family in mammalian cells (Hong 2005).

Name	localisation	AA length	snare motif position	GenBank identification	synonym	type
Syntaxin1	PM	288	202–254	Q16623	HPC-1	Qa
Syntaxin2	PM	288	201–253	P32856	Epimorphin	Qa
Syntaxin3	PM	289	201–253	NM_004177		Qa
Syntaxin4	PM	297	210–262	Q12846		Qa
Syntaxin5	Go	301	219–271	U26648		Qa
Syntaxin6	TGN/end	255	173–225	AJ002078		Qc
Syntaxin7	EE/LE	261	175–227	U77942		Qa
Syntaxin8	EE/LE	236	155–207	NP_004844		Qc
Syntaxin10	TGN	249	167–219	AF035531		Qc
Syntaxin11	TGN/LE	287	214–266	O75558		Qa
Syntaxin13	EE	276	188–240	NP_803173	Syntaxin12	Qa
Syntaxin16	TGN	325	240–292	NP_001001433		Qa
Syntaxin17	ER	302	172–224	NP_060389		Qa
Syntaxin18	ER	335	253–305	Q9P2W9		Qa
SNAP-23	PM	211	24–76 and 156-208	NP_003816	Syndet	Qb/Qc
SNAP-25	PM	206	29–81 and 150-202	NP_003072		Qb/Qc
SNAP-29	Go/End	258	60–112 and 206-258	O95721	GS32	Qb/Qc
VAMP1	SV	118	34–86	P23763	Synaptobrevin1	R
VAMP2	SV	116	32–84	NP_055047	Synaptobrevin2	R
VAMP3	EE/RE	100	15–67	NP_004772	Cellubrevin	R
VAMP4	TGN/EE	141	53–105	NP_973723		R
VAMP5	PM	116	6–58	NP_006625		R
VAMP7	LE/Ly/PM	220	126–178	NP_005629	Ti-VAMP	R
VAMP8	EE/LE	100	13–65	NP_003752	Endobrevin	R
Ykt6	Go	198	139–191	AAB81131		R
Sec22a	ER/IC	282	135–187	AAD43013		?
Sec22b	IC/cis-Go	215	135–187	NP_004883	ERS-24	R
Sec22c	ER/IC	250	135–185	AAD02171		?
Bet1	IC/cis-Go	118	36–88	NP_005859		Qc
GS15	Go	111	25–77	AAF37877		Qc
GS27	IC/Go	212	130–182	O14653	Membrin, Gos-27	Qb
GS28	Go	250	170–222	O95249	GOS-28	Qb
Vti1a	trans-Go	217	132–184	BI830707 and BF805294	Vti1-rp2	Qb
Vti1b	EE/LE	232	146–198	NP_006361	Vti1-rp1	Qb
Slt1	ER	259	173–225	BC008455	Use1, p31	Qc
Sec20	ER	228	132–184	NP_001196	Bnip1	?

PM: plasma membrane; Go: Golgi apparatus; cis- Go: cis-Golgi compartments; trans-Go: trans-Golgi compartments; TGN: trans-Golgi network; End: endosomes; EE: early endosomes; LE: late endosomes; RE: recycling endosomes; Ly: Lysosomes; ER: endoplasmic reticulum; IC: ER-Golgi intermediate compartments; SV: synaptic vesicles.

Compared to the well preserved SNARE motif, the N-terminal region of the different SNAREs are very diverse (Figure 1.6). Qa SNAREs, also called syntaxins, possess a three helical motif in their N-terminal region. Qb and Qc SNAREs don't have a specific motif at their N-terminal region. On the other hand, most of the R-SNAREs have a profilin-like fold also referred as a longin domain in their N-terminal region (Daste et al, 2015). The presence and function of the different N-terminal regions of the SNAREs are not fully understood. It is suggested that they are necessary for the interaction with regulators such as the Sec1/Munc18 (SM) family or with tethering factors. Some reports have demonstrated that

the N-terminal region is not essential for fusion events (Wang et al, 2001). Most of the SNAREs also contain a transmembrane domain connected to the SNARE motif by a linker. The SNAP25 family miss the transmembrane domain so the anchorage to the membrane is performed via a post translational modification (Gerst 1999; Jahn and Scheller 2006).

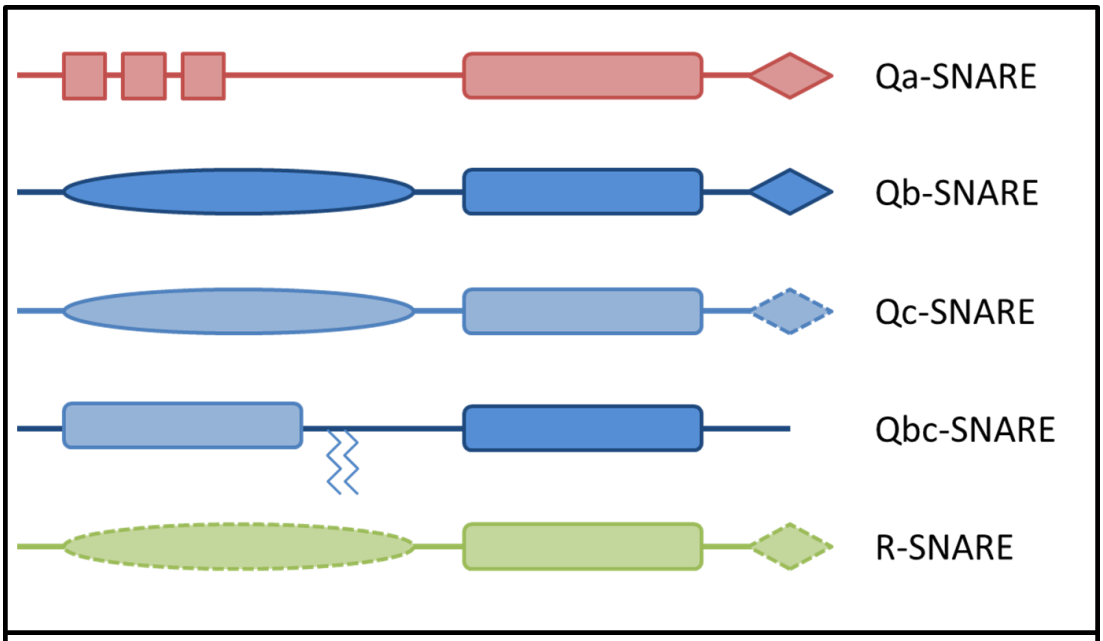

Figure 1.6. Structure of the different subfamilies of SNAREs. The red squares represent the antiparallel triple helix bundles present in the N-terminal of Qa-SNAREs. Ovoid shapes represent the various N-terminal domains of Qb-, Qc- and R-SNAREs. The rectangular shapes represent the SNARE motif. Qbc-SNARE represents the SNAP25 family possessing two SNARE motifs, a Qb and Qc motif, linked by a linker that is often palmitoylated (zigzag lines). Diamonds represents the transmembrane domains of the SNAREs. Shapes in dashed lines are domains missing in some members of the subfamilies. Qc SNARE motifs are represented in light blue and Qb SNARE motifs in dark blue. (Jahn and Scheller, 2006).

SNAREs are thought to act as follows. A v-SNARE is packed together with cargo proteins during the formation of a vesicle so after budding of the vesicle interaction between the v-SNARE and a t-SNARE is possible for membrane fusion. SNAREs have a potential role in the formation of vesicles via the interaction of coat proteins, notably from COPI and II complexes (Mossessova, Bickford, and Goldberg 2003; Rein et al. 2002). After the traffic of the vesicle to the target compartment, tethering factors are necessary to position and gather the vesicle to the exact position of the t-SNARE. The SNAREs spatially close interact and form a *trans*-SNARE complex which is believed to catalyse the fusion of the membranes. Once the fusion is performed, the complex becomes a *cis*-SNARE complex that needs to be disassembled and the components recycled for further use. Intervention of α-SNAP and NSF are required for disassembly in an ATP dependent manner. Once recycled,

the v-SNARE is relocalised to its original compartment by retrograde transport and t-SNAREs are reorganised for the next fusion (Jahn and Scheller 2006).

As outlined above, to mediate their action, SNARE proteins work together with tethering factors for the fusion of the membranes. Two classes of tethering factors are able to intervene; homodimers containing long stretches of predicted coiled-coil and hetero-oligomers known as multi-subunit tethering complexes. SM family proteins have also been proposed to have a role in the assembly and regulation of SNARE proteins but the molecular mechanism remain unclear (Archbold et al. 2014; Gerst 1999). As described previously, the most important regulators of the SNARE complex are NSF and α-SNAP as they disassemble the *cis*-SNARE complex in an ATP-dependent manner to recycle all the SNARE elements.

The different targets investigated in this study are SNAREs and are described in more detail below. They were chosen for their roles in functions thought to be important for secretion of proteins and that could potentially improve secretory capacity if manipulated. Some targets were chosen not for their function but because they participate in complex with other SNAREs and to determine if engineering of a complex rather than one component would enhance secretory productivity. Interestingly, a number of the targets selected have a role in the autophagosome which has also been identified as a potential target for manipulation for the improvement of recombinant protein production.

1.6.1. Vesicle associated membrane proteins or VAMPs

1.6.1.1. VAMP3

All the VAMPs (vesicle associated membrane proteins) are R-SNAREs. VAMP3 or cellubrevin, is ubiquitously expressed and was first reported in 1993 as a result of the screening of a genomic library (McMahon et al. 1993). VAMP3 is a 100 amino acid long protein cleaved by the tetanus toxin light chain. It has been demonstrated that VAMP3 interacts with the syntaxin4/SNAP23 complex and syntaxin16/Vti1a/syntaxin6 complex (Mallard et al. 2002), playing a role in the retrograde transport from the early/recycling endosome to the TGN. VAMP3 is known to be localised in early and recycling endosomes (Galli et al. 1994; Jovi et al. 2014; McMahon et al. 1993). VAMP3 is preferentially present in tubular membranes where it facilitates fusion of recycling endosomes and the Golgi. VAMP3 is suggested to regulate the recycling of various proteins such as integrins (Luftman et al. 2009; Skalski and Coppolino 2005), transferrin and their receptors from endosomes to

the plasma membrane (McMahon et al. 1993) as well as α-granule transport in platelets (Feng et al., 2002; Polga´r et al., 2002) and retrograde transport of mannose-6 phosphate receptor to the Golgi (Ganley et al., 2008). VAMP3 is also involved in fusion at the plasma membrane with different t-SNAREs (syntaxin1/SNAP-25, syntaxin1/SNAP-23 and syntaxin4/SNAP-25) (Hu, Hardee, and Minnear 2007). A study in murine C3 cells demonstrated that depletion of both VAMP3 and YKT6 caused a complete block in secretion suggesting a major role in fusion of secretory carriers (Gordon et al. 2017).

1.6.1.2. VAMP4

VAMP4 is a 141 amino acid protein discovered in 1998 (Advani et al. 1998) and is only expressed and highly conserved in vertebrates (Zeng et al. 2003). It is known to be part of the SNARE complex including STX16, Vti1a and STX6 responsible for retrograde traffic between the early/recycling endosome and the TGN (Mallard et al. 2002; Zeng et al. 2003). Depletion of VAMP4 results in abolition of anterograde transport of GPI-anchored and transmembrane proteins (Hirata et al. 2015) suggesting that VAMP4 is important for recycling of critical molecules for post-Golgi anterograde transport. In Hela cells, depletion of VAMP4 leads to disruption of the organisation of the Golgi apparatus demonstrating the importance of the retrograde transport and the central role of VAMP4 (Okayama et al. 2012). VAMP4 is predominantly localised at the TGN through a 51 residue section of amino acids present in its N-terminus (Zeng et al. 2003) and interaction with SNAP47 (Kuster et al. 2015).

VAMP4, by its function in specialised cells, has been reported to be involved in exocytosis in PC12-27 cells (Cocucci et al. 2008), release of lytic granules in NK cells (Krzewski et al. 2011) and maturation of secretory granules in PC12 and atT-20 cells (Shitara et al. 2013). Through such reports it is thought that VAMP4 has a central role in regulated exocytosis. VAMP4 is also localised at hippocampal synapses and is implicated in asynchronous release and spontaneous release in neuronal cell lines (Ramirez and Kavalali 2012). A group working on Hela cells reported that overexpression of VAMP4 leads to abolition of the need of tethering and regulatory elements (Laufman, Hong, and Lev 2011). VAMP4 also has a role in activity-dependent bulk endocytosis of synaptic vesicle (Nicholson-Fish et al. 2015)

1.6.1.3. VAMP7

VAMP7, also called tetanus-insensitive VAMP (Ti-VAMP), is a 220 amino acid long protein discovered in 1998 (Advani et al. 1998). The N-terminal of VAMP7 is suggested to have a

profilin like structure (Hong 2005). VAMP7 is localised to the Golgi apparatus (Chaineau, Danglot, and Galli 2009) and is the only SNARE to be localised to the late endosome (Pols et al. 2013). VAMP7 interacts with different SNARE complexes; the syntaxin4/SNAP23 complex which is suggested to mediate fusion of lysosomes with the plasma membrane (Rao et al. 2004) and syntaxin17/SNAP29 complex required for the fusion of autophagosomes and lysosomes (Takáts et al. 2018). By mediating the fusion of vesicles from the Golgi, late endosomes and lysosomes, VAMP7 is involved in several cellular functions such as phagocytosis, cell migration, membrane repair, and mitosis (Daste et al. 2015). VAMP7 also has roles in autophagosome biosynthesis (Moreau and Rubinsztein 2012), autophagosome-lysosome fusions (Takáts and Juhász 2013) and autophagosomal secretion (Fader, Aguilera, and Colombo 2012). VAMP7 may also have a general role in exocytosis. It is known to have a role in regulated exocytosis in HeLa cells (Chaineau et al. 2009) and to be involved in the release of lytic granules in NK cells (Krzewski et al. 2011) whereas it has only a minor role in constitutive exocytosis in HSY cells (Oishi et al. 2006). VAMP7 contributes to sphingolipid and Golgi homeostasis and is involved in transport of GPI-anchored proteins to the plasma membrane (Molino et al. 2015)

1.6.1.4. VAMP8

VAMP8, also called endobrevin, is a 100 amino acid long protein that was discovered in 1998 by Advani et al. (1998). Expression of VAMP8 is ubiquitous but enriched in epithelial cells such as kidney, intestine, pancreas and lung cells (Hong 2005). VAMP8 is localised in endosomes and was suggested to be involved in fusion between the early and late endosome (Wong et al., 1998). Endobrevin interacts with the SNARE complex, STX7/Vti1b/STX8, to mediate homotypic fusion of early and late endosomes (Antonin et al, 2000). VAMP8 also interacts with the STX4/SNAP23 complex in pancreatic acinar cells, playing a major role in regulated exocytosis of zymogen granules (Wang et al., 2004). Involvement in regulated exocytosis of this complex has also been observed in mast cells (Paumet et al. 2000). Wang et al. (2007) have suggested that VAMP8 might play the role of an R-SNARE for the entire endocrine system with a critical role in parotid and lacrimal acinar cells and other exocrine tissues. Fu et al. (2018) have also reported that VAMP8 interacts with syntaxin17 and SNAP29, two SNAREs involved in autophagosome fusion with the lysosome. By coupling with syntaxin2, VAMP8 is involved in cytokinesis too (Low et al. 2003). VAMP8 regulates compound exocytosis, a mode of secretion were secretion is enhanced by vesicle-to-vesicle fusion at the plasma membrane (Thorn and Gaisano 2012).

1.6.2. Syntaxins and synaptosome associated proteins (SNAPs)

1.6.2.1. Syntaxin7 or STX7

Syntaxin7 or STX7 was first reported in 1998 (Siew Heng Wong et al, 1998). It is a protein of 261 amino acids length, primarily linked to the early endosome and widely expressed as shown by Northern blot experiments (Siew Heng Wong et al. 1998). Syntaxin7 has also been associated with later compartments in the endocytic pathway and suggested to be involved in cycles between the plasma membrane and early endosomes (Prekeris et al, 1999). Due to its function in the endocytic pathway and localisation in early/late endosomes and lysosomes, STX7 is suggested to have a function in the formation of late endosomes and lysosomes (Nakamura et al. 2000). Syntaxin7 forms a complex with Vti1b, syntaxin8 and either VAMP7 or 8 (Pryor et al. 2004), depending on the fusion event (homotypic fusion or late endosome-lysosome fusion (Hong 2005)). He and Linder (2009) have observed that palmitoylation of STX7 is essential for its compartmentalisation, a lack of this PTM results in retention of STX7 at the plasma membrane. STX7 has also been reported to be implicated in phagocytosis, notably in the maturation process involving STX13 in phagocytic cells (Collins et al. 2002) and tumour necrosis factor exocytosis in macrophages (Murray et al. 2005).

1.6.2.2. Syntaxin17 or STX17

Discovered in 1998 by Steegmaier et al (1998), syntaxin3 was used as a bait in a two-hybrid screen to capture syntaxin17, a 303 amino acid long protein. STX17 is a distant member of the mammalian syntaxin family and does not have an equivalent in yeast (Steegmaier et al. 1998). It is expressed ubiquitously with an abundance in rich smooth ER cell membranes such as in steroidogenic cells (Steegmaier et al. 2000). STX17 localisation is dependent on the nutrient environment. In nutrient rich situations STX17 is localised to the ER (tubular and smooth ER), mitochondria and cytosol, otherwise STX17 is associated with the autophagosome (Itakura and Mizushima 2013) and mitochondria associated membranes (Hamasaki, Furuta, et al. 2013). Such localisation indicates roles at the mitochondrial and autophagosome levels.

STX7 possess two adjacent hydrophobic domains whereas other syntaxin only have one and a C-terminal luminal tail. Both hydrophobic domains are used for membrane anchoring but no function has been reported yet for the c-terminal luminal tail (Muppirala, Gupta, and Swarup 2011). STX17 activity is regulated in the early secretory pathway by tyrosine phosphorylation (Muppirala, Gupta, and Swarup 2012). In rich nutrient conditions, STX17

promotes mitochondrial fission by controlling localisation and activity of Drp1. Syntaxin17 is present on raft-like structures of the ER-mitochondria contact sites (Arasaki et al. 2015). Under starvation conditions, STX17 relocalises to mitochondria associated membranes and promotes formation of autophagosomes by interacting with ATG14L (Hamasaki, Shibutani, and Yoshimori 2013). STX17 plays a role in regulation of ER Ca^{2+} homeostasis and in mitochondrial dynamics by interacting with the protein Rab32. Syntaxin17 plays a role in responding to nutrient conditions and coordinates action between the ER, autophagosome and mitochondria under unfavourable nutrient conditions (Arasaki et al. 2015).

Syntaxin17 also plays a role in autophagy and notably in the fusion of the autophagosome with the endosomes and lysosomes. For fusion of the autophagosome, synxtaxin17 forms a *trans*-SNARE with SNAP29 and VAMP8 (Hubert et al. 2016). It has been suggested that depletion of syntaxin17 can inactivated mTOR, a major negative regulator of autophagy (Hegedus et al. 2013). Two reports have reported that this role is conserved through evolution (Hegedus et al. 2013). Without STX17, autophagosomes accumulate in the cell without degradation due to lack of fusion with lysosomes (Itakura, Kishi-Itakura, and Mizushima 2012).

Syntaxin17 also forms a complex with SNAP29 and VAMP7 to mediate the fusion of mitochondrial derived vesicles and endosomes or lysosomes. It is the last eukaryotic common ancestor suggesting that management of mitochondrial damage could have been one of the first vesicle transport pathways in cells (McLelland et al. 2016). A siRNA screen of several SNAREs to identify proteins necessary for constitutive secretion reported that STX17 is necessary for secretion (Gordon et al. 2010). STX17 might have roles other than membrane fusion, notably in specific cell lines where it has been observed to predominantly localise in the nucleus (Q. Zhang et al. 2005).

1.6.2.3. Syntaxin18 or STX18

STX18 was first reported in 2000 by Hatsuzawa et al. (2000) as a result of a yeast two-hybrid screen using α-SNAP as a bait. Syntaxin18 or STX18 is a 335 amino acid long protein principally located in the ER and plays a role in transport between the ER and Golgi. STX18 is involved in membrane traffic between the ER and the Golgi and interacts notably with RINT-1 and ZW10 which regulates its functions (Arasaki et al. 2006). STX18 forms a complex with Sec20, Use1 and Sec22b, playing a role in recycling traffic (Hong 2005). An siRNA screen confirmed that STX18 is essential for retrograde traffic from the Golgi (Gordon et al.

2010). This retrograde function is suggested to be essential to maintain the organisation of the smooth/rough ER and ER exit sites (Iinuma et al. 2009). Roles in ER mediated phagocytosis and Procollagen VII secretion have been reported for STX18 in J774 cells and HeLa cells respectively (Hatsuzawa et al. 2006; Nogueira et al. 2014) suggesting interaction of STX18 with a wide range of proteins.

1.6.2.4. SNAP29

SNAP29 (synaptosome associate protein of 29 kDA) is a 258 amino acids protein discovered in 1998 by Steegmaier et al. (1998) widely expressed in different tissues. SNAP29 belongs to the SNAP25 family which contains two SNARE motifs and do not possess a C-terminal membrane domain anchoring them to membranes (Hong 2005). For membrane anchoring, members of the SNAP25 family tend to use palmitoylation but SNAP29 uses instead an asparagine-proline-phenylalanine protein binding motif in the N-terminal (Rapaport et al. 2010). This binding domain gives SNAP29 a great versatility in its interactions with other proteins, notably syntaxins (Steegmaier et al. 1998) confirmed *in vitro*. It has been reported that the binding of syntaxins to SNAP29 increases their ability to bind to vesicles associated with SNAREs and that the presences of these vesicles also increases the binding of SNAP29 to syntaxins (Hohenstein and Roche 2001).

Due to the variety of interactions possible for SNAP29, it has been suggested that the protein has numerous functions. SNAP29 has been reported as being localised at the outer kinetochore, playing a role in kinetochore assembly and avoiding mis-segregation and/or formation of fragmented nuclei (Morelli et al. 2016). Through the formation of the *trans*-SNARE, SNAP29/STX17/VAMP8, SNAP29 controls fusion of autophagosomes with lysosomes (Itakura et al. 2012; Takáts and Juhász 2013). The association of the *trans*-SNARE is dependent on *O*-linked β-N-acetylglucosaminylation of SNAP29 which prevents association of the complex (Guo et al. 2014). SNAP29 might also have a role in platelet α-granule secretion regulation and thrombus stability in mouse platelets (Williams et al. 2016). Moreover, SNAP29 has roles in regulation of the secretion of neuronal secretory vesicles (Su et al. 2001) and lamellar granules in keratinocytes (Sprecher et al. 2005). The role of SNAP29 in endocytic recycling of transferrin and β1-integrin suggests a prominent role in endocytic recycling events that have also been observed (Rapaport et al. 2010).

The multiple roles of SNAP29 suggest that it is a general regulator of SNARE complex disassembly and has some function in *trans*-SNARE recycling post membrane fusion. This is probably due to its interactions with most of the syntaxins and its non-specific localisation.

This would also explain why so few members of the SNAP25 family are present if SNAP29 acts as a general participant in *trans*-SNARE complex (Steegmaier et al. 1998).

1.7. Aims of this study

For the last few decades, the biopharmaceutical market has expanded rapidly with the approval of complex molecules by the regulatory authorities produced from cultured mammalian cells, particularly monoclonal antibodies. Mammalian cell hosts are the system of choice for the production of monoclonal antibodies due to their capacity to correctly fold and assemble the different polypeptides required to generate a full length monoclonal antibody (HC and LC) and their ability to undertake human-like PTMs, particularly *N*-glycosylation. CHO cells have to date been optimised for secretory recombinant protein production via various approaches as outlined in the introduction to this thesis. In particular, cell line engineering has been attempted through strategies such as the manipulation of cell metabolism, apoptosis engineering and engineering of the secretory pathway by manipulating the vesicle traffic and formation. To date few such engineered systems have made it to manufacturing processes yet the opportunity remains to enhance the CHO chassis via cell engineering. The few studies available in the area of engineering of vesicle trafficking have suggested that the approach can be successful and overcome existing bottlenecks in CHO cells. The overall goal of this project was to investigate the increase of the production of secreted recombinant protein yields from CHO cells by engineering of the secretory pathway. The approach selected was the manipulation of proteins belonging to the SNARE family involved in vesicle traffic and formation. The outcome of this strategy was evaluated in two different environments, industry and academia, to determine the relevance and transferability of the strategy.

CHAPTER 2: Materials and Methods

2.1. DNA manipulation and cloning

2.1.1. DNA plasmid sources

Plasmids pMRXIP-SNAP29, pMRXIP-STX18, pMRXIP-STX7 and pMRXIP-STX17 were outsourced from Addgene where they were deposited by Noboru Mizushima (Addgene plasmid # 45923, # 45918, # 45921 and # 45909). Plasmids pEGFP-VAMP8, pEGFP-VAMP7, pEGFP-VAMP4, pEGFP-VAMP3 were deposited by Thierry Galli (Addgene plasmid # 42311, # 42316, # 42313 and # 42310). The plasmid pcDNA™3.1/Hygro$^{(+)}$ was sourced from Thermo Fisher Scientific.

2.1.2. Polymerase chain reaction for fragment amplification

Polymerase Chain Reaction (PCR) experiments were carried out using a Phusion High-Fidelity DNA polymerase (Thermo Fisher Scientific, UK). Typically, the PCR mix was 4 µL of 5 x Phusion HF buffer, 0.4 µL of 10 mM dNTPs (Invitrogen, USA), 0.8 µL of both forward and reverse primers at 100 µM, less than 100 ng/µL of cDNA or 20 ng/µL plasmid, 0.2 µL polymerase and nuclease-free water (Thermo Fisher Scientific, UK) for a final volume of 20 µL. The primers were designed using SnapGene software (GSL Biotech LLC, USA) and the Oligo Analysis Tool (Eurofins, UK). The amplification cycle started with an initial denaturation at 98˚C for 30 sec followed by 30 or 35 cycles of 98˚C for 10 sec, 58 to 62˚C for 30 sec (depending on the melting temperature (Tm) of the primers), 72˚C for 30 sec for each 1 kb of the desired fragment length. The final step was a final extension cycle at 72˚C for 7 min. All the different primer sets used in this work are detailed in Appendix 1.

2.1.3. Enzymatic digest of plasmid DNA

All restriction enzyme digests were done using FastDigest™ enzymes (Thermo Fisher Scientific, UK) unless specified. The manufacturer's recommendations were followed for the different conditions. Generally, 1 µL of enzyme was used to digest 1 µg of DNA at 37˚C for 30 min in a reaction volume of 20 µL.

2.1.4. Agarose gel electrophoresis for DNA observation and analysis

Agarose gels were composed of 1 x TAE buffer (50 x TAE buffer; 2 M Tris, 50 mM EDTA, 20 mM acetic acid) containing 0.5 to 2% agarose. Agarose was dissolved by microwaving the

solution. After cooling down the mixture, 3 µL/50 mL gel of ethidium bromide (Invitrogen, USA) was added and the gel was casted into an electrophoresis tank. Once solidified, 1 x TAE buffer was used as electrophoresis buffer. When necessary, a loading dye was added to the DNA mixture (Promega, USA) (FastDigest buffer already includes a loading dye). A DNA ladder (Promega, UK) was loaded alongside the samples to help determine the sizes of the DNA fragments. Routinely, agarose gel electrophoresis was performed at 80 V for one hour. For visualization of the DNA fragments, the gel was exposed under UV light using a G Box (Syngene, UK).

2.1.5. DNA purification

After extraction from an agarose gel, DNA fragments were purified using the Wizard® SV Gel and PCR Clean-Up System (Promega, USA). The manufacturer's protocol was followed and the last elution step was performed using 50 µL of nuclease-free water. The DNA solution obtained was quantified using a nanodrop ND 1000 spectrophotometer (NanoDrop technologies, USA).

2.1.6. Ligation of DNA fragments

To ligate 2 digested DNA fragments with compatible ends, T4 ligase (Promega, USA) was used following the manufacturer's specifications. Typically, the quantity of backbone (acceptor fragment) and insert (donor fragment) was calculated using a ratio of 1:3 (backbone to insert ratio) and 100 ng of backbone with the following equation:

$$\frac{ng\ of\ backbone\ \times\ kb\ size\ of\ insert}{kb\ size\ of\ backbone} \times\ molar\ ratio = ng\ of\ insert$$

The reactional volume was 10 µL incubated overnight at 4˚C.

2.1.7. Generation of DH5α *Escherichia coli* competent cells

A DH5α *E. coli* strain was prepared for calcium chloride transformation. An isolated colony was picked from an overnight petri dish culture in Lysogeny Broth (LB) media with agar (1% w/v of peptone, 0.5% w/v of yeast extract, 1% w/v of NaCl, and 1.5% w/v of agar) and used to inoculate 5 mL of LB media (1% w/v of peptone, 0.5% w/v of yeast extract, 1% w/v of NaCl). The starter culture was incubated overnight at 37˚C, 150 rpm and used to inoculate 2 x 50 mL of Super Optimal Broth (SOB) media (2% w/v of peptone, 0.5% w/v of yeast extract, 0.1% w/v of NaCl, 2.5 mM KCl, 10 mM $MgCl_2$) in 250 mL Erlenmeyer flasks the next day. The cultures were grown at 37˚C, 150 rpm until reaching an absorbance A600 of 0.4-0.6.

Cultures were then transferred to chilled 50 mL tubes and harvested at 3000 *g* for 15 min at 4˚C. The pellets were resuspended in 10 mL ice-cold 100 mM $CaCl_2$ previously filter-sterilized and incubated on ice for 30 min. After a second spin at 4000 *g* for 15 min at 4˚C, the pellets were gently resuspended into 2 mL ice-cold $CaCl_2$, pooled together and 1 mL sterile 80% glycerol was added to the cells. Cells were dispensed as 100 µL aliquots in cryotubes and flash-frozen on dry ice. Once flash-frozen the aliquots were kept at -80˚C.

2.1.8. Transformation of DNA into competent cells

An aliquot of competent DH5α cells was thawed on ice. 3 µL of plasmid or 10 µL of ligation mix was added to cells then incubated for 30 min on ice. A heat shock at 42˚C for 90 sec was performed to transform the cells. After 2 min recovery on ice, 900 µL of LB media was added to the competent cells and the cells were incubated for an hour at 37˚C, 180 rpm. At the end of the incubation step, 100 µL of competent cells was spread on a LB media agar plate containing the appropriate selection marker (ampicillin at 100 µg/mL or kanamycin at 50 µg/mL). The plates were placed at 37˚C overnight.

2.1.9. Plasmid DNA amplification

Depending on the quantity of DNA needed, two scales of plasmid DNA amplification were used; QIAprep Spin Miniprep kit and HiSpeed Plasmid Maxi kit (Qiagen, UK). Depending on the desired scale, 5 mL in a 50 mL tube or 250 mL in a 1 L Erlenmeyer flask of LB media containing selection antibiotics was inoculated with a colony containing the desired plasmid. Cultures were incubated overnight at 37˚C, 150 rpm. The next day the cells were harvested at 3000 *g* for 20 min and the pellets were processed using the appropriate kit. For quantification, a nanodrop ND 1000 was used.

2.1.10. DNA sequencing

All sequencing was outsourced to Genewiz UK Ltd. The DNA samples were sent as 10 µL aliquots at 100 ng/µL.

2.1.11. Plasmid linearization and DNA precipitation

2.1.11.1. University of Kent procedure

FspI enzyme (New England Bioloabs, USA) was used to linearize the plasmid, the ratio used was 1 µL of enzyme for 10 µg of DNA. The mixture was incubated overnight at 37˚C. To check the full linearization of the plasmid a small volume (1 µL) was analysed by agarose gel electrophoresis.

The different precipitation steps were performed in a laminar flow hood to avoid contamination. After linearization, the DNA was precipitated with 0.1 volume of 3 M sodium acetate pH 5.2 and 2.5 volume 95% ethanol chilled at -20˚C. The mix was centrifuged at 17000 *g* for 30 min at 4˚C. The supernatant was discarded and 1 volume of 70% ethanol chilled at -20˚C added. A second centrifugation at 17000 *g* for 5 min at 4˚C was performed. Decanted pellet was left to air-dry. Finally, the pellet was resuspended in 50 µL of sterile-filtered TE buffer (HiSpeed Plasmid Maxi kit (Qiagen, UK)) and left overnight at room temperature. A small volume was then used (2 µL) for quantification.

2.1.11.2. Fujifilm Diosynth Biotechnologies procedure

NheI enzyme (New England Bioloabs, USA) was used to linearize the plasmid, the ratio used was 1 µL of enzyme for 10 µg of DNA. The mixture was incubated overnight at 37˚C. To check the full linearization of the plasmid a small volume (1 µL) was analysed by agarose gel electrophoresis.

The different precipitation steps were performed in a laminar flow hood to avoid contamination. The linearized DNA was transferred to a 2 mL tube and 0.1 volumes of 3 M, pH 5.2 sodium acetate (Sigma Aldrich, USA) was added. The DNA was precipitated by adding 2.5 volumes of ice-cold 95% ethanol. To improve the precipitation, the tube was incubated 1 hour at -80˚C. The precipitated DNA was centrifuged at top speed for 30 min at 4˚C and the supernatant discarded. One volume of 70% ice-cold ethanol was added to wash the pellet and another centrifugation at top speed for 10 min at 4˚C performed. The supernatant was discarded again and the pellet was left to air dry. To resolubilize the pellet, 55 µL of water (Sigma Aldrich, USA) was added and the tube was incubated overnight at 37˚C. The next day 5 µL was used for quantification using a Qubit 4 fluorometer (Invitrogen, USA) following the manufacturer's protocol.

2.2. Cell culture

2.2.1. Suspension cell lines

2.2.1.1. CHO-S cells

The CHO-S cell line was a serum-free cell line originated from the laboratory of Professor Nicole Borth. CHO-S cells were routinely seeded at 0.2 x 10^6 viable cells/mL in 20 mL of CD-CHO media (Life Technologies, USA) containing 8 mM L-glutamine (Sigma Aldrich, USA) in a

125 mL Erlenmeyer flask (Corning, USA). Cells were manually gassed. Flasks were incubated in a HT multitron standard incubator (Infors, CH) at 37˚C, 140 rpm. When CO_2 monitoring was essential, cells were inoculated in 125 mL Erlenmeyer flasks with vented caps (Corning, USA) and incubated in a New Brunswick™ S41i incubator (Eppendorf, USA) at 37˚C, 140 rpm and 5% CO_2. Stably transfected CHO-S cells were cultivated under the same conditions as the host cell line except with the addition of selection agent in the media, Hygromycin B at 750 µg/mL (Thermo Fisher Scientific, USA) or Puromycin at 7.5 µg/mL (Sigma Aldrich, USA). Tube spin vessels were also used with a working volume of 10 mL in 50 mL conical bottom tubes (Sarstedt, DE) or 50 mL conical bottom tubes with vented cap (Corning, USA) when necessary and incubated at 37˚C, 240 rpm, 5% CO_2. Cells were passaged every 3-4 days.

2.2.1.2. Clone 27 (Fujifilm Diosynth Biotechnologies) CHO cells

Clone 27 is a CHO-DG44 derived cell line used as a host at Fujifilm Diosynth. Clone 27 was routinely seeded at 0.2 x 10^6 viable cells/mL in 30 mL of CD-DG44 media (Life Technologies, USA) containing 8 mM L-glutamine (Thermo Fisher Scientific, USA)) and 0.18% (v/v) pluronic F-68 (Thermo Fisher Scientific, USA) in a 125 mL Erlenmeyer flask with vented caps (Corning, USA). Flasks were incubated in a Certomat CT Plus incubator (Sartorius, DE) at 37˚C, 125 rpm, 5% CO_2 and 80% humidity. Cells were passaged every 3 days.

Stably transfected Clone 27 cells were cultivated in FDB-MAP (SAFC, USA) containing 8 mM L-glutamine and a selection pressure, Methotrexate (MTX) at 175 nM (Sigma aldrich, USA) or Puromycin at 10 µg/mL (Sigma Aldrich, USA). Stably transfected Clone 27 cell lines were maintained every 3-4 days. Tube spin vessel were also used with a working volume of 10 mL in 50 mL spin tubes bioreactor with vented caps (TPP, CH) and incubated in a Certomat CT Plus incubator (Sartorius, DE) at 37˚C, 200 rpm, 5% CO_2 and 80% humidity.

2.2.2. Adherent cell lines

2.2.2.1. Flp-In ™ CHO cells

Flp-In™ CHO cells are adherent cells commercially available from Thermo Fisher Scientific. The cells were maintained in DMEM media (Thermo Fisher Scientific, USA) complemented with 10% (v/v) Foetal Bovine Serum (Gibco, USA). Five mL of media was inoculated in T25 tissue culture flasks (Sarstedt, DE) and incubated in a MCO-200 Sanyo incubator (Sanyo, JP) at 37˚C, 5% CO_2.

2.2.3. Cell maintenance

2.2.3.1. Suspension cells

Culture viability and cell concentration were determined by processing a sample (0.6 to 1 mL) of the culture with a Vi-CELL cell counter (Beckman Coulter, USA). The cell suspension was diluted at the desired level in pre-warmed media and returned as soon as possible in the incubator under the conditions described in 2.2.1.

2.2.3.2. Adherent cells

Adherent cells were observed under a microscope to determine the level of confluency. When confluency reached 90-100%, media was removed and cells were washed with PBS. One mL of pre warmed 0.25% trypsin-EDTA (Thermo Fisher Scientific, USA) was added to the cells and the flask returned to the incubator for 5 min. After incubation, cells were dislodged by pipetting and 4 mL of pre warmed media was added to stop trypsin action. A few drops of the dislodged cell mixture were used to inoculate fresh media. If a precise cell number was required, a cell count was performed using a Vi-CELL before dilution to the desired concentration.

2.2.4. Antibiotic kill curve

2.2.4.1. University of Kent procedure

Kill curves were performed with different concentrations of hygromycin B (0, 100, 250, 500, 750 and 1000 µg/mL) and puromycin (0, 1, 2.5, 5, 7.5 and 10 µg/mL) with the CHO-S cell line. The cells were grown in 6-well plates at 1 x 10^5 viable cell/mL in a volume of 2 mL of CD-CHO media with 8 mM L-glutamine and the desired antibiotic concentration. Time points were taken at day 2, 4 and 7 for cell concentration and culture viability using a Vi-CELL instrument. The working concentrations arrived at from those experiments were 750 µg/mL for hygromycin B and 7.5 µg/mL for puromycin. Plates were incubated at 37˚C, 5% CO_2.

2.2.4.2. Fujifilm Diosynth Biotechnologies procedure

A kill curve was performed for puromycin (7.5, 10 and 15 µg/mL) with mpDG44/ADA 7 cell line. Cells were inoculated at 2 x 10^5 viable cells in 1 mL of FDB-MAP media containing 8 mM L-glutamine and the desired puromycin concentration in a 24 well plate. Plates were incubated at 37˚C, 10% CO_2 and 80% humidity. Culture viability and cell concentration were recorded after 5 days incubation using a Vi-CELL cell counter.

2.2.5. Stably expressing cell line generation

2.2.5.1. University of Kent procedure

After a culture viability check, 1 x 10^7 viable cells were pelleted at 200 *g* for 5 min and resuspended in 0.7 mL of CD-CHO with 8 mM L-glutamine, 20 µg of linearized DNA was added to the cells and the mixture was poured into a Gene Pulser® cuvette (Biorad, USA). Cells were electroporated using a Gene Pulser Xcell™ Electroporation system (Biorad, USA) with the following parameters; 300 V, 900 µF and 4 mm cuvettes. Electroporated cells were resuspended into 18 mL of media in a T75 tissue culture flask (Sarstedt, DE). Cuvettes were rinsed with 1.2 mL of media. After an overnight incubation at 37˚C, 5% CO_2, the selection pressure agent was added to obtain the desired concentration in a final volume of 25 mL.

2.2.5.2. Fujifilm Diosynth Biotechnologies procedure

After a culture viability check, 5 x 10^6 viable cells were centrifuged at 180 g for 10 min and resuspended in 100 µL of SF buffer provided in the SF Cell line 4D-Nucleofector™ X Kit L (Lonza, CH). The cells were placed into the nucleocuvettes and 8 µg of linearized DNA was added. The cells were electroporated using program FF-137 (parameters not communicated) of the 4D-Nucleofector™ System (Lonza, CH). Post-nucleofection, 400 µL of pre-warmed FDB-MAP containing 1 x HT supplement (Thermo Fisher Scientific, USA) and 8 mM L-glutamine were added into the cuvettes and they were incubated at 37˚C for 15 min. After incubation, 20 mL of pre-warmed FDB-MAP containing 1 x HT supplement and 8 mM L-glutamine in a T75 flask were inoculated with the transfected cells. The flasks were incubated at 37˚C, 10% CO_2 overnight. Next day, cells were centrifuged for 10 min at 180 g and the media was replaced by FDB-MAP media containing and 8 mM L-glutamine and the selection pressure agent (175 nM MTX or 7.5 µg/mL puromycin). Flasks were placed in the incubator for a recovery period of 2-3 weeks.

2.2.6. Transient transfection experiments

2.2.6.1. University of Kent procedures

2.2.6.1.1. Lipofectamine 2000

Lipofectamine 2000 (Invitrogen, USA) was used to transfect Flp-In cells. First, 500 µL of growth media in a 24-well plate were inoculated with 6 x 10^4 viable cells. The next day, 0.8 µg of DNA was diluted in 50uL Opti-MEM™ (Thermo Fisher Scientific, USA) and gently mixed while 2 µL of lipofectamine was added to 50 µL of Opti-MEM and incubated for 5 minutes at room temperature. After incubation, the diluted DNA and lipofectamine were

mixed gently together and incubated for 20 minutes at room temperature. To finish, 100 µL of the complexes were added to each well and the cells incubated at 37˚C, 5% CO_2 for 72 hours.

2.2.6.1.2. Novachoice

Prior to transfection, the desired vessels and media were inoculated at 1 x 10^6 viable cells/mL in 96-DWP or 0.5 x 10^6cells/mL in spin tubes. 1 µg/mL DNA was added to 0.1 times the total volume of media followed by 1 µL of Novachoice (Roche, CH) reagent and 0.5 µL of booster for every millilitre of media used. After a 20-min incubation step at room temperature, the mix was added to the freshly inoculated culture and the cells were incubated at desired parameters depending on the vessel used.

2.2.6.1.3. Electroporation

The protocol was similar to the stable cell line generation (see section 2.2.5.1) except the DNA concentration used was 40 µg (non-linearized) instead of 20 µg and the absence of selection pressure.

2.2.6.2. Fujifilm Diosynth Biotechnologies procedures

2.2.6.2.1. Novachoice

Prior to transfection, 10.8 mL of CD-DG44 media with 8 mM L-glutamine and 0.18% pluronic F-68 was inoculated at 1 x 10^6 viable cells/mL in spin tubes. 1 µg/mL DNA was added to 1.2 mL of CD-DG44 media with 8 mM L-glutamine followed by 12 µL of Novachoice (Roche, CH) reagent and 6 µL of booster before a 20-min incubation step at room temperature. After incubation, the mix was added to the freshly inoculated culture and the cells were incubated at 37˚C, 5% CO_2, 200 rpm for the amount of time needed.

2.2.6.2.2. Electroporation

The protocol was similar to the stable cell line generation (see section 2.2.5.2) except for the DNA concentration used (8 or 16 µg DNA) and the absence of selection pressure.

2.2.7. Limiting dilution cloning

Before starting, 96-well plates were filled with 100 µL of the adequate media except for the well A1 and stored at 37˚C. The day following stable transfection, cells were diluted to 2 x 10^4 viable cells/mL and 200 µL was placed into the well A1 of a 96-well plate. A series of 1:2 dilutions were undertaken through the column A of the plate. At the last well 100 µL was

discarded to have the same volume across the whole plate. With a multichannel pipette, 100 µL was added to the first column to give a total volume of 200 µL/well. Using 100 µL from the first column, a 1:2 dilution was performed in the second column and carried through the whole plate with the removal of 100 µL in the last column. The final volume of each well was made to 200 µL with pre-warmed media. After inoculating the plates, they were incubated for 2-3 weeks at 37˚C, 5% CO_2. Wells were constantly checked by microscopy to detect the formation of single colonies in wells. When the confluency was sufficient (around 70%) and monoclonality confirmed, wells containing single colonies were expanded into 24-well plates, 6-well plates, T-25 flasks, T-75 flasks and then spin tubes or 125 mL Erlenmeyer flasks. Figure 2.1 is a graphical explanation of the dilution across the 96 well plate.

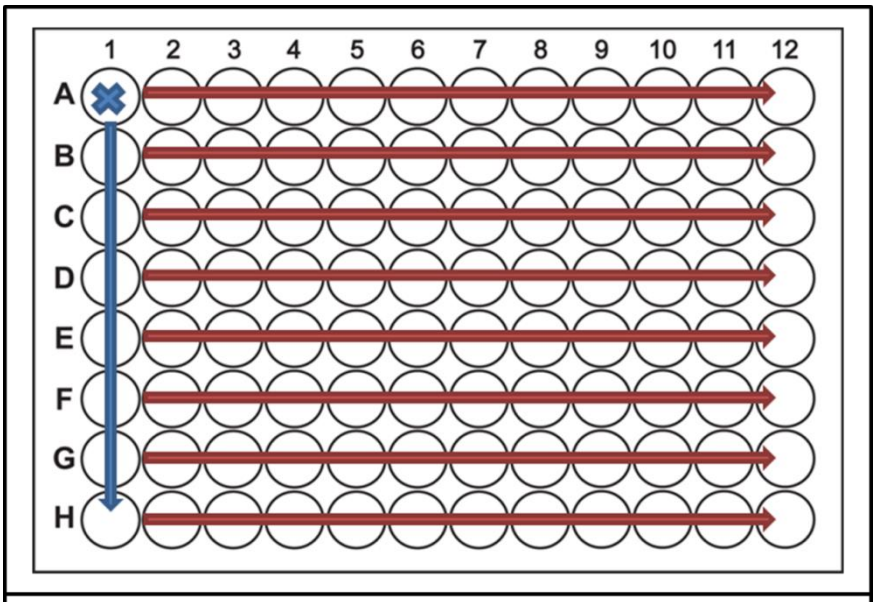

Figure 2.1. Graphical representation of the dilution performed for limiting dilution cloning in 96 well plates. First set of dilutions (represented by the blue arrow) starts in well A1 by the addition of 200 µL of cells at 2 x 10^4 viable cells/mL. A dilution of 1:2 is performed in the first column before making the volume to 200 µL. A second set of dilutions (represented by the red arrows) is a set of 1:2 dilutions across the plate.

2.2.8. Cell line revival after cryopreservation

2.2.8.1. University of Kent procedure

A cryovial was thaw gently in the water bath. The content of the vial was then transferred to a 50 mL tube and 40 mL of pre warmed CD-CHO media containing 8 mM L-glutamine was added drop by drop. Cells were centrifuged at 200 *g* for 5 min. The pellet was resuspended in 20 mL of fresh media and transferred to a 125 mL Erlenmeyer flask that was then incubated at 37˚C, 140 rpm.

2.2.8.2. Fujifilm Diosynth Biotechnologies procedure

A cryovial was thaw gently in the water bath. The content of the vial was resuspended in 20 mL of pre warmed CD-DG44 media containing 8 mM L-glutamine and 0.18% pluronic F-68 added drop by drop. A cell concentration and culture viability count was performed. Cells were diluted to a concentration of 0.2 x 10^6 viable cells/mL and incubated at 37˚C, 125 rpm, 5% CO_2 and 80% humidity.

2.2.9. Cryopreservation of cell lines

2.2.9.1. University of Kent procedure

After verification of the viability of the culture using a Vi-CELL instrument, 1 x 10^7 viable cells were centrifuged at 200 *g* for 5 min. The cells were resuspended in 1 mL of CD-CHO media containing 8 mM L-glutamine and 7.5% (v/v) DMSO (Sigma Aldrich, USA) and transferred to a CryoTube™ vial (Nunc, USA). Vials were kept overnight at -80˚C in a Nalgene Mr Frosty before being transferred into liquid nitrogen storage.

2.2.9.2. Fujifilm Diosynth Biotechnologies procedure

After verification of the culture viability using a Vi-CELL device, 1 x 10^7 viable cells were centrifuged at 180 *g* for 10 min. The cells were resuspended in 1.5 mL of FDB-MAP media containing 10% (v/v) DMSO (Sigma Aldrich, USA)) and transferred to a cryovial. Vials were kept overnight at -80˚C in a Nalgene Mr Frosty before being transferred into liquid nitrogen storage.

2.2.10. Mini-pool cell line generation procedure

After electroporation and addition of the selection pressure, 96-well plates were inoculated at 5000 cells/well. The plates were incubated at 37˚C, 10% CO_2 for 3 weeks. After 3 weeks, the confluency and monoclonality of the wells were evaluated by eye or using a Cell Metric® CLD plate reader (Solentim, UK) and 48 wells were selected. The content of the selected wells (200 µL) was transferred to a 24-well plate, and 800 µL of FDB-MAP containing 8 mM L-glutamine and 175 nM MTX added and incubated at 37˚C, 10% CO_2. After 5 days of growth, 200 µL of supernatant was sampled from each well to quantify the antibody concentration using the Octet instrument (see section 2.3.6). This quantification was used to rank the mini-pools and select 8 mini-pools to progress in T25 flasks containing 5 mL media and then in spin tubes containing 10 mL of media. The spin tubes were incubated at 37˚C, 200 rpm, 5% CO_2 and 80% humidity.

2.2.11. Fed-batch over grow or FOG cultures

250 mL flasks with vented caps were inoculated at 0.2 x 10^6 viable cells/mL in 60 mL FDB-MAP media containing 8 mM L-glutamine. The flasks were incubated at 37˚C, 125 rpm, 80% humidity and 5% CO_2. During the FOG the following parameters were monitored: cell concentration, culture viability, concentration of glucose, glutamine, glutamate, lactate and ammonium. Cell concentration and culture viability were monitored daily from day 2 using a Vi-CELL cell counter. Metabolite levels were evaluated daily from day 3 using a YSI 2950 metabolic analyser (YSI, USA). Every other day from day 4, 1 mL of culture was sampled, centrifuged 5 min at 1400 *g* and both pellet and supernatant were kept at -20˚C. Regarding the feed regime, the cultures was fed from day 2 with 2% (v/v) HyClone™ Cell Boost 7A (GE healthcare, USA) and 0.2% (v/v) HyClone™ Cell Boost 7B (GE healthcare, USA), 0.5% (v/v) 200 mM L-glutamine when the glutamine concentration was below 0.22 g/L. Glucose (Sigma Aldrich, USA) was added when the concentration dropped under 3 g/L. The volume of glucose added to the culture was calculated using the following formula:

$$Glucose\ feed\ volume\ (mL) = \frac{(4 - current\ glucose\ concentration(g/L))}{stock\ glucose\ concentration\ (g/L)} \times startingvolume\ (mL)$$

FOG experiments were stopped after 14 days of culture or when the viability of the culture dropped under 70%.

2.2.12. Tissue culture in 96 Deep Well Plates (DWP)

Deep well plate culture system was used to screen at a small scale numerous conditions in an environment mimicking flask culture. The deep well plate system is composed of 2 distinct parts, the single use 96-DWP plate and the reusable lid. The lid was composed of a stainless steel lid, blue microfiber filter inlay, green ePTFE filter inlay and a silicone seal to maintain the culture aerated and sterile as represented in Figure 2.2B. Lids were assembled, autoclave and dried before use. 96 deep well plates were inoculated at the desired cell concentration before the lid was placed on top and clamped into position. Plates were incubated at 37˚C, 90% humidity, 5% CO_2 and 375 rpm.

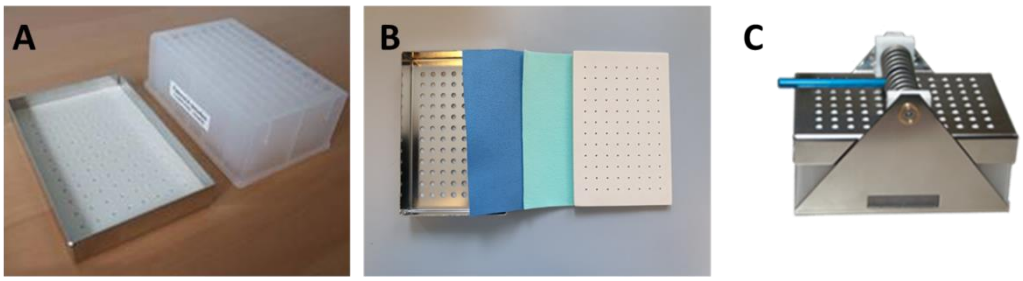

Figure 2.2. Equipment for 96-DWP tissue culture. **A**, image of a 96-DWP and its assembled lid. **B**, Image of the different layers of the lid, from left to right: stainless steel lid, blue microfiber filter inlay, green ePTFE filter inlay and a silicone seal. **C**, Image of a 96-DWP with lid in its holder.

2.3. Protein analysis

2.3.1. Total protein extraction from cell pellets

A known number of cells (generally between 1 and 2 x 10^6 viable cells/mL) was centrifuged at 1500 *g* for 5 min and the supernatant discarded. For each 1 x 10^6 cell pellet, 100 µL of extraction buffer (20 mM Hepes pH 7.2, 100 mM NaCl, 1% Triton X-100, 10 mM β-glycerophosphate, 1mM Na_3VO_4, 50 mM NaF and a tablet of cOmplete™ mini EDTA-free Protease Inhibitor cocktail (Roche, CH) for every 10 mL of buffer) was added to the cells. After incubation for 30 min on ice, the extract was centrifuged at 17000 *g* for 5 minutes in order to pellet all the cell debris. The protein extract was kept at -20˚C or -80˚C for longer periods.

2.3.2. SDS-PAGE

2.3.2.1. Sample preparation procedure

To prepare the samples, 5 x sample buffer (10% (v/v) glycerol, 120 mM Tris-HCl pH 6.8, 2% (w/v) SDS, few grains of bromophenol bleu, few grains of pyronin G and 4% (v/v) β-mercaptoethanol if reducing buffer) was added to the desired amount of protein lysate diluted in distilled water to a 1 x final buffer concentration. Samples were vortex thoroughly, boiled for 5 min at 95˚C and loaded into the polyacrylamide gels or stored at -20˚C.

2.3.2.2. Gel preparation and electrophoresis

Sodium dodecyl sulphate polyacrylamide gels (SDS-PAGE) were composed of two phases, the stack (5% acrylamide; 5% (v/v) acrylamide/Bis solution 37.5:1 (Biorad, USA), 125 mM Tris-HCl pH 6.8, 1% (w/v) SDS, 1% (w/v) Ammonium persulfate, 0.1% TEMED) and the separating phase between 8 and 12% acrylamide (8-12% (v/v) acrylamide/Bis solution 37.5:1 (Biorad, USA), 375 mM Tris-HCl pH 8.8, 1% (w/v) SDS, 1% (w/v) ammonium persulfate, 0.06% TEMED) set in a Novex cassette (Life Technologies, USA). After loading of the samples on the gels, electrophoresis were performed in running buffer (200 mM glycine, 25 mM Tris-HCl, 0.1% (w/v) SDS, pH 8.8) at 100 V for 30 min and then at 150 V until desired migration.

2.3.3. Western blot analysis

After SDS-PAGE, the polyacrylamide gel was inserted in between 2 sheets of 3 mm CHR Whatman paper (GE healthcare, USA) in direct contact with an Amersham Protran 0.45 NC nitrocellulose membrane (GE healthcare, USA). The stack was inserted in a cassette fitting in a transfer tank. Transfer of the proteins from the gel to the nitrocellulose membrane was performed in transfer buffer (100 mM glycine, 12.5 mM Tris-HCl, 0.1% (w/v) SDS, 20% (v/v) methanol) at 4˚C for 1 hour at 750 mA. Non-specific interactions were blocked by incubating the membrane in a 5% (w/v) solution of marvel milk for 30 min. Two washes with 0.1% TBST buffer (150 mM NaCl, 2.5 mM KCl, 25 mM Tris-HCl, 0.1% (v/v) tween20, pH 7.6) were performed before incubating the membrane with a solution containing the primary antibody of choice (diluted antibody, 150 mM NaCl, 2.5 mM KCl, 25 mM Tris-HCl, 0.1% (v/v) tween20, pH7.6, 3% (w/v) bovine serum albumin (Sigma Aldrich, USA)) at 4˚C overnight on a rocking table. All sources and dilutions for the antibodies used in this project are reported in Table 2.1. The following day, the membrane was washed 4 times with 0.1% TBST for 10 min with agitation. Once the washes were finished, the membrane was incubated for 1 hour at room temperature with a 5% (w/v) marvel milk solution containing a secondary antibody coupled to Horseradish peroxidase. Four new washes with 0.1% TBST for 10 minutes were then performed. To detect signal, the membrane was incubated for 1 min with 2 mL of Pierce™ ECL substrate (Thermo Fisher Scientific, USA) before exposing it to an Amersham Hyperfilm ECL film (GE Healthcare, USA) and developing using a Optimax 2010 developer (PROTEC GmbH & Co, DE).

Table 2.1. List of the antibodies used and sources for western blot analysis during this work.

Name	Type	Dilution	target	coupled	specie	origin
Anti-GFP	Primary	1:5000	GFP	/	mouse	CRUK
Anti-β-actin	Primary	1:5000	β-actin	/	mouse	Sigma
Anti-α-tubulin	Primary	1:5000	α-tubulin	/	mouse	Sigma
Anti-SNAP29	Primary	1:1000	SNAP29	/	mouse	Santa Cruz Biotechnologies
Anti-STX18	Primary	1:1000	STX18	/	mouse	Santa Cruz Biotechnologies
Anti-STX7	Primary	1:1000	STX7	/	mouse	Santa Cruz Biotechnologies
Anti-Heavy chain	Primairy	1:10000	Human IgG (γ-chain specific)	/	rabbit	Sigma
Anti-rabbit	Secondary	1:1000	Rabbit IgG	Horseradish peroxidase	goat	Sigma
Anti-mouse	Secondary	1:1000	Mouse IgG	Horseradish peroxidase	goat	Sigma

2.3.4. Densitometry

Densitometry using ImageJ (NIH, USA) was undertaken to evaluate target protein expression in cell lines. After western blot analysis, signals obtained for protein of interest were analysed and compared to the house keeping protein β-actin which was used to normalise the level of signal and define the relative level of expression of the protein of interest in each sample.

2.3.5. Flow cytometry

Fluorescent profiles were recorded using a BD FACSJazz flow cytometer. For analysis, 2 x 10^6 viable cells were harvested at 200 *g* for 5 min and resuspended in 1 x phosphate buffered saline buffer before processing on the flow cytometer. Cell line profiles were obtained by recording of 10000 events (cells). All the results were analysed using the BD FACS Software.

2.3.6. Bradford assay

To determine the protein concentration of samples, 1 mL of Bradford reagent (120 mM Coomassie Blue G250, 15% (v/v) ethanol, 8.5% (v/v) phosphoric acid) was added to 50 µL of sample (diluted or not). The mixture was incubated 10 min at room temperature before using a calibrated spectrophotometer to determine the absorbance at 595 nm. A standard curve of known bovine serum albumin amounts was used to determine the concentration of unknown protein samples.

2.3.7. Octet measurements

Protein samples were centrifuged at 1400 *g* for 5 min and 200 µL of sample (diluted or not) was placed into a 96-well plate. The columns 11 and 12 were reserved for media (used during the experiment) and the regeneration buffer (10 mM glycine pH 1) respectively. Before measurement, the Dip and Read ™ Protein A biosensors (PALL FortéBio, USA) were

soaked in media for 10 minutes. Titre measurements were done using a Octet® QK^e system and the results analysed using the Octet Qke system analysis (version 9.0) with a 5PL unweighted curve fitting curve.

2.3.8. Cellometer analysis

The cellometer vision CBA commercialised by Nexcelom bioscience is an imager used to determine cell density and viability but also carry out fluorescence measurements. This device had been used to measure GFP levels in cell sample and obtained transfection efficiency data. To do so, 20 µL of cell culture was inserted in one chamber of a SD100 slide. This slide was then inserted into the cellometer for GFP measurement.

2.4. Microscopy techniques

2.4.1. Coverslip treatment with poly-L-lysine

Round glass coverslips were inserted in a 24-well plate and covered with 0.01% poly-L-Lysine w/v in sterile water (Sigma Aldrich, USA). After a 20 min incubation at room temperature, wells containing the coverslip were rinsed 3 times with sterile water and air dried before use.

2.4.2. Cell culture for microscopy

For microscopic studies, the culture of cells was required to be in a specific manner. The concentration of cells should be low to avoid cells growing over each other, but also not too low so as to have cells to observe and have a representative view. As such, cells were inoculated at 4 x 10^5 viable cells/mL for 2 days at 37˚C and 5% CO_2.

2.4.3. Coverslip preparation

After growing the cells on coverslips, the culture media was aspirated and a PBS wash was performed. The cells were fixed by incubating 1 mL of pre-warmed 4% (w/v) paraformaldehyde diluted in PBS solution for 20 min at room temperature. Following incubation, the paraformaldehyde solution was discarded and 3 PBS solution washes were undertaken. The coverslips were then mounted on slides using 10 µL 10% phenylenediamine w/v (Sigma Aldrich, USA) diluted in Mowiol 4-88 (Harco, UK) and left overnight at 4˚C to dry in the dark. The next day, the edges of the coverslips were sealed using nail varnish to prevent drying and oxidation.

2.5. Statistical analysis

Two statistical tests were used in this study, one way ANOVA and a student t-test. When comparing more than 2 means, one way ANOVA was performed followed by a post-hoc Tukey analysis with a confidence interval of 95% considered as significant. The means sharing a letter do not have a statistical difference. For comparison of two means, a student t-test was performed, rejecting the null hypothesis if a p-value <0.05 was obtained.

CHAPTER 3: Molecular Cloning of Target SNARE Proteins and Subsequent SNARE CHO Cell Line Engineering

3.1. Introduction

As outlined in the introduction section of this thesis, in the biopharma industry mammalian cells (e.g. HEK, VERO, and NS0) are commonly used for the production of biotherapeutic recombinant proteins, however one cell line predominates, the Chinese hamster ovary (CHO) cell line. CHO cell lines are the workhorse of industry for the production of biotherapeutic proteins with over 30% of approved products produced in CHO derived cell lines (Walsh 2014). Since their first isolation and description in 1956 (Puck 1958), CHO cells have been continuously studied and optimised for protein production (specifically production of post-translationally modified proteins at a commercial scale for use in humans) over the years (Wurm 2004) to give specific productivities (the amount of protein made per cell) of up to 90 pg/cell/day and viable cell concentrations of 10 x 10^6 cells/mL and beyond for extended periods of time in fed-batch culture mode. Cell culture process and media optimisation have been part of the reason for the improvements in cell growth, increased viable cell numbers and increased cell specific productivity and culture yields (referred to as titre) but will not be discussed in detail here. Cell line engineering has, for the last 20 or more years, been an important consideration and approach for the improvement of CHO cells with regard to all the different major attributes studied for improvement. These include manipulation of the glycosylation pattern (Amann et al. 2018), cell metabolism (Pereira, Kildegaard, and Andersen 2018) and apoptosis engineering (Lee et al. 2009). The work described in this thesis is focused on the engineering of the secretory pathway of the cell, a pathway that encompasses co-translational polypeptide synthesis into the ER, folding, assembly, post-translational modification and secretion of secreted proteins.

Several approaches have been reported on the manipulation of the secretory pathway in CHO cells with the aim of enhancing its protein folding, assembly and secretory capacity, such as; (i) the amelioration of the translocation of the polypeptide into the ER through manipulation of the peptide signal sequence (Kober et al. 2013) and (ii) signal recognition

particle (SRP) elements (Le Fourn et al. 2014), (iii) overexpression of chaperones within the ER (Borth et al. 2005; Chung et al. 2004), (iv) engineering of the unfolded protein response (UPR, Tigges and Fussenegger 2006) and (v) engineering of vesicle trafficking and formation (Peng et al. 2011; Peng and Fussenegger 2009). This last strategy, engineering of vesicle trafficking and formation, is probably the least explored of these different areas and was the main approach investigated in this project. With regard to vesicle formation and targeting, the SNARE family is a potential target area for manipulation with members of this family being involved in vesicle sorting and formation. Moreover, studies have successfully reported the manipulations of a small number of SNARE proteins in CHO cells to deliver an increase in recombinant protein production (Peng, Guetg, Tigges, et al. 2010; Peng and Fussenegger 2009).

To study the effect(s) of manipulation of a gene of interest (and hence the functional protein), two approaches have been widely used over the years; overexpressing or knocking down/out of the gene of interest (Fischer et al. 2015). Genomic knockout is used to delete the effect of disadvantageous genes or to determine the impact of unknown gene function using a range of techniques mainly involving designer nucleases such as CRISPR/cas9 (Grav et al. 2015). Knockdown approaches can also be used (e.g. siRNAs) where gene silencing may be lethal. On the other hand, overexpression is used to increase the beneficial effect of an existing gene, change the balance of gene expression, alleviate potential bottlenecks or to introduce the effect of an ectopic gene. With specific regard to the SNARE proteins, these have essential roles in vesicle trafficking and fusion so an overexpression strategy was used in this study.

This chapter is focused on describing all the experiments undertaken to obtain monoclonal CHO cell populations overexpressing specific SNARE proteins. Firstly, all the processes for the generation of mammalian expression vectors for the SNARE proteins fused with an eGFP tag are described. Expression analysis was then carried out for the proteins of interest before proceeding to the generation of stably expressing CHO cell lines. Once the expression of the protein of interest in the different cell lines was confirmed, monoclonal populations were derived from the stably expressing cell lines. To finish, monoclonal populations were selected with regards to target SNARE protein expression and the stability of the expression in the cell lines. The overall result was the generation of CHO-S monoclonal cell lines stably expressing SNARE proteins for further characterisation and application to recombinant protein production.

3.2. Generation of mammalian expression vectors for the expression of the SNARE genes of interest

3.2.1. VAMP expressing vectors

From a survey of the literature (Aoyagi et al. 2016; Cocucci et al. 2008; Mallard et al. 2002; Nozawa et al. 2017; Oishi et al. 2006; Peng et al. 2011; Tran, Zeng, and Hong 2007), 4 VAMP proteins, VAMP3, VAMP4, VAMP7 and VAMP8, were judged to potentially have a significant impact on the capacity/efficiency of the secretory pathway (see section 1.6 and 3.5). For the different selected VAMP proteins, plasmids containing the Human encoding gene were obtained from Addgene; pEGFP-VAMP3 (plasmid #42310), pEGFP-VAMP4 (plasmid #42313), pEGFP-VAMP7 (plasmid #42316) and pEGFP-VAMP8 (plasmid #42311), having been deposited in the collection by Thierry Galli. The different genes were all provided in the pEGFP-C3 plasmid which is a mammalian expression vector using neomycin or G418 as a selection marker. The different genes were fused to an eGFP gene to express a fused protein with an eGFP tag in the N-terminal position. As neomycin or G418 can result in poor selection with the CHO-S host cell line used in this study and can result in unstable integration (data not shown), it was decided to subclone the eGFP-VAMP fusions into a new mammalian expression vector, the commercially available pcDNA3.1/Hygro(+) vector which has a hygromycin B selection gene for the selection of stably expressing cells.

To generate the pcDNA3.1Hygro/VAMP3 construct, the coding sequence for VAMP3 fused to an eGFP tag was digested from the original pEGFP-VAMP3 using XbaI and NheI restriction enzymes. After digestion, two bands were obtained at the respective size of 1173 bp and 3920 bp as determined by agarose gel electrophoresis analysis (Figure 3.1A). The lower band containing the fragment of interest was excised from the gel and purified before being ligated into the pcDNA3.1/Hygro(+) backbone previously digested with XbaI and NheI. Ligation was successful using a 3:1 ratio (insert:vector) and several colonies obtained were used to extract DNA after cultivation overnight at 37^{o}C in 5 mL LB media with 100 µg/mL ampicillin. From analytical digestion with XbaI and NheI, two fragments at 1173 bp and 5501 bp were expected for successful ligations, one colony showed the required DNA pattern (Figure 3.1B). The region containing VAMP3 and the eGFP gene was then sequenced to check for any anomalies in the sequence, such as point mutations, and was found to be correct.

The pcDNA3.1Hygro/VAMP4 construct was generated by digesting the sequence containing the fused protein from pEGFP-VAMP4 using BamHI and NheI restriction enzymes. Two bands were obtained at the respective size of 1198 bp and 3932 bp by agarose gel electrophoresis analysis (Figure 3.1C). The smaller band, containing the gene of interest, was extracted from the agarose gel, purified and ligated into the pcDNA3.1/Hygro(+) vector previously digested with BamHI and NheI. Ligation was successful using a 3:1 ratio (insert: vector) and several of the resulting colonies were used to extract DNA after growth overnight at 37^{o}C in 5 mL LB media with 100 µg/mL ampicillin. One colony showed the required DNA pattern as determined by agarose gel electrophoresis analysis, with two bands expected at 1198 bp and 5563 bp after analytical digestion with BamHI and NheI (Figure 3.1D). The region containing VAMP4 and the eGFP gene was confirmed as correct by sequence analysis.

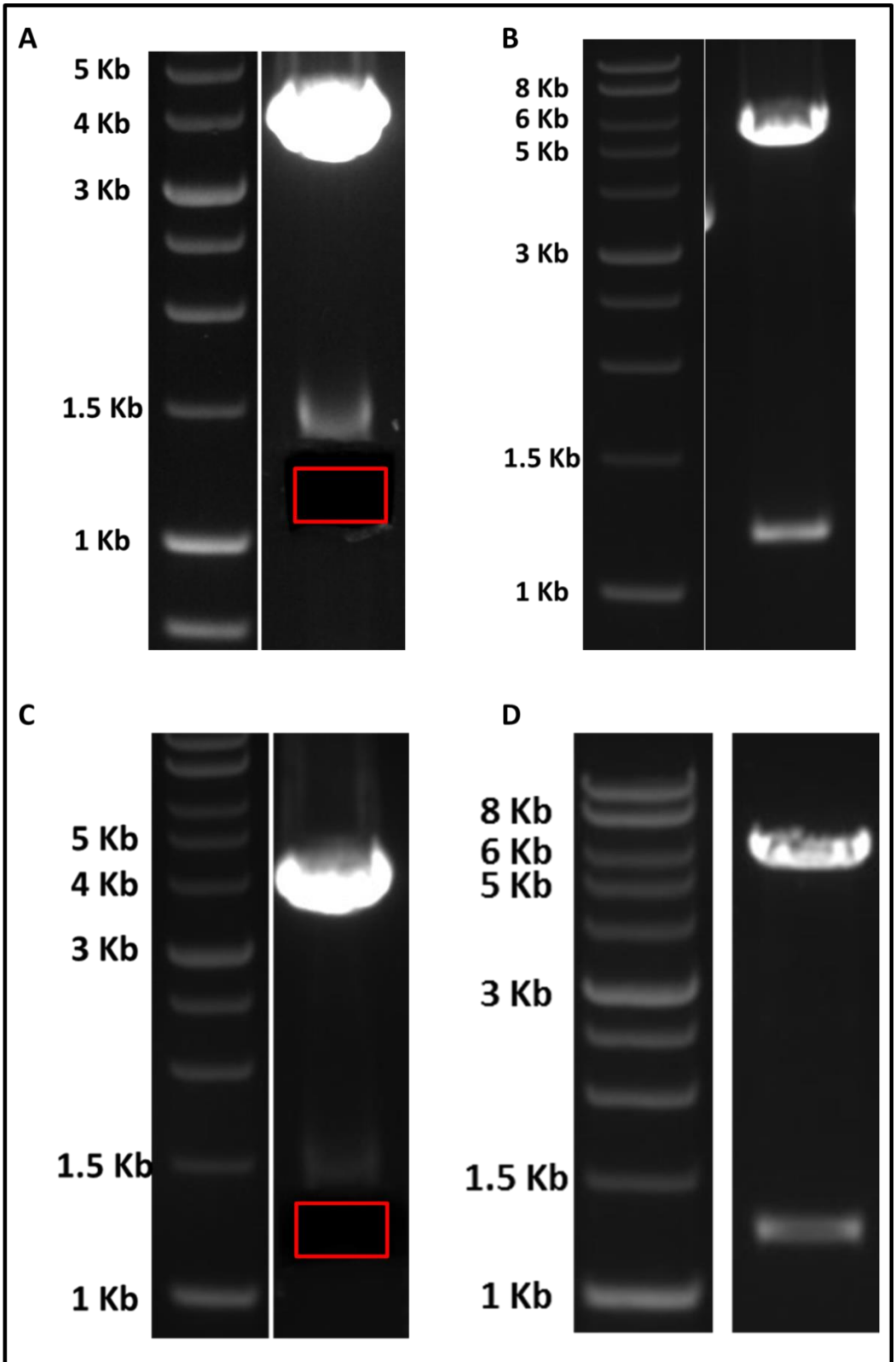

Figure 3.1. Agarose gel electrophoresis analysis of digested DNA. **A**, Digestion of pEGFP-VAMP3 with XbaI and NheI expecting bands at 1173 bp and 3920 bp. **B**, Successful analytical digest of pcDNA3.1Hygro/VAMP3 using XbaI and NheI with bands expected at 1173 bp and 5501 bp. **C**, Digestion of pEGFP-VAMP4 using BamHI and NheI obtaining expected bands at 1198 bp and 3932 bp. **D**, Successful test digest of pcDNA3.1Hygro/VAMP4 using BamHI and NheI with expected bands at 1198 bp and 5563 bp. Red squares outline excised bands for ligation.

The pcDNA3.1Hygro/VAMP7 construct was created in a similar manner to the pcDNA3.1Hygro/VAMP4 construct in that the original pEGFP-VAMP7 construct was digested using BamHI and NheI restriction enzymes generating two fragments of 3932 bp and 1437 bp in size. The smaller band carrying the region of interest was excised, purified and ligated into the pcDNA3.1/Hygro(+) vector co-digested with the same restriction enzymes. Ligation was successful using a 3:1 ratio (insert: vector) and several colonies obtained were used to extract DNA after cultivation overnight at 37^{o}C in 5 mL LB media with 100 μg/mL ampicillin. When performing a test digest with HindIII and SmaI, two fragments of 1828 bp and 5172 bp were anticipated for a successful ligation. One colony showed the desired pattern after digestion (Figure 3.2A). To confirm the success of the ligation, the region containing VAMP7 and the eGFP gene was sequenced.

The generation of the pcDNA3.1Hygro/VAMP8 construct was more technical due to the potential presence of methylation at the XbaI site used for digestion. To prevent the potential methylation, the bacterial strain used for transformation and DNA amplification was changed from a DH5α *E. coli* strain to a SCS110 *E. coli* strain. The SCS110 strain is lacking the genes *dam* (DNA adenine methylase) and *dcm* (DNA cytosine methyltransferase), two essential genes for DNA methylation in *E. coli*. Once demethylated pEGFP-VAMP8 was obtained, digestion was performed using NheI and XbaI restriction enzymes. Two fragments of 1166 bp and 3920 bp were observed after agarose gel electrophoresis analysis (Figure 3.2B). The smaller, required fragment was extracted, purified and ligated with the pcDNA3.1/Hygro backbone digested with the XbaI and NheI restriction enzymes. Ligation was successful using a 3:1 ratio (insert: vector) and several colonies obtained were used to extract DNA after cultivation overnight at 37^{o}C in 5 mL LB media with 100 μg/mL ampicillin. When performing a test digest with the SmaI restriction enzyme, two fragments of 1309 bp and 5358 bp were expected. One colony demonstrated the banding pattern indicative of successful ligation (Figure 3.2C). To confirm the success of the ligation, the region containing VAMP7 and the eGFP gene was sequenced.

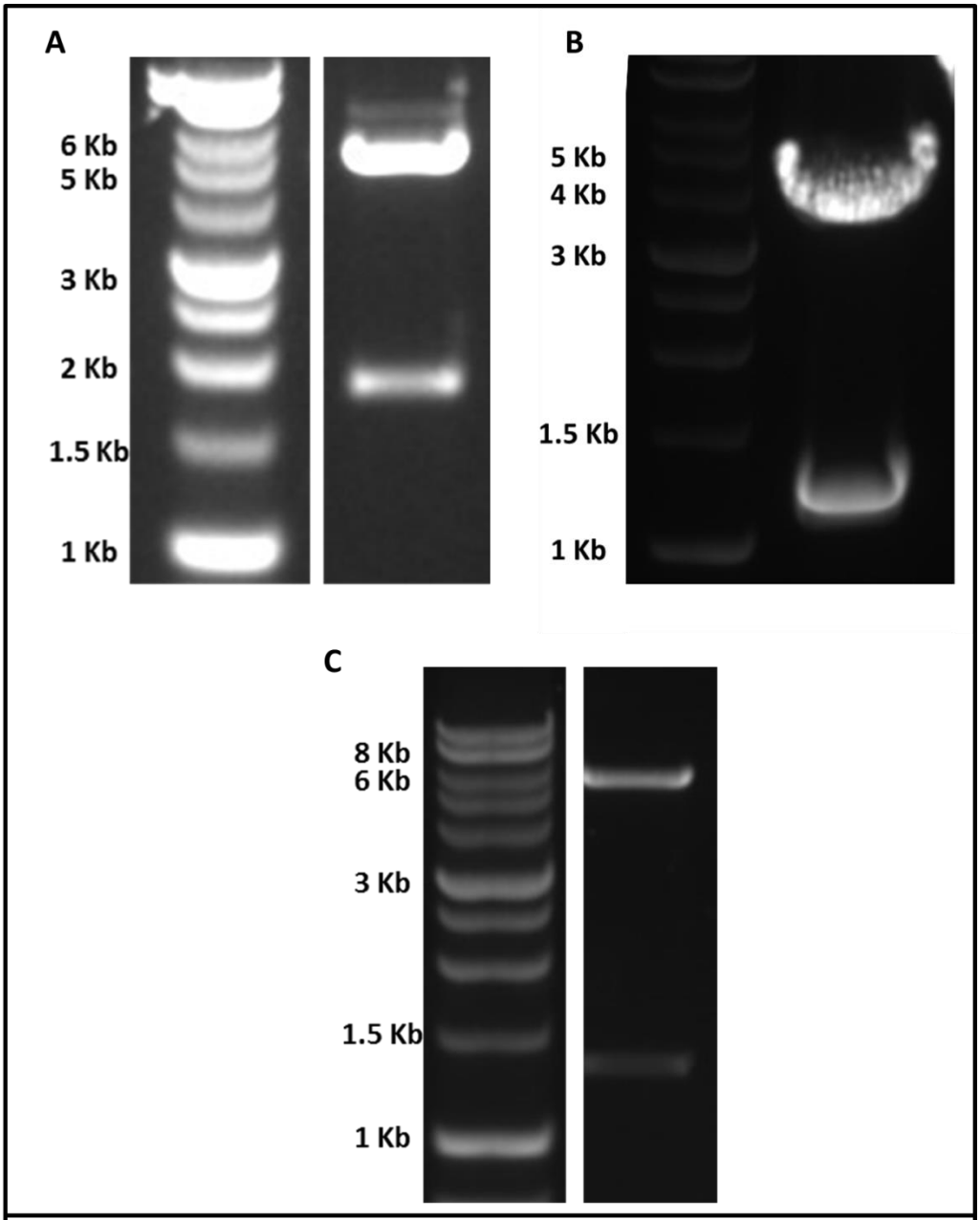

Figure 3.2. Agarose gel electrophoresis analysis of digested DNA. **A**, Successful test digest of pcDNA3.1Hygro/VAMP7 using SmaI with expected bands at 1828 bp and 5172 bp. **B**, Digestion of pEGFP-VAMP8 after demethylation using NheI and XbaI with expected bands at 1166 bp and 3920 bp. **C**, Successful analytical digest of pcDNA3.1Hygro/VAMP8 using SmaI obtaining expected bands at 1309 bp and 5358 bp.

To be able to distinguish any effect upon transfection of the constructs into CHO-S host cells specific to the vector or the eGFP tag (i.e. not due to the presence of the target SNARE gene but due to other sequences in the vector), a control pcDNA3.1Hygro/GFP construct was generated. To achieve this, eGFP was excised from a donor vector (a gift from Tulshi Patel) using HindIII and BamHI restriction enzymes to result in the release of a 738 bp band containing the eGFP gene and 5505 bp band from the remainder of the vector. The

fragment containing the eGFP gene was excised, purified and ligated into the pcDNA3.1/Hygro(+) backbone digested with the same enzymes. Ligation was successful using a 3:1 ratio (insert: vector) and several colonies obtained were used to extract DNA after cultivation overnight at 37^{o}C in 5 mL LB media with 100 µg/mL ampicillin. An analytical digest on a successful clone using BamHI and HindIII restriction enzymes was performed, resulting in the generation of two bands at 738 bp and 5579 bp of size as expected (Figure 3.3A). Sequencing of the eGFP region was also undertaken to confirm the presence of the correct nucleotide sequence.

Once all the described vectors were generated, the plasmids were amplified by growth of transformed DH5α competent *E.coli* cells and then 250 mL of LB media containing 100 µg/mL ampicillin were inoculated for each constructs and large stocks of DNA generated using the HiSpeed Plasmid Maxi kit in preparation for future experiments. Appendix 2 presents the different vector maps for each of the newly generated plasmids which are summarised in Table 3.1.

Table 3.1. List of vectors described in Chapter 3.

Name	Backbone	Gene of interest	Tag	restriction sites used for cloning	Mammalian selection	Origin
pcDNA3.1/Hygro(+)	/	/	/	/	Hygromycin B	Thermo Fisher
pEGFP-VAMP3	pEGFP-C3	VAMP3	N-term fused eGFP	XbaI/NheI	Hygromycin B	Addgene, plasmid #42310
pEGFP-VAMP4	pEGFP-C3	VAMP4	N-term fused eGFP	BamHI/NheI	Hygromycin B	Addgene, plasmid #42313
pEGFP-VAMP7	pEGFP-C3	VAMP7	N-term fused eGFP	BamHI/NheI	Hygromycin B	Addgene, plasmid #42316
pEGFP-VAMP8	pEGFP-C3	VAMP8	N-term fused eGFP	XbaI/NheI	Hygromycin B	Addgene, plasmid #42311
pcDNA3.1Hygro/VAMP3	pcDNA3.1/Hygro(+)	VAMP3	N-term fused eGFP	XbaI/NheI	Hygromycin B	This work
pcDNA3.1Hygro/VAMP4	pcDNA3.1/Hygro(+)	VAMP4	N-term fused eGFP	BamHI/NheI	Hygromycin B	This work
pcDNA3.1Hygro/VAMP7	pcDNA3.1/Hygro(+)	VAMP7	N-term fused eGFP	BamHI/NheI	Hygromycin B	This work
pcDNA3.1Hygro/VAMP8	pcDNA3.1/Hygro(+)	VAMP8	N-term fused eGFP	XbaI/NheI	Hygromycin B	This work
pcDNA3.1Hygro/GFP	pcDNA3.1/Hygro(+)	eGFP		HindIII/BamHI	Hygromycin B	This work
pMRXIP-STX7	pMRXIP GFP-Ci2	STX7	N-term fused eGFP	/	Puromycin	Addgene, plasmid #45921
pMRXIP-STX17	pMRXIP GFP-Ci2	STX17	N-term fused eGFP	/	Puromycin	Addgene, plasmid #45909
pMRXIP-STX18	pMRXIP GFP-Ci2	STX18	N-term fused eGFP	/	Puromycin	Addgene, plasmid #45918
pMRXIP-SNAP29	pMRXIP GFP-Ci2	SNAP29	N-term fused eGFP	/	Puromycin	Addgene, plasmid #45923
pMRXIP-GFP	pMRXIP GFP-Ci2	eGFP		BamHI	Puromycin	This work

3.2.2. Syntaxin (STX) and SNAP expressing vectors

As described for the VAMP proteins in section 3.2.1, a literature research was performed to identify appropriate genes/proteins to target and 3 syntaxin and one SNAP proteins were selected as candidates for the project, STX7, STX17, STX18 and SNAP29 (Arasaki et al. 2015; Gordon et al. 2010; Ward et al. 2000)(see section 1.6 and 3.5). Plasmids containing the human sequence of the selected four genes were procured from Addgene, pMRXIP-STX7 (plasmid #45921), pMRXIP-STX17 (plasmid #45909), pMRXIP-STX18 (plasmid #45918) and pMRXIP-SNAP29 (plasmid #45923), these being deposited in the collection by Noboru Mizushima. All the genes of interest were fused with an N-terminal eGFP gene to give a fused protein with a eGFP tag in the N-terminal position. The different plasmids obtained

from Addgene were not modified and used as provided. The pMRXIP GFP-Ci2 backbone plasmid into which these gene sequences had been cloned is a mammalian expression vector with a puromycin selection marker. Having a different selection marker from the VAMP expressing vector was convenient to allow the potential generation of STX/SNAP and VAMP co-expressing stable cell lines.

Nonetheless, it was necessary to generate a control vector to determine any effect of the backbone or the eGFP tag in subsequent experiments on the CHO cell. To do so, a vector only expressing eGFP, pMRXIP-GFP, was generated in this backbone by removing the gene coding for STX17 in the pMRXIP-STX17 plasmid. To do this, pMRXIP-STX17 was digested using the BamHI restriction enzyme and two bands at 918 bp and 6815 bp were obtained. The larger band was extracted (Figure 3.3B), purified and re-ligated to itself to generate pMRXIP-GFP. After successful ligation, several colonies were used to extract DNA after cultivation overnight at 37^{o}C in 5 mL LB media with 100 µg/mL ampicillin. After analytical digestion with BamHI, a unique fragment at 6815 bp was expected. One colony showed the desired banding pattern (Figure 3.3C).

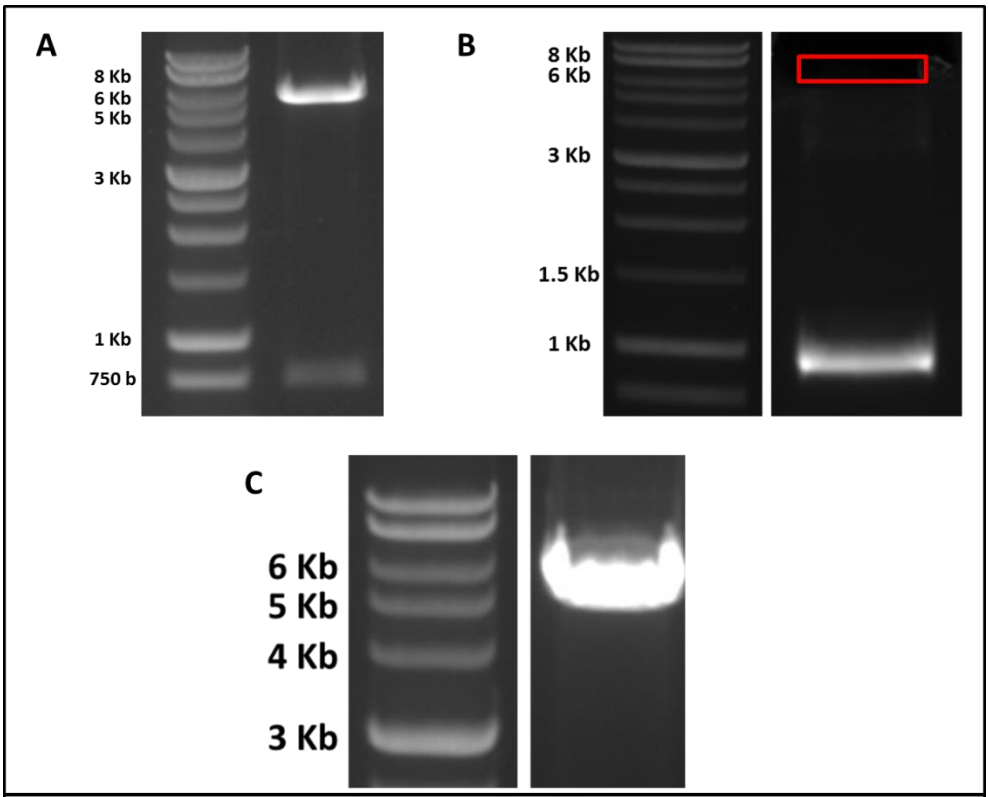

Figure 3.3. Agarose gel electrophoresis analysis of DNA digestion. **A**, Successful test digest of pcDNA3.1Hygro/GFP using BamHI and HindIII with expected bands at 5579 bp and 738 bp. **B**, Digestion of pMRXIP-STX17 using BamHI with expected bands at 6815 bp and 918 bp. Red squares signals the position of the extracted band. **C**, Successful analytical digest of pMRXIP-GFP using BamHI with one expected band at 6815 bp. Red square indicates excised band.

Subsequent to the generation of the control vector, the constructs were bulked up by inoculation of 250 mL of LB media with 100 µg/mL ampicillin with DH5α transformed cells. DNA was extracted and purified from the culture using the HiSpeed Plasmid Maxi kit for later use.

3.3. Generation of stably expressing CHO-S cell lines

3.3.1. Initial confirmation of expression of the eGFP tag of the fused proteins

To simplify the study and detection of the different proteins of interest, vectors expressing fused proteins with eGFP at the N-terminal had been generated. eGFP is a fluorescent protein of 26.9 kDa widely used in biology. It has the advantage of its visualization being non-invasive making it a powerful tool for observation *in vivo*. Despite this, some precautions need to be considered in using this as a tag to follow expression of the tagged protein of interest (in this case the STXs and VAMPs). eGFP, like every other protein, needs to be properly folded to maintain its fluorescence activity. The fusion with membrane proteins having high structural restraints and the presence of a linker could possibly cause the misfolding of the eGFP tag. Further, the presence of eGFP alone does not confirm the presence of the target gene as it is possible that the eGFP could be cleaved from the target protein which is then degraded whilst the eGFP remains. It was therefore necessary to confirm the presence of both the eGFP and the fusion protein at the appropriate size before undertaking studies with such constructs.

To determine if the fused proteins generated maintained their fluorescent signal, a transient transfection of commercially available, adherent CHO Flp-In cells was performed with the different vectors generated in section 3.2 above. 24-well tissue culture plates were inoculated with CHO Flp-In cells at 1.2 x 10^5 viable cells/mL and transfected using Lipofectamine 2000 (see protocol 2.2.6.1.1) and 0.8 µg DNA. After 72 h of incubation, cells were observed using a Leica MZFL III microscope and a Leica CD300F camera to detect the presence of eGFP expression. Figure 3.4 shows the results obtained from this transient transfection experiment. For all the constructs, a fluorescence signal was detected demonstrating that the eGFP was present and properly folded. Differences in the intensity of fluorescence were observed with a notably low signal with the pcDNA3.1Hygro/VAMP7 and pMRXIP-STX18 constructs which may suggest low expression of these compared to the

other constructs. This experiment successfully showed that the eGFP tag was properly processed in the ER and fluorescence was detectable.

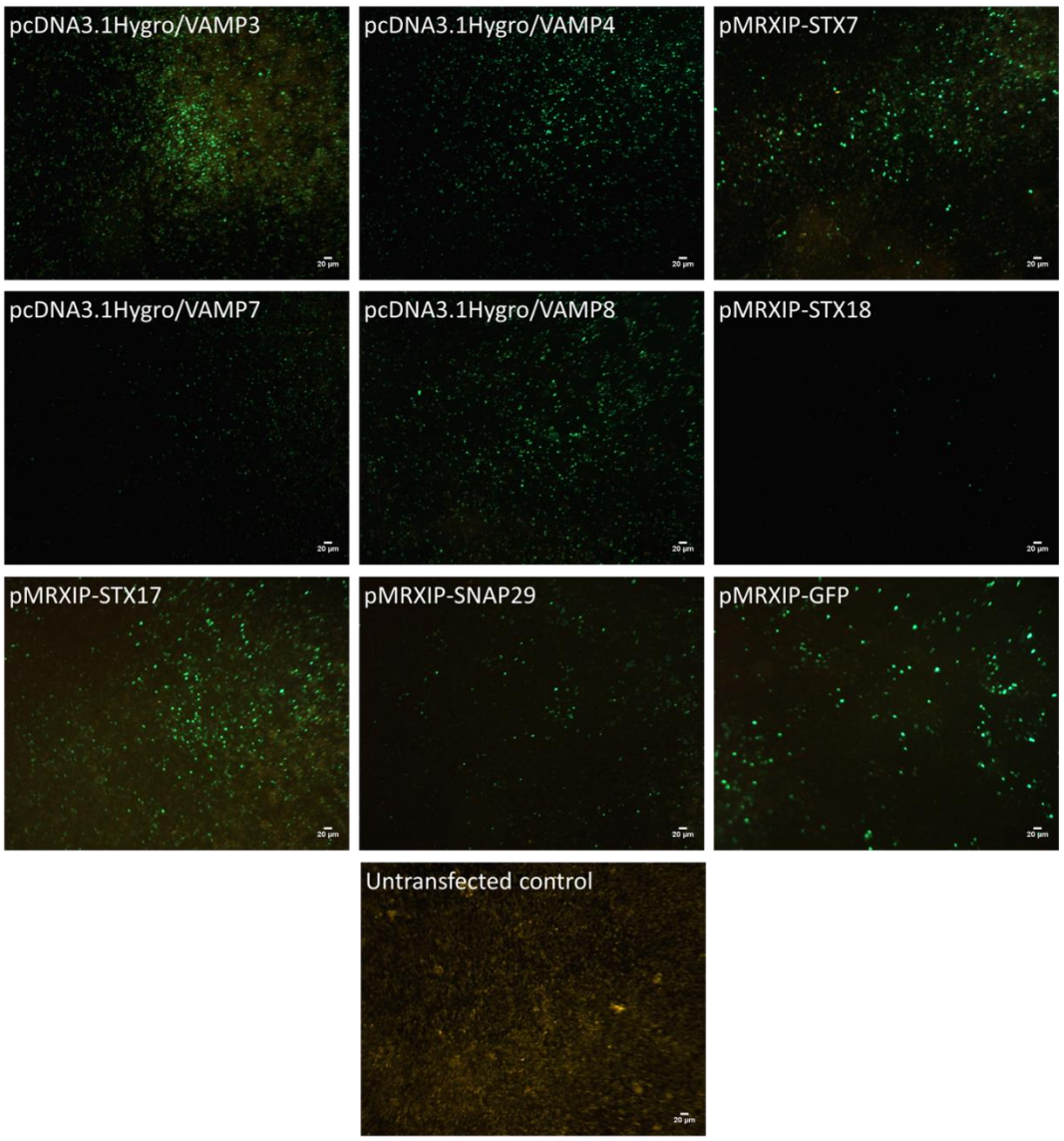

Figure 3.4. Fluorescent image analysis of transiently transfected cells. CHO Flp-In cells were transiently transfected with 0.8 µg of pcDNA3.1Hygro/VAMP3, pcDNA3.1Hygro/VAMP4, pcDNA3.1Hygro/VAMP7, pcDNA3.1Hygro/VAMP8, pMRXIP-STX7, pMRXIP-STX17, pMRXIP-STX8, pMRXIP-SNAP29 and pMRXIP-GFP using Lipofectamine 2000. After 72 h incubation, cells were observed using a Leica MZFL III microscope (x10 magnification) with an excitation wavelength of 488 nm and pictures taken using a Leica CD300F camera. The untransfected control was observed under the same parameters as the other cell lines except the light intensity that was higher.

3.3.2. Titration of hygromycin B and puromycin to determine the appropriate amount that kills the host CHO-S cell in the absence of the selection marker for use in stable cell line generation

In order to generate stably expressing cell lines, selection agent (hygromycin B or puromycin depending on the vector) needed to be added at the appropriate concentration for successful selection of cells stably expressing the selection marker. The concentration of antibiotic to use was determined by generating kill curves. For this, CHO-S cells were cultivated in 6 well plates at 1 x 10^5 viable cells/mL in media containing a specific amount of selection agent. Growth and cell viability were then monitored at day 2, 4 and 7 post addition of selection agent using a Vi-CELL instrument (see protocol 2.2.4.1).

Concentrations from 0 to 1000 µg/mL were tested for hygromycin B (Figure 3.5A). No or little difference in culture viability was observed for the cells incubated with 0, 100, 250 and 500 µg/mL hygromycin B until day 4, after which the culture viability reduced except for the 100 µg/mL condition. When cells were incubated in the presence of 750 or 1000 µg/mL hygromycin B, culture viability was reduced below 50% after 4 days and below 10% after 7 days and cells incubated with concentration of 750 and 1000 µg/mL didn't grow. As concentrations of 750 and 1000 µg/mL of hygromycin B gave a similar result with regard to the observed culture viability and cell concentration after 7 days, the concentration of 750 µg/mL was chosen as the working concentration for the generation of stable cell lines.

For determining the appropriate puromycin selection concentration to use, the following concentrations were tested; 0, 1, 2.5, 5, 7.5 and 10 µg/mL (Figure 3.5B). No impact on cell growth or culture viability was observed for concentrations from 0 to 2.5 µg/mL. The culture viability was 49% for 7.5 µg/mL and 14% for 10 µg/mL after 4 days, showing a higher impact of 10 µg/mL on culture viability. With regard to the cell growth, only the concentrations of 7.5 and 10 µg/mL inhibited cell growth. The effect on culture viability and cell growth were judged sufficient at 7.5 µg/mL compared to 10 µg/mL to use as a working concentration for stable cell line selection in future experiments

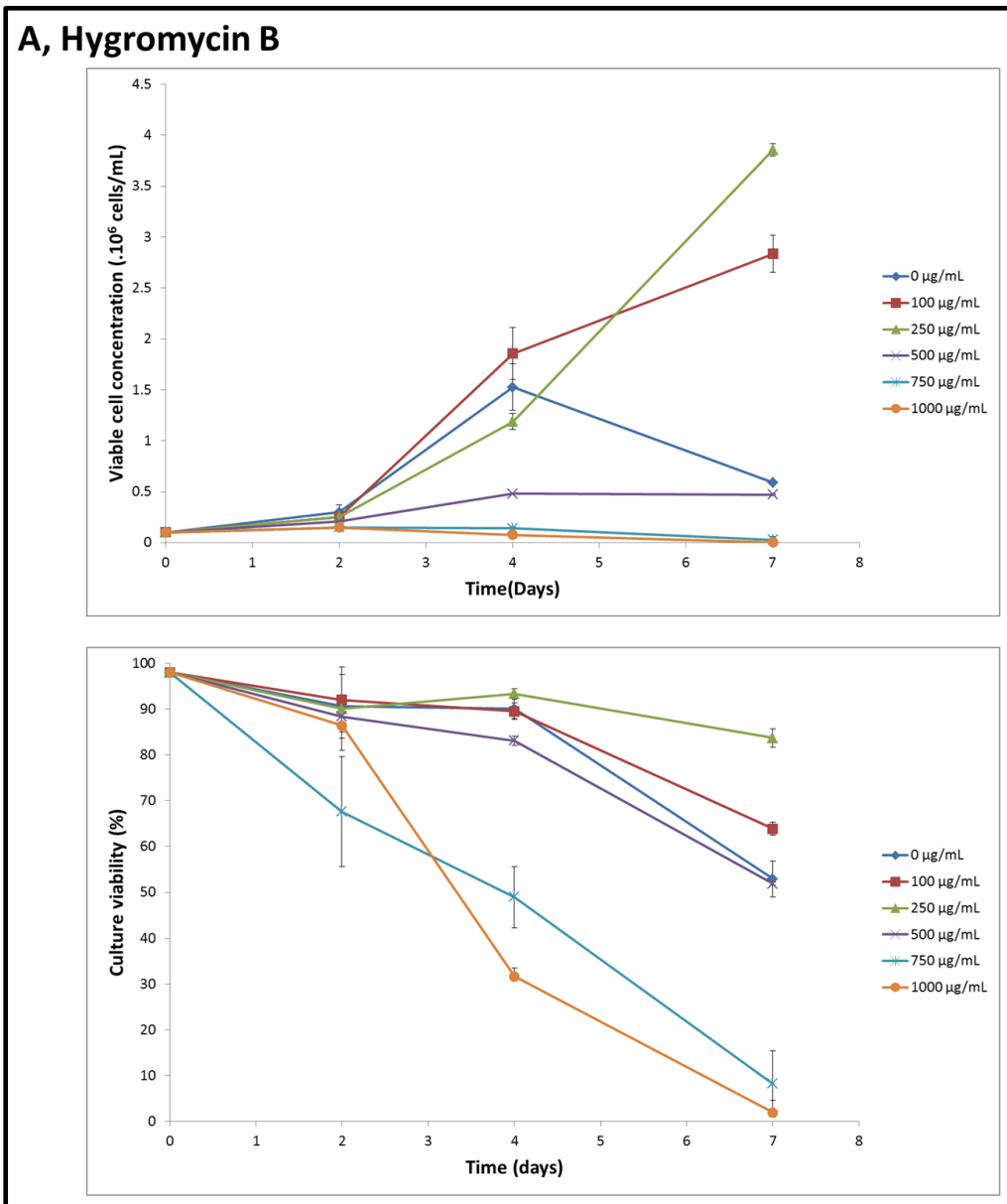

Figure 3.5. Viable cell number and culture viability of CHO-S cells cultivated with different concentration of selection agents (A) Hygromycin B and (B) Puromycin. Cells were grown in 6-well plate with the appropriate concentration of antibiotic and time points were taken at day 2, 4 and 7. Error bars are representative of 2 biological repeats except for day 2 at 1000 µg/mL of hygromycin B.

B, Puromycin

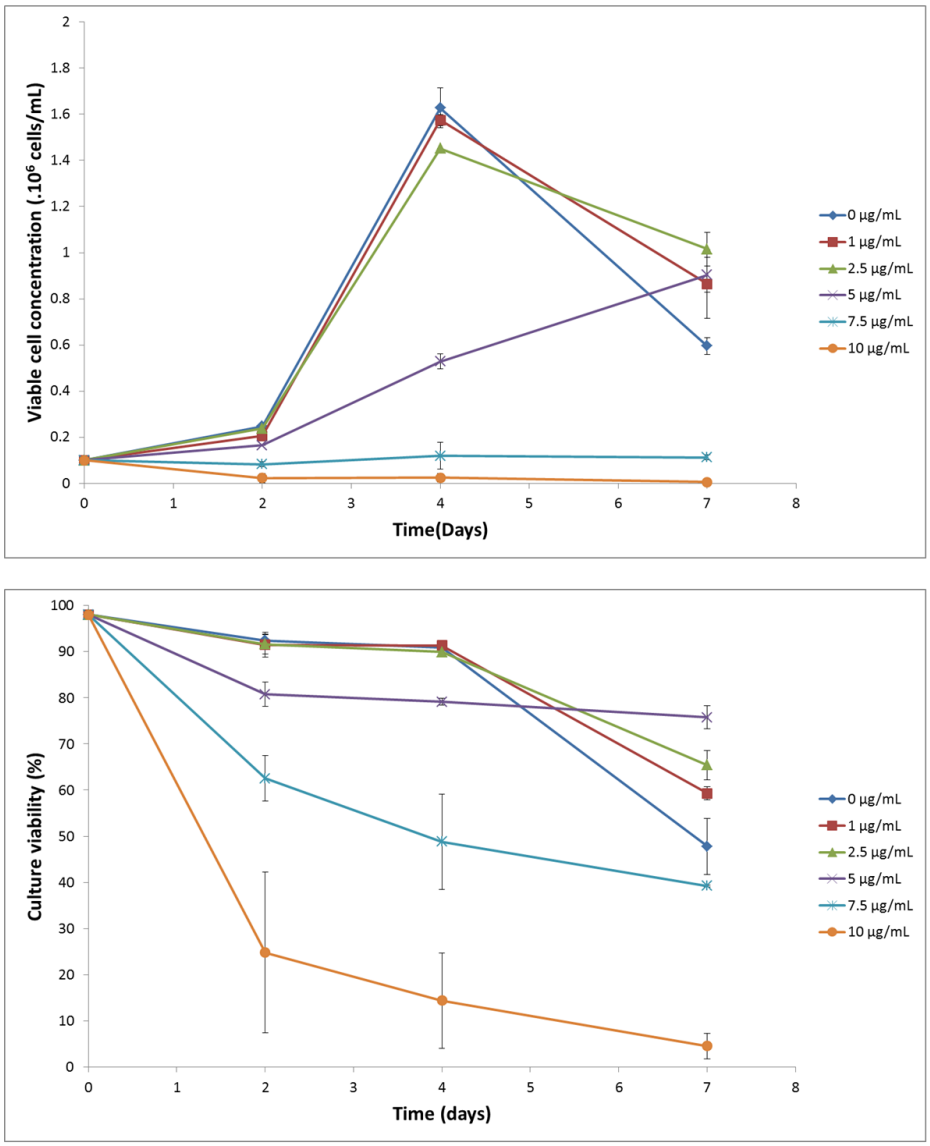

Figure 3.5(cont.). Viable cell number and culture viability of CHO-S cells cultivated with different concentration of selection agents (A) Hygromycin B and (B) Puromycin. Cells were grown in 6-well plate with the appropriate concentration of antibiotic and time points were taken at day 2, 4 and 7. Error bars are representative of 2 biological repeats except for day 2 at 1000 µg/mL of hygromycin B.

3.3.3. Stable CHO-S cell line generation and selection

After determination of an effective concentration of the selective agents (750 µg/mL of hygromycin B and 7.5 µg/mL puromycin) and the generation of the different expression vectors (see section 3.2), stably eGFP-SNARE expressing CHO-S cell lines were generated. CHO-S cells were electroporated with 20 µg of linearized DNA using a Gene Pulser Xcell™ Electroporation system (protocol 2.2.5.1). The following day, the selection agent was added

at the appropriate concentration to apply the necessary selection pressure to generate stably expressing cell pools. After 2 weeks of recovery, cell growth and culture viability were determined using a Vi-CELL instrument. If appropriate cell numbers and culture viability were observed (these being >60% viability and >0.5 x 10^6 cells/mL), the cells were used to inoculate 20 mL of media in a 125 mL Erlenmeyer flask (protocol 2.2.3.1). The different cell lines generated are summarised in Appendix 3.

3.3.4. Analysis of target eGFP-SNARE fusion protein expression in stable CHO-S cell pools

Following the creation of the different stably expressing CHO-S cell pools, further investigation needed to be undertaken to confirm the expression of the fusion proteins of interest. Indeed, electroporation is a random integration technique where the desired gene could be integrated into a silenced region. Moreover, the method used for selection (hygromycin B and puromycin) only assures the enrichment of cells stably expressing the resistance gene. To confirm expression of the fused proteins, pellets from the stably expressing cell pools were extracted for SDS-PAGE and western blot analysis (protocol 2.3.2).

Figure 3.6A shows the results obtained after western blot analysis of the different pellets extracted from the VAMPs engineered stable CHO-S cell pools. The expected molecular weights are 38, 43, 51 and 38 kDa for VAMP3, VAMP4, VAMP7 and VAMP8 fused with eGFP. After probing with an anti-GFP antibody, signal was detected for VAMP3, VAMP4 and VAMP8 at the expected size (Figure 3.6A). No extra bands were observed confirming the integrity of the fused proteins and that the eGFP had not been cleaved from the VAMP protein. No signal was obtained for the eGFP-VAMP7 cell pools, even after several repeats of the extraction. Several attempts to generate CHO-S/eGFP-VAMP7 cell pools were attempted and all were unsuccessful. The reason for this is not known and will be discussed later.

The same analysis was performed for the CHO-S eGFP-STX/SNAP stably expressing cell pools, CHO/STX7, CHO/STX17, CHO/STX18, CHO/SNAP29 and CHO/MRXIP-GFP. The expected size for the different constructs were 57, 60, 65, 56 and 27 kDa for STX7, STX17, STX18, SNAP29 fused with eGFP and the control (pMRXIP-GFP). Western blot analysis (Figure 3.6B) with an anti-GFP antibody showed a positive signal at the expected sizes for STX7, STX17, SNAP29 and the STX control. Two bands were observed for STX7, a main one

at the expected size (57 kDa) and a less intense band of a smaller size directly below the main band (Figure 3.6B). The smaller band could correspond to eGFP-STX7 protein lacking a particular PTM or be the effect of protease activity trimming one end of the polypeptide sequence. STX7 is subjected to several phosphorylations which modifies it molecular weight (Achuthan et al. 2008), potentially accounting for the difference in the band sizes observed. Western blot analysis of the ectopic expression of the eGFP-STX18 fused protein showed a lot of cleavage of the eGFP tag (Figure 3.6C). A signal at the expected size was observed (65 kDa) but the tag was predominately removed as shown by the more intense band at 27 kDa. This set of experiments confirmed that for most of the targets a fused protein containing a correctly folded eGFP was obtained and that the cell pools were suitable for further analysis.

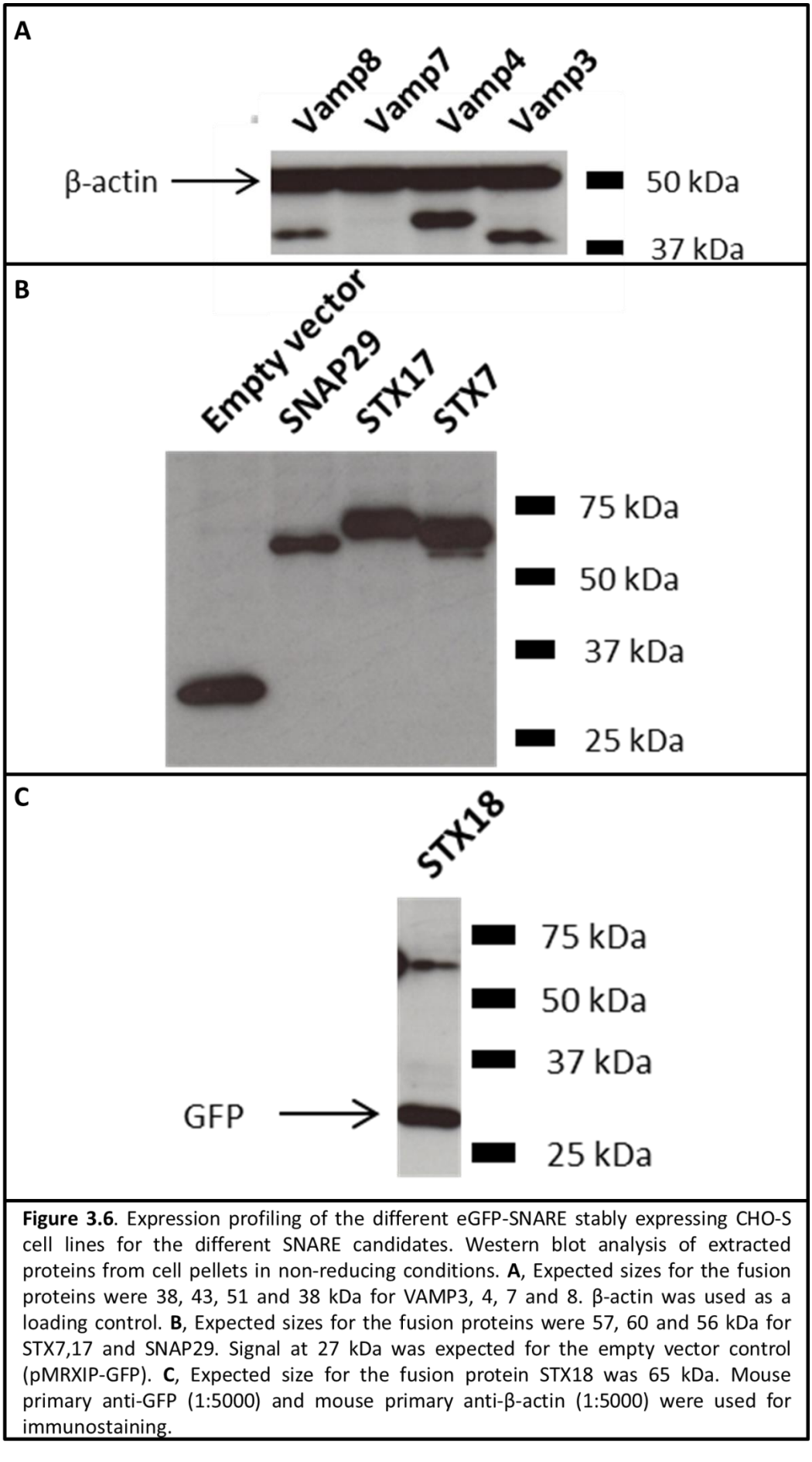

Figure 3.6. Expression profiling of the different eGFP-SNARE stably expressing CHO-S cell lines for the different SNARE candidates. Western blot analysis of extracted proteins from cell pellets in non-reducing conditions. **A**, Expected sizes for the fusion proteins were 38, 43, 51 and 38 kDa for VAMP3, 4, 7 and 8. β-actin was used as a loading control. **B**, Expected sizes for the fusion proteins were 57, 60 and 56 kDa for STX7,17 and SNAP29. Signal at 27 kDa was expected for the empty vector control (pMRXIP-GFP). **C**, Expected size for the fusion protein STX18 was 65 kDa. Mouse primary anti-GFP (1:5000) and mouse primary anti-β-actin (1:5000) were used for immunostaining.

3.4. Monoclonal CHO-S eGFP-SNARE expressing cell line generation

3.4.1. Limiting dilution cloning for generation of monoclonal cell lines from the CHO-S SNARE engineered cell pools

Using the stably expressing cell pools generated under section 3.3 above, monoclonal cell lines were created. This was achieved using limiting dilution cloning. For each cell pool, a series of limiting dilutions were made in 3 x 96-well sterile tissue culture plates in order to obtain a sufficient number of monoclonal cell lines. Once the plates were prepared and the cells added as described in section 2.2.7, they were incubated at 37^{o}C in a 5% CO_2 atmosphere for 3 weeks while monitoring for out-growth and signs of contamination using a bright field microscope. After recovery, the cell lines were characterised via a process detailed in figure 3.7. All the stable cell lines generated in section 3.3 were subjected to the limiting dilution process including the controls, CHO/3.1HGFP and CHO/MRXIP-GFP.

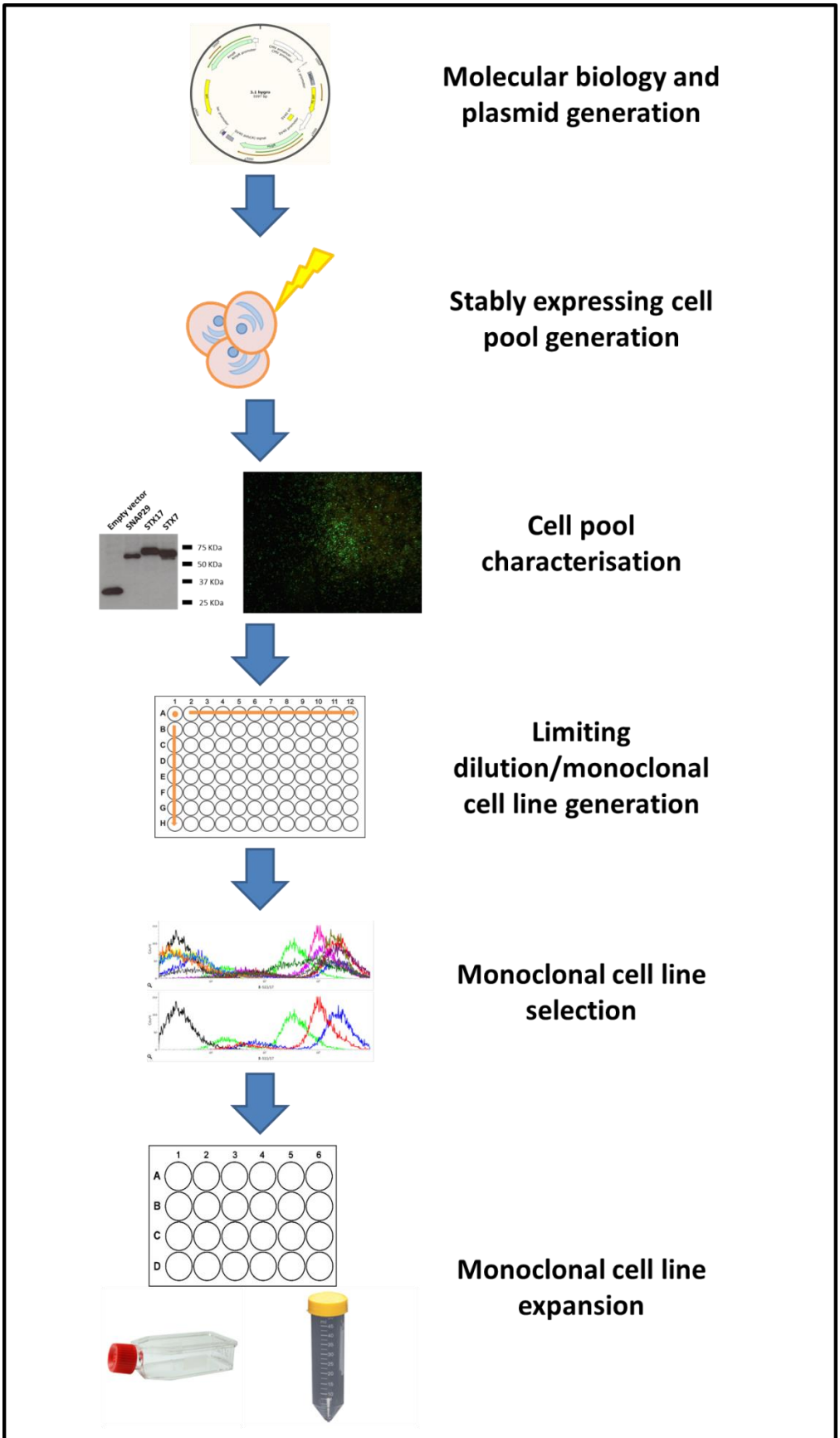

Figure 3.7. Graphical representation of the process used in this project for the generation and selection of monoclonal CHO-S cell lines expressing the target eGFP-SNARE proteins from the initial cell pools.

3.4.2. Monoclonal cell line selection for further study

From the polyclonal stably expressing cell pools generated earlier in the project, monoclonal populations were created using the method described in Figure 3.7. Initially, 12 clones were selected after recovery and the selection was based on 2 parameters; monoclonality (presence of only one cell initially in the well) and confluency (>60%). These requirements were evaluated by bright field microscopy. Monoclonal cell lines were named with the following pattern; name of the parental cell pool with the addition of a letter A-L (e.g. CHO/V4 K for the CHO-S VAMP4 K monoclonal cell line).

Selected cells were grown in a well of a 24-well plate and then in a well of a 6-well plate before the fluorescence was determined using a FACSJazz device. As the different proteins of interest were eGFP fused proteins, it was assumed that the level of expression of eGFP was correlated to the level of expression of the fusion protein. This assumption was undertaken to simplify the selection process. The measurement of eGFP expression using a flow cytometer was also helpful in determining if a population was likely to be monoclonal. The process of limiting dilution cloning relies on microscopic observation which can be error prone. The presence of a single main peak by flow cytometry fluorescence analysis would provide further evidence of the likelihood of the monoclonality of the cell population.

Figure 3.8 shows the results obtained for the VAMP expressing monoclonal cell lines using the flow cytometer FACSJazz with the 12 clones selected after limiting dilution cloning. Generally, for the eGFP-VAMP expressing cell lines, the different monoclonal populations had the same profile with a slight shift of population to the right compared to the control cells corresponding to an increase in fluorescence that is assumed to be due to eGFP expression. For VAMP3 monoclonal populations, only one clone (CHO/V3 J) showed a clear increase in fluorescence compared to the control observed as a shift in signal to the right. All the other clones had a similar eGFP expression comparable to the host cell line (Figure 3.8). For VAMP4 and 8, no noticeable difference between the different clonal populations was detected, despite a shift to the right in eGFP intensity compared to the control. The 3 clones with the biggest shift were selected for further study. In all cases for the CHO/V3, CHO/V4 and CHO/V8 monoclonal cell lines, only one major peak was observed suggesting the presence of one population of engineered cells and hence a monoclonal population. Further, whilst different expression of the eGFP-VAMP3 was observed suggesting the CHO-S cells can tolerate a range of over-expression of this SNARE, only a small increase in

expression of the eGFP-VAMP4 and eGFP-VAMP8 was observed and all at approximately the same intensity suggesting that the CHO-S cells can only tolerate a small increase in the expression of these SNAREs and hence no highly expressing cells survive the selection process.

The monoclonal populations obtained with the eGFP control demonstrated a diverse profile of expression across the clones isolated (Figure 3.8). The 3 populations had different expression profiles and were much higher in expression than the eGFP-VAMP fusions. A second peak was observed in the different control populations suggesting that the populations were not monoclonal (Figure 3.8). Even if the smaller peak was minor, this subpopulation could eventually outgrow the higher expressing population. Due to the lack of choice, these likely polyclonal cell lines were selected as controls but this information was kept in mind for future analysis.

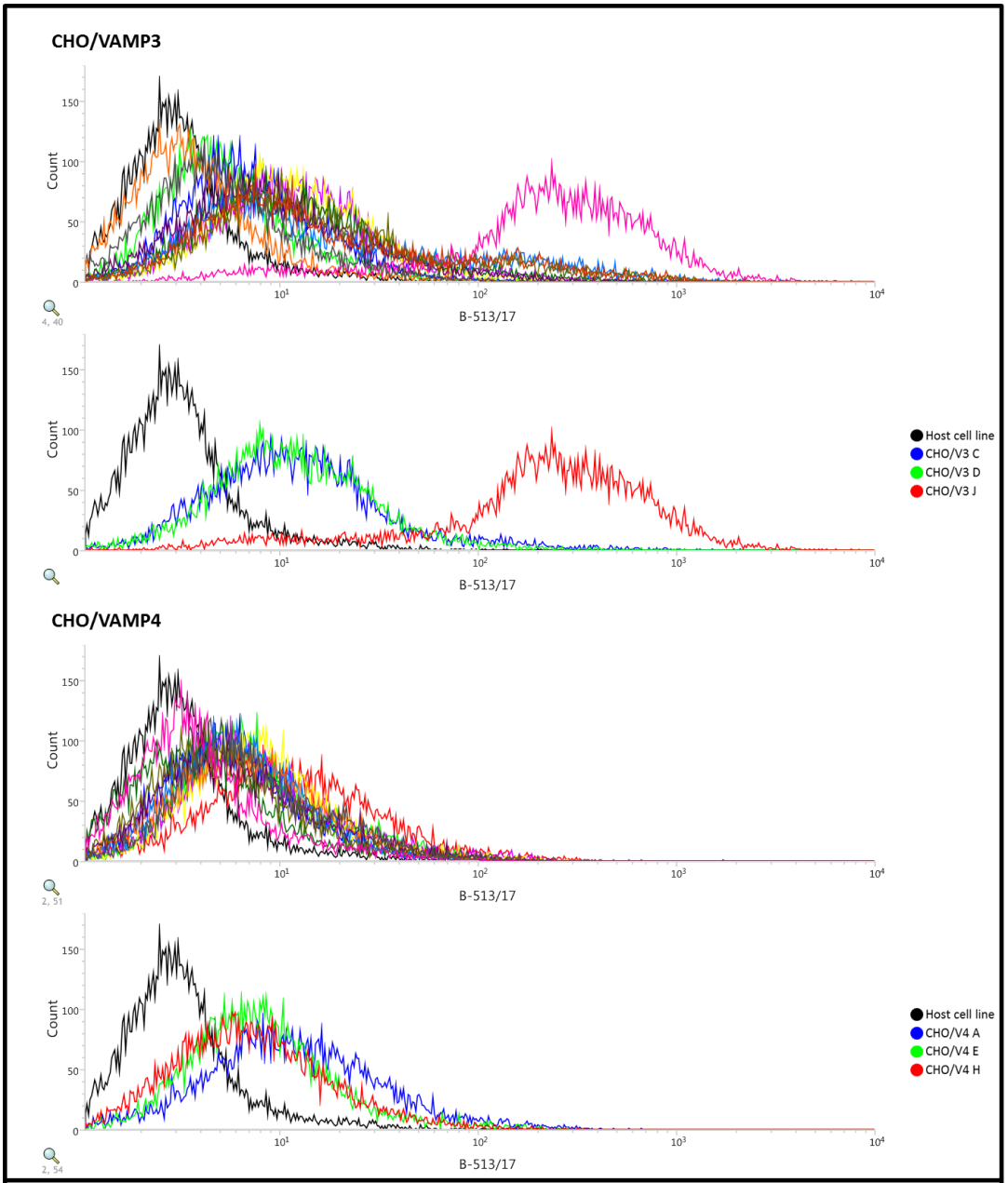

Figure 3.8. GFP signal analysis of the different clones after limiting dilution by flow cytometry. Cells were cultivated in 6-well plate for 6 days, 2 mL of culture was spun and resuspendend in 1 mL of PBS. For each cell line, 10000 events were recorded using a FACSJazz flow cytometer. Upper graphs represent signal of all the clones (black for the host cell line and colours for the different clones) for a specific cell line while bottom graphs only focus on clones selected for further analysis. Excitation wavelength used was 488 nm.

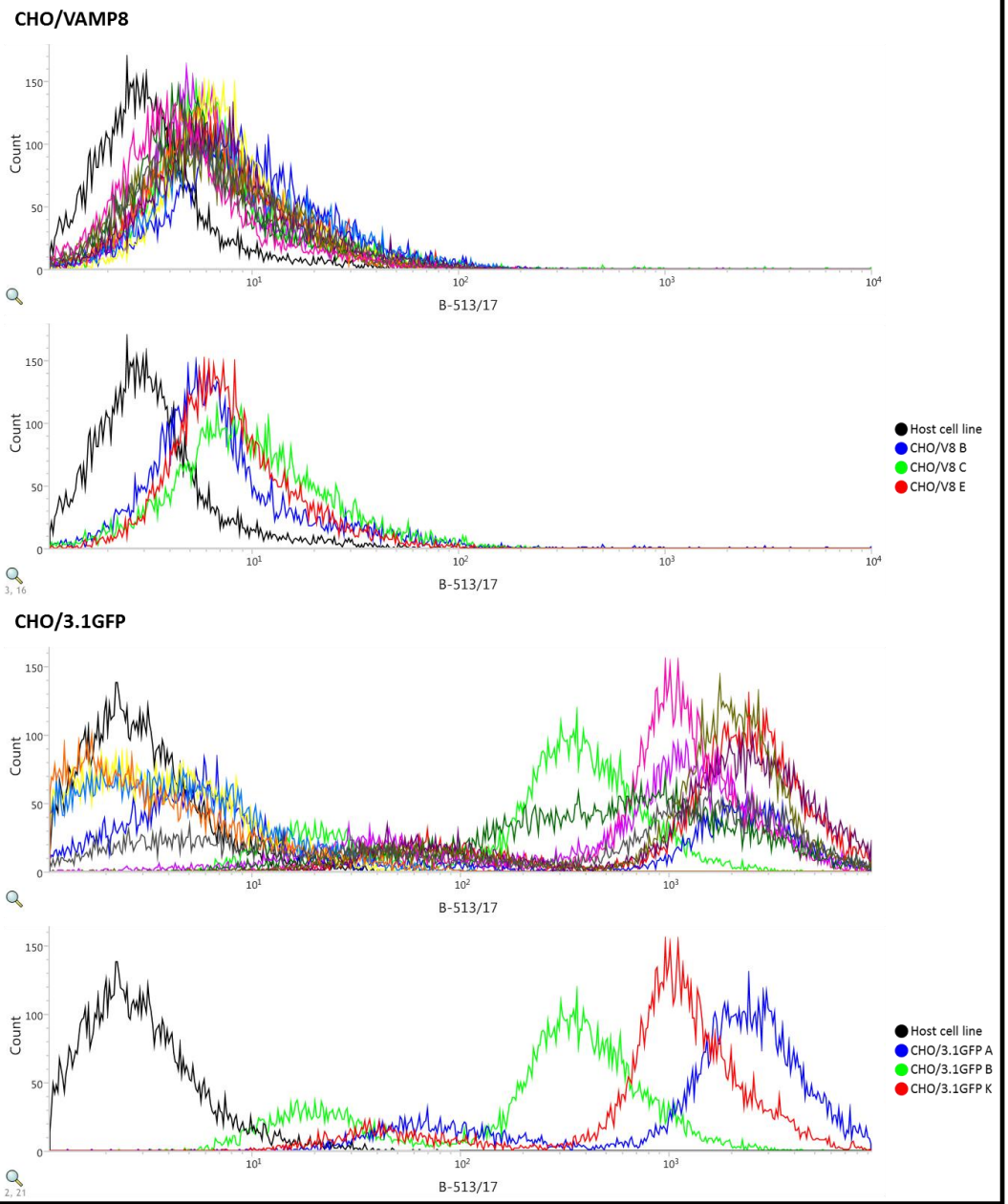

Figure 3.8 (cont.). GFP signal analysis of the different clones after limiting dilution by flow cytometry. Cells were cultivated in 6-well plate for 6 days, 2 mL of culture was spun and resuspendend in 1 mL of PBS. For each cell line, 10000 events were recorded using a FACSJazz flow cytometer. Upper graphs represent signal of all the clones (black for the host cell line and colours for the different clones) for a specific cell line while bottom graphs only focus on clones selected for further analysis. Excitation wavelength used was 488 nm.

The same process for selecting clonal cell lines for further study was executed for the syntaxin/SNAP expressing cell lines. For the different clonal populations obtained after limiting dilution cloning, the profiles of eGFP expression were more varied than observed with the VAMPs with relative low, mid and high expressers (compared to the control) isolated (Figure 3.9). For the different clones of CHO/STX7, a clear and large shift to the

right was noticeable for most clones compared to the control although among those clones there was an almost identical fluorescence profile. 3 were selected for expansion and further study.

CHO/STX17 expressing clonal populations had different fluorescence profiles with relative low, mid and high expression. This was the preferred outcome after limiting dilution cloning providing a diversity of expression across the clones and an ability to select the different levels of expression for later study (Figure 3.9). Among the 12 clones expressing STX18 selected after limiting dilution cloning, only 3 showed a fluorescence profile with a shift to the right confirming eGFP expression. The previous analysis of the STX18 pool revealed low expression of eGFP-STX18 and cleavage of the eGFP tag (see Figure 3.6C). The monoclonal populations isolated based on eGFP expression were expressing a relative mid and high profile of expression but this would need to be characterised further to confirm whether the fluorescence signal was due to eGFP only expression or if the full fusion protein was expressed. SNAP29 expressing cell lines were observed at relatively low or high fluorescence measurements compared to the control. The clones showing low expression were not selected. 3 clones among the high expressing profiles were selected and used for expansion. The MRXIP-GFP control expressing cell lines surprisingly showed only a small shift in the different populations evaluated and all the clones had a comparable profile. 3 clones were selected for further study

It was observed that several clones selected for expansion had a broad eGFP signal (CHO/STX17 C, CHO/STX17 J, CHO/SNAP29 I) but an absence of two distinct peaks. These cell lines could be polyclonal but there was no definitive data to confirm this. Moreover, in this project the generation of monoclonal cell lines was not an absolute requirement but rather a manner to obtain cell lines with different profiles of SNARE expression for further evaluation. These cell lines were considered appropriate for such further study.

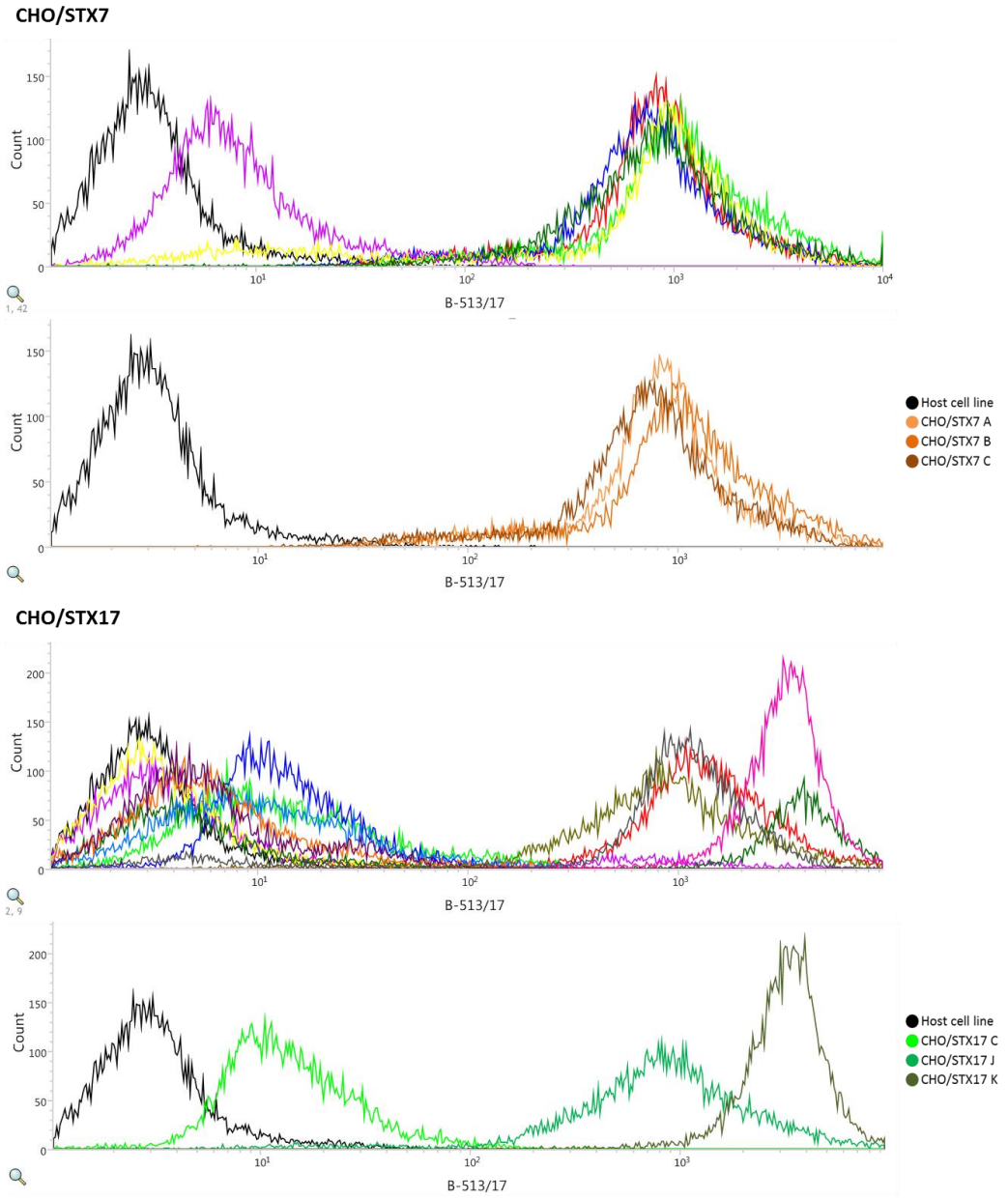

Figure 3.9. GFP signal analysis of the different clones after limiting dilution by flow cytometry. Cells were cultivated in 6-well plate for 6 days, 2 mL of culture was spun and resuspendend in 1 mL of PBS. For each cell line, 10000 events were recorded using a FACSJazz flow cytometer. Upper graphs represent signal of all the clones (black for the host cell line and colours for the different clones) for a specific cell line while bottom graphs only focus on clones selected for further analysis. Excitation wavelength used was 488 nm.

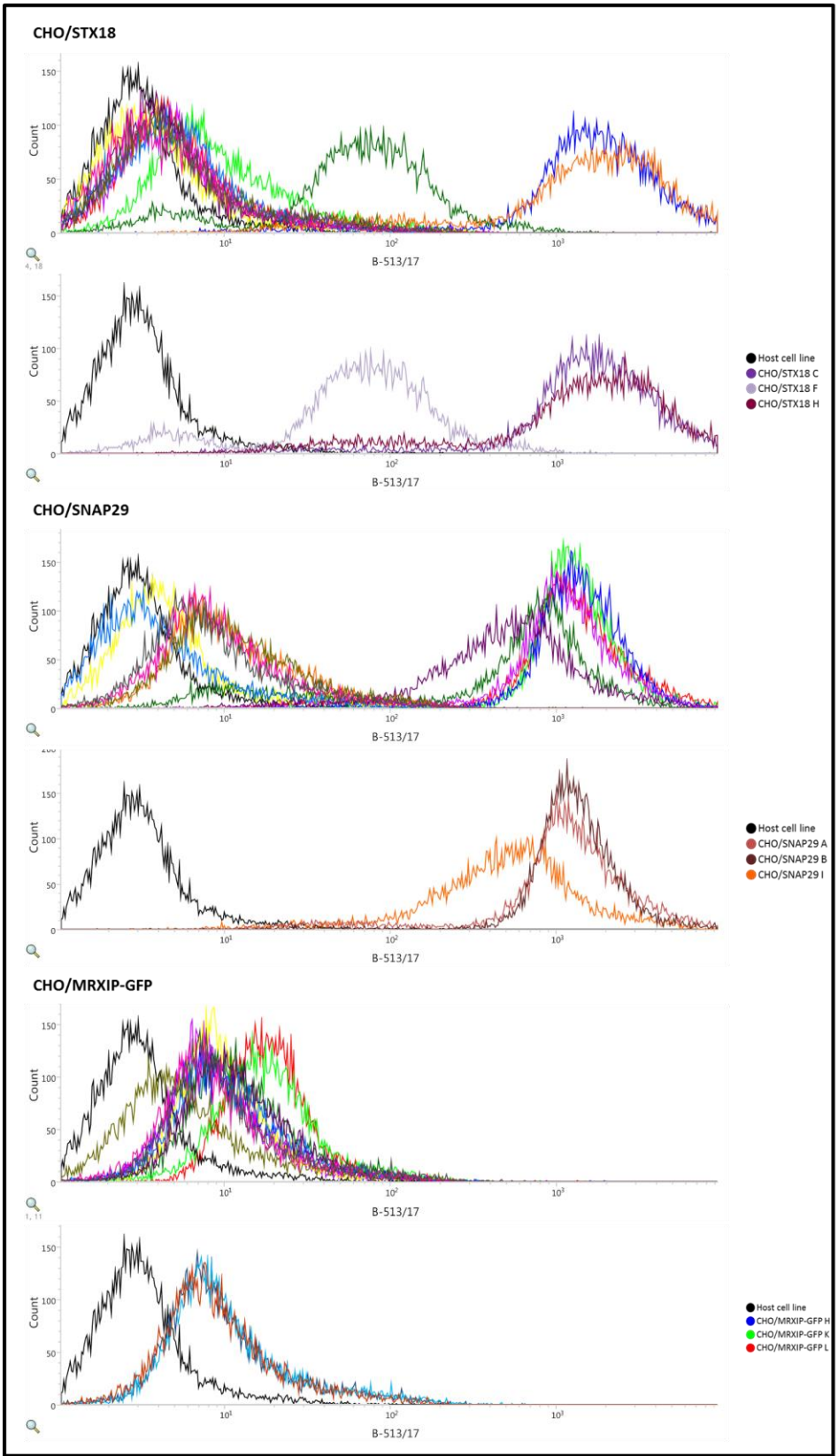

Figure 3.9 (cont). GFP signal analysis of the different clones after limiting dilution by flow cytometry. Cells were cultivated in 6-well plate for 6 days, 2 mL of culture was spun and resuspendend in 1 mL of PBS. For each cell line, 10000 events were recorded using a FACSJazz flow cytometer. Upper graphs represent signal of all the clones (black for the host cell line and colours for the different clones) for a specific cell line while bottom graphs only focus on clones selected for further analysis. Excitation wavelength used was 488 nm.

3.4.3. Evaluation of the stability of EGFP-SNARE expression in CHO-S monoclonal cell lines over time

For further analysis of the impact of SNARE over-expression on CHO-S cells, 3 clones were selected for each construct and expanded until reaching a shaken culture condition in spin tubes. When the different cell lines were adapted to the shaken environment (culture viability >90%), profiles of expression were assessed once again using flow cytometry. This was to confirm that the expression observed during isolation of the cell lines was maintained. Figure 3.10 shows the results obtained from the fluorescence measurement of cells cultured in a shaken environment. Surprisingly, most of the VAMP expressing clones had lost the expression of eGFP. Only CHO/V4 A and CHO/V3 D had retained eGFP expression. CHO/V4 A showed a similar expression profile in the shaken environment to that previously observed in the static flask whereas the CHO/V3 D profile had changed. The CHO/V3 D profile showed a less pronounced shift to the right compared to static conditions. Moreover, it was possible to distinguish 2 populations, one expressing eGFP at a low amount and one not appearing to express eGFP at all (Figure 3.10).

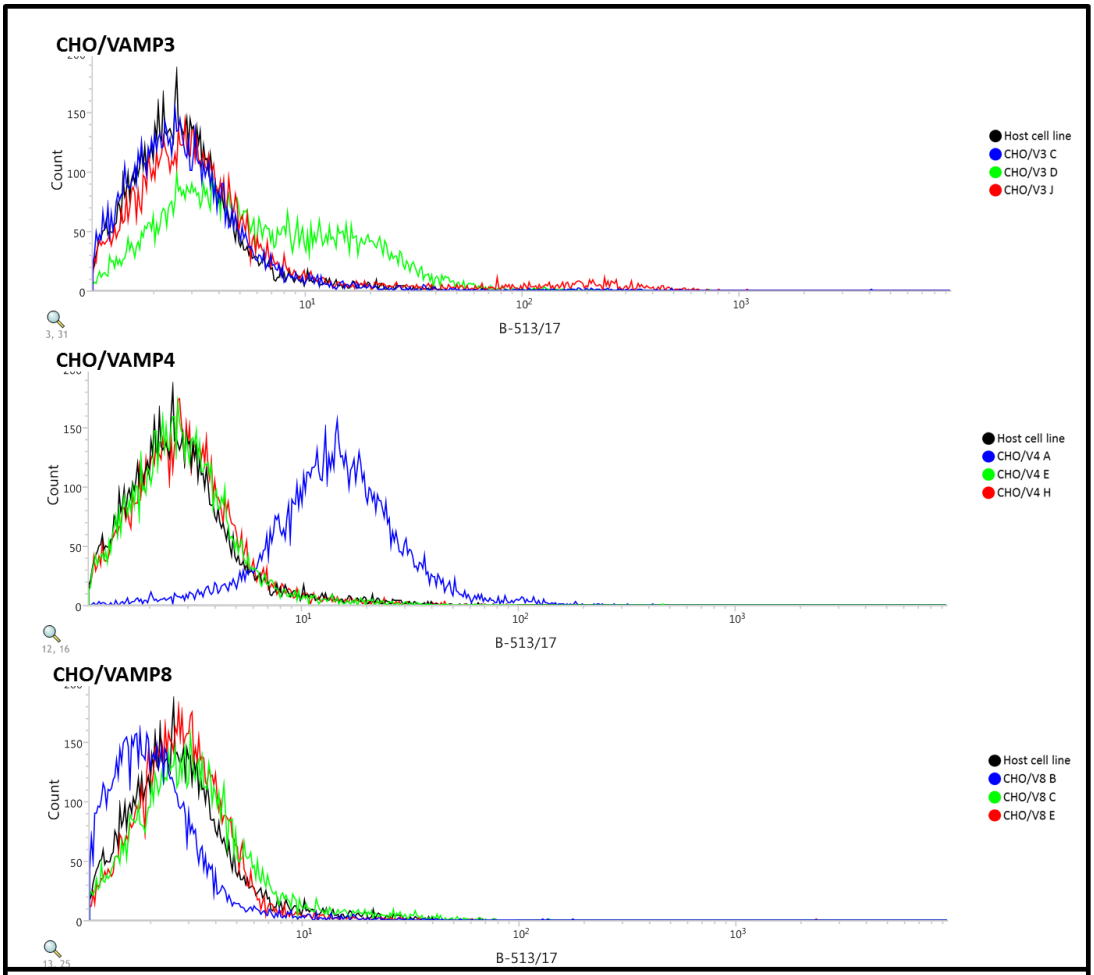

Figure 3.10 GFP signal analysis of the selected clones after subculture in spin tubes to determine stability of expression over time. Cells were cultivated in spin tubes for 2 days, 1 mL of culture was spun and resuspendend in 1 mL of PBS. For each cell line, 10000 events were recorded using a FACSJazz flow cytometer. Excitation wavelength used was 488 nm.

On-the-other-hand, the STX/SNAP over-expressing clones appeared to have retained eGFP expression much better than the VAMP cell lines suggesting that over-expression of the STX/SNAP is more tolerated in the CHO-S cell lines and maintained through generations. However, for the different CHO-S clones expressing STX7, whereas they showed a very similar profile to that observed in the static environment, adaptation to a shaken environment appeared to have resulted in a reduction in the relative amount of eGFP expression (the shift to the right was less prominent, Figure 3.10). With regard to the cell lines expressing STX17, CHO/STX17 K appeared to express less eGFP in shaken environment. CHO/STX17 K had a comparable expression level to CHO/STX17 J. The low expresser, CHO/STX17 C, appeared to have two distinct populations (two peaks) in the shaken environment with no change in the levels of expression. No evident alteration was observed for the clones expressing STX18 between the shaken cultured cells and the

previous data generated on the static cells. For SNAP29 over-expressers, one of the high expressing cell lines (CHO/SNAP29 B) appeared to have lost some eGFP expression compared to the other (CHO/SNAP29 A) cell line (Figure 3.10). The profile of eGFP expression of CHO/SNAP29 I was broader in the shaken environment and suggested the presence of a second peak. No difference was observed when comparing the profiles of the MRXIP-GFP cell lines in static and shaken environment (Figure 3.10).

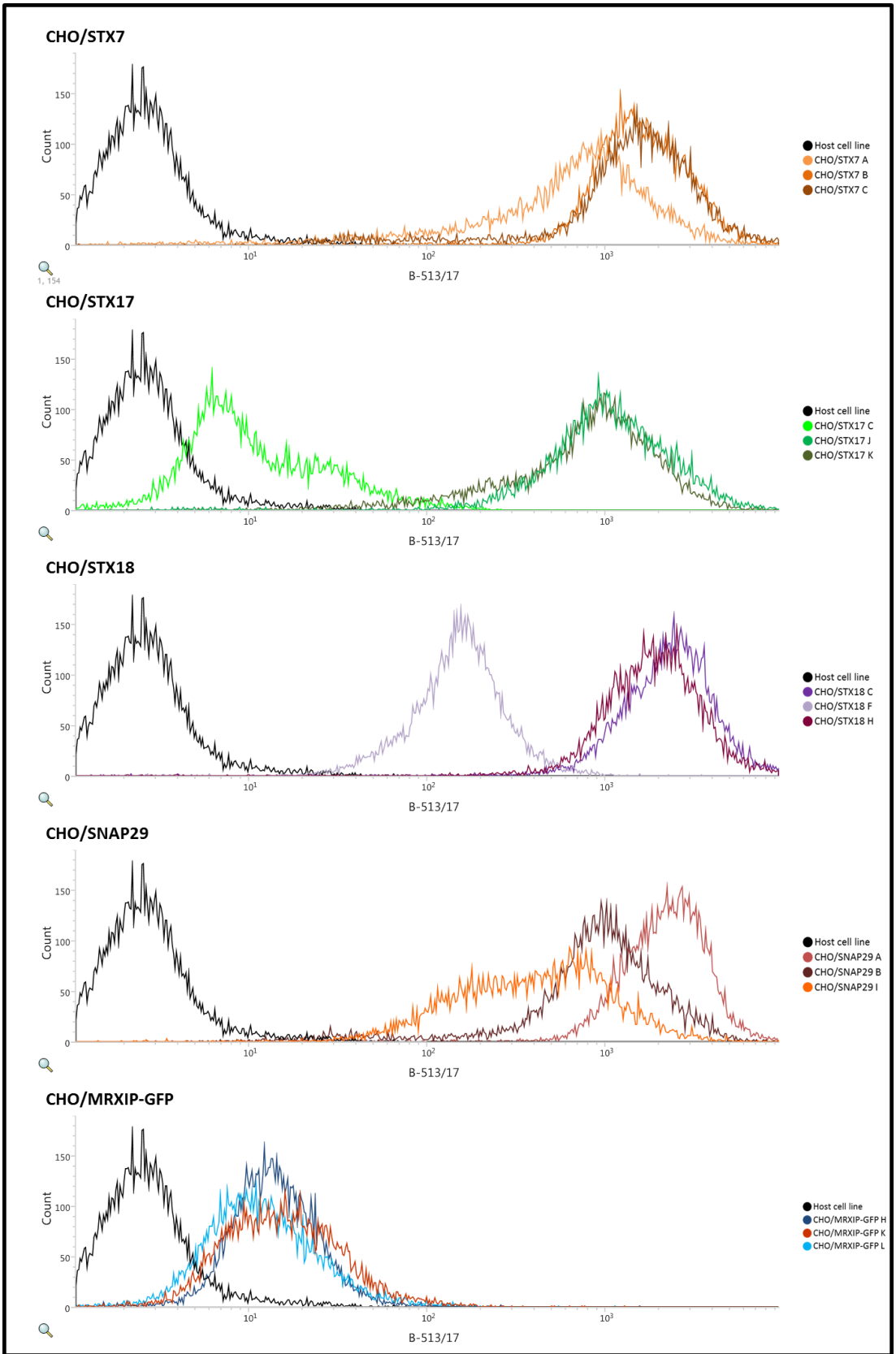

Figure 3.10 (cont). GFP signal analysis of the selected clones after subculture in spin tubes to determine stability of expression over time. Cells were cultivated in spin tubes for 2 days, 1 mL of culture was spun and resuspendend in 1 mL of PBS. For each cell line, 10000 events were recorded using a FACSJazz flow cytometer. Excitation wavelength used was 488 nm.

3.5. Discussion

The work described in this chapter is focused on the molecular cloning of target eGFP-SNAREs into appropriate mammalian gene expression vectors with antibiotic selection markers. This in order to generate engineered CHO-S cell lines necessary for further study around the impact of over-expression of the SNAREs on CHO cell secretory recombinant protein production. Thus, the secretory pathway is the main point of interest, and particularly vesicle trafficking and formation. The first step in the study was to select potential candidate target proteins for manipulation that may be able to impact the secretory pathway in order to improve recombinant protein secretion, the overall goal of the study. Based on the findings of previous reports into manipulation of some of the SNARE family (Peng, Guetg, Abellan, et al. 2010) and work reported by Gordon et al. (2010) on the identification of SNAREs necessary for constitutive secretion, the work here was focussed upon assessing the impact of SNARE over-expression in CHO cells on recombinant protein secretion capacity.

From a survey of the literature and availability of genetic constructs, a number of potential different candidates emerged as targets for SNARE manipulation; VAMP3, VAMP4, VAMP7, VAMP8, STX7, STX17, STX18 and SNAP29. A siRNA screen in HeLa (Gordon et al. 2010) identified STX17, STX18 and SNAP29 as necessary for constitutive secretion of proteins suggesting a potential bottleneck in secretion at the level of these proteins which overexpression could alleviate. VAMP8, known to involved in compound exocytosis (Thorn and Gaisano 2012), has already been successfully used to increase production of recombinant protein in CHO-K1 cells (Peng et al. 2011) and was chosen as a control. VAMP3 and VAMP4 were selected due to their possible role on the Golgi structure and fusion events at the membrane. Indeed, depletion of VAMP4 in HeLa cells affects the structure of the Golgi apparatus (Shitara et al. 2013) while VAMP3 is necessary for fusion events at the plasma membrane in several *trans*-SNARE complexes (Hu et al. 2007). STX7 and VAMP7 were selected due to their involvement in *trans*-SNARE complexes with other targets such as VAMP8 or SNAP29 for further co-expression analysis. Once these targets were selected, genetic constructs for their stable expression in mammalian cell lines were generated. At the start of this work, the sequences of the candidate genes were only predicted for CHO cells in the different databases (http://www.chogenome.org/, as at 2015). All the sequences for the genes used were therefore from human. The different sequences for the genes are now available (https://www.ensembl.org/Cricetulus_griseus_crigri/Info/Index, as

at August 2018). To confirm the high degree of homology between both species for the different genes, nucleotide sequence alignments were performed using BLASTn bioinformatic tool (https://blast.ncbi.nlm.nih.gov/Blast.cgi?PAGE_TYPE=BlastSearch). The results of the alignment are detailed in Table 3.2. In the particular case of the candidate genes, identity of over 80% was observed between Human and Chinese hamster genes. Moreover, ectopic expression of human genes in CHO cells is common and has been successful (Fischer et al. 2015). Further, the use of the human gene can offer an advantage in that this can remove any natural gene expression control elements within the CHO sequence that might limit the ability to over-express a given gene sequence. Hence, use of human sequences in this project was performed while keeping the information in mind for further analysis.

Table 3.2. Results of nucleotide sequence alignment using BLASTn between the Human and the Chinese Hamster candidate genes.

gene	CHO gene Ensembl ID	CHO genome used	identity to human gene (%)	NCBI Reference Sequence ID for the hit sequence	E value
VAMP3	ENSCGRT00000002866.1	CriGri_1.0	243/288(84%)	NM_004781.3	4.00E-84
VAMP4	ENSCGRT00000024637.1	CriGri_1.0	379/397(95%)	NM_003762.4	0
VAMP7	ENSCGRT00000023866.1	CriGri_1.0	614/662(93%)	NM_005638.5	0
VAMP8	ENSCGRT00000015951.1	CriGri_1.0	250/285(88%)	NM_003761.4	5.00E-96
STX7	ENSCGRT00000018077.1	CriGri_1.0	697/779(89%)	NM_001326579.1	0
STX17	ENSCGRT00000024318.1	CriGri_1.0	589/670(88%)	NM_017919.2	0
STX18	ENSCGRT00000014508.1	CriGri_1.0	900/1008(89%)	NM_016930.3	0
SNAP29	ENSCGRT00000014256.1	CriGri_1.0	528/614(86%)	NM_004782.3	0

Plasmids with the human genes of interest were initially sourced from Addgene. In all cases the target genes were fused to an eGFP gene at the N-terminal for the expression of a fusion protein with a fluorescence tag. Here, the different genes of interest were fused to eGFP via a tandem repeat (Yu et al. 2015) with no specific sequence used as a linker but only a stuffer region providing enough space for proper folding. The presence of a eGFP reporter gene is a valuable tool for protein detection and non-invasive visualisation of expression in cells (Tsien 1998). However, even though the tag may not interfere with the expression of the individual SNAREs, this does not confirm that the tag does not interfere with the activity/function of the tagged protein.

Originally, VAMP candidates were provided inserted in a pEGFP-C1 plasmid backbone with a selection based on neomycin or G418 antibiotic resistance. Previous experiments (data not shown) in the laboratory had found the generation of stably expressing cell lines using this selection to be difficult and unstable cell lines were produced. To solve this issue, the different genes of interest were sub-cloned into a commercially available

pcDNA3.1/Hygro(+) plasmid with a resistance gene for hygromycin B. On-the-other-hand, the different syntaxin/SNAP plasmids were provided in another plasmid called pMRXIP GFP-Ci2 conferring a puromycin resistance to the cells. Those constructs weren't modified but used as provided. As VAMP and syntaxin/SNAP proteins interact together in vesicle formation and trafficking (Hong 2005; Jahn and Scheller 2006), the fact these were under different selection agents meant it would be possible to determine any additional effect if more than one component of a *trans*-SNARE complex was expressed. These could also be used to determine if a specific component is limiting in the *trans*-SNARE complex as it is suggested that some R-SNAREs and Q-SNAREs might be replaced by other SNAREs (Gordon et al. 2010). Control vectors (pcDNA3.1Hygro/GFP and pMRXIP-GFP) were also generated to determine any background effect from stable integration of these plasmids and the selection process on the CHO cell (Stepanenko and Heng 2017).

To confirm the expression of the full length fusion proteins with a correctly folded eGFP tag from the newly generated vectors, the fluorescent signal as a result of expression of the constructs was investigated by transient transfection in adherent CHO Flp-In cells. GFP fluorescence is obtained through its fluorophore and its correct folding is required to give activity. The fluorescent images taken 72 h after the transient transfection showed that the transfected cells were fluorescent, suggesting that the eGFP tag was correctly folded. These results agree with the studies where the fusion genes VAMP4, VAMP7, STX17 and STX18 were originally reported (Itakura et al. 2012; Mallard et al. 2002; Martinez-Arca et al. 2000). The differences in signal intensity (notably for STX18 and VAMP7) for the different constructs may be explained by several factors. As the transfection approach was the same for all constructs, the most probable explanation is that the over-expression of these SNAREs is not well tolerated by the cell or that these are turned over rapidly and hence the amount of expressed eGFP-fusion protein observed is low in comparison to the other constructs. Stable cell line generation subsequently undertaken was also difficult with these two constructs, providing further evidence that the over-expression of these fusion proteins is not tolerated in CHO cells.

In order to generate the different stably expressing cell lines, the working concentration for the different selection agents was determined. From the results in section 3.3.2, a working concentration of 750 µg/mL of hygromycin B and 7.5 µg/mL of puromycin were used. All the stably expressing CHO-S SNARE engineered cell lines were generated by electroporation (Appendix 3) which results in delivery of the plasmid DNA to the nucleus

and random integration of the linearized plasmid into the genome of the host cell. By this nature of integration, the genes of interest may be silenced or have low expression levels due to positional effects (Davami 2016). To determine the eGFP-SNARE fusion protein expression profiles of the different polyclonal pool populations, protein extraction from cells and subsequent western blot analysis for the eGFP-SNARE fusion proteins was undertaken. After incubation with an anti-GFP antibody, an expression signal for the full length fused protein was obtained for all the constructs except for eGFP-VAMP7 and eGFP-STX18. For cells expressing STX18, two bands were detected at 65 kDa and 27 kDa corresponding to the size of the full fusion protein and the eGFP alone. A stronger signal was detected for the eGFP than the full protein suggesting a more abundant presence of cleaved but properly folded eGFP. This indicates cleavage of the eGFP tag. The cleavage of the eGFP tag may be due to the presence of a cleavage motif in the linker sequence. Indeed, full size fusion protein and eGFP were detected and in the case of mis/unfolding of the fusion protein, both parts of the fusion protein would have been degraded. After analysis of the linker region on synlinker (http://synlinker.syncti.org/, National University of Singapore), no common cleavage recognition motif was found.

Regarding eGFP-VAMP7 stably expressing CHO-S cells, no eGFP signal was obtained after blotting with an anti-GFP antibody for either the full fusion protein or any fragment containing the eGFP. This was unexpected because a fluorescent signal was detected during the transient transfection suggesting at least proper folding of the eGFP. Several protein extractions and generation of stably expression cell lines were unsuccessful. The most likely reasons for this are that either the eGFP-VAMP7 fusion protein (with the human VAMP7 sequence) is toxic to the cells and hence cells expressing this do not survive or that the protein is rapidly degraded. No further studies were undertaken during this work to ascertain if either of these possibilities was correct.

Overexpressing ectopic proteins can be a burden on the cell and have detrimental effects. For example, when heterologous proteins are being translated, overload of the ER capacity to fold proteins can trigger the UPR pathway (Chakrabarti, Chen, and Varner 2011). This pathway leads to recovery of a normal state or apoptosis. Different levels of ectopic protein expression may be needed to observe when the ER capacity is destabilised. One way to obtain different levels of expression is the use of promoters with different transcription rates. This strategy requires the creation of a different vector for each promoter used. In this study, we used instead the property of random integration by electroporation. Indeed

after electroporation, cells integrate a different amount of DNA into their genome in different locations giving a polyclonal population. Potentially every cell expresses the protein of interest at a different level due to integration of different copy number of the genes, positional effects, and different translational and protein folding capacities across cells. By performing limiting dilution cloning to obtain monoclonal cell lines, cell lines derived from a unique cell, it is theoretically possible to obtain cell lines expressing the target recombinant fusion protein at different levels. Further, monoclonal populations have become a standard in industrial processes in order to obtain a population with homogeneous genetic information.

The monoclonal cell lines were generated through two steps of selection. The first was after the recovery step where clones were selected based on clonality and confluency. From 3 x 96-well plates initially setup for each construct, 12 clones were selected. The second step was a screening of the 12 selected clones for expression of each eGFP-SNARE fusion construct based on fluorescence measurements. Flow cytometry was used to determine the relative level of expression of the fused protein. This approach does not however, allow the investigator to determine if SNARE protein function is impaired by the presence of the eGFP tag.

When analysing the data obtained by flow cytometry, a difference in the shift of the curves between the eGFP-VAMP and eGFP-syntaxin/SNAP expressing cell lines was noticeable. The different nature of the backbone into which these genes were cloned and expressed from may explain the variation observed. For all the proteins of interest, at least 3 clones with fluorescent signal above from the host cell lines were obtained, although the magnitude of the difference in expression differed between the constructs.

After selection of the different clones based on the fluorescence by flow cytometry, they were expanded from 6 well plates to spin tubes. Normally, the CHO-S cells used were cultured in suspension but for the limiting dilution cloning and the expansion period following it, the different clones spent a period of time in a static environment (≈2 month). CHO cells were initially a static cell line and were adapted to suspension culture resulting in changes in gene expression (Shridhar et al. 2017). The level of eGFP-SNARE fusion protein expression was determined in the cells for selection purposes in a static environment so the change to suspension culture could result in a change in the expression profile in the different clones. Therefore, in order to determine whether any changes in the level of expression of the eGFP were observed, flow cytometry was performed after adaptation of

the cells to the shaken environment. Some changes were expected due to the drastic change of environment, increasing the risk of loss of the gene of interest. Surprisingly, most of the VAMP expressing clones had lost eGFP expression when adapted to the shaken environment while the selection pressure was present. Gene position and structure at the integration site have a great impact on the stability of integration, but the presence of the selection pressure should preserve gene integration. Moreover, Böhm et al. (2004) showed that expression of a gene of interest was lost over time (2 months) only when selection pressure was absent. On-the-other-hand, the syntaxin/SNAP expressing cell lines profile changed much less and the general profile was maintained. The difference between the VAMP and syntaxin/SNAP expressing cell lines may be explained by the difference in the backbone, or by the very nature of the proteins being expressed. If the over-expression of the VAMP proteins is toxic to the cell one would expect over time that those with expressing the protein at a low level would 'out-grow' those with higher expression levels so that with every culture passage the expression observed would be reduced. This could be investigated by following the expression of the eGFP-VAMP fusion protein in culture over time.

Another phenomenon was also observed during the second round of flow cytometry on the cells growing in suspension. In a few populations there was clear evidence of a polyclonal population (presence of two or more distinct peaks) where this had not been observed. In all cases, the fluorescent peaks were close together denoting a small difference in the fluorescent expression. This may have arisen as a result of the initially selected cell line not being monoclonal or during subsequent adaptation and culturing of the cells in suspension culture. In order not to reduce the number of cell lines for each target, the potential polyclonal populations were not discarded.

3.6. Summary of the main findings from the work in this chapter

This chapter summarises the processes undertaken for the generation of all the cell lines required for the remainder of the project. After focusing on a limited number of targets, VAMP3, VAMP4, VAMP7, VAMP8, STX7, STX17, STX18 and SNAP29, picked from literature reports, mammalian expression vectors of these fused N-terminally to eGFP were generated. The expression of the different fused proteins was checked using fluorescent microscopy and western blot analysis after transient transfection. Stably expressing CHO-S

cell pools were then generated and subjected to limiting dilution cloning to generate monoclonal populations with different levels of eGFP-SNARE fusion protein expression. After selection of the different monoclonal populations based on fluorescence levels, only the syntaxin/SNAP expressing clones provide adequate expressing monoclonal cell lines. The generated cell lines were then characterised further, particularly the ability of these to secrete a target recombinant biotherapeutic protein and in relation to the relative levels of eGFP-SNARE fusion protein over-expression. This work is outlined in the next chapter.

CHAPTER 4: Assessment of the Impact of Over-expression of Target SNAREs in CHO-S Cells on the Cell and Recombinant Protein Expression

4.1. Introduction

As described previously in this thesis, cell line engineering processes classically use one of two approaches, either the overexpression of a beneficial gene or the repression of a detrimental gene. Here, cell line engineering was undertaken via the generation of cell pools and clonal lines overexpressing ectopic proteins, VAMPs or syntaxin/SNAP fused to an eGFP tag (see Chapter 3). After generation of these engineered cell lines as described in Chapter 3, the next step was to determine how the introduced characteristics impacted upon the cell lines compared to the parental cell line control. In this regard, a number of key parameters can be evaluated with regard to improving recombinant protein production from a new host. Three such parameters which are fundamental to recombinant protein expression from cell hosts are cell growth and survival (this reflects the rate of growth, the biomass that is accumulated and then for how long this is maintained), cell productivity and titre (reflecting both cell specific productivity and overall product yield from the culture) and the product quality (including correct folding and assembly of polypeptides and post-translational modifications). Once these 3 parameters have been investigated and characterised, the stability of these parameters over time (referred to as the "stability of the cell line") are monitored to confirm that a recombinant cell line does not lose the desired characteristics over time (Chen et al. 2012; Li et al. 2016).

Introduction or the overexpression of a gene into a host cell might have consequences on the engineered cell line growth properties and culture durability and viability. Indeed, placing a burden on the ER by overexpression of proteins that are directed into the ER can activate the UPR (Schröder and Kaufman 2005), which acts to initially try to alleviate the burden on the ER by upregulation of chaperones and foldases in the ER whilst simultaneously slowing entry of new polypeptides into the ER. If the burden cannot be reduced or, in a timely manner, apoptosis is induced (Xu, Bailly-Maitre, and Reed 2005). Indeed, in general the overexpression of either endogenous or exogenous genes and proteins can lead to a disturbance of the homeostasis of the cell, a perceived cell stress and

impaired cell growth and performance with regard to recombinant protein production. Moreover, expression of ectopic proteins can be toxic to the cells and hence produce undesired effects on growth and culture viability leading to cell death. On-the-other-hand, overexpression of proteins involved in proliferation such as cyclin-dependent kinase like 3 (Jaluria et al. 2007) or vasolin containing protein (Doolan et al. 2010) can result in the manifestation of desired characteristics.

In order to assess the impact of cell engineering on growth rate and cell doubling time, experiments can be performed to generate data that allows the plotting of the viable cell concentration through time on a log scale to determine the different growth phases of culture (exponential, stationary and decline phase). The curves obtained can be used to extrapolate the growth rate during the exponential phase of growth using the following equation

$$\mu = \frac{dX}{dt} \times \frac{1}{X} \text{ or } X = X_0.e^{\mu t}$$

where X_0 is the initial cell concentration, μ is the growth rate and t is time.

Productivity or titre are terms used to describe the concentration of recombinant protein of interest produced. The culture yield or titre can be calculated as a concentration (e.g. often mg/mL or g/L of the target protein of interest) or a specific productivity (pg/cell/day of product of interest). Specific productivity is a more precise measurement than titre or culture yield, giving the average quantity of product produced per cell over time. It is calculated by plotting the change in integral viable cell concentration (IVC) against the change in product concentration over time and using the following equation

$$C(t) = qp(t) \times \int_{t0}^{t} V(t)dt$$

where C(t) is the product concentration, qp(t) is specific productivity over a specified time period and $\int_{t0}^{t} V(t)dt$ is the integral viable cell concentration across the specified time period.

This chapter describes the characterisation of those cell lines generated in Chapter 3 and any impact of the over-expression of the proteins of interest on cell growth and secreted recombinant protein productivity. After the limiting dilution and selection process, experiments were undertaken to confirm the correct ectopic expression of the fused molecule in the different cell lines. Once correct expression was confirmed, the effect of

the overexpression on the cell lines with regard to growth was assessed at different scales (shake flasks and spin tubes). Any impact on secretory productivity of model recombinant biotherapeutic proteins was then assessed under different conditions and with different recombinant model proteins. The end result is the characterisation of monoclonal cell lines expressing eGFP-SNARE fused protein of interest with defined cell growth profiles and productivity assessments under different conditions and scales. Comparison between different scales was also performed to determine reproducibility of prediction.

4.2. Characterisation of different selected syntaxin/SNAP expressing cell lines

After limiting dilution cloning of the engineered cell pools, 2 or 3 clones for each syntaxin/SNAP construct were obtained. Investigations were then undertaken to confirm expression of the intact fusion protein and an active fluorescent tag in the stably transfected pools (see section 3.3) and on the monoclonal cell lines.

4.2.1. Microscopy studies confirm the presence of a correctly processed eGFP tag in the different eGFP-syntaxin/SNAP fusion protein engineered CHO-S cells

To determine the presence and correct folding of the eGFP tag in the eGFP-syntaxin/SNAP engineered CHO-S cells, fluorescence microscopy was performed to detect the eGFP fluorescence signal within the cells. For the different cell lines, cells were immobilised on coverslips after poly-L-lysine treatment (see 2.4.1). The cells were then observed using a LS620 microscope (Etaluma, USA) and fluorescent images collected. Figure 4.1 shows representative images collected for the engineered cell lines. All the eGFP-SNARE cell lines, except the CHO/MRXIP-GFP H cell line, contained a fluorescence signal confirming the presence of correctly folded eGFP tag (Figure 4.1). Differences in fluorescence intensity were observed between the different cell lines, notably between the different cell lines expressing the same protein of interest. For example, CHO/SNAP29 A had a stronger signal compared to CHO/SNAP29 B whilst no fluorescence signal above background was observed in the CHO/MRXIP-GFP H cell line. This result did not follow the expression profile as would be predicted from the previously undertaken flow cytometry analysis (see section 3.4.3) and likely reflects changes in the relative expression profiles since the flow cytometry analysis. Further, the flow cytometry analysis profile represents that from 10000 cells

whilst the microscopy analysis shows relative expression across a small number of cells. Regardless, this experiment successfully confirmed that the majority of the generated monoclonal cell lines had correct processing of the eGFP tag and a diversity in fluorescent intensity (and hence presumably of the fusion protein and syntaxin) as expected from the selection of cell lines with different profiles by flow cytometry after the limiting dilution process (see section 3.4.2).

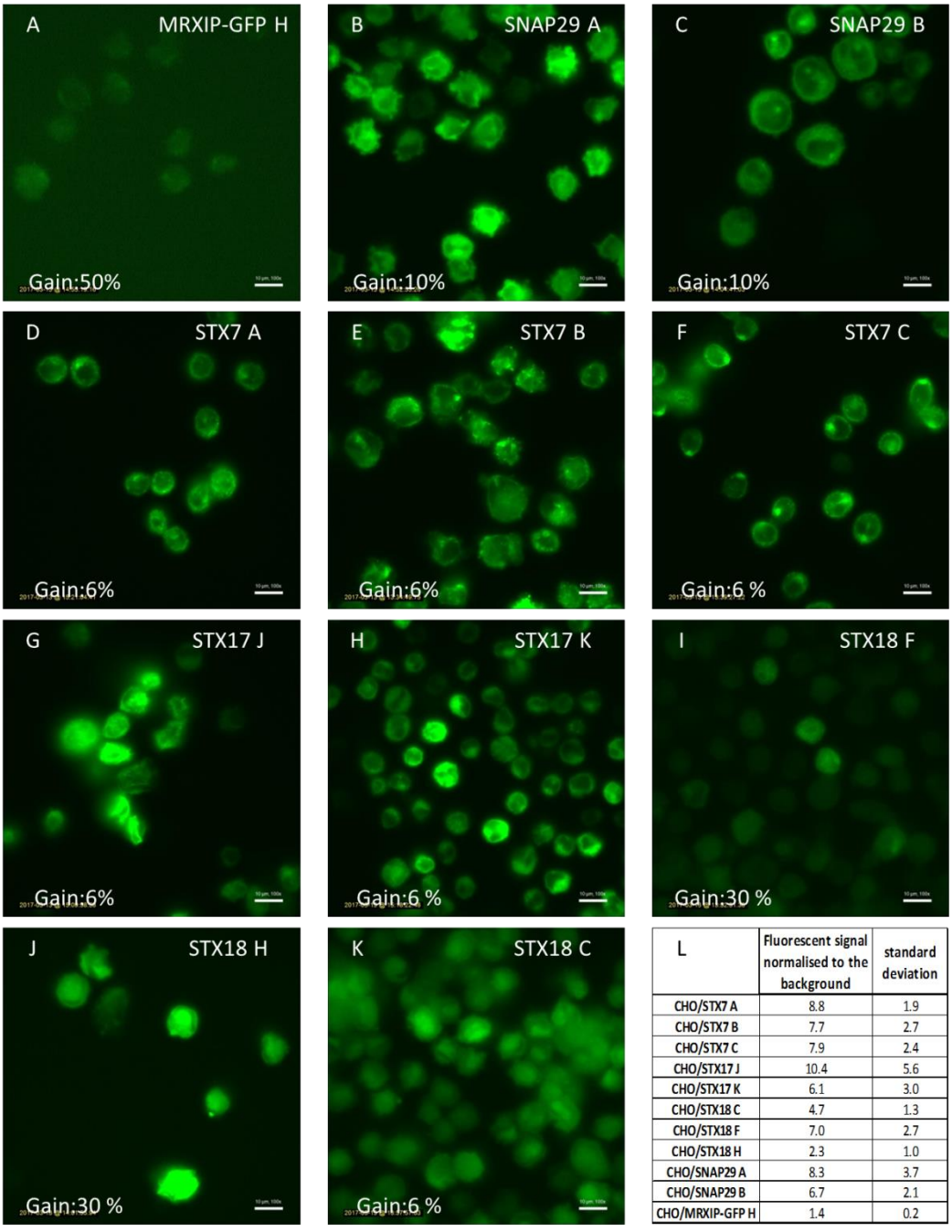

L	Fluorescent signal normalised to the background	standard deviation
CHO/STX7 A	8.8	1.9
CHO/STX7 B	7.7	2.7
CHO/STX7 C	7.9	2.4
CHO/STX17 J	10.4	5.6
CHO/STX17 K	6.1	3.0
CHO/STX18 C	4.7	1.3
CHO/STX18 F	7.0	2.7
CHO/STX18 H	2.3	1.0
CHO/SNAP29 A	8.3	3.7
CHO/SNAP29 B	6.7	2.1
CHO/MRXIP-GFP H	1.4	0.2

Figure 4.1. Fluorescent image analysis of the different monoclonal populations of eGFP-syntaxin/SNAP engineered CHO-S cells. After poly-L-lysine treatment of coverslips, cells were grown for 3 days on the coverslips before being fixed. Observation of the cells and image collection was undertaken using a LS620 microscope (Etaluma, USA). The gain was not consistent through the experiment and is indicated for each individual image. Magnification was 100X and the scale bar represents 10 µm. **A-K**, microscopic images for the different monoclonal cell lines. **L**, analysis of the average GFP fluorescence intensity for each cell in images A to K normalised to the background using ImageJ.

4.2.2. Western blot relative expression analysis of the eGFP-syntaxin/SNAP fused protein in the different CHO-S engineered monoclonal populations

Until this point, the CHO-S eGFP-syntaxin/SNAP engineered monoclonal cell lines had been selected based upon their fluorescence signal intensity from the eGFP moiety of the fused protein and not on the expression of the intact fused protein. Indeed, to facilitate selection it was assumed that the level of fluorescence was correlated to the expression of the fused protein. Although previous experiments had shown the expression of intact proteins in the stably expressing CHO-S engineered pools (see section 3.3.4), the expression profile and potential for fragmentation or cleavage of the eGFP from the fusion protein in the different monoclonal population could be different due to the selection and expansion procedure following limiting dilution cloning.

For every eGFP-syntaxin engineered CHO-S monoclonal cell line, total protein was extracted from a set number of viable cells and detection of the overexpressed eGFP-syntaxin fusion protein was assessed by western blot analysis using an anti-GFP antibody. Indicative resulting signals detected are shown in Figure 4.2A. A signal at the expected size was detected for all the different engineered cell lines except for CHO/STX18 H and CHO/STX18 C. The expected band sizes were 57, 60, 65 and 56 kDa for the STX7, STX17, STX18 and SNAP29 fused protein with eGFP. Low signal was detected for CHO/STX18 F even after a long exposition times (30 min) (Figure 4.2A). A similar experiment was then undertaken with the different eGFP-STX18 expressing cell lines using an antibody specific for STX18. Figure 4.2B confirmed that endogenous STX18 could be detected in all of the CHO-S engineered and host cells lines but that no expression of the exogenous eGFP-STX18 protein was detectable in the CHO/STX18 H cell line whilst for the CHO/STX18 F cell line there was a strong positive signal at the expected size (65 kDa). No data was obtained for CHO/STX18 C, the cell line was lost before the experiment so no material was available. Thus, this data shows that except for the CHO/STX18 H and C cell lines, there was a signal at the expected size of the eGFP-syntaxin/SNAP fusion protein confirming expression of the intact protein of interest.

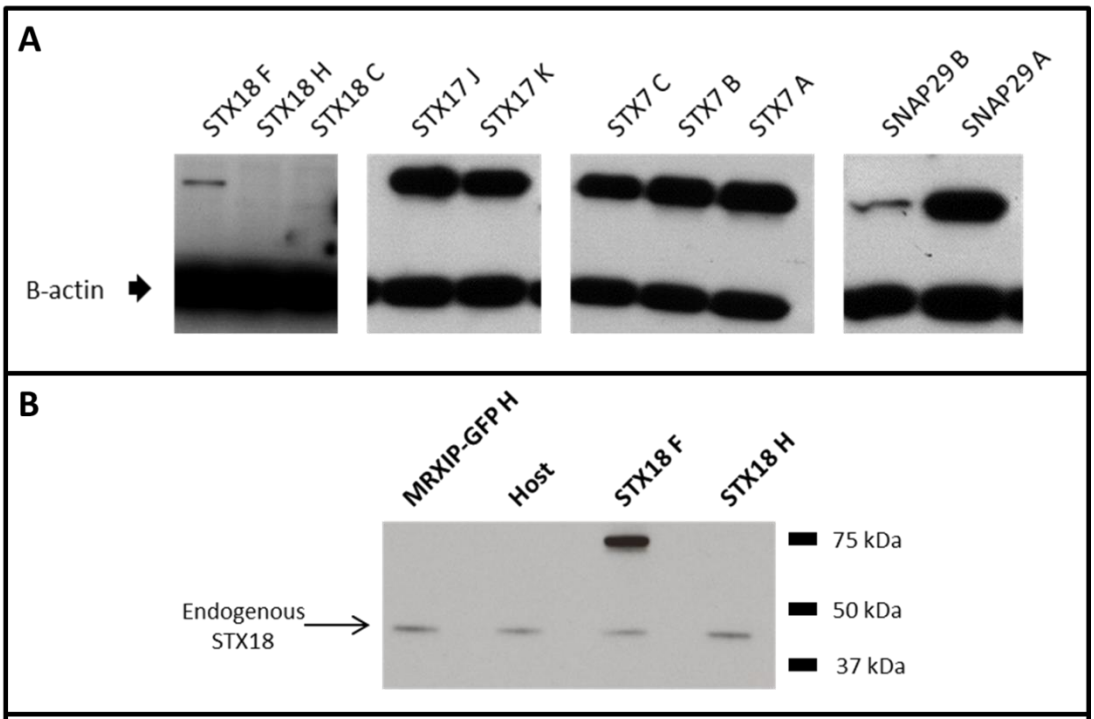

Figure 4.2. Expression analysis by western blot of eGFP-syntaxin/SNAP fusion protein expression in the different monoclonal cell lines. **A**, Anti-GFP (1:5000) and anti-β-actin (1:5000) antibodies were used for the detection of the fused proteins and the house keeping gene β-actin. **B**, Anti-STX18 antibody (1:1000) used for the detection of endogenous and ectopic STX18 and STX18 fused protein. Protein amount loaded into gels were identical for the different cell lines (A, 8 µg of protein B, 15 µg of protein).

In order to try and ascertain the relative difference in expression between individual clones of the eGFP-syntaxin/SNAP fusion protein, densitometry analysis was undertaken (Figure 4.3) based on the signal obtained in Figure 4.2A to rank the expression between the different clones. Indeed, one of the goals of generating monoclonal population was to obtain cell lines with different profiles of expression. After normalizing the signal intensity from the western blot experiment with the expression of the house keeping gene β-actin, it was determined that CHO/STX17 J had a higher level of expression than CHO/STX17 K (around 1.2 times more). CHO/SNAP29 B was expressing 2.5 times less than CHO/SNAP29 A, 0.52 compared to 1.32. For STX7 expressing cell lines, CHO/STX7 C (0.86) was expressing less than CHO/STX7 A and B (1.08 and 1.05). The difference of expression between CHO/STX7 A and B was small.

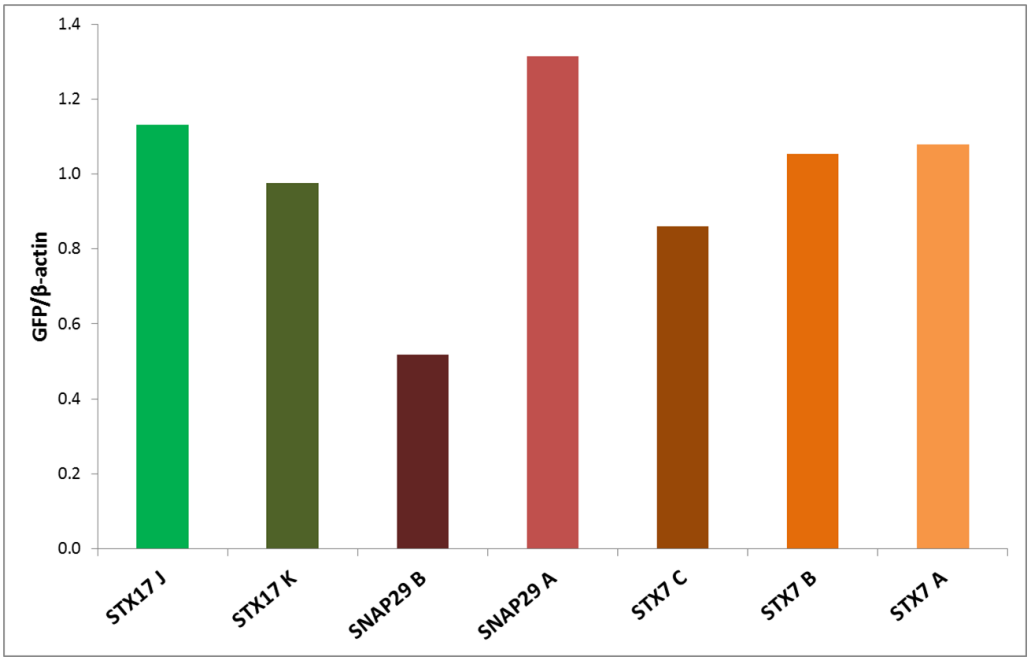

Figure 4.3. Quantification of the relative expression levels of the eGFP-syntaxin/SNAP fusion proteins in the different cell lines using densitometry from the images in Figure 4.2 (n=1). Densitometry was performed with ImageJ on the signal from Figure 4.2. and β-actin signal was used to determine reference expression levels.

4.2.3. Analysis of growth profiles during batch culture of the different eGFP-syntaxin/SNAP CHO-S engineered cell lines

After confirming the expression of the full length eGFP-syntaxin fusion protein and the correct folding of the eGFP tag in the different CHO-S engineered cell lines, the different monoclonal cell lines were further characterised with respect to growth characteristics. The viable cell concentration and culture viability were therefore monitored during batch culture to determine if there was any effect of the overexpression of the target proteins on cell growth compared to the host cell line. Experiments were also performed in shake flasks and spin tubes to determine if a change of scale or vessel in further experiments would impact upon the cell growth characteristics.

4.2.3.1. Growth assessment of SNARE engineered CHO-S cells in shake flasks

Cell lines were grown in 125 mL Erlenmeyer flasks with a vented cap and the cultures were initially inoculated at a concentration of 0.2 x 10^6 viable cells/mL with a viability >95% from an exponentially growing culture. The viable cell concentration and culture viability were then monitored daily using a Vi-CELL instrument. All cell lines were analysed with triplicate cultures being setup. Cells were incubated at 37˚C, 5% CO_2 and with shaking at 140 rpm.

The media used for the experiment was different for the engineered syntaxin/SNAP cell lines (CD-CHO + 8 mM L-glutamine + 7.5 µg/mL puromycin) compared to the host cell line (CD-CHO + 8 mM L-glutamine) in that the selection agents was maintained in the engineered cell lines.

Figure 4.4 shows the growth curve for the appropriate controls, the initial CHO-S non-engineered host cell line and two CHO-S eGFP expressing cell lines designated CHO/MRXIP-GFP L and H. These cell lines were expressing eGFP only from the same vector backbone and selection as the syntaxin engineered CHO-S cell lines. The CHO/MRXIP-GFP L eGFP expressing cell line and the original CHO-S host cell line showed a similar exponential phase growth profile whereas the CHO/MRXIP-GFP H control appeared to potentially have a faster growth rate during exponential phase and reached a peak viable cell concentration at 6.73 x 10^6 cells/mL. The growth phase for the CHO/MRXIP-GFP H cell line was also longer compared to the other cell lines. Despite the visual differences in the growth profiles described (Figure 4.4), there was no significant difference in the growth profiles as determined by one way ANOVA analysis of the means of the viable cell numbers at the different time points except on days 6 and 8, which showed a difference between the CHO-MRXIP-GFP H cell line and the other two.

The culture viability of the CHO/MRXIP-GFP L cell line started to decrease from day 4 under the batch culture conditions, falling below 10% on day 11 (Figure 4.4). CHO/MRXIP-GFP H showed a drop in culture viability only from day 7, but the reduction was more abrupt and the culture had a viability <10% by day 10 compared to the other CHO/MRXIP-GFP cell line. The non-engineered host cell line culture viability decreased from day 5 with the culture viability falling below 10% by day 10, although the culture was continued until day 13 to be able to compare this with the other cell lines. No statistical difference in the culture viability between the cell lines was discerned in the first 4 days of culture. As no statistical difference was found between the non-engineered host cell line and those engineered to express eGFP alone, it was decided to compare the growth results of the different engineered eGFP-syntaxin monoclonal population to the host cell line and CHO/MRXIP-GFP H. This would allow comparison to the original host cell and to cells which had been engineered to have the additional transcriptional and translational burden of eGFP expression and had been through the selection process but were not expressing the target syntaxin protein.

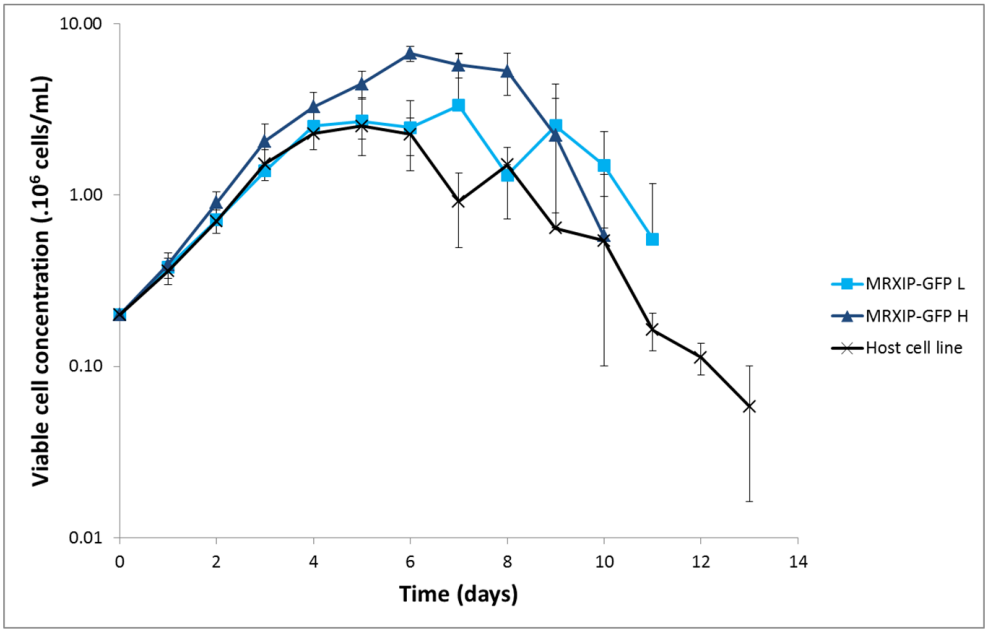

	Day 1	Day 2	Day 3	Day 4	Day 5	Day 6
MRXIP-GFP H	A	A	A	A	A	A
MRXIP-GFP L	A	A	A	A	A	B
Host cell line	A	A	A	A	A	B

	Day 7	Day 8	Day 9	Day 10	Day 11
MRXIP-GFP H	A	A	A	A	
MRXIP-GFP L	A	B	A	A	A
Host cell line	A		A	A	A

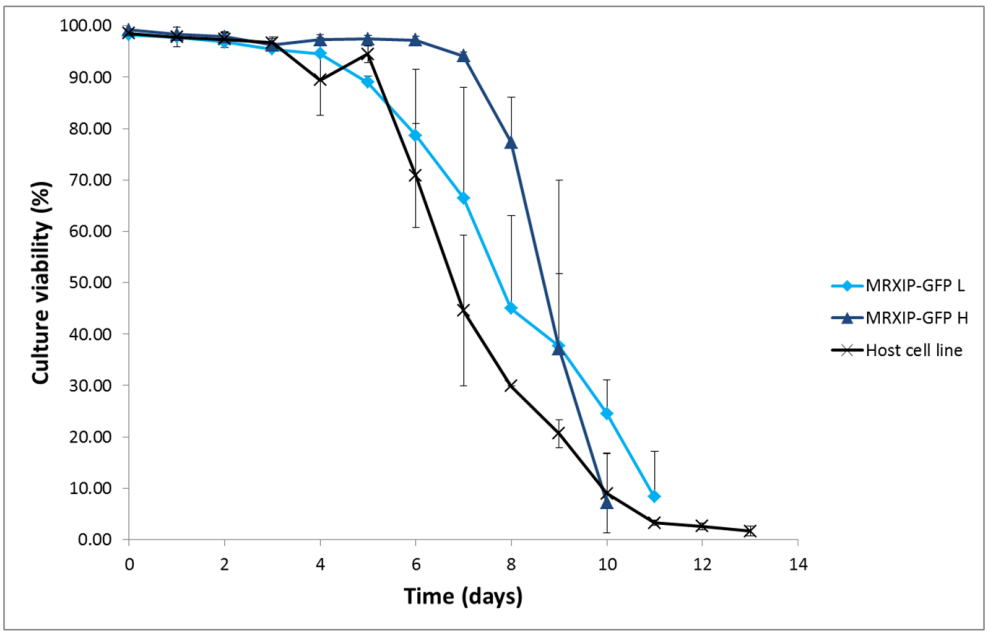

	Day 1	Day 2	Day 3	Day 4	Day 5	Day 6
MRXIP-GFP H	A	A	A	A	A	A
MRXIP-GFP L	A	A	A	A	B	A B
Host cell line	A	A	A	A	A	B

	Day 7	Day 8	Day 9	Day 10	Day 11
MRXIP-GFP H	A	A	A	A	
MRXIP-GFP L	A B	B	A	A	A
Host cell line	B		A	A	A

Figure 4.4. Cell growth and culture viability profiles of the different control cell lines CHO/MRXIP-GFP H, L (engineered to express eGFP alone) and the original host cell line (CHO-S) during batch cultivation in shake flasks. Cultures were inoculated at 0.2 x 10^6 viable cells/mL with culture viability >95%. Cultures were stopped when viability was <10%. Tables show one way ANOVA analysis followed by a Tukey test. Means that do not share a letter are statistically different. Error bars represent the standard deviation from the mean (n=3 except for CHO-S at day 8 where n=1).

After establishing the growth characteristics of the control cell lines, the profiles of the eGFP-syntaxin/SNAP engineered cells were compared to these. When comparing the STX7 expressing cell lines with the controls, there was no consistent pattern between the different eGFP-STX7 cell lines and the control with regard to cell growth (Figure 4.5). Up until day 4 the growth profiles were similar, however at this point they diverged from each other. CHO/STX7 A had a longer exponential phase than the host cell line and CHO/STX7 C, and the duration of its exponential phase was similar to CHO/STX7 B and the CHO/MRXIP-GFP H control although it didn't obtain as high viable cell concentration (3.97×10^6 cells/mL). The CHO/STX7 C exponential phase was shorter compared to the other cell lines and the maximum viable cell concentration reached, 1.70×10^6 cells/mL, was the lowest of all cell lines in this comparison. Among the STX7 expressing cell lines, CHO/STX7 B had the longest exponential phase and reached the highest viable cell concentration of 6.47×10^6 cells/mL on day 7. The STX7 expressing cell lines were all terminated at day 10 when the culture viability dropped below 10%. No statistical difference between the different STX7 engineered cell lines and the host cell line was observed when comparing the viable cell concentrations across the culture. It was clear from the error bars that even within triplicate cultures there was variability.

When the culture viability of STX7 expressing cells was considered, the culture viability of the CHO/STX7 C cell line declined first, beginning at day 3 (Figure 4.5). CHO/STX7 A had an almost identical culture viability profile as the host cell line with a decline in viability at day 4 until day 10. The CHO/STX7 B cultures showed an unusual profile with an initial drop in viability at the start of the experiment until day 2, whereupon its viability increased until day 5, after which the culture viability then decreased until the end of the experiment at day 10. Statistical analysis showed that across the 5 first days of culture there was no statistical difference in the culture viabilities, however after this there were statistical differences between cell lines as shown in Figure 4.5.

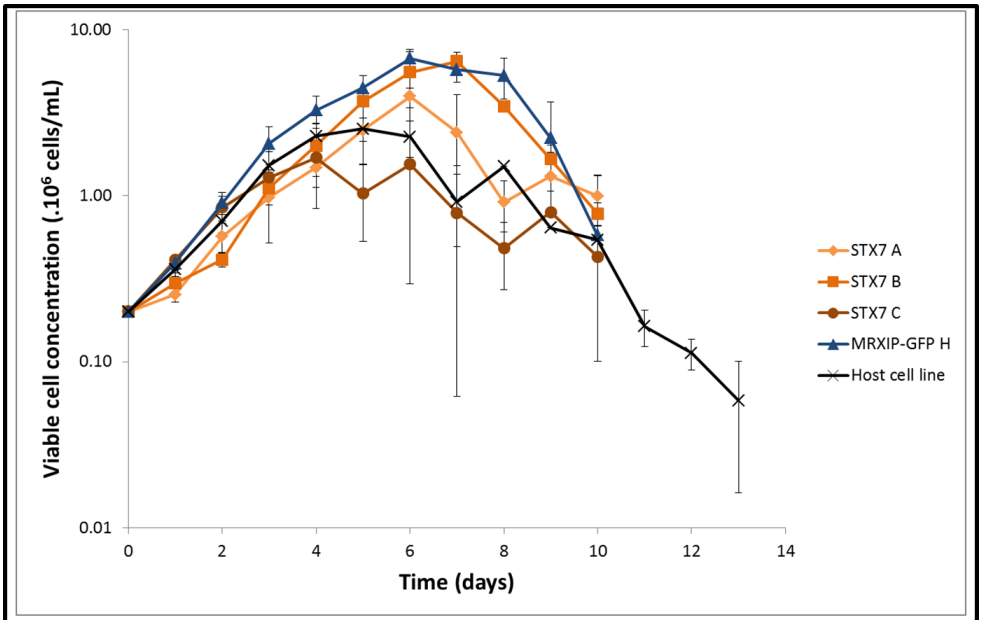

	Day 1	Day 2	Day 3	Day 4	Day 5	Day 6
STX7 A	C	B C	B	B	B C	A
STX7 B	B C	C	A B	A B	A B	A
STX7 C	A B	A B	A B	A B	C	A
MRXIP-GFP H	A	A	A	A	A	A
Host cell line	A	A B C	A B	A B	B C	A

	Day 7	Day 8	Day 9	Day 10
STX7 A	B	B	A	A
STX7 B	A	A	A	A
STX7 C	B	B	A	A
MRXIP-GFP H	A	A	A	A
Host cell line	B		A	A

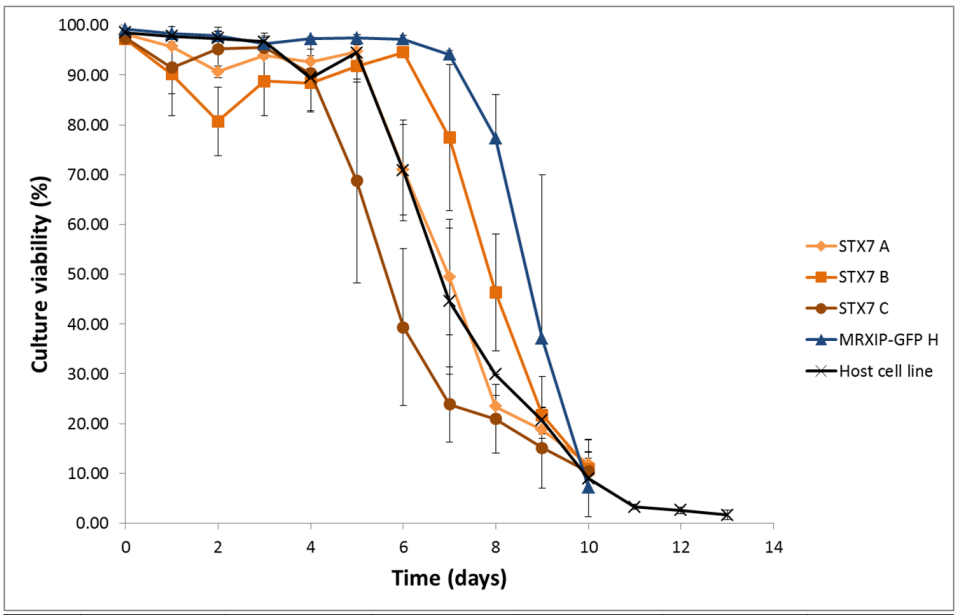

	Day 1	Day 2	Day 3	Day 4	Day 5	Day 6
STX7 A	A	A B	A	A	A	B
STX7 B	A	B	A	A	A B	A B
STX7 C	A	A	A	A	B	C
MRXIP-GFP H	A	A	A	A	A	A
Host cell line	A	A	A	A	A	B

	Day 7	Day 8	Day 9	Day 10
STX7 A	B C	C	A	A
STX7 B	A B	B	A	A
STX7 C	C	C	A	A
MRXIP-GFP H	A	A	A	A
Host cell line	C		A	A

Figure 4.5. Growth and culture viability profiles of the different eGFP-STX7 engineered cell lines CHO/STX7 A, B, C, and the control CHO/MRXIP-GFP H and host CHO-S cell line in shake flask batch culture. Cultures were inoculated at 0.2 x 10^6 viable cells/mL with viability >95%. Cultures were stopped when viability was <10%. Tables represent one way ANOVA analysis followed by a Tukey test. Means that do not share a letter are statistically different. Error bars represent the standard deviation from the mean (n=3 except for CHO-S at day 8 where n=1).

When the growth profiles of the cell lines engineered to express eGFP-STX17 were considered, a significant difference in growth was demonstrated compared to the control CHO/MRXIP-GFP H cell line (Figure 4.6). Both of the eGFP-STX17 cell lines had a slower growth rate, and reached lower maximum viable cell concentrations than the eGFP expressing control cell line. When compared to the non-engineered host cell line, CHO/STX17 J and K cell lines obtained similar cell concentrations (2.53×10^6, 3.05×10^6 and 2.49×10^6 viable cells/mL for the host cell line, CHO/STX17 K and CHO/STX17 J respectively) but their growth profile was slower (see Figure 4.6). The CHO/STX17 K and J cell lines followed a similar exponential phase of growth until day 6 at which point the growth profiles diverged. At this point the viable cell concentration of the CHO/STX17 J cell line began to decline whilst the viable cell number of the CHO/STX17 K cell line was maintained and was statistically different from day 10 to 12.

When comparing the culture viabilities of the different eGFP-STX17 cell lines (Figure 4.6), a decrease in culture viability for CHO/STX17 K was observed at day 1 before an increase until day 5. From day 6, the viability of CHO/STX17 K culture reduced slowly until day 13 with this culture lasting longer than the other cell lines. Viability of the CHO/STX17 J cultures started to decline from day 6 in line with that observed for the host cell line, but at a slower rate. The CHO/MRXIP-GFP H culture viabilities began to decline later than the other cell lines (day 7) but at a faster rate. The monitoring of the growth profiles of the STX17 engineered cell lines under batch culture conditions demonstrated that the CHO/STX17 K cultures maintained higher cell concentrations and maintained higher culture viability than the other cell lines at the end of the batch culture.

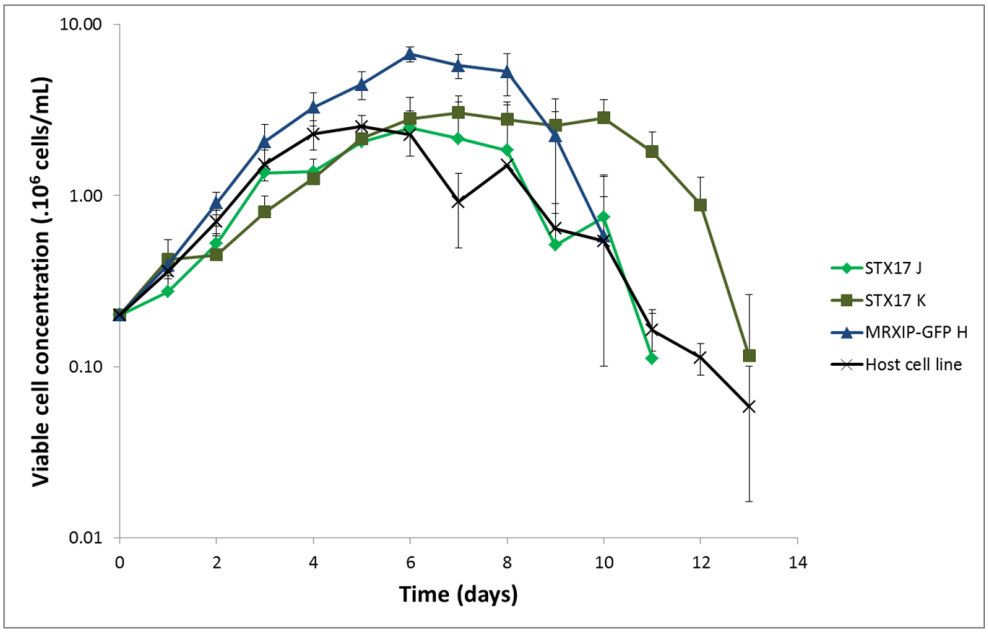

	Day 1	Day 2	Day 3	Day 4	Day 5	Day 6
STX17 J	A	B	A B	B	B	B
STX17 K	A	B	B	B	B	B
MRXIP-GFP H	A	A	A	A	A	A
Host cell line	A	A B	A B	A B	B	B
	Day 7	**Day 8**	**Day 9**	**Day 10**	**Day 11**	**Day 12**
STX17 J	B	B	A	B	B	
STX17 K	B	A B	A	A	A	A
MRXIP-GFP H	A	A	A	B		
Host cell line	B		A	B	B	B

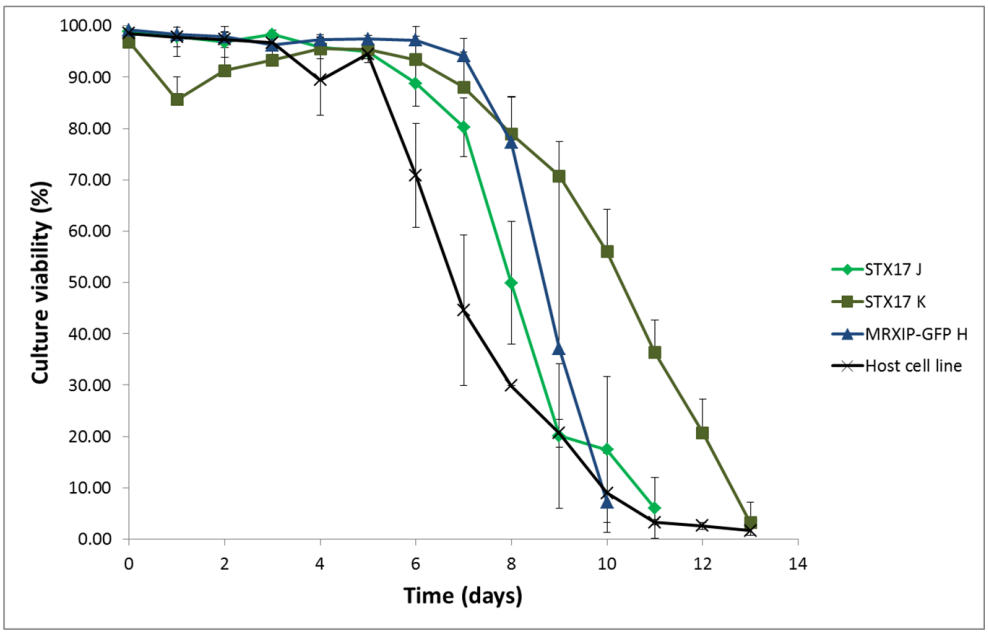

	Day 1	Day 2	Day 3	Day 4	Day 5	Day 6
STX17 J	A	A	A	A	A	A
STX17 K	B	A	B	A	A	A
MRXIP-GFP H	A	A	A B	A	A	A
Host cell line	A	A	A B	A	A	B
	Day 7	**Day 8**	**Day 9**	**Day 10**	**Day 11**	**Day 12**
STX17 J	A	B	B	B	B	
STX17 K	A	A	A	A	A	A
MRXIP-GFP H	A	A	A B	B		
Host cell line	B		B	B	B	B

Figure 4.6. Growth and culture viability profiles of the different CHO/STX17 K, J engineered cells, CHO/MRXIP-GFP H eGFP control and original host CHO-S cell line under batch culture conditions in shake flasks. Cultures were inoculated at 0.2 x 10^6 viable cells/mL with viability >95%. Cultures were stopped when viability dropped below 10%. Tables show results from one way ANOVA analysis followed by a Tukey test. Means that do not share a letter are statistically different. Error bars represent the standard deviation from the mean (n=3 except for CHO-S at day 8 where n=1).

Figure 4.7 shows the growth curve profiles for the cell lines expressing STX18 alongside the different controls. The first 4 days of exponential growth were more-or-less identical across the different cell lines, although the engineered cell lines expressing STX18 achieved higher viable cell concentrations than the host cell line, but not the GFP expressing control cell line. CHO/STX18 H cultures had a shorter exponential phase and attained lower cell concentrations on average, 5.43 x 10^6 cells/mL, compared to CHO/STX18 F, C and CHO/MRXIP-GFP H cultures. The CHO/STX18 C cultures attained similar viable cell concentrations to the control CHO/MRXIP-GFP H cultures, whilst CHO/STX18 F cultures reached higher viable cell concentrations (8.16 x 10^6 compared to 6.73 x 10^6 and 5.57 x 10^6 for CHO/MRXIP-GFP H and CHO/STX18 F respectively). The duration of the batch cultures was similar for the three STX18 expressing cell lines, showing a decrease in viable cell concentrations from day 7 for CHO/STX18 C and F cultures and day 8 for CHO/STX18 H cultures. When the culture viability was compared across the different STX18 expressing cell lines (Figure 4.7), the 3 clones had almost identical profiles with a rapid decline in viability from day 5 until the end of the culture at day 9.

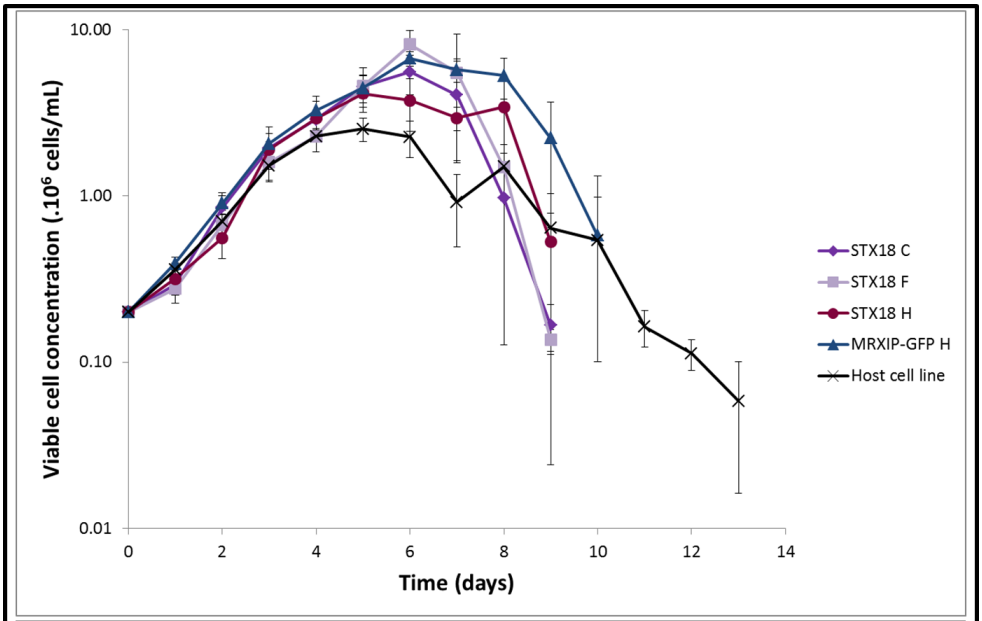

	Day 1	Day 2	Day 3	Day 4	Day 5	Day 6
STX18 C	A	A	A	A	A	A B C
STX18 F	A	A	A	A	A	A
STX18 H	A	A	A	A	A	B C
MRXIP-GFP H	A	A	A	A	A	A B
Host cell line	A	A	A	A	A	C

	Day 7	Day 8	Day 9
STX18 C	A	B	B
STX18 F	A	B	B
STX18 H	A	A B	A B
MRXIP-GFP H	A	A	A
Host cell line	A		A B

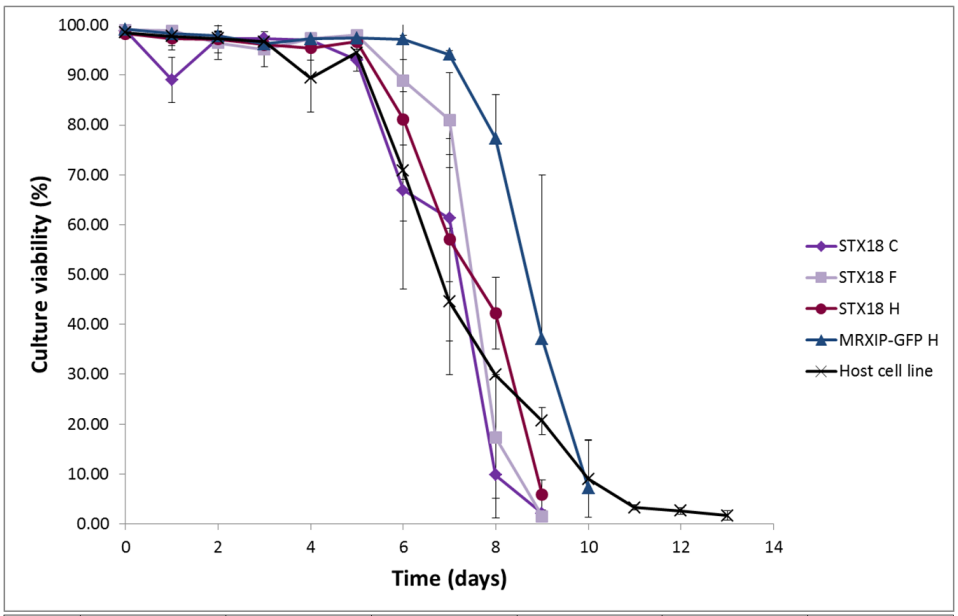

	Day 1	Day 2	Day 3	Day 4	Day 5	Day 6
STX18 C	B	A	A	A	C	A
STX18 F	A	A	A	A	A	A
STX18 H	A	A	A	A	A B	A
MRXIP-GFP H	A	A	A	A	A B	A
Host cell line	A	A	A	A	B C	A

	Day 7	Day 8	Day 9
STX18 C	A B C	C	A
STX18 F	A B	C	A
STX18 H	B C	B	A
MRXIP-GFP H	A	A	A
Host cell line	C		A

Figure 4.7. Growth and culture viability profiles of the different CHO/STX18 C, F, H, and CHO/MRXIP-GFP H and CHO-S host cell lines during batch culture in shake flasks. Cultures were inoculated at 0.2 x 10^6 viable cells/mL with viability >95%. Cultures were stopped when viability was <10%. Tables represent analysis by one way ANOVA followed by a Tukey test. Means that do not share a letter are statistically different. Error bars represent the standard deviation from the mean (n=3 except for CHO-S at day 8 where n=1).

Figure 4.8 shows the growth curves for CHO/SNAP29 A and B engineered cell lines, including the control cell lines, the original CHO-S and eGFP expressing CHO/MRXIP-GFP H cell line. CHO/SNAP29 B cultures showed slower growth compared to the other cell lines but reached higher viable cell concentrations than the host cell line. CHO/SNAP29 B cultures also had a longer exponential phase (until day 9) than the other cell lines, being 3 days longer than CHO/MRXIP-GFP H and CHO/SNAP29 A cultures. From day 9, CHO/SNAP29 B cultures maintained superior viable cell concentrations compared to the other cell lines while showing a slow decrease in viable cell concentration with time. The CHO/SNAP29 A culture growth curves were similar to the control CHO/MRXIP-GFP H profiles with an exponential phase until day 6 and a decline phase starting at day 8. CHO/SNAP29 A cultures achieved similar viable cell concentrations compared to the control CHO/MRXIP-GFP H cultures (5.75×10^6 cells/mL compared to 6.73×10^6 cells/mL).

When comparing the culture viabilities of the cell lines as shown in Figure 4.8, it was observed that the CHO/SNAP29 A culture viabilities decreased from day 3, slowly at first and more drastically from day 6. CHO/SNAP29 B culture viabilities started to decline at the same time as the control CHO/MRXIP-GFP H culture viability at day 6. However, whereas CHO/MRXIP-GFP H culture viability dropped suddenly, CHO/SNAP29 B culture viability reduced slowly over time until day 13 and was still 19.6% at day 13 when the culture was terminated.

Whereas the growth profiles of the majority of the engineered cell lines did not show any significant difference with the host and control cell lines, the CHO/SNAP29 B and CHO/STX17 K engineered cell lines demonstrated the ability to maintain viable cell concentrations at a higher amount longer than the other cell lines with an observed slow culture viability decrease for both cell lines towards the end of culture.

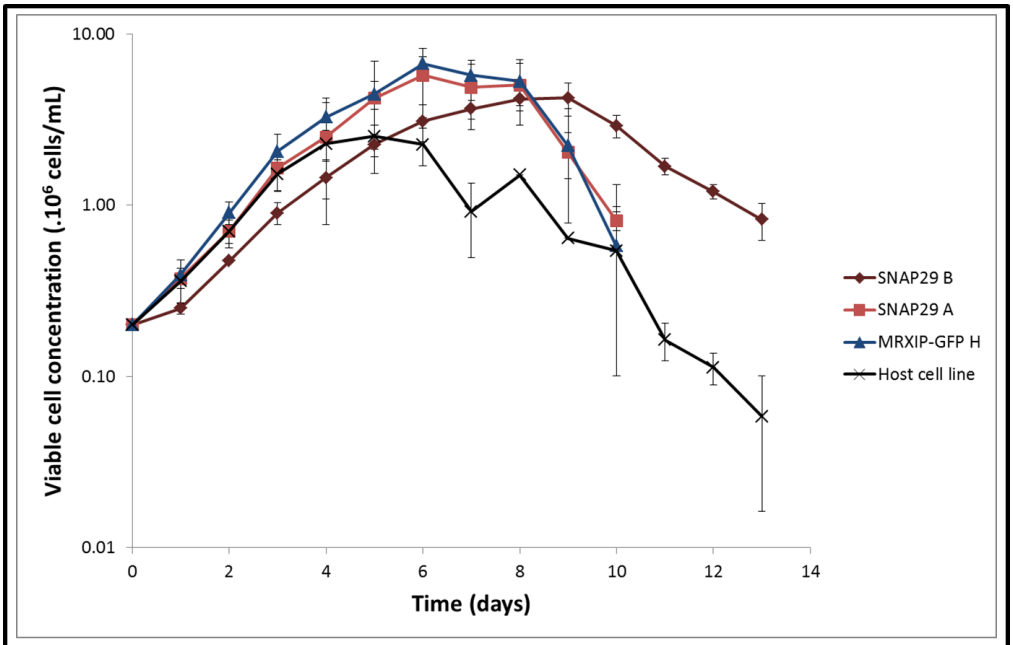

	Day 1	Day 2	Day 3	Day 4	Day 5	Day 6	Day 7
SNAP29 A	A	A B	A B	A	A	A B	A
SNAP29 B	A	B	B	A	A	B	A B
MRXIP-GFP H	A	A	A	A	A	A	A
Host cell line	A	A B	A B	A	A	B	B

	Day 8	Day 9	Day 10	Day 11	Day 12	Day 13
SNAP29 A	A	A B	B			
SNAP29 B	A	A	A	A	A	A
MRXIP-GFP H	A	A B	B			
Host cell line		B	B	B	B	B

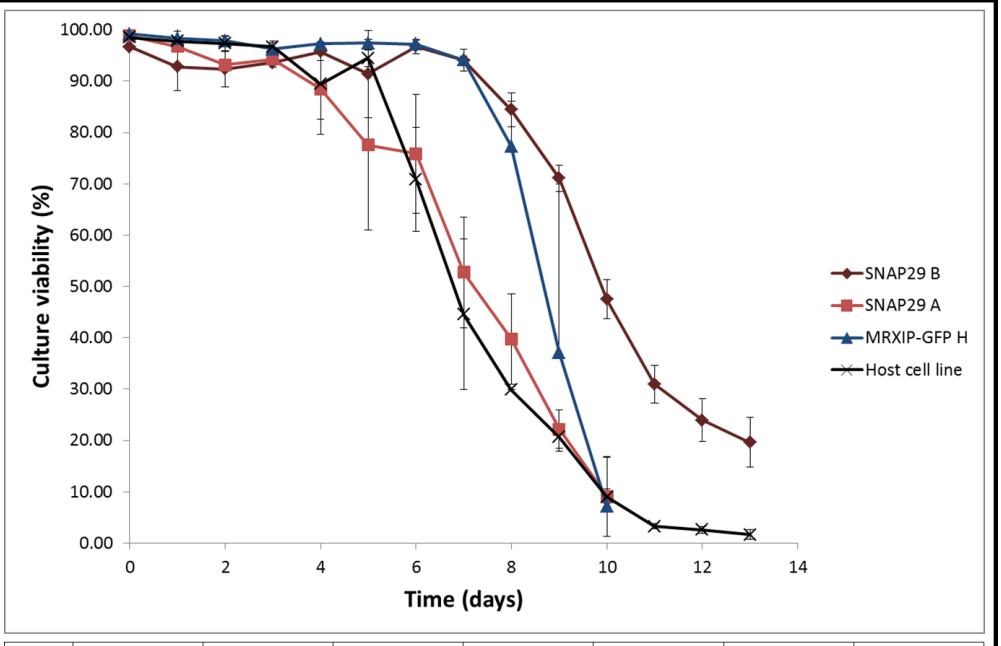

	Day 1	Day 2	Day 3	Day 4	Day 5	Day 6	Day 7
SNAP29 A	A	A B	A B	A	A	B	B
SNAP29 B	A	B	B	A	A	A	A
MRXIP-GFP H	A	A	A B	A	A	A	A
Host cell line	A	A B	A	A	A	B	B

	Day 8	Day 9	Day 10	Day 11	Day 12	Day 13
SNAP29 A	B	B	B			
SNAP29 B	A	A	A	A	A	A
MRXIP-GFP H	A	A B	B			
Host cell line		B	B	B	B	B

Figure 4.8. Growth and culture viability profiles of the different engineered cell lines CHO/SNAP29 A, B, and eGFP control CHO/MRXIP-GFP H and original CHO-S host cell line under batch culture in shake flasks. Cultures were inoculated at 0.2 x 10^6 viable cells/mL with viability >95%. Cultures were stopped when viability was <10%. Tables represent one way ANOVA analysis followed by a Tukey test. Means that do not share a letter are statistically different. Error bars represent the standard deviation from the mean (n=3 except for CHO-S at day 8 where n=1).

4.2.3.2. Growth assessment of SNARE engineered CHO-S cells in spin tubes

Batch culture growth profiles of a number of the syntaxin/SNAP engineered cells were also generated when grown in spin tubes. The aim of this experiment was to investigate if there was any impact of change of scale on the cell growth and culture viability of the cell lines to be further studied. Spin tubes and Erlenmeyer flasks are different in their geometry so the shaking pattern and gas intake are different. Cells were grown in a 10 mL culture volume and inoculated at 0.2 x 10^6 viable cells/mL with an initial viability >95%. Spin tubes with vented cap were used and cells were incubated at 37˚C, with shaking at 220 rpm and in a 5% CO_2 atmosphere. Cell numbers and culture viability were monitored everyday throughout cultures using a Vi-CELL instrument.

Figure 4.9 shows the results obtained using spin tubes for culturing the cell lines CHO/STX18 F, CHO/STX17 K, CHO/SNAP29 B, the eGFP control CHO/MRXIP-GFP H and the original CHO-S host cell line. CHO/SNAP29 B, CHO/MRXIP-GFP H and the host cell line had similar growth rates under these conditions, whilst CHO/STX18 F cultures had a faster growth rate and CHO/STX17 K had a slower growth profile. CHO/STX18 H cultures reached a maximal viable cell concentration of 14.3 x 10^6 cells/mL at day 5 of culture under these conditions. The exponential phase lasted until day 5 for the different cell lines before they entered a stationary phase or decline phase (CHO/STX18 F). Interestingly, a lag phase was observed for the different cell lines in the first 24 h, this might be due to the fact cells were subculture in 125 mL Erlenmeyer flasks prior the experiment.

Figure 4.9 reveals the different culture viability measurements across the batch culture. All the cell lines showed a decrease in culture viability from day 5, some more rapidly than others (CHO/STX18 H). It was also observed that CHO/STX17 K cultures maintained lower culture viability compared to the other cell lines across days 2-5 of culture (viability around 90%). CHO/SNAP29 B and CHO/MRXIP-GFP H cell lines maintained higher levels of culture viability longer than the other cell lines.

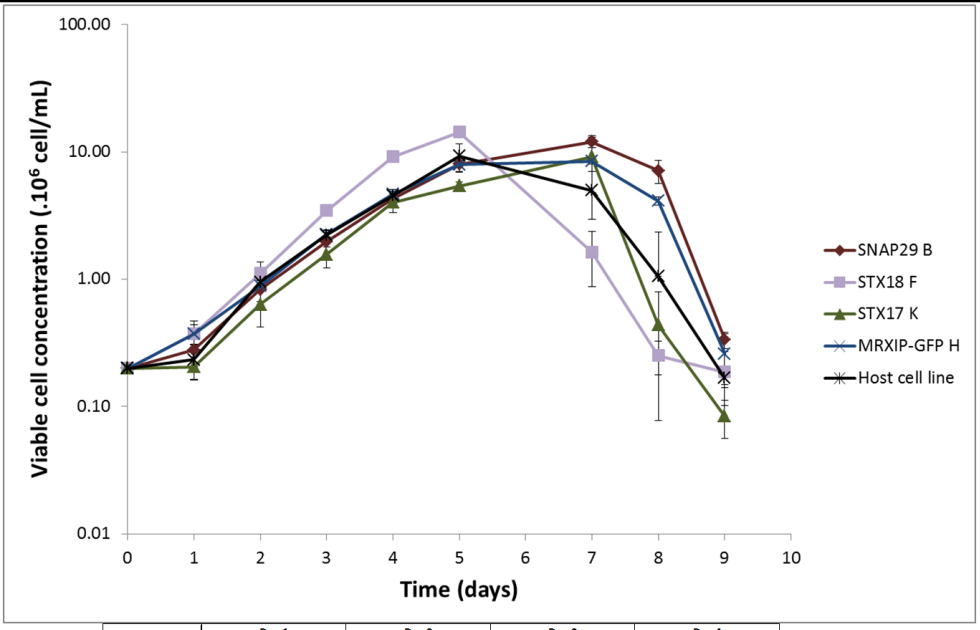

	Day 1	Day 2	Day 3	Day 4
STX17 K	A	A	C	B
STX18 F	A	A	A	A
SNAP29 B	A	A	B C	B
MRXIP-GFP H	A	A	B	B
Host cell line	A	A	B C	B

	Day 5	Day 6	Day 7	Day 8	Day 9
STX17 K	C	A B	C	B	B
STX18 F	A	C	C	A B	A B
SNAP29 B	B C	A	A	A	A
MRXIP-GFP H	B C	A B	B	A B	A B
Host cell line	B	B C	C	A B	A B

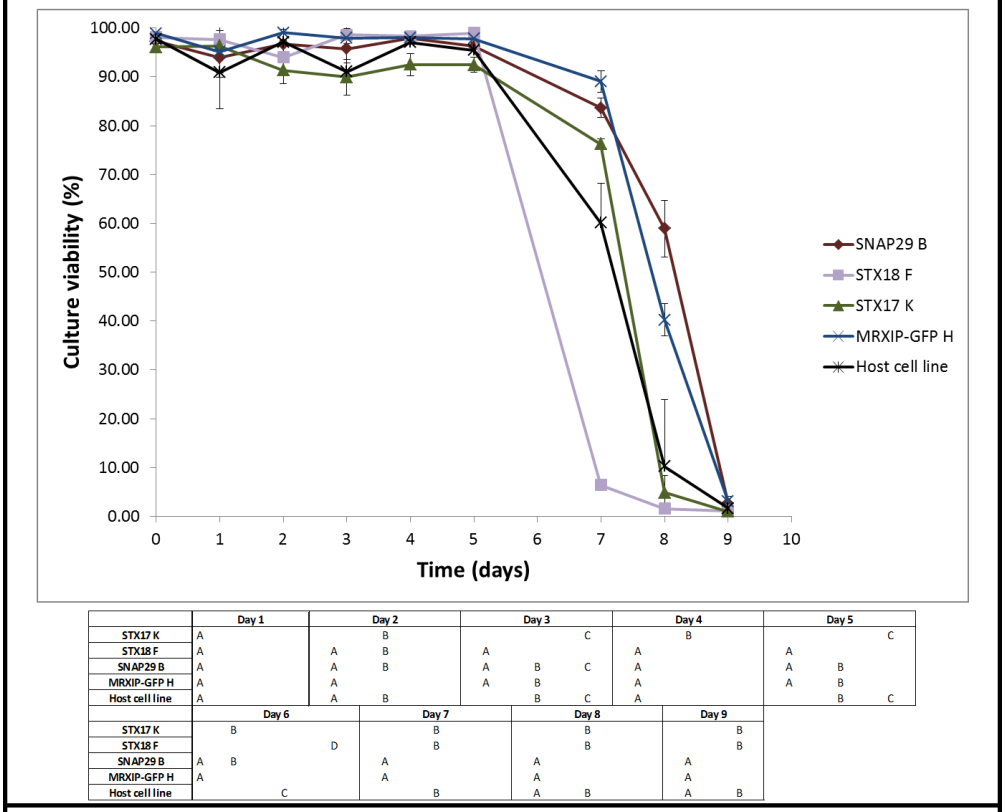

	Day 1	Day 2	Day 3	Day 4	Day 5
STX17 K	A	B	C	B	C
STX18 F	A	A B	A	A	A
SNAP29 B	A	A B	A B C	A	A B
MRXIP-GFP H	A	A	A B	A	A B
Host cell line	A	A B	B C	A	B C

	Day 6	Day 7	Day 8	Day 9
STX17 K	B	B	B	B
STX18 F	D	B	B	B
SNAP29 B	A B	A	A	A
MRXIP-GFP H	A	A	A	A
Host cell line	C	B	A B	A B

Figure 4.9. Growth and culture viability profiles of different eGFP-syntaxin/SNAP engineered and control cell lines when cultured in batch culture in spin tubes. Cultures were inoculated at 0.2 x 10^6 viable cells/mL with viability >95%. Cultures were stopped when culture viability was <10%. Tables represent one way ANOVA analysis followed by a Tukey test. Means that do not share a letter are statistically different. Error bars represent the standard deviation from the mean (n=3).

4.3. Characterisation of the impact of engineering over-expression of syntaxins and SNAP in CHO-S cells on recombinant protein productivity

After characterisation of the growth profiles of the different eGFP-syntaxin/SNAP over-expressing generated cell lines, transient transfection experiments were undertaken to determine if there was any effect of overexpression of the candidate SNAREs on secreted recombinant protein production. Transient transfection is a rapid technique to express recombinant material from a cell line (Geisse 2009). The advantages compared to stably expressing cell lines are that the method is rapid and can generate material in a few days and can be easy to optimise at small scale. The disadvantage is that the recombinant DNA is quickly lost from cells as cells grow and divide and that the number of copies of DNA introduced into each cell can be very variable. For the purposes of the studies here, two model commercial recombinant proteins were used, Adalimumab and Etanercept. Adalimumab (trade name Humira) is an IgG1 molecule acting as a TNF-inhibitor used to treat inflammatory type arthritis (Burmester et al. 2013). Etanercept (trade name Enbrel) is a fused protein of the TNF receptor and the constant heavy chain fragment of an IgG1. As for Adalimumab, Etanercept is also used to treat inflammatory type of arthritis (Scott 2014). The adalimumab plasmid, pAdalimumab, used in this study was previously generated by Linas Tamošaitis and the Etanercept plasmid, pEtanercept, by James Budge.

4.3.1. Rapid screening of the eGFP-syntaxin/SNAP engineered CHO-S monoclonal populations for any impact on the secretory productivity of a recombinant protein at small scale

Transient transfection in 96-DWPs was performed to determine if the overexpression of the syntaxin proteins had any effect on the secretory productivity of the cells. 96-DWPs are a vessel used for rapid screening of large amounts of different conditions in small volumes. The control cell lines (CHO-S, CHO/MRXIP-GFP H) and the engineered cell lines (CHO/MRXIP-GFP L, CHO/SNAP29 A, CHO/SNAP29 B, CHO/STX17 J, CHO/STX17 K, CHO/STX18 C, CHO/STX18 F, CHO/STX18 H, CHO/STX7 A, CHO/STX7 B and CHO/STX7 C) were transiently transfected with 1 µg/mL DNA of Adalumimab or Etanercept plasmid using the NovaCHOice reagent. Due to the low volume in the wells (300 µL), 2 plates were incubated in parallel for each condition; one to generate material for recombinant protein analysis and one dedicated to profiling of cell concentrations and culture viabilities. Cells

were incubated at 37˚C, 5% CO_2, in a 90% humidity atmosphere with shaking at 375 rpm. Cell pellets and supernatant were harvested 5 days after transfection for analysis.

4.3.1.1. Determination of the expression of the recombinant protein Etanercept

Figure 4.10 shows western blots analysis of Etanercept amounts in day 5 supernatants after probing with an anti-heavy chain antibody the amount of material generated across the different cell lines investigated. Samples were analysed under non-reduced conditions and normalised by loading the same volume of supernatant. Several bands were observed (Figure 4.10) and correspond to alternative forms of the recombinant protein produced. Under non-reducing conditions, disulphide bonds are preserved so only the full size molecule should be recognised (upper band, Figure 4.10). However, whilst the full, intact molecule was observed, a band corresponding to half size was also detected that corresponds to half-molecule forms (one unit of heavy chain and one unit of TNF receptor) and heavy chain fragments present in the media after breaking of the disulphide bonds. Indeed, release into the media by dying cells of enzymes with thioredoxin like activity is known to cause reduction of recombinant product (Koterba, Borgschulte, and Laird 2012; Trexler-Schmidt et al. 2010). On the blot, the upper band detected around 250 kDa represents the intact product and the lower band represents the signal from detection of half molecule (association of heavy chain fused to the TNF receptor fragment).

When the relative amounts of product were assessed by western blot across the different cell lines, compared to the controls, a more intense band was obtained for the analysis of the supernatant material of the replicates from the CHO/STX17 J and CHO/STX17 K cell lines (Figure 4.10). The CHO/STX17 J banding was stronger than that from the CHO/STX17 K cultures. When investigating the STX18 expressing clones, CHO/STX18 F and H cell lines showed a stronger Etanercept banding compared to the controls whereas the analysis of material from the STX18 C engineered cell line showed no observable difference in banding intensity compared to the control. CHO/STX18 C and CHO/STX18 H cell lines demonstrated no expression of eGFP-SNARE target, hence the difference of signal between the cell lines was probably due to the cell line performance. The amount of Etanercept from the STX18 F cell line was higher than that from the STX18 H cell line as indicated by the stronger banding pattern.

The data presented in Figure 4.10 for the relative amount of Etanercept in the culture supernatant from the CHO/SNAP29 A cell line was striking in that lack of a signal for the full

length molecule whereas for material from the CHO/SNAP29 B cell line there was a strong band present which was more intense than that from the controls. For analysis of material from the STX7 expressing cell lines (Figure 4.10), CHO/STX7 C and B appeared to have weaker expression than the controls. On-the-other-hand, supernatant material from the CHO/STX7 A cell line appeared to give a slightly stronger intensity band than the controls for 2 of the replicate cultures while one had a similar intensity to the controls.

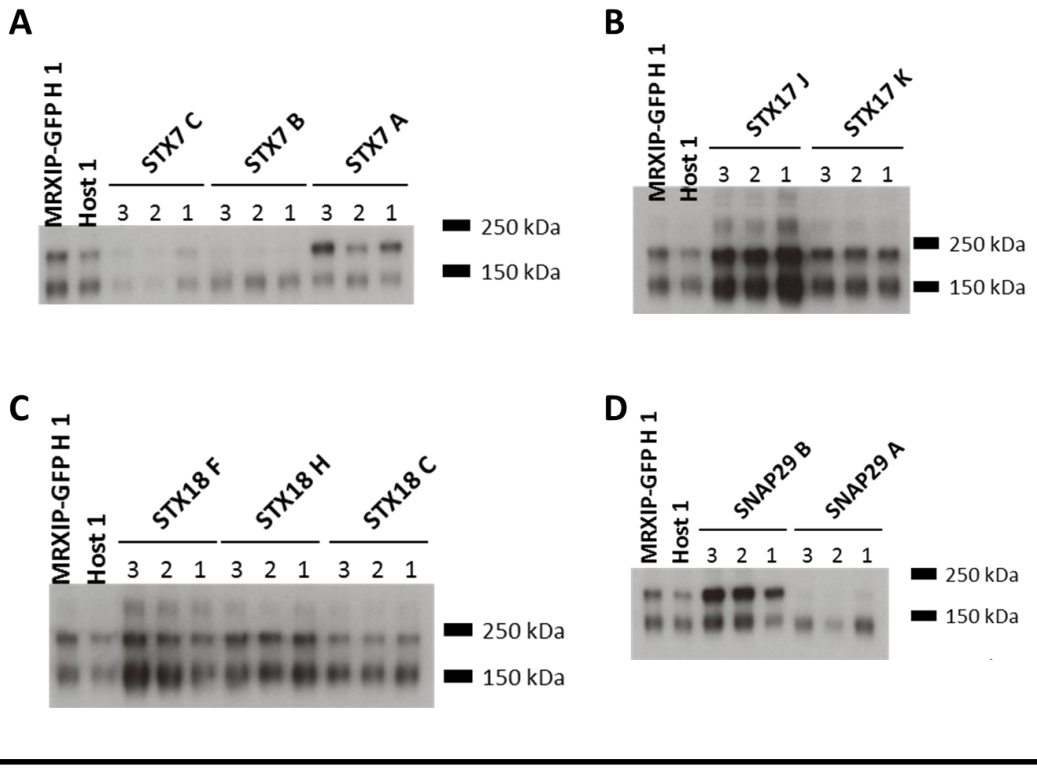

Figure 4.10. Western blot analysis of supernatant from day 5 after transient transfection of the different syntaxin/SNAP engineered cell lines with the plasmid pEtanercept in 96-DWPs. Equal volumes of culture supernatant were loaded for the different cell lines and anti-heavy chain antibody (1:10000) was used for signal detection. Results are separated as following: **A**, cell lines expressing GFP-STX7; **B**, cell lines expressing GFP-STX17; **C**, cell lines expressing GFP-STX18 and **D**, cell lines expressing GFP-SNAP29. Expected sizes are around 250 kDa for full size molecule and around 150 kDa for half molecule.

Whilst western blotting is a powerful technique for confirming the presence of a specific protein and the relative amounts between samples, it is only a semi-quantitative method at best. A more quantitative measurement of the amount of Etanercept in supernatant samples was therefore also undertaken using a commercially available Octet instrument and appropriate probes and standards to determine concentrations in the supernatants. Octet measurements were therefore undertaken on the different samples to determine their product concentration. Due to the low volumes from the 96 DWPs available, only one

measurement of each biological replicate was undertaken (no technical triplicate). Figure 4.11 summarises the Etanercept product titres obtained on day 5 supernatants after transient transfection of the different controls and syntaxin engineered cell lines. The host cell line and the two CHO/MRXIP-GFP control clones had a similar concentration of Etanecept present in the supernatant samples. The supernatant samples from the CHO/STX7 B and CHO/STX7 C cultures had similar amounts of Etanercept present to the controls whilst that from the SNAP29 A cell line was very variable across the 3 cultures (Figure 4.11). The remaining syntaxin/SNAP engineered cultures all showed an increase in Etanercept amounts in the supernatant compared to the control cultures. Two cell lines had higher Etanercept concentrations than the others or the controls, CHO/STX17 J and CHO/STX18 F with concentrations of 9.94 and 8.91 µg/mL respectively. The other cell lines, CHO/STX17 K, CHO/STX18 C, CHO/STX18 H, CHO/SNAP29 B and CHO/STX7 A yielded similar concentrations of Etanercept, all superior to the controls. As described above, the samples from the CHO/SNAP29 A cultures showed a huge variability in measurement. Specific productivity was not calculated due to the low number of data points.

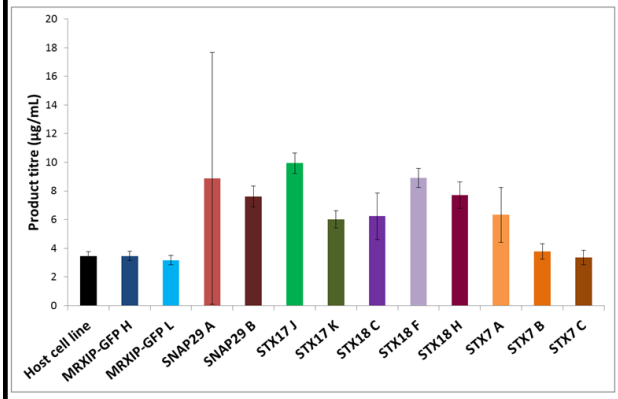

	Day 5					
Host cell line					E	F
MRXIP-GFP H					E	F
MRXIP-GFP L						F
SNAP29 A						
SNAP29 B	A	B	C			
STX17 J	A					
STX17 K			C	D	E	
STX18 C		B	C	D		
STX18 F	A	B				
STX18 H	A	B	C			
STX7 A		B	C	D		
STX7 B				D	E	F
STX7 C					E	F

Figure 4.11. Etanercept concentrations in the supernatants of the different syntaxin/SNAP engineered CHO-S cell lines as determined using an Octet instrument on day 5 of batch culture following transient transfection with pEtanercept in 96-DWPs. Error bars show the standard deviation from the mean (n=3). One way ANOVA analysis was performed on the mean followed by Tukey tests. Means sharing a letter are not significantly different. Results for CHO/SNAP29 A were not included in the statistical analysis due to their high variability.

Figure 4.12 shows the viable cell concentration at day 5 of batch culture after transfection for the different engineered cells and controls. CHO/STX17 J, CHO/STX18 H and CHO/STX7 A cell lines had low viable cell concentrations after 5 days of culture compared to the other cell lines and controls. CHO/MRXIP-GFP controls had higher viable cell concentrations 5

days post-transfection than the initial host cell line and all other cell lines. CHO/SNAP29 A and B cultures had similar viable cell concentrations after 5 days, higher than the host cell line. The CHO/STX17 K cultures had a much higher viable cell number compared to CHO/ STX17 J ($7.59.10^6$ and $1.37.10^6$ cells/mL respectively) on day 5 of the culture. CHO/STX18 C and CHO/STX18 F cultures had a similar viable cell concentration to the host cell line 5 days post-transfection whereas CHO/STX18 H cultures had a reduced viable cell concentration. Each clone of CHO/STX7 had a different viable cell concentration 5 days post-transfection during batch culture. CHO/STX7 C had a similar viable cell number to the host cell line while the CHO/STX7 B viable cell concentration was higher than that of the host. CHO/STX7 A cultures had a low viable cell concentration compared to the host cell line. No link between titre and viable cell line concentration was observed. Indeed, CHO/MRXIP-GFP H and L did not have a higher titre than that from other cell lines despite having higher viable cell concentrations on day 5 whereas CHO/STX17 J, CHO/STX18 H and CHO/STX7 A with lower viable cell concentrations had higher Etanercept titre.

Two profiles were noted for culture viability across the cell lines investigated (Figure 4.12), cell lines having a viability >80% after 5 days or having a viability between 50 and 70%. The host cell line and the empty vector controls had culture viabilities over 80%, as did CHO/SNAP29 B, CHO/STX17 K, CHO/STX18 C and CHO/STX18 F cultures. Cell lines CHO/STX17 J, CHO/STX18 H and CHO/STX7 A had a much lower viable cell concentration at day 5 but also had reduced culture viability compared to the other cell lines.

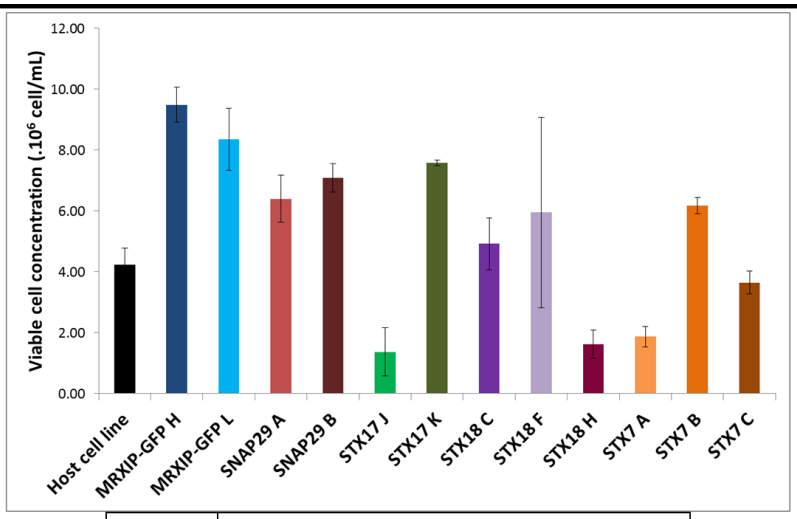

	Day 5						
Host cell line				D	E	F	G
MRXIP-GFP H	A						
MRXIP-GFP L	A	B					
SNAP29 A	A	B	C	D	E		
SNAP29 B	A	B	C	D			
STX17 J							G
STX17 K	A	B	C	D			
STX18 C			C	D	E	F	
STX18 F		B	C		E		
STX18 H							G
STX7 A						F	G
STX7 B		B	C	D	E		
STX7 C					E	F	G

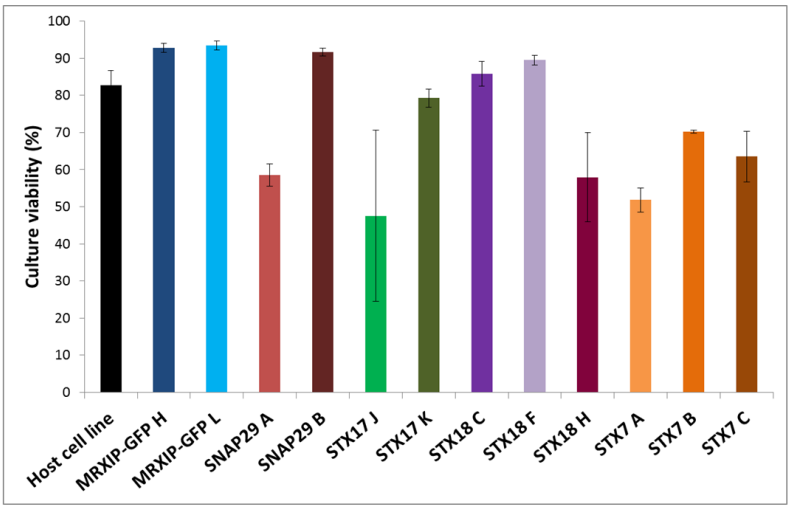

	Day 5				
Host cell line	A	B	C		
MRXIP-GFP H	A	B			
MRXIP-GFP L	A				
SNAP29 A				D	E
SNAP29 B	A	B			
STX17 J					E
STX17 K	A	B	C	D	
STX18 C	A	B	C		
STX18 F	A	B			
STX18 H				D	E
STX7 A					E
STX7 B		B	C	D	E
STX7 C			C	D	E

Figure 4.12. Viable cell concentration and culture viability of the different eGFP-syntaxin/SNAP engineered CHO-S and control cell lines monitored at day 5 after transient transfection with pEtanercept in 96-DWP batch culture. Error bars represent the standard deviation of the mean (n=3). One way ANOVA analysis was performed on the mean followed by Tukey tests. Means sharing a letter are not significantly different.

4.3.1.2. Determination of the expression of the recombinant protein Adalimumab

As for the Etanercept analysis, Figure 4.13 shows western blot analysis for the transient experiment in DWPs for secreted Adalimumab production from the control and different syntaxin/SNAP engineered cell lines. As for the results for the Etanercept analysis, samples were analysed under non-reduced conditions and normalised by using identical volumes. The upper band observed corresponds to the full IgG molecule (250 kDa), the middle band corresponds to half molecule (>150 kDa) and the lower band corresponds to heavy chain (>100 kDa) (Figure 4.13). A more intense signal was obtained for the different replicates of CHO/STX17 J and CHO/STX17 K cell line supernatants compared to the controls and samples from the CHO/STX17 J cell line replicates had a stronger signal than CHO/STX17 K. For STX18 expressing cell lines, CHO/STX18 F and CHO/STX18 H had stronger band intensities for the IgG expression than the controls while the samples from the CHO/STX18 C cell line had a similar band intensity. Analysis of samples from the CHO/SNAP29 B cell line had a strong band intensity compared to the controls whereas samples from the CHO/SNAP29 A cell line had a weaker signal compared to the controls (Figure 4.13). Samples from CHO/STX7 A and B had similar band intensities as the controls suggesting that the amount of IgG expressed was similar whilst samples from the transient transfection of the CHO/STX7 C cell line had a lower band intensity compared to the controls.

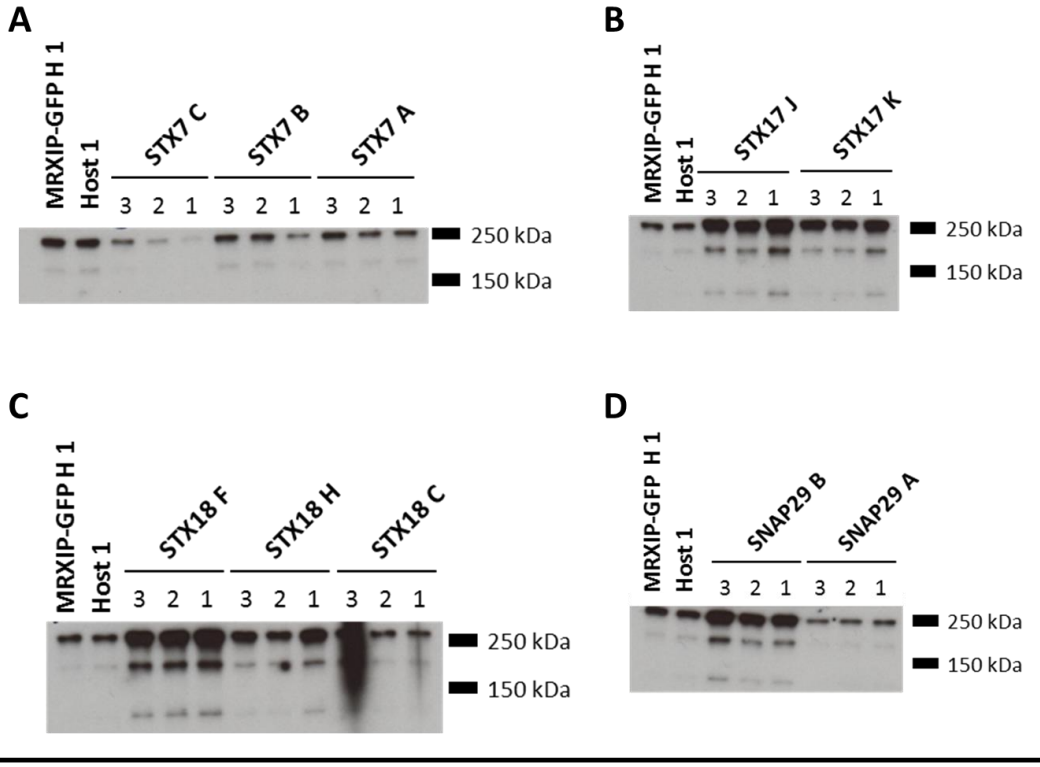

Figure 4.13. Western blot analysis of supernatant samples from day 5 batch cultures after transient transfection of the different syntaxin/SNAP engineered CHO-S cell lines with the plasmid pAdalimumab in 96-DWPs. Equal volumes of supernatant were loaded for the different conditions and anti-heavy chain antibody (1:10000) was used for signal detection. Results are separated as following: **A**, cell lines expressing GFP-STX7; **B**, cell lines expressing GFP-STX17; **C**, cell lines expressing GFP-STX18 and **D**, cell lines expressing GFP-SNAP29. Expected sizes are around 250 kDa for full size molecule, around 150 kDa for half molecule and around 100 kDa for the heavy chain.

Figure 4.14 shows the Octet analysis measurement on the different supernatants on day 5 after transient transfection with pAdalimumab to determine IgG concentration. The host cell line and CHO/MRXIP-GFP H and L cell lines had a similar IgG titre after 5 days. The CHO/STX18 H cell line yielded the highest average titre of 8.1 µg/mL of Adalimumab although there was high variability between the replicate samples. The CHO/STX18 F, CHO/STX17 J and CHO/SNAP29 B engineered cell lines all yielded a similar concentration of IgG product as determined by the Octet analysis to that of the CHO/STX18 H cell line without as much variability across the replicate samples. The titre of the cell lines expressing STX7 were more-or-less identical and not significantly different from the controls as was the IgG yield from the CHO/SNAP29 A, CHO/STX17 K and CHO/STX18 C cell lines (Figure 4.14).

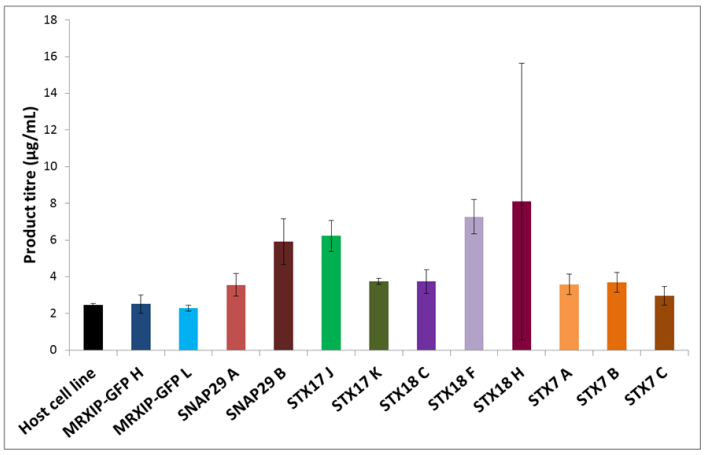

	Day 5
Host cell line	B
MRXIP-GFP H	B
MRXIP-GFP L	B
SNAP29 A	B
SNAP29 B	A
STX17 J	A
STX17 K	B
STX18 C	B
STX18 F	A
STX7 A	B
STX7 B	B
STX7 C	B

Figure 4.14. IgG titre results obtained by Octet measurement of supernatants from day 5 following the transient transfection with pAdalimumab in 96-DWPs of the different syntaxin/SNAP engineered and control cell lines. Error bars show the standard deviation from the mean (n=3). One way ANOVA analysis was performed on the mean followed by Tukey tests. Means sharing a letter are not significantly different. Results for CHO/STX18 H were not included in the statistical analysis due to their high variability.

When the viable cell number 5 days post-transfection of the Adalimumab plasmid into the different cell lines was investigated, a similar pattern to that observed in the transient DWP experiment for Etanercept was observed (Figure 4.15). On day 5, the CHO/MRXIP-GFP H and L cell lines had the highest viable cell concentrations whereas CHO/STX17 J, CHO/STX18 H and CHO/STX7 A cell lines had low viable cell concentrations at day 5 compared to the other cell lines (Figure 4.15). The host cell line had a comparable viable cell concentration to the CHO/SNAP29 A, CHO/STX18 C and CHO/STX7 B cell lines. Cell lines CHO/SNAP29 B and CHO/STX17 K had similar viable cell concentrations but these were statistically lower than the control CHO/MRXIP-GFP cell lines. The viable cell concentration in CHO/SNAP29 B cell line cultures was higher than that of the CHO/SNAP29 A cell line whilst CHO/STX17 K had a considerable difference in viable concentration compared to the CHO/STX17 J cell line. Cell lines expressing STX7 also had different viable cell concentrations on day 5 after transfection for each clone, with CHO/STX7 B having the highest and CHO/STX7 A the lowest (Figure 4.15).

Culture viability was also monitored at day 5 of the culture after transient transfection and culture viabilities are reported in Figure 4.15. The two different groups or trends observed for the previous transient transfection with pEtanercept with regard to culture viability were once again observed. The two groups were split into those with cultures with a viability of approximately 80% such as the controls (host cell line, CHO/MRXIP-GFP H and L)

and cell lines with a culture viability around 50%. Except for cell line CHO/STX18 C, it was noted that cell lines with low viable cell concentration had also lower culture viabilities.

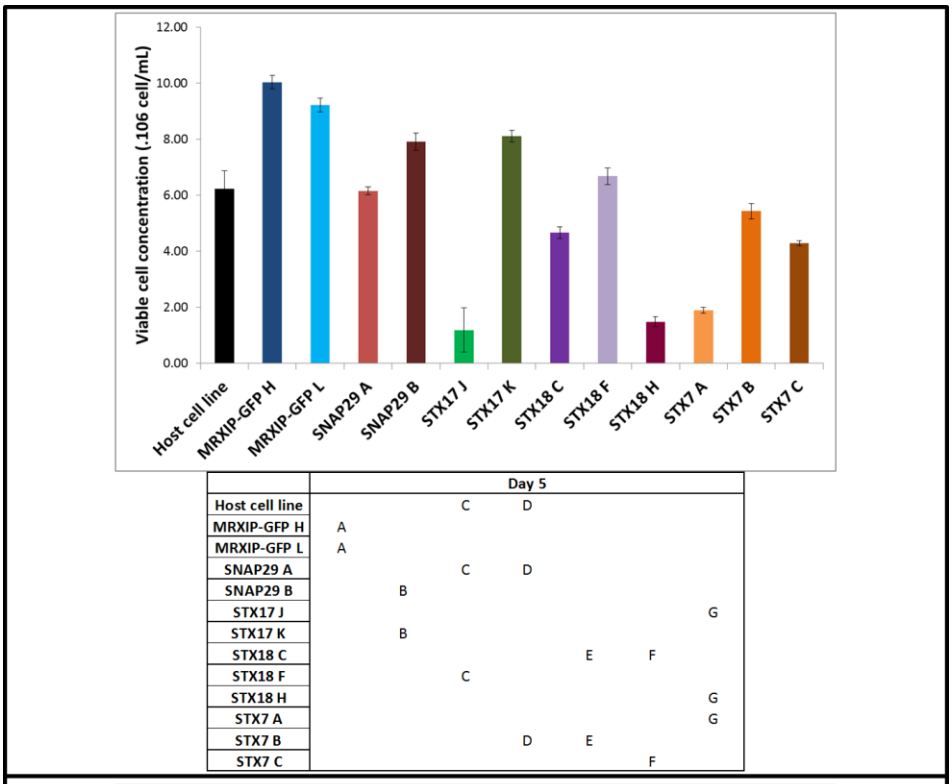

	Day 5
Host cell line	C D
MRXIP-GFP H	A
MRXIP-GFP L	A
SNAP29 A	C D
SNAP29 B	B
STX17 J	G
STX17 K	B
STX18 C	E F
STX18 F	C
STX18 H	G
STX7 A	G
STX7 B	D E
STX7 C	F

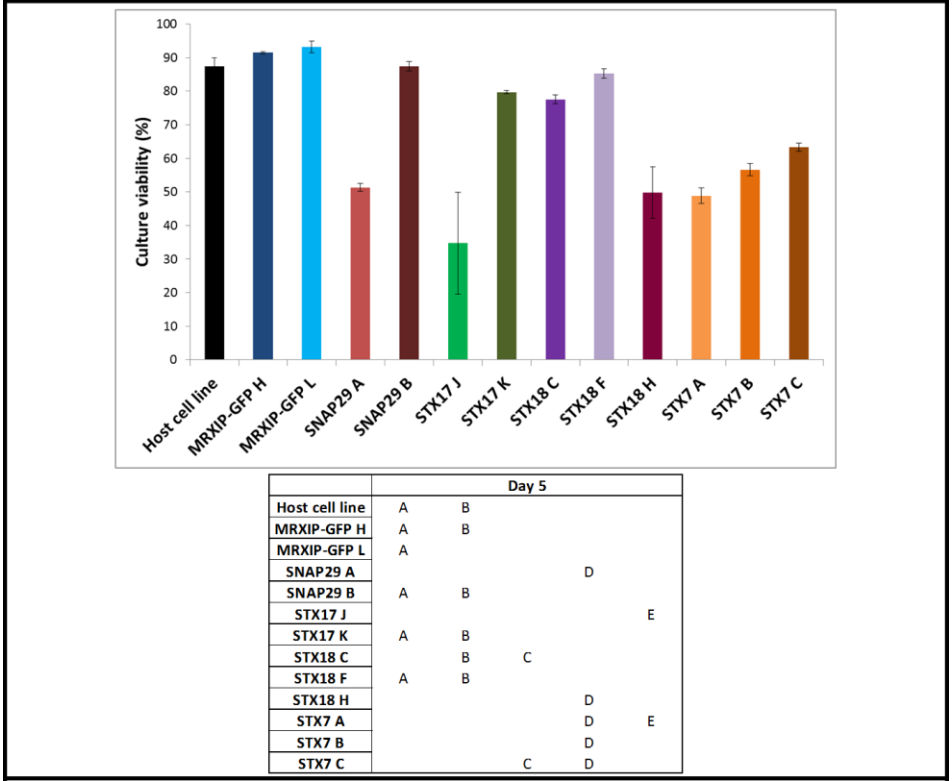

	Day 5
Host cell line	A B
MRXIP-GFP H	A B
MRXIP-GFP L	A
SNAP29 A	D
SNAP29 B	A B
STX17 J	E
STX17 K	A B
STX18 C	B C
STX18 F	A B
STX18 H	D
STX7 A	D E
STX7 B	D
STX7 C	C D

Figure 4.15. Viable cell concentration and culture viability monitored at day 5 after transient transfection with pAdalimumab of the different clonal cell lines in 96-DWPs. Error bars represent the standard deviation of the mean (n=3). One way ANOVA analysis was performed on the means followed by Tukey tests. Means sharing a letter are not significantly different.

4.3.2. Investigating the impact of syntaxin/SNAP engineering of CHO-S cells on secretory productivity under fed-batch culture conditions

The previous work described in the above sections assessed the impact of SNARE engineering of CHO cells on the secretory productivity of two model biotherapeutic proteins under batch culture conditions. A common procedure to increase product titre and cell growth is to implement a feed strategy in the process (Xie, Zhou, and Robinson 2003), turning the process into a fed batch culture. Through the culture, cells will consume different metabolites present in the media at different rates and produce by-products such as lactate and ammonium that are toxic to the cells (Hassell, Gleave, and Butler 1991; Lao and Toth 1997). Feeding strategies are specifically design to supply the cells with fresh metabolites that are reduced or depleted from the media and maintain high levels of carbon source in order to ensure cells obtain the highest possible maximum viable cell concentration in the shortest possible time and then to maintain the cells in a stationary phase whilst production of the target biotherapeutic protein is achieved. The choice of the feed and the feeding strategy vary depending on the cell line and media used. In the case of the work here, a commercially available efficient feed B was used because it is recommended by the manufacturer when the principal media is CD-CHO. The fed batch experiments undertaken here were completed using spin tubes which are vessels with a typical working volume of 10 mL, providing more material for analysis than the 96 DWPs.

Cultures were initially inoculated at 0.5 x 10^6 viable cells/mL with a viability >95%. Transient transfection was then undertaken with 1 µg/mL DNA using NovaCHOice reagent with either the pEtanercept or pAdalimumab expression plasmids to allow transient expression of the target molecules. The starting volume of the culture was 10 mL in spin tubes with two sampling points, day 3 and 5 post-transfection. After sampling on day 3, 15% v/v Efficient feed B was added to cultures as a feed strategy. Cultures were incubated at 37˚C with shaking at 240 rpm and 5% CO_2 was supplemented manually.

4.3.2.1. Fed-batch analysis of Adalumimab expression from syntaxin/SNAP engineered CHO-S cells

Western blot analysis on day 5 post-transfection supernatant samples allowed an initial qualitative assessment of relative product yields from the different cell lines investigated (Figure 4.16). There was a small visual difference between the banding intensity, and hence expression, of the IgG molecule from the host cell line and from the CHO/MRXIP-GFP H cell

lines that had a more intense band (Figure 4.16). The banding pattern, and hence IgG expression, from the CHO/STX17 J samples were more intense than the controls and CHO/STX17 K and STX18 F whilst those from the CHO/STX17 K cell line were also more intense than those from the controls. For samples from the CHO/STX18 F cell line, the band intensity was much more similar to that from the CHO/MRXIP-GFP H samples. The expression, as determined by western blot, from the CHO/SNAP29 B cell line was higher than the controls and the CHO/SNAP29 A cell line. The expression from the other cell lines showed no consistent patterns between replicates and cell lines (Figure 4.16).

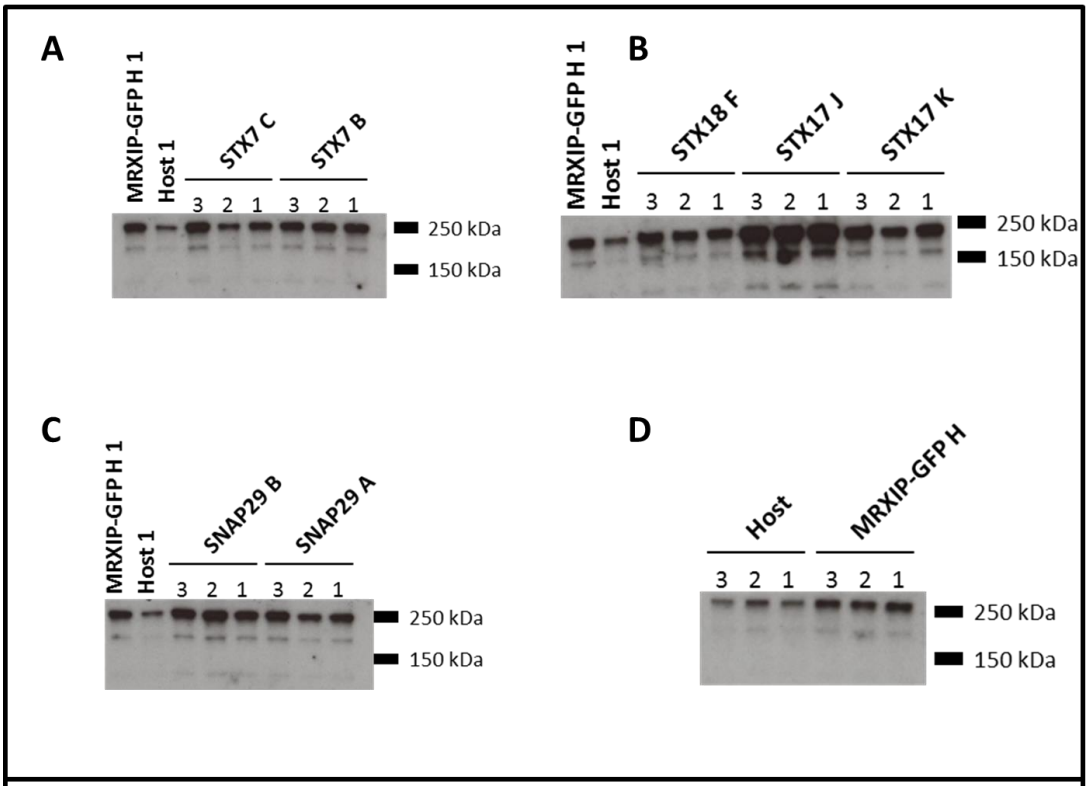

Figure 4.16. Western blot analysis of supernatant samples from day 5 post-transfection fed-batch cultures of the different syntaxin/SNAP engineered cell lines with the plasmid pAdalimumab. Equal volumes of supernatant were loaded for the different conditions and anti-heavy chain antibody (1:10000) was used for signal detection. Results are separated as following: **A**, cell lines expressing GFP-STX7; **B**, cell lines expressing GFP-STX17 or GFP-STX18; **C**, cell lines expressing GFP-SNAP29 and **D**, Host cell line and GFP expressing cell line. Expected sizes are around 250 kDa for full size molecule, around 150 kDa for half molecule and around 100 kDa for the heavy chain.

The western blot analysis in figure 4.16 suggested that under fed-batch conditions some of the cell lines yielded higher IgG concentrations than the control samples and therefore a more quantitative analysis was undertaken. Figure 4.17 presents Octet analysis of supernatant samples from day 3 and 5 for the transient production of Adalimumab under the described fed-batch conditions. The CHO/STX17 J cell line, with a final concentration at

day 5 of 3.04 µg/mL (5-fold more than the host cell line), had the highest concentration of IgG in agreement with the western blot data. The supernatants from cell lines CHO/STX17 K, CHO/STX7 B and CHO/STX18 F also had a significantly higher concentration of IgG compared to the host cell line whereas the cell lines CHO/MRXIP-GFP H, CHO/SNAP29 A and B had a similar titre to the controls (Figure 4.17). The titre profiles between the different cells lines at day 5 were reflective of those at day 3 and there was not a large increase in titre between day 3 and 5, suggesting that most of the expression of the recombinant product happened in the first 3 days. Compared to the experiment carried in 96 DWPs (see section 4.2.3), the range of titres obtained were reduced.

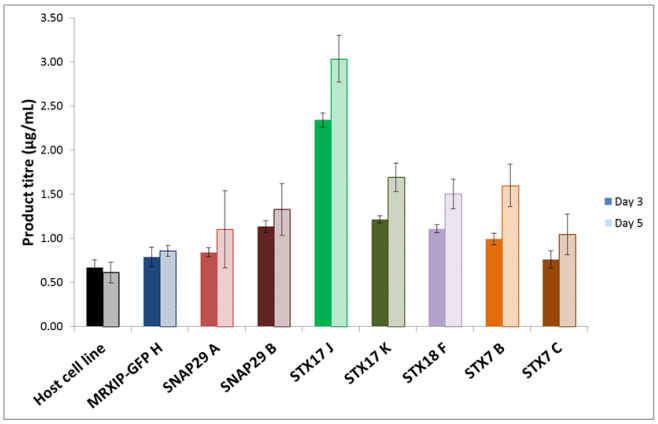

	Day 5		
Host cell line			D
MRXIP-GFP H		C	D
SNAP29 A	B	C	D
SNAP29 B	B	C	
STX17 J	A		
STX17 K	B		
STX18 F	B	C	
STX7 B	B		
STX7 C	B	C	D

Figure 4.17. IgG titre results as determined by Octet measurements on supernatants from day 3 and 5 after transient transfection with pAdalimumab in fed-batch cultures of the control and syntaxin/SNAP engineered CHO-S cell lines. Plain bars represent day 3 data and patterned bars represent day 5 data. Error bars show the standard deviation from the mean (n=3). One way ANOVA analysis was performed on the means from day 5 followed by Tukey tests. Means sharing a letter are not significantly different.

When the viable cell concentrations form the fed-batch cultures were analysed (Figure 4.18), different profiles were obvious. The host cell line and CHO/STX17 J cell line viable cell number declined during across the whole culture period. Cell lines CHO/STX18 F and CHO/SNAP29 B initially showed a decline in viable cell numbers before increasing between day 3 and 5. Some cell lines had a constant increase in viable cell number across the experiment such as CHO/STX7 B, CHO/MRXIP-GFP H and CHO/STX17 K. Cell lines CHO/SNAP29 A and CHO/STX7 C cultures had a small increase in viable cell number at day 3 before decreasing in viable cell concentration. With regard to monitoring culture viability (Figure 4.18), all the cell lines had a decreased in viability at day 3 compared to the initial viability at the start of the experiment. The decrease in viability was more prominent for the SNAP29 B cell line than the other cell lines. From day 3 (feed day), culture viability

either recovered or did not (Figure 4.18) in individual cell lines. During the culture it was also noticed that the host cell line formed clumps of cells (visual observation).

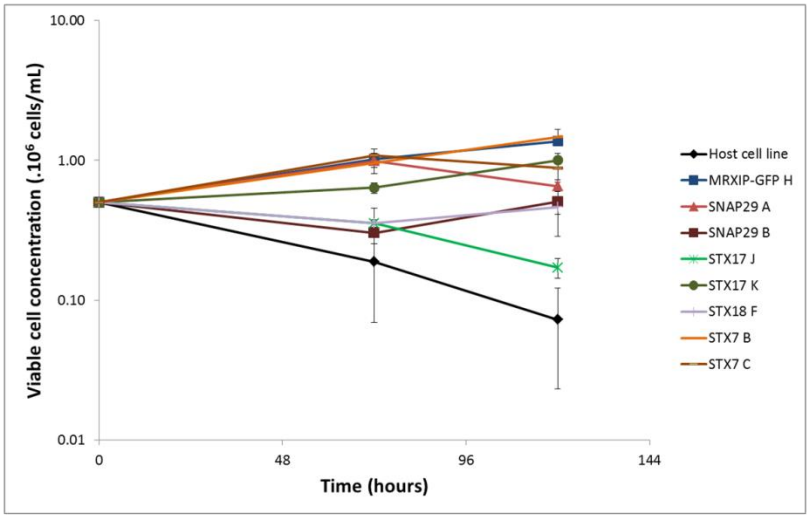

	Day 3			Day 5				
Host cell line			C					F
MRXIP-GFP H	A			A				
SNAP29 A	A					C	D	
SNAP29 B			C				D	E
STX17 J			C					E	F
STX17 K		B			B			
STX18 F			C				D	E
STX7 B	A			A				
STX7 C	A				B	C		

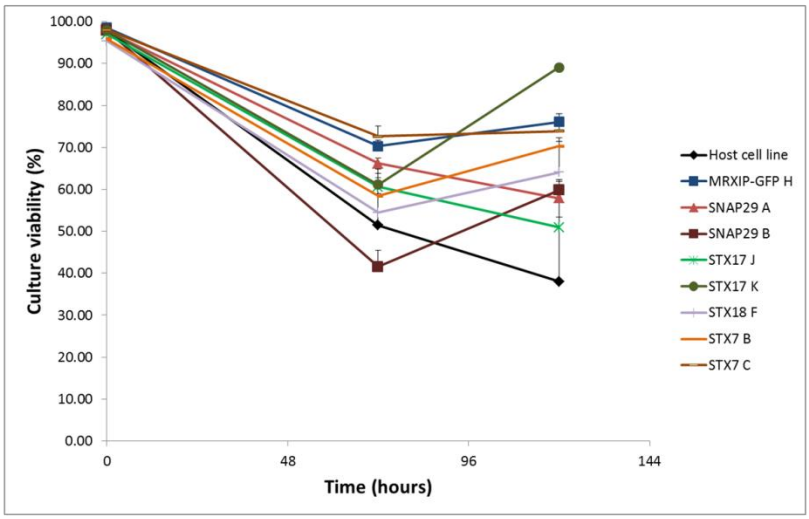

	Day 3					Day 5			
Host cell line				D	E	A			D
MRXIP-GFP H	A	B					B		
SNAP29 A	A	B	C				B	C	
SNAP29 B					E		B	C	
STX17 J	A	B	C	D				C	D
STX17 K	A	B	C	D		A			
STX18 F			C	D			B	C	
STX7 B		B	C	D			B		
STX7 C	A					A	B		

Figure 4.18. Viable cell concentration and culture viability monitoring of the different cell lines transiently transfected with pAdalimumab in fed-batch cultures. Error bars show the standard deviation from the mean (n=3). One way ANOVA analysis was performed on the means followed by Tukey tests. Means sharing a letter are not significantly different.

The cell specific productivity was also calculated for the different cell lines for the production of Adalimumab and the results are displayed in Figure 4.19. The CHO/STX17 J cell line had the highest specific productivity at 1.32 pg/cell/day of Adalumimab. All the other cell lines had specific productivity between 0.01 to 0.49 pg/cell/day but were not statistically higher than that of the control cell lines. Some cell lines displayed a high variability for their specific productivity value between replicate cultures than others, notably the host cell line. Clumping observed of the host cell line during the experiment might explain this as determination of viable cell numbers is more difficult when the cells are clumped. Indeed, calculation of specific production relies on determining viable cell concentration values and having non homogenous mixtures (notably with the presence of cells clumps) will result in the calculation of incorrect viable cell numbers and hence specific productivities.

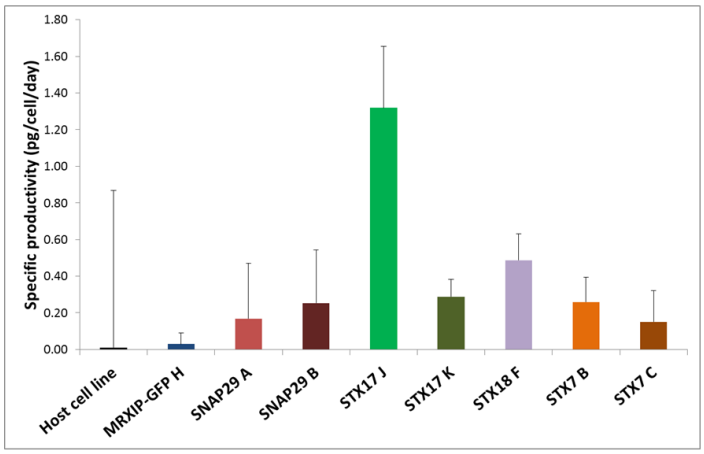

	Qp
Host cell line	B
MRXIP-GFP H	B
SNAP29 A	B
SNAP29 B	B
STX17 J	A
STX17 K	B
STX18 F	A B
STX7 B	B
STX7 C	B

Figure 4.19. Calculated cell specific productivity for the different syntaxin/SNAP engineered CHO-S cell lines transiently transfected with pAdalimumab during fed-batch culture. Error bars show the standard deviation from the mean (n=3). One way ANOVA analysis was performed on the means followed by Tukey tests. Means sharing a letter are not significantly different.

4.3.2.2. Fed-batch analysis of Etanercept expression from syntaxin/SNAP engineered CHO-S cells

As for the model IgG used to asses impact on secretory productivity of the engineered syntaxin/SNAP CHO-S cells, the expression of the model Fc-TNFR fusion protein was also assessed under fed-batch culture conditions. Figure 4.20 reports the relative expression of as determined by western blot analysis on non-reduced supernatant samples at day 5 post-transfection from transient production of Etanercept. The intensity of the bands observed after incubation of the membrane with anti-heavy chain showed similar expression levels

from the host cell line and the CHO/MRXIP-GFP H control cell line. The expression from the CHO/SNAP29 A cell line was similar to the control while that from the CHO/SNAP29 B cell line was lower than the controls (Figure 4.20). The expression from the CHO/STX7 C and B cell lines was also similar to that observed from the controls. Analysis of samples from the CHO/STX17 J cell line suggested that expression was higher for at least two biological replicates as indicated by a more intense band. Analysis of CHO/STX18 F samples suggested that there might be a small increase in the expression of Etanercept compared to the controls but this was not the case for the CHO/STX17 K cell line where the band intensity was less than that for the controls.

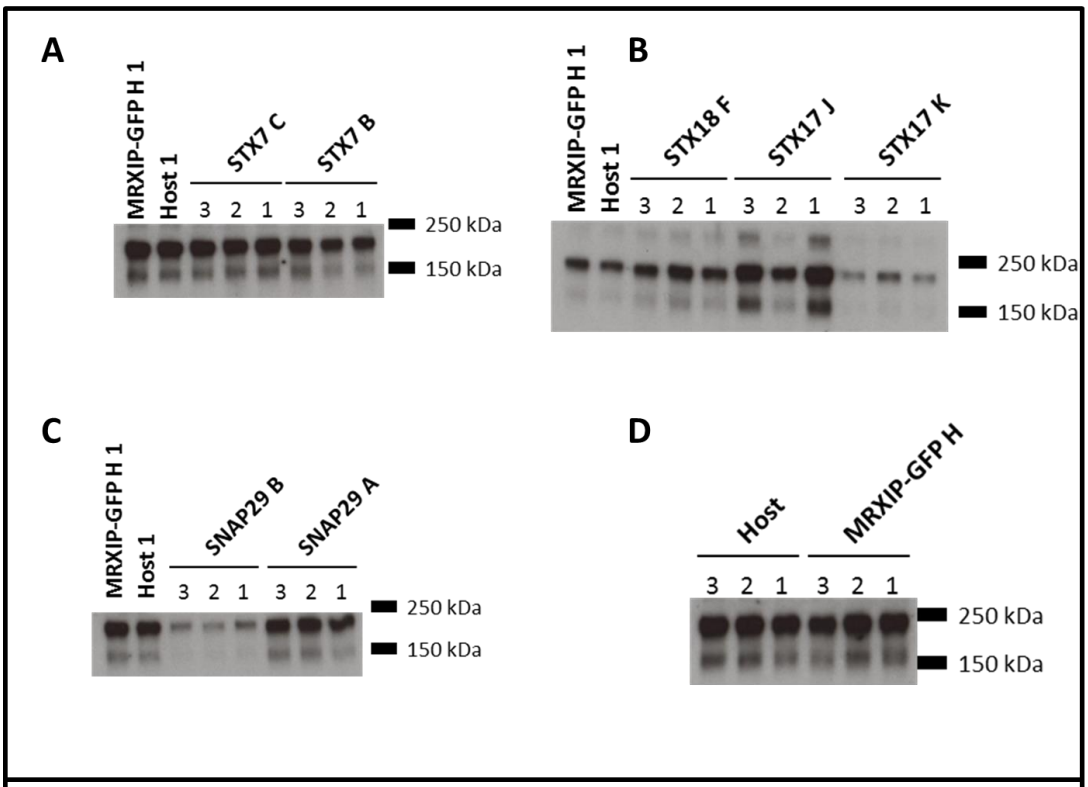

Figure 4.20. Western blot analysis of supernatant samples from day 5 of a fed-batch culture after transient transfection of the different syntaxin/SNAP engineered cell lines with the plasmid pEtanercept. Equal volumes of supernatant were loaded for the different conditions and anti-heavy chain antibody (1:10000) was used for signal detection. Results are separated as following: **A**, cell lines expressing GFP-STX7; **B**, cell lines expressing GFP-STX17 or GFP-STX18; **C**, cell lines expressing GFP-SNAP29 and **D**, Host cell line and GFP expressing cell line. Expected sizes are around 250 kDa for full size molecule and around 150 kDa for half molecule.

In addition to the qualitative analysis of samples by western blot, more quantitative Octet based analysis was also undertaken and the results are reported in Figure 4.21. From this analysis the CHO/MRXIP-GFP H, CHO/SNAP29 B and particularly CHO/STX17 K cell lines showed a decrease in product titre from day 3 to day 5. This wasn't observed in the

experiment using Adalumimab plasmid (see section 4.2.5.1). A possible explanation, especially for CHO/STX17 K could be the mixing of the sample days during analysis as this decrease was not obvious from the western analysis. Cell line CHO/STX17 J had the highest titre at day 5 of 4.16 µg/mL whilst cell lines CHO/SNAP29 A, CHO/STX18 F, CHO/STX17 K, CHO/STX7 B and CHO/STX7 C expressed more-or-less the same amount of Etanercept as the host cell line. For the majority of the cell lines, it was observed that the difference in titre between day 3 and day 5 was small, implying that the majority of the recombinant protein production had been completed before day 3 and that the feeding on day 3 did not positively impact on the production of the Etanercept material. This may also reflect the transient nature of the expression whereby the plasmid is diluted out from cells as they divide such that expression can be rapidly lost as the cells grow and divide.

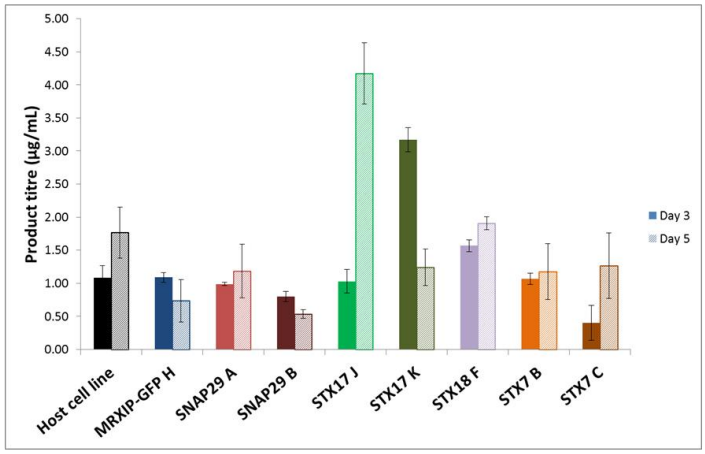

	Day 5	
Host cell line	B	
MRXIP-GFP H		C
SNAP29 A	B	C
SNAP29 B		C
STX17 J	A	
STX17 K	B	C
STX18 F	B	
STX7 B	B	C
STX7 C	B	C

Figure 4.21. Assessment of Etanercept titre by Octet analysis on supernatants from day 3 and 5 after the transient transfection of the different syntaxin/SNAP engineered CHO-S cell lines with pEtanercept in fed-batch cultures. Plain bars represent day 3 data and patterned bars represent day 5 data. Error bars show the standard deviation from the mean (n=3). One way ANOVA analysis was performed on the mean from day 5 followed by Tukey tests. Means sharing a letter are not significantly different.

Figure 4.22 reports the viable cell concentration and culture viability recorded on days 3 and 5 of the transient transfection experiment. The host cell line showed a decrease in viable cell concentration from day 0 to day 5 while the CHO/MRXIP-GFP H control showed an increase in viable cell concentration during the experiment (Figure 4.22). Several cell lines showed little change in their viable cell concentration during the experiment, including CHO/STX7 C, CHO/SNAP29 A, CHO/STX18 F. Cell lines CHO/SNAP29 B, CHO/STX17 K and CHO/STX7 B had a decrease in viable cell concentration from day 0 to day 3 before increasing between days 3 and 5.

When comparing the culture viability of the different cell lines during the transient expression of the recombinant protein Etanercept (Figure 4.22), all cell lines had a decrease in culture viability from day 0 to day 3. CHO/SNAP29 B was the cell line with the greatest decrease with a culture viability <30% at day 3. Only two cell lines, CHO/STX17 J and the host cell line showed a decrease in culture viability across the whole experiment while the other cell lines showed an increase in culture viability from day 3 to 5. CHO/MRXIP-GFP H had the highest viability on day 5 at 73.5%.

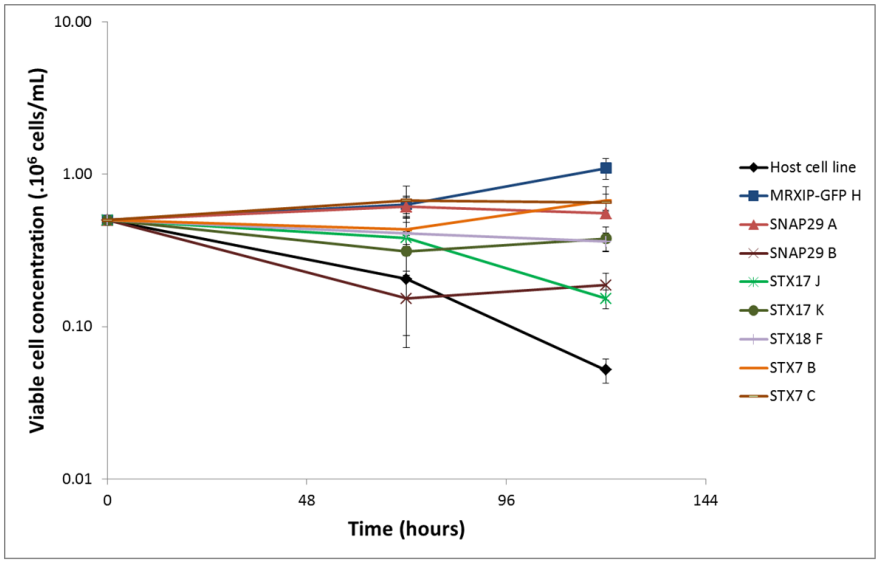

	Day 3			Day 5				
Host cell line			C					E
MRXIP-GFP H	A	B		A				
SNAP29 A	A	B			B	C		
SNAP29 B			C				D	E
STX17 J		B	C				D	E
STX17 K			C			C	D	
STX18 F	A	B	C			C	D	
STX7 B	A	B	C		B			
STX7 C	A				B			

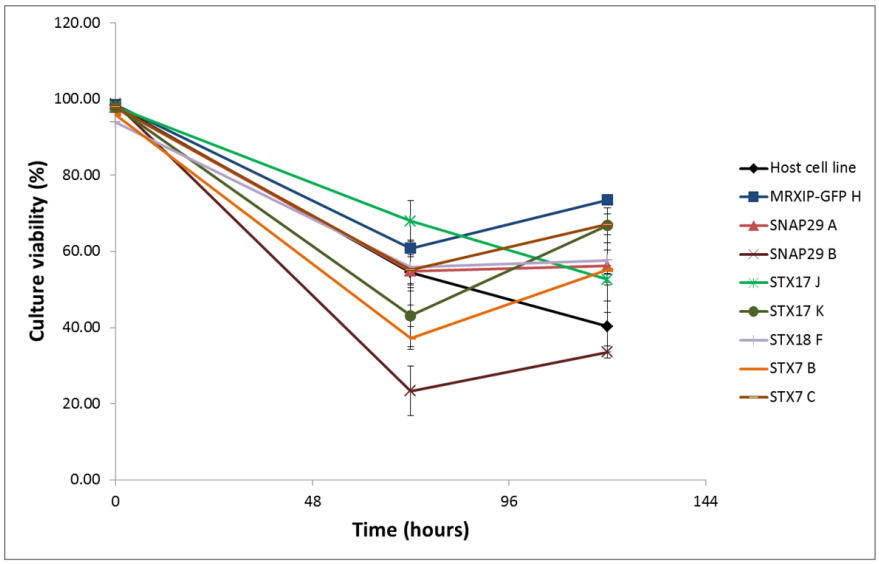

	Day 3				Day 5			
Host cell line	A	B					C	D
MRXIP-GFP H	A				A			
SNAP29 A	A	B				B	C	
SNAP29 B				D				D
STX17 J	A					B	C	
STX17 K		B	C		A	B		
STX18 F	A	B			A	B		
STX7 B			C	D		B	C	
STX7 C	A	B			A	B		

Figure 4.22. Viable cell concentration and culture viability of the different syntaxin/SNAP CHO-S engineered cell lines transiently transfected with pEtanercept in fed-batch cultures. Error bars show the standard deviation from the mean (n=3). One way ANOVA analysis was performed on the means followed by Tukey tests. Means sharing a letter are not significantly different.

The calculated specific productivity for the transient experiment for the production of Etanercept for the different cell lines is reported in Figure 4.23. Three cell lines appeared to have a negative specific productivity or qp in this experiment, which is clearly not possible and reflects the fact that the product titre decreased between day 3 and day 5 while the viable cell concentration was increasing. The highest specific productivity was from the CHO/STX17 J cell line for the transient production of Etanercept at 5.9 pg/cell/day.

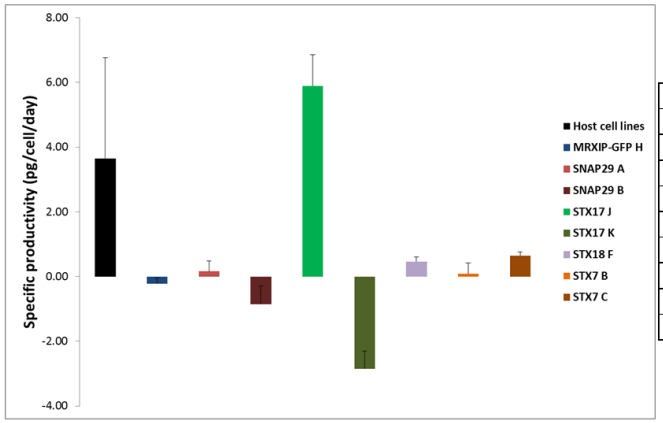

	Qp			
Host cell line	A	B		
MRXIP-GFP H			C	D
SNAP29 A			C	D
SNAP29 B			C	D
STX17 J	A			
STX17 K				D
STX18 F		B	C	
STX7 B			C	D
STX7 C		B	C	

Figure 4.23. Calculated specific productivity for the different syntaxin/SNAP engineered CHO-S cell lines transiently transfected with pEtanercept in fed-batch culture. Error bars show the standard deviation from the mean (n=3). One way ANOVA analysis was performed on the means followed by Tukey tests. Means sharing a letter are not significantly different.

4.3.3. Larger scale transient expression of Etanercept and Adalimumab from the syntaxin/SNAP engineered CHO-S cells

A larger scale transient experiment was performed to allow monitoring of the culture through a longer period of time (more sampling points) and study the impact on productivity of the syntaxin/SNAP engineered cell lines. Using larger volumes and 13 different cell lines required transfection of larger numbers of cells. The method of transfection used for this transient transfection was electroporation instead of NovaCHOice reagent. Compared to NovaCHOice, electroporation is a method able to transfect effectively and easily a higher number of cells (Kim and Eberwine 2010). The change of scale and method of transfection allowed an investigation into any impact on the productivity of the method and scale.

Cell lines were electroporated with 40 µg DNA of pEtanercept or pAdalimumab using 1 x 10^7 viable cells in order to inoculate 125 mL Erlenmeyer flasks with vented caps at 0.3 x 10^6 viable cells/mL in 20 mL of CD-CHO supplemented with 8 mM L-glutamine. Cells were

incubated at 37˚C, 5% CO_2 and 140 rpm. Cell growth and culture viability were monitored every 2 days from day 2 using a Vi-CELL instrument. Alongside the Erlenmeyer flasks, 96-DWPs were inoculated with the same electroporated cell lines. Two DWPs were inoculated for each recombinant protein, one sampled at day 2 and the other at day 4. The goal was to confirm the capability of 96 DWPs to mimic the results obtained at the larger scale.

4.3.3.1. Larger scale transient expression of Etanercept from the syntaxin/SNAP engineered CHO-S cells

4.3.3.1.1. Impact on secreted Etanercept productivity of syntaxin/SNAP engineering of CHO-S cells

Western blot analyses on supernatant samples harvested at day 8 of batch culture are reported in Figure 4.24. Samples were analysed under non-reducing conditions and normalised by loading equal volumes. Controls showed the same banding intensity (host cell line, CHO/MRXIP-GFP H and L) indicative of similar expression of Etanercept. The CHO/SNAP29 B cell line had higher expression than CHO/SNAP29 A and the controls as shown by a more intense band whilst expression from the CHO/SNAP29 A cell line was lower than for the controls. The expression from the CHO/STX7 C and B and CHO/STX18 H cell lines was similar to the controls. On-the-other-hand, the CHO/STX18 F cell line appeared to have mainly half-molecule product in the supernatant, suggesting degradation in the supernatant or secretion of only half-molecule. Expression from the CHO/STX17 J cell line was higher than the controls whilst that from the CHO/STX17 K was similar to the controls.

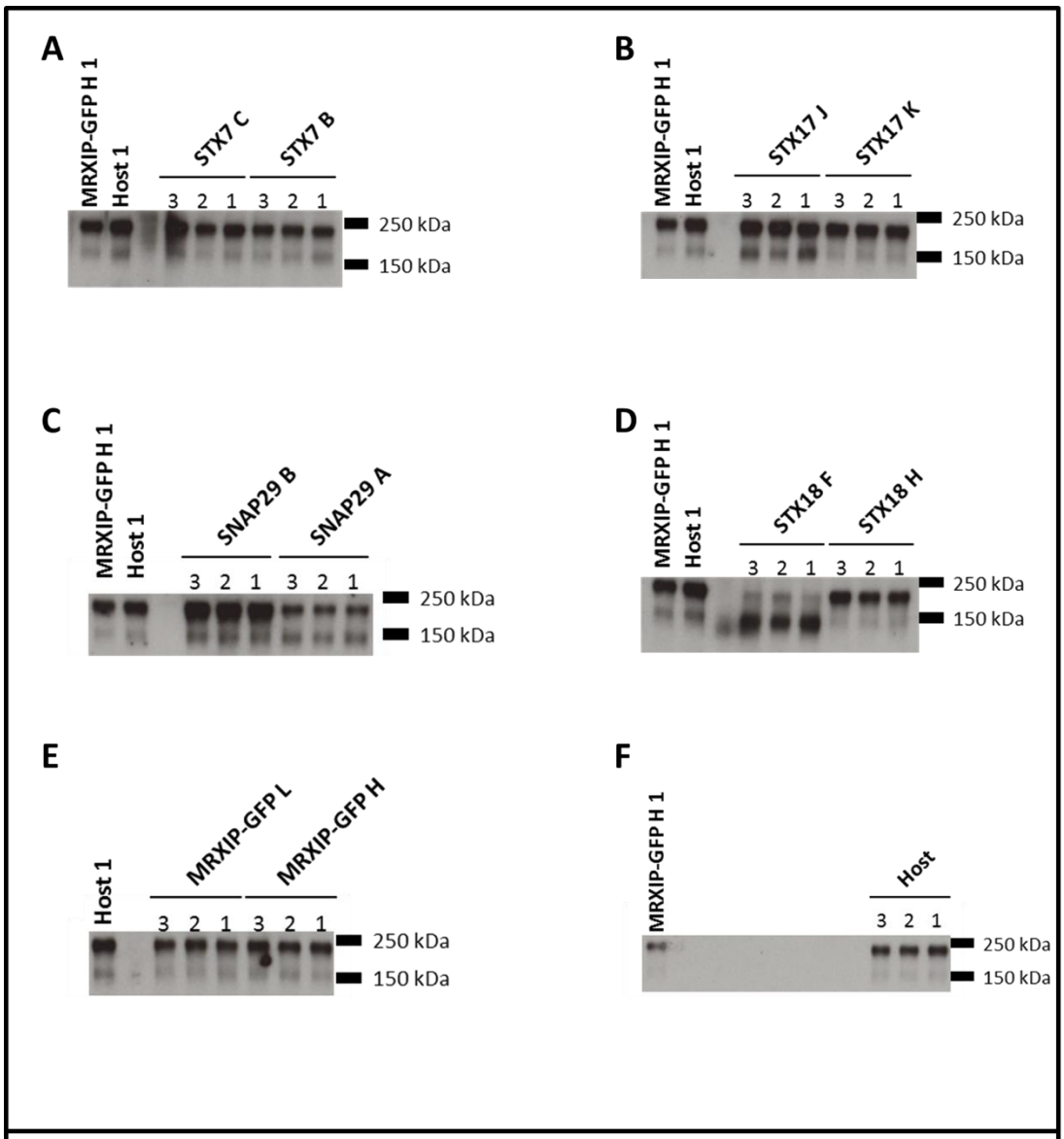

Figure 4.24. Western blot analysis of supernatant samples on day 8 of batch culture after transient transfection of the syntaxin/SNAP engineered CHO-S cells with pEtanercept in 125 mL Erlenmeyer flasks. Equal volumes of supernatant were loaded for all samples and anti-heavy chain antibody (1:10000) was used for signal detection. Results are separated as following: **A**, cell lines expressing GFP-STX7; **B**, cell lines expressing GFP-STX17; **C**, cell lines expressing GFP-STX18; **D**, cell lines expressing GFP-SNAP29; **E**, GFP-expressing cell lines and **F**, Host cell line . Expected sizes are around 250 kDa for full size molecule and around 150 kDa for half molecule

Figure 4.25 summarises the Etanercept titre measured in supernatant samples by Octet for each sampling day when transiently expressing Etanercept. The cell line yielding the highest concentration at day 8 was CHO/SNAP29 B at 5.38 µg/mL, 1.6 times more than the host cell lines or CHO/MRXIP-GFP H cell line. The cell line CHO/STX17 J also gave a similar yield at day 8 as the CHO/SNAP29 B cell line. All the other cell lines yielded very similar concentrations at day 8.

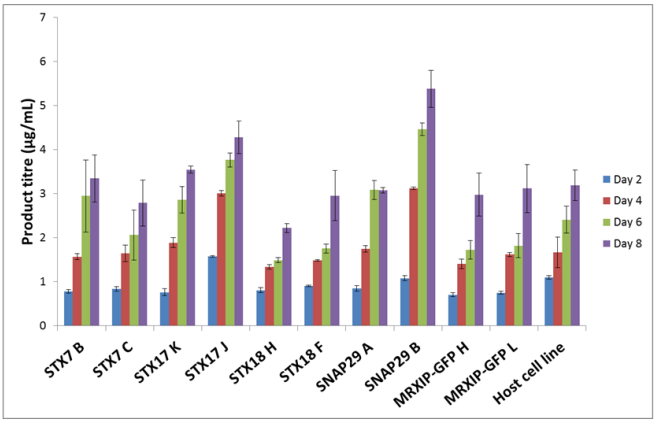

	Day 8			
STX7 B		B	C	D
STX7 C			C	D
STX17 K		B	C	
STX17 J	A	B		
STX18 H				D
STX18 F			C	D
SNAP29 A			C	D
SNAP29 B	A			
MRXIP-GFP H			C	D
MRXIP-GFP L		B	C	D
Host cell line		B	C	D

Figure 4.25. Assessment of product titre across different days of batch culture for the different syntaxin/SNAP engineered CHO-S cell lines when transiently expressing Etanercept. Error bars show the standard deviation from the mean (n=3). One way ANOVA analysis was performed on the mean each day followed by Tukey tests. Means sharing a letter are not significantly different.

Figure 4.26 reports viable cell number and culture viability data across the batch culture and transient expression of pEtanercept. The viable cell concentration trend was similar for the different cell lines except for the untransfected control and CHO/STX18 H cell line. The cell lines showed no or little growth until day 2, suggesting a lag phase and from there the viable cell number increased until day 6 before plateauing or decreasing. The untransfected control had a more rapid and exponential growth without any lag phase reaching a maximal viable cell concentration on day 4 of 7.51 x 10^6 cells/mL. No plateau was observed for the untransfected control and viable cell concentration decreased continuously from day 4 to 8. Even with a delay in growth compared to the untransfected control, the CHO/STX18 F cell line reached the highest viable cell concentration of 8.45 x 10^6 cells/mL on day 6. Most of the cell lines achieved comparable viable cell concentrations on day 6. Cell line CHO/STX18 H was the only one to show a decrease in viable cell concentration from the beginning of the experiment.

The culture viability profile was similar also for all the transfected cells (Figure 4.26) except the untransfected control. Culture viability was decreased at day 2 from where it started to recover until day 6. At day 6 the culture viability dropped until day 8. CHO/STX18 H had the biggest decrease in viability at day 2 but recovered rapidly. The untransfected control had no drop in culture viability until day 4 where upon viability reduced rapidly. It was observed that some of the cell lines maintained higher culture viabilities than others at day 8, notably CHO/SNAP29 B which had a culture viability of 90% at this time (Figure 4.26).

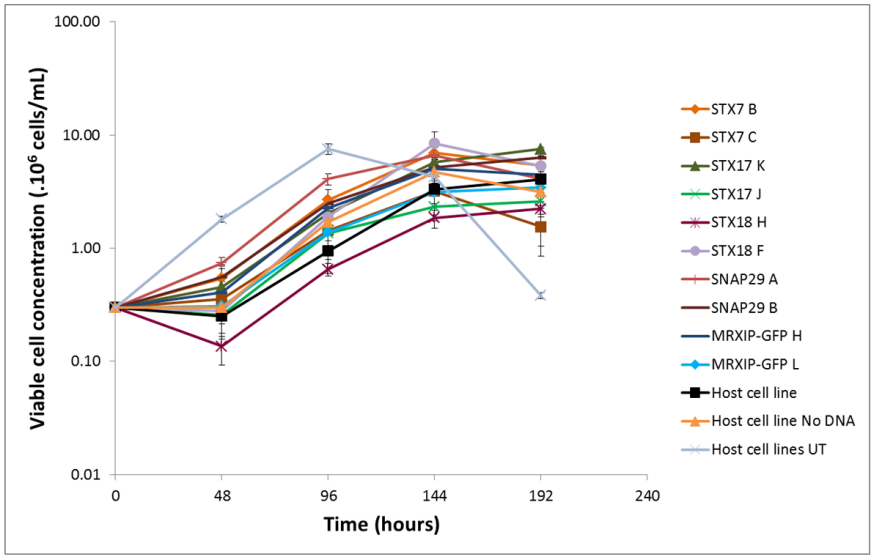

	Day 2	Day 4	Day 6	Day 8
STX7 B	B C D	B C	A B	A B C
STX7 C	C D E	C D E	D E	D E
STX17 K	B C D	C D E	A B C D	A
STX17 J	C D E	C D E	E	C D E
STX18 H	E	E	E	D E
STX18 F	C D E	C D E	A	A B C
SNAP29 A	B	B	A B C	B C D
SNAP29 B	B C	C	A B C D E	A B
MRXIP-GFP H	C D E	C D	B C D E	B C D
MRXIP-GFP L	C D E	C D E	D E	B C D
Host cell line	D E	D E	C D E	B C D
Host cell line No DNA	C D E	C D E	B C D E	C D E
Host cell lines UT	A	A	B C D E	E

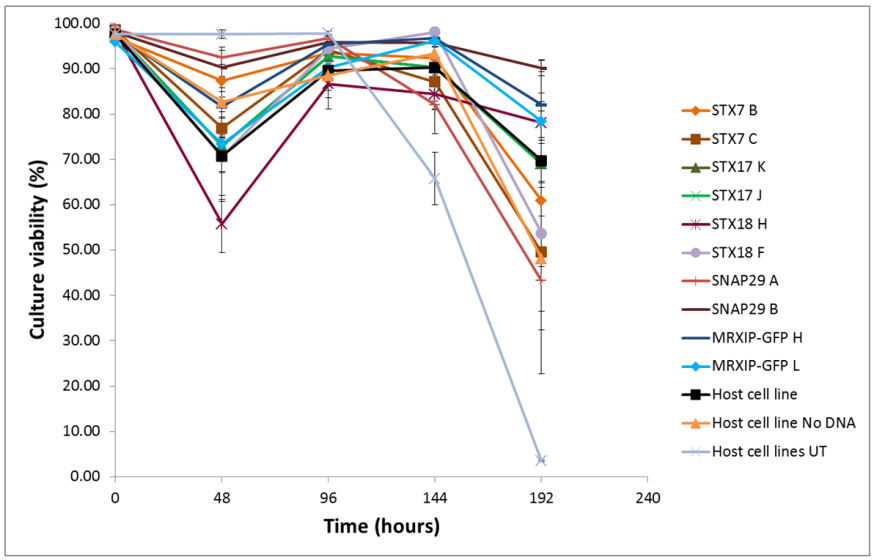

	Day 2	Day 4	Day 6	Day 8
STX7 B	A B C D	A B C	A B C	A B C
STX7 C	B C D	A B C	A B C	B C
STX17 K	A B C D	A B C	A B	A
STX17 J	C D E	A B C	A B C	A B C
STX18 H	E	C	B C	A B
STX18 F	D E	A B C	A	B C
SNAP29 A	A B	A B	C	C
SNAP29 B	A B C	A B	A B	A
MRXIP-GFP H	A B C D	A B C	A B	A B
MRXIP-GFP L	C D	A B C	A B	A B
Host cell line	D E	A B C	A B C	A B C
Host cell line No DNA	A B C D	B C	A B C	B C
Host cell lines UT	A	A	D	D

Figure 4.26. Viable cell concentration and culture viabilities on the different sampling days across batch culture after transient transfection of the different syntaxin/SNAP engineered cells with pEtanercept. Error bars show the standard deviation from the mean (n=3). One way ANOVA analysis was performed on each day followed by Tukey tests. Means sharing a letter are not significantly different.

Figure 4.27 reports the cell specific productivity of the different cell lines for the transient production of Etanercept. CHO/STX17 J had the highest cell specific productivity of 0.25 pg/cell/day. Whilst CHO/SNAP29 B yielded the highest overall titre at day 8 of culture, its specific productivity was not different from the host cell line and the different controls.

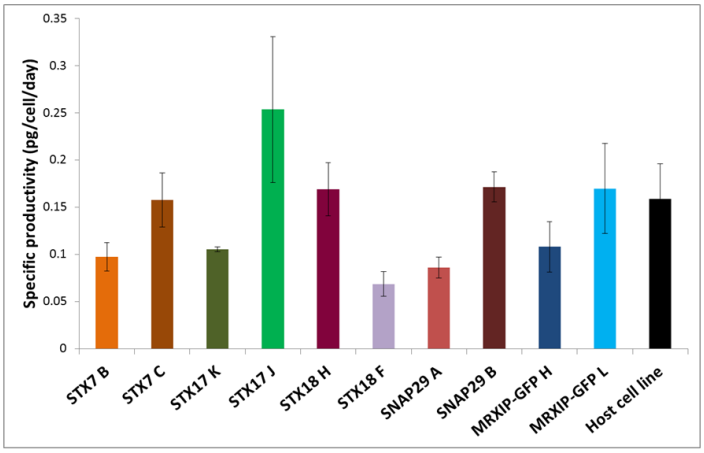

	Specific productivity		
STX7 B		B	C
STX7 C	A	B	C
STX17 K		B	C
STX17 J	A		
STX18 H	A	B	
STX18 F			C
SNAP29 A		B	C
SNAP29 B	A	B	
MRXIP-GFP H		B	C
MRXIP-GFP L	A	B	
Host cell line	A	B	C

Figure 4.27. Calculated specific productivity for the different syntaxin/SNAP CHO-S engineered monoclonal populations after transient transfection of pEtanercept in 125 mL flasks under batch culture conditions. Error bars show the standard deviation from the mean (n=3). One way ANOVA analysis was performed followed by Tukey tests. Means sharing a letter are not significantly different.

4.3.3.1.2. Evaluation of the performance of the different syntaxin/SNAP engineered CHO-S cell lines at two different scales, 96-DWP and 125 mL Erlenmeyer flasks, for scalability purposes

Figure 4.28 shows the comparison of Etanercept product titre at day 2 and 4 as determined by Octet analysis between the two culturing systems, 96-DWPs and shaking Erlenmeyer flask batch cultures. For the statistical analysis, a t-test was used instead of one way Anova analysis because Anova analysis is designed for analysis of multiple components whereas a t-test is more relevant for comparison of one mean against another. After statistical analysis between the conditions at day 2 and 4, no significant difference was found in the titres between the culture systems for the majority of the cell lines except for that from cell lines CHO/SNAP29 A and B at day 4 and CHO/STX18 F, CHO/SNAP29 B and CHO/MRXIP-GFP L at day 2. Even when statistical difference was confirmed, the difference between the two conditions was small.

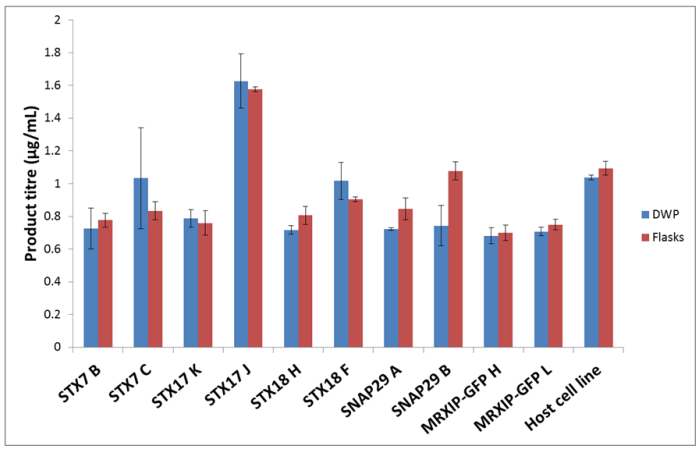

	p Value	Difference DWP and spin tube ? (Y/N)
STX7 B	0.543	N
STX7 C	0.336	N
STX17 K	0.627	N
STX17 J	0.63	N
STX18 H	0.068	N
STX18 F	0.162	N
SNAP29 A	0.032	Y
SNAP29 B	0.013	Y
MRXIP-GFP H	0.664	N
MRXIP-GFP L	0.166	N
Host cell line	0.097	N

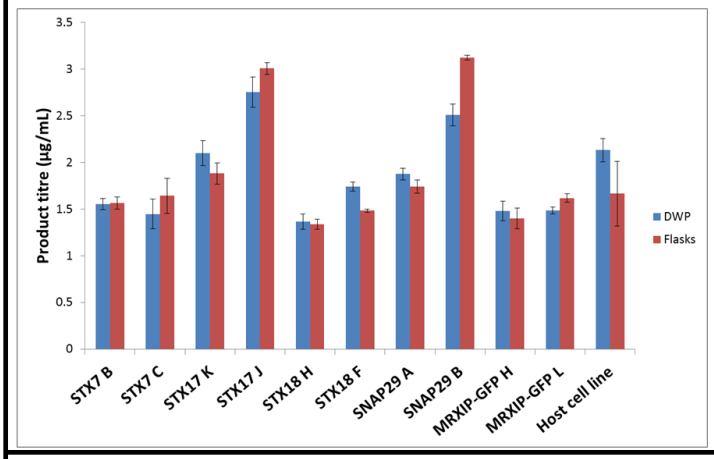

	p Value	Difference DWP and spin tube ? (Y/N)
STX7 B	0.811	N
STX7 C	0.244	N
STX17 K	0.1	N
STX17 J	0.065	N
STX18 H	0.639	N
STX18 F	0.001	Y
SNAP29 A	0.071	N
SNAP29 B	0.001	Y
MRXIP-GFP H	0.4	N
MRXIP-GFP L	0.017	Y
Host cell line	0.095	N

Figure 4.28. Comparison of the Etanercept product titre in supernatants from days 2 and 4 from 96-DWP and 125 mL flask experiments. Error bars show the standard deviation from the mean (n=3). T-test was performed to compare the different concentration between the two conditions.

4.3.3.2. Larger scale transient expression of Adalimumab from the syntaxin/SNAP engineered CHO-S cells

4.3.3.2.1. Impact on secreted adalimumab productivity of syntaxin/SNAP engineering of CHO-S cells

Western blot analysis of supernatant samples from day 8 of batch culture after transient transfection with pAdalimumab of the different syntaxin/SNAP engineered CHO-S cell lines (Figure 4.29) demonstrated that the host cell line and the different empty vector controls had a similar level of Adalimumab expression. The CHO/SNAP29 B sample had a more intense band than samples from the CHO/SNAP29 A cell line and the controls, indicative of higher expression. The band intensity from the CHO/SNAP29 A samples suggest that the level of expression from this cell line is reduced compared to the host cell line and

CHO/MRXIP-GFP control cell lines. The expression from the CHO/STX17 K cell line was higher than the controls as indicated by a more intense band, whereas the expression from the CHO/STX17 J cell line was similar to the controls. The CHO/STX7 C samples had two biological replicates with a band intensity higher than the controls whereas the last replicate had an intensity similar to the controls. The CHO/STX7 B cell line yield similar expression profiles to the controls. Finally, the CHO/STX18 H cell line had lower expression of Adalimumab than the controls whereas two of the CHO/STX18 F cell line generally had similar levels of expression compared to the controls.

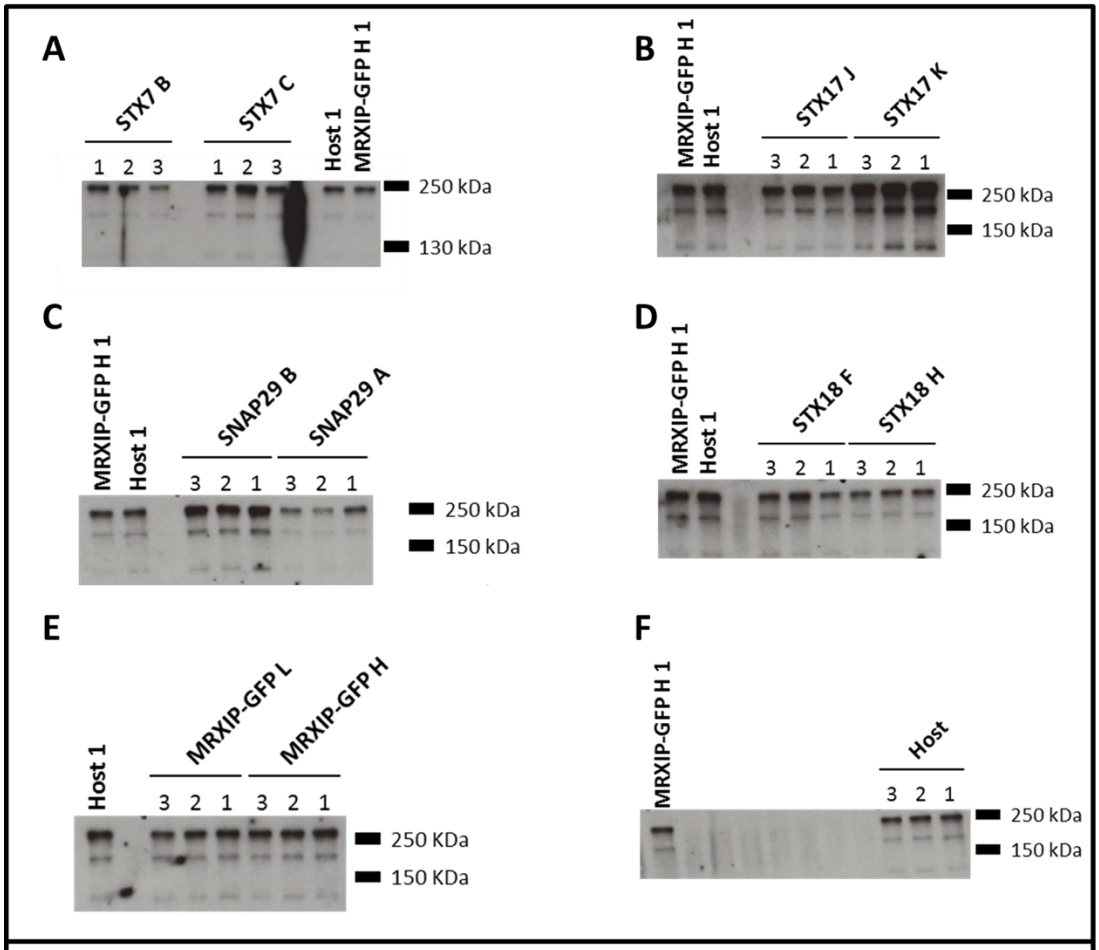

Figure 4.29. Western blot analysis of supernatant samples at day 8 of batch culture after transient transfection of the syntaxin/SNAP engineered CHO-S cell lines with pAdalimumab in 125 mL Erlenmeyer flasks. Equal volumes of supernatant were loaded for the different conditions and anti-heavy chain antibody (1:10000) was used for signal detection. Results are separated as following: **A**, cell lines expressing GFP-STX7; **B**, cell lines expressing GFP-STX17; **C**, cell lines expressing GFP-STX18; **D**, cell lines expressing GFP-SNAP29; **E**, GFP-expressing cell lines and **F**, Host cell line . Expected sizes are around 250 kDa for full size molecule, around 150 kDa for half molecule and around 100 kDa for the heavy chain.

More quantitative Adalimumab product titres across the different days of the batch culture transient expression with pAdalimumab are reported in Figure 4.30. The cell line with the highest product titre at day 8 was CHO/STX17 K at 3.18 µg/mL. The host cell line and the empty vectors had similar product titres with no statistical difference between them. The cell lines CHO/STX7 B and CHO/STX7 C also yielded a similar amount of Adalimumab. The cell line CHO/STX17 K expressed considerably more Adalimumab than the CHO/STX17 J cell line (2.5 times more) whilst the CHO/STX18 F cell line expressed 2.6 times more than the CHO/STX18 H cell line and the CHO/SNAP29 B cell line 2.2 times more than the CHO/SNAP29 A cell line. The CHO/SNAP29 B, CHO/STX18 F and CHO/ STX17 J cell lines yielded a higher Adalimumab titre than the host cell line which was statistically different (Figure 4.30).

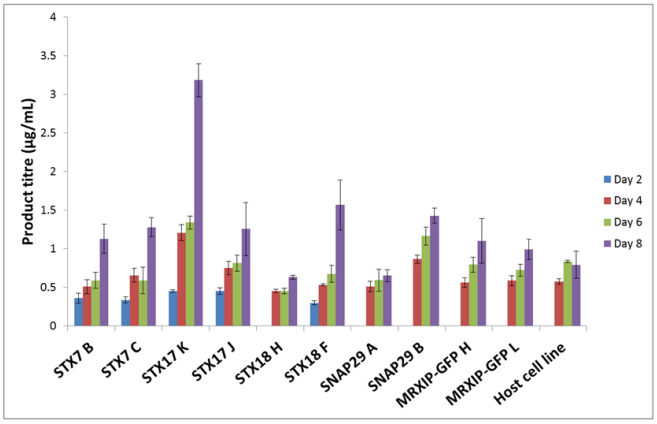

	Day 8				
STX7 B		B	C	D	E
STX7 C		B	C		
STX17 K	A				
STX17 J		B	C	D	
STX18 H					E
STX18 F		B			
SNAP29 A				D	E
SNAP29 B		B			
MRXIP-GFP H		B	C	D	E
MRXIP-GFP L		B	C	D	E
Host cell line			C	D	E

Figure 4.30. Product titre analysis across the different days of batch culture for the different syntaxin/SNAP engineered CHO-S cell lines when transiently expressing Adalimumab. Error bars show the standard deviation from the mean (n=3). One way ANOVA analysis was performed on the means of each day followed by Tukey tests. Means sharing a letter are not significantly different.

Figure 4.31 reports growth data of the cell lines during the batch culture transient Adalimumab expression experiment. The cell growth profiles appear similar for the different transfected cell lines except for the untransfected cell line. A lag phase was observed between day 0 and day 2 with no growth or decrease in viable cell concentration. After day 2, all the cell lines went into exponential cell growth until day 6. At day 6 the viable cell numbers plateaued except for the CHO/STX18 F cell line that decreased in viable cell number. The CHO/STX18 F cell line obtained the highest viable cell concentration at 7.86 x 10^6 cells/mL on day 6. This was more than the untransfected control that had a maximum viable cell concentration of 6.41 x 10^6 cells/mL on day 6.

The culture viability profiles of the transient experiment are also reported in Figure 4.31. All the transfected cell lines showed a drop in culture viability at day 2 compared to day 0 but recovered from there until day 6. At day 6 the culture viability plateaued or declined. This was different for the host cell lines that showed recovery and maintenance of culture viability from day 2 until the end of the experiment. Some of the transfected cell lines, such as CHO/SNAP29 B and CHO/STX17 K, maintained high viability until the last day of the experiment with a culture viability around 93%. The untransfected control showed no reduction in culture viability at day 2 but this started to decrease slowly from day 4 before a drastic fall at day 6 (Figure 4.31).

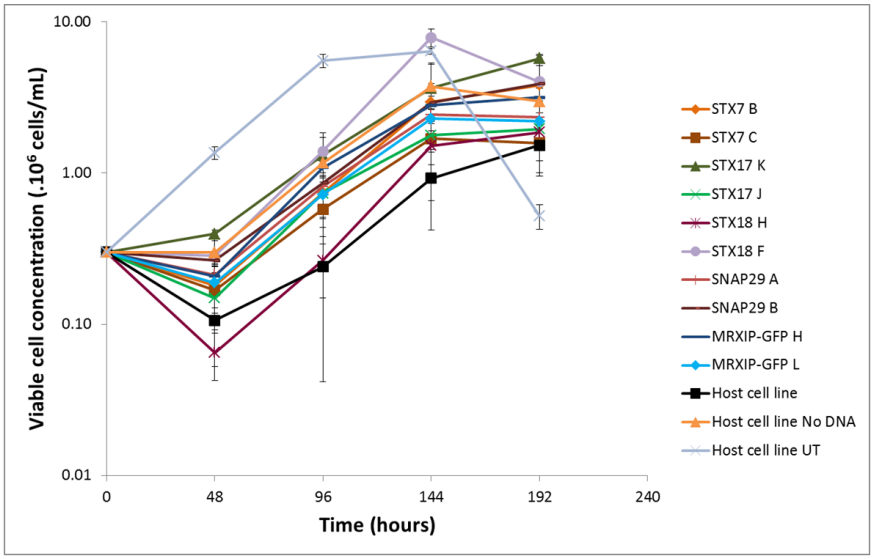

	Day 2	Day 4	Day 6	Day 8
STX7 B	C D E	B C	C D	A B C
STX7 C	C D E	B C	C D	B C D
STX17 K	B	B	C	A
STX17 J	C D E	B C	C D	B C D
STX18 H	E	C	C D	B C D
STX18 F	B C D	B	A	A B
SNAP29 A	B C D E	B C	C D	B C D
SNAP29 B	B C D	B C	C D	A B C
MRXIP-GFP H	C D E	B C	C D	B C
MRXIP-GFP L	C D E	B C	C D	B C D
Host cell line	D E	C	D	C D
Host cell line No DNA	B C	B C	B C	B C D
Host cell line UT	A	A	A B	D

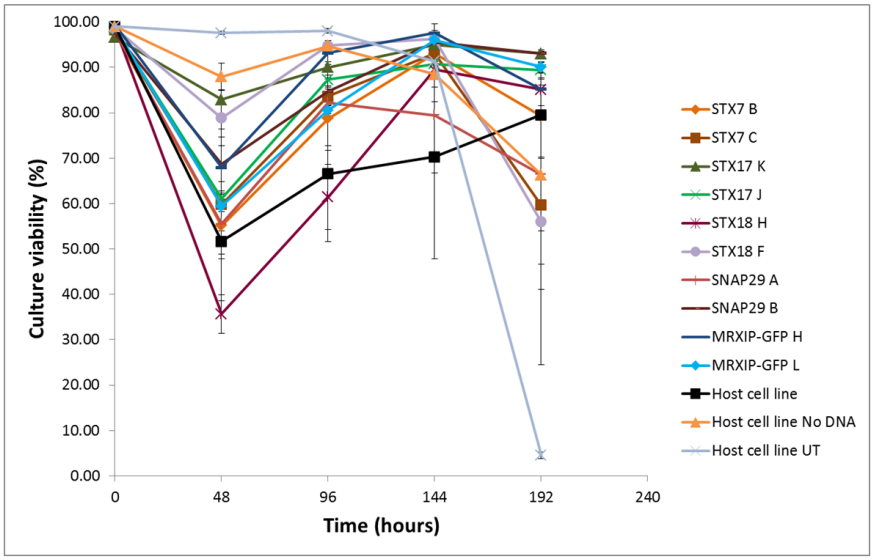

	Day 2	Day 4	Day 6	Day 8
STX7 B	E F	B C	A	A
STX7 C	D E	A B C	A	A
STX17 K	A B C	A B	A	A
STX17 J	D E	A B	A B	A
STX18 H	F	D	A B	A
STX18 F	A B C D	A B	A	A
SNAP29 A	E	A B C	A B	A
SNAP29 B	B C D E	A B	A	A
MRXIP-GFP H	C D E	A B	A	A
MRXIP-GFP L	D E	B C	A	A
Host cell line	E F	C D	B	A
Host cell line No DNA	A B	A B	A B	A
Host cell line UT	A	A	A B	B

Figure 4.31. Viable cell concentration and culture viability profiles for the different sampling days after transient transfection of the syntaxin/SNAP engineered CHO-S cells with pAdalimumab. Error bars show the standard deviation from the mean (n=3). One way ANOVA analysis was performed on each day followed by Tukey tests. Means sharing a letter are not significantly different.

Figure 4.32 reports the specific productivity measurements for the different cell lines when transiently expressing the model molecule, Adalimumab. Not all the data points were used to calculate the specific productivity, with only the data from day 4 to 8. Some cell lines had a low titre of the product of interest at day 2 and the measurements were below the limit of detection when using the Octet instrument. These points were therefore not included in the calculation of specific productivity for all the cell lines. The highest specific productivity achieved was 0.14 pg/cell/day by the CHO/STX17 K cell line. The cell lines CHO/STX7 B, CHO/STX7 C, CHO/STX17 J were also statistically superior to the host cell line (Figure 4.32).

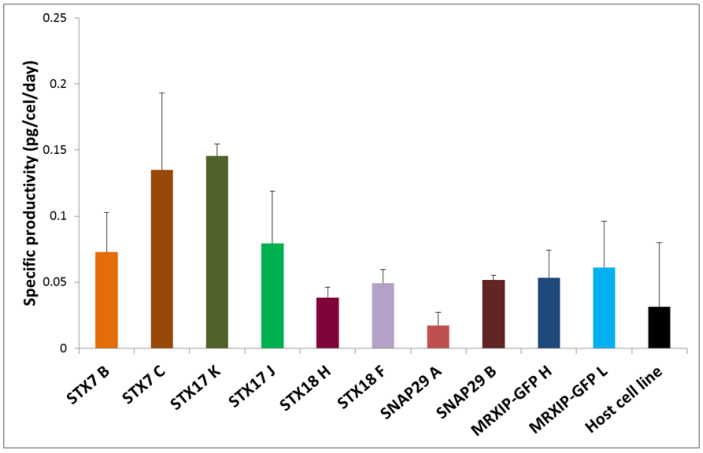

	Specific productivity		
STX7 B	A	B	C
STX7 C	A	B	
STX17 K	A		
STX17 J	A	B	C
STX18 H			C
STX18 F		B	C
SNAP29 A			C
SNAP29 B		B	C
MRXIP-GFP H		B	C
MRXIP-GFP L	A	B	C
Host cell line			C

Figure 4.32. Calculated specific productivity for the different syntaxin/SNAP CHO-S engineered monoclonal populations after transient transfection of pAdalimumab in 125 mL flasks under batch culture conditions. Error bars show the standard deviation from the mean (n=3). One way ANOVA analysis was performed followed by Tukey tests. Means sharing a letter are not significantly different.

4.3.3.2.2. Evaluation of the performance of the different syntaxin/SNAP engineered CHO-S cell lines at two different scales, 96-DWP and 125 mL Erlenmeyer flasks, for scalability purposes

Comparison of the two methods of culture wasn't possible for Adalimumab expression from the syntaxin/SNAP CHO-S engineered cell lines. Indeed, no detectable expression could be determined for DWP samples at day 2 or day 4 for most of the cell lines. Only 3 cell lines gave detectable expression, CHO/STX17 K, CHO/STX17 J and CHO/SNAP29 B at day 4. To perform technical triplicates, the samples needed to be diluted and this resulted in the sample concentration being below the limit of detection of the instrument explaining the lack of data for the early points at day 2. Where comparisons were possible, the data between the scales was comparable (Figure 4.33).

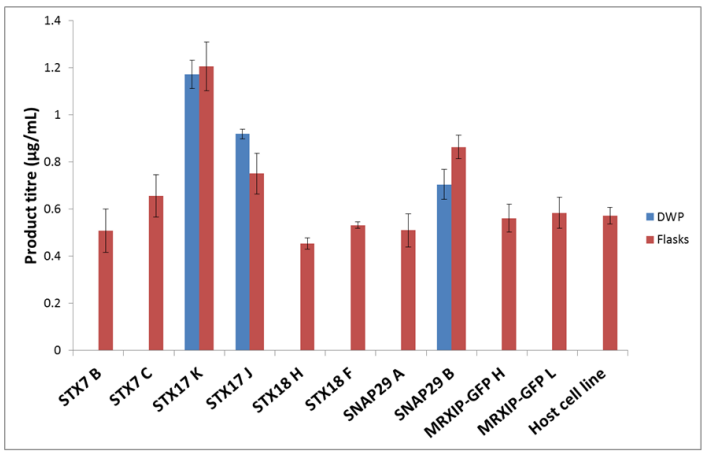

	p Value	Difference DWP and spin tube ? (Y/N)
STX17 K	0.654	N
STX17 J	0.031	Y
SNAP29 B	0.027	Y

Figure 4.33. Comparison of the product titre of supernatants from day 4 between 96-DWP and 125 mL flasks under batch culture conditions. Due to low concentrations in the samples and the need to dilute them, most of the values for the DWP conditions were under the limit of detection. Error bars show the standard deviation from the mean (n=3). T-test was performed to compare the different concentration between the two conditions.

4.4. Discussion

This chapter is focused on the characterisation of the different monoclonal syntaxin/SNAP engineered CHO-S cell populations generated and described in Chapter 3. The investigated cell lines overexpressing SNARE-eGFP fused proteins were analysed with respect to how the engineering, and level or amount of over-expression, impacted upon the growth properties of the cells and/or the secretory capacity of the cell using model recombinant proteins. To assess any impact on secretory capacity, transient transfection experiments were performed and any impact on cell growth or secretory productivity assessed.

After the selection of the different monoclonal populations in Chapter 3 and their adaptation to suspension environment, cells were cryopreserved for further use. When the cells were revived for the studies described in this chapter, some cell lines never recovered or were lost at different stages due to adaptation problems. No noticeable trend was observed with regard to a particular effect of overexpression of specific targets of interest that related to non-recovery from cryopreservation or death of the culture after recovery over time. The CHO/SNAP29 I cell line did not recover from cryopreservation whilst the cell lines CHO/STX17 C and CHO/STX18 C did initially recover from cryopreservation but were subsequently lost during subculture.

To confirm proper folding of the eGFP tag in the different monoclonal cell lines, microscopy analysis was performed. The different cell lines demonstrated fluorescent expression at

different levels, except for the CHO/MRXIP-GFP H cell line, indicative of varying eGFP and hence syntaxin/SNAP expression. The intensity differences by microscopy observation related to the flow cytometry profiles of the monoclonal cell lines; cells with low fluorescence intensity as determined by fluorescence microscopy analysis had a smaller shift in their fluorescence intensity compared to control samples as determined by flow cytometry analysis. Surprisingly, no fluorescence could be detected in the CHO/MRXIP-GFP H cell line by microscopy whereas analysis on the parental cell line (microscopy, western blot analysis and flow cytometry) suggested the presence of a properly folded eGFP protein. As the cell lines were prepared in a similar manner, the most probable reason for absence of fluorescence is a rapid turnover in the cells so the amount of fluorescence observed was low and not detectable under the conditions this experiment was undertaken.

The different clonal populations obtained after limiting dilution cloning had all been exposed to a stressful selection process. Previous data showed that the parental cell lines were not all expressing predominantly the intact fusion protein such as CHO/STX18 (see section 3.3.4). Western blot analysis using an anti-GFP antibody on cell lysates was therefore performed to determine the relative level of expression of the fused protein for each cell line. Except for cell lines expressing STX18, detection of a signal for the intact fusion protein was at the expected size. For cell lines expressing STX18, only CHO/STX18 F had a weak signal after long exposure of the membrane to film (30 min) when using the anti-GFP antibody. Western blot analysis with a specific antibody for the detection of STX18 was then performed for STX18 expressing cell lines. Low or an absence of signal could be an indication of degradation of the fusion protein or cleavage of the eGFP tag. A Fluorescent signal was observed by flow cytometry and fluorescence microscopy analysis so cleavage of the eGFP tag could be a viable explanation as to why the full length product was not observed. When analysing samples with the anti-STX18 antibody, the CHO/STX18 F cell line samples contained two bands as expected, one for the full size fusion protein around 65 kDa and one representing the endogenous STX18 expression of the protein. A stronger signal for the endogenous protein in CHO/STX18 H compared to the controls would have suggested a cleavage between the eGFP and the syntaxin but still overexpression of the protein of interest. Here, the most plausible explanation is cleavage of the eGFP and degradation of the syntaxin part, leaving a free functional eGFP tag responsible for the signal in the microscopy and flow cytometry experiments. No analysis was performed on

the CHO/STX18 C cell line because it perished during subculture and no successful revival was achieved.

Further analysis on western blot data was undertaken using densitometry and the free software ImageJ. Densitometry is a technique to measure band signal intensity and compare the relative intensity of different bands. Due to the use of anti-β-actin antibody in parallel with the anti-GFP antibody, detection of levels of β-actin was possible. β-actin is a house keeping gene that is assumed to be expressed to the same extent across cells from the same parental host cell line (i.e. is invariant). The signal for β-actin was used as normaliser to compare the relative level of expression of the fused proteins across the different cell lines. It was then possible to quantify the differences in expression, for example CHO/STX17 J expressed 1.2 times more of STX17-eGFP fused protein than CHO/STX17 K. These results generally correlated with the flow cytometry results and the fluorescence microscopy observations.

After confirming the relative level of expression of the specific SNARE-eGFP fusion proteins in each selected cell line and confirmation of the expression of an intact fusion protein with a correctly processed eGFP tag, growth profiles under batch-culture conditions were generated to determine if the overexpression of the different ectopic proteins had any effect on the growth of the cells. Indeed, overexpression of proteins in cells generates an additional burden on the cell. Moreover, when overexpression is chosen for the study of a protein function, strong promoters are typically used, potentially saturating the cellular capacity with the production of one protein (Xia et al. 2006). This can be detrimental to the cell and activate stress pathways in response such as the unfolded protein response (UPR). On the other hand, overexpression of proteins involved in controlling cell proliferation can also enhance culture viability and cell growth (Doolan et al. 2010; Jaluria et al. 2007).

When comparing the growth of the host cell line and the eGFP expressing only controls CHO/MRXIP-GFP H and L, no statistical difference was generally observed. Nonetheless, whilst CHO/SMRXIP-GFP L had an almost identical growth profile to the host cell line, the CHO/MRXIP-GFP H cell line appeared to have a faster growth rate and reached higher viable cell concentrations. This probably reflects biological diversity within the host cell population that becomes apparent when the host cell line is cloned. Nevertheless, this data suggests that the introduction of the backbone alone expressing eGFP and a resistance gene for puromycin did not confer any dis/advantage on cell growth.

The analysis of the growth and culture viability profiles of the control and syntaxin/SNAP engineered cell lines showed no significant impact of the ectopic expression of the fusion protein on growth. However, the culture viability and duration of culture was impacted in some of the engineered cell lines compared to the controls with extended periods of growth or stationary phase. The cell lines with lower over-expression of STX17, CHO/STX17 K, and SNAP29, CHO/SNAP29 B, were positively impacted with regard to the duration of cell growth but not high expression cell lines. STX17 and SNAP29 are proteins involved in autophagy and notably the formation of the autophagosome and fusion with the lysosome (Burgo et al. 2012; Guo et al. 2014; Hegedus et al. 2013; Kumar et al. 2018; Morelli et al. 2014). The autophagosome is a double-membrane vesicle, encapsulating unwanted molecules such as protein aggregates, damaged mitochondria, and no longer required proteins, that will fuse with a lysosome for degradation of the content (Shibutani and Yoshimori 2014). Autophagy is triggered by stress such as energy deprivation or nutrient starvation (He and Klionsky 2009) which are generally experienced by the cell during batch culture late in the culture. By potentially influencing the formation and maturation of the autophagosome, over-expression of STX17 and SNAP29 might well improve the degradation and turnover of proteins and thus allow amino acids to be liberated to maintain protein synthesis and support other metabolic pathways, hence allowing the cell lines to maintain higher culture viability levels for longer periods. In support of this, other reports have shown that engineering of the autophagosome can lead to prolonged culture times (Lee et al. 2013; Lee and Lee 2012).

After analysing the impact of the ectopic over-expression of the different eGFP-syntaxin/SNAP fusion proteins of interest on growth profiles, transient transfection was performed to determine the effect on the transient secretory productivity of the cell lines. Any effects on secretory productivity were studied using two models proteins, Adalimumab and Etanercept. IgG molecules were chosen as model proteins because they are relevant in an industrial context with therapeutic antibodies representing around 25% of approved molecules by the FDA (Walsh 2014).

The first transient transfection experiment was undertaken using a 96-DWP culturing approach and NovaCHOice transfection reagent. DWPs are a convenient platform for the rapid screening of multiple cell lines and conditions. The western blot analysis confirmed the cells could transiently produce the model recombinant proteins. Western blot is only a semi-quantitative method but relative comparisons were possible between the different

cell lines, especially when samples are processed in the same way. It was possible to detect an increase in secretory productivity from the cell lines CHO/SNAP29 B, CHO/STX17 J and CHO/STX18 F compared to the control and host cell lines for both model proteins. The results were then confirmed by a more quantitative method using an Octet instrument that allowed the determination of the actual concentration of the target molecule in the supernatant.

Cell line CHO/STX17 K also showed an increase in productivity but to a smaller extent than STX17 J. The CHO/STX17 J cell line was shown to express more fusion protein than the CHO/STX17 K cell line and the impact on productivity might therefore be proportional to the over-expression of STX17-eGP protein. This was the opposite for the SNAP29 expressing cell lines. Indeed, CHO/SNAP29 B that expressed lower levels of fusion protein than CHO/SNAP29 A was more productive. In this case, high levels of SNAP29 might be toxic for the cell or have an antagonist effect on productivity explaining the difference between the clonal populations. No obvious relationship between growth and productivity was observed in that experiment.

The impact of the over-expression of ectopic eGFP-SNAREs on productivity was also studied under fed-batch culture conditions. Fed-batch cultures are a process where the culture media is supplemented during culture to replace depleted components and consists of carbon sources (usually glucose for CHO cells), vitamins, amino acids and other metabolites. Initial assessment of relative product titres was undertaken using western blot analysis with anti-heavy chain antibody. When the expressed molecule of interest was Adalimumab, a stronger band signal for the product IgG from cell lines CHO/STX18 F, CHO/STX17 K, CHO/STX17 J and CHO/SNAP29 B was observed, suggesting higher expression of the model molecule compared to the controls. CHO/STX17 J gave the strongest signal, in agreement with the batch culture experiments. When the preliminary results were compared to the quantitative results obtained by Octet analysis, they agreed. Indeed, CHO/STX17 J produced the highest titre of model protein at 3.04 µg/mL at day 5. CHO/SNAP29 B, CHO/STX17 K and CHO/STX18 F also obtained statistically higher titre than the host cell line. When comparing those results with the batch experiment in 96-DWPs, the trend was similar. Higher expression was obtained for the cell lines CHO/STX17 K, J CHO/STX18 F and CHO/SNAP29 B suggesting that either the scale up or the change in culture conditions had no impact when expressing Adalimumab. On-the-other-hand, in the transient transfection experiment for expression of Etanercept, the preliminary results

obtained by western blot analysis of the supernatant at day 5 suggested that only CHO/STX17 J seemed to have a positive effect on titre. This did not relate to the findings in the previous experiment (see section 3.2.4) where higher concentrations were obtained also for CHO/STX17 K, CHO/STX18 F and CHO/SNAP29 B in batch cultures.

The viable cell concentration and culture viability was also monitored at day 3 and 5 for both fed-batch experiments. One noticeable observation was the slow growth of the different cell lines under these conditions. Most cell lines had only at most doubled, reaching concentrations below 1 x 10^6 viable cells/mL. This was surprising when compared to the growth profiles in spin tubes under batch conditions where cells concentrations at day 5 were >5 x 10^6 cells/mL. The transfection protocol might explain a delay in growth due to the stress applied to the cells but a similar protocol was applied to the 96-DWP experiment where some cell lines reached high viable cell concentrations (> 8 x 10^6 cells/mL for CHO/MRXIP-GFP H and L). Another possible parameter that might influence these results was the use of spin tubes without vented caps. The spin tubes were gassed manually at the beginning of the experiment and at day 3, whereas vented caps help to maintain a constant supply of oxygen and CO_2 to control pH in the culture over time. Moreover, cells were inoculated at a high starting concentration (0.5 x 10^6 cells/mL) which may have impacted on the growth. When monitoring culture viability, the same trend was observed across the different conditions tested. The culture viability was decreased at day 3 and then recovered at day 5. This was possibly the effect of the transfection on day 0 and then the addition of the efficient feed B on day 3.

There was also a difference observed in the titre obtained between the 96-DWP experiment and the spin tube fed-batch experiment. Whilst both used the same transfection protocol, the titre was two times higher from the 96-DWP experiment. The low viable cell concentration and poor growth in the spin tube experiment is a likely explanation for the difference in titre between the experiments. Another explanation could be the loss of expression, as the majority of the product was shown to be generated in the first 3 days of culture, before the feeding. Indeed, transient transfection is not a method designed to support prolonged expression over time such as stably cell line generation.

A larger scale batch culture transient expression experiment was also undertaken in 125 mL Erlenmeyer flasks to determine the reproducibility of results when scaling up the process. In this case the method of transient transfection was different, electroporation was used. The resulting analysis of the amount of Etanercept product in the cell culture supernatants

by western blot analysis of day 8 samples suggested higher expression of Etanercept in CHO/STX17 J and CHO/SNAP29 B confirmed by quantitative Octet measurements. Those results were in line with the other experiment in different scales when expressing Etanercept, cell lines overexpressing STX17 and SNAP29 at specific levels conferred an increase in recombinant protein production. It was also observed that the cell line CHO/STX18 F supernatant from day 8 gave an intense signal but for a sized product that corresponded to only half of the molecule. CHO/STX18 F achieved low culture viability at day 8 when expressing Etanercept while achieving high viable cell concentration. Release of the intracellular content of numerous cells affects product degradation notably by unleashing enzymes with thioredoxin-like activity into the media. Those enzymes reduce the disulphide bonds and only the half-molecule of the product of interest remains.

When producing Adalimumab, an intense signal was observed for CHO/SNAP29 B and for CHO/STX17 K but not J. In the case of production of Adalimumab, titre measurement only correlated with the preliminary results of CHO/STX17 K whereas CHO/SNAP29 B had similar titre to the controls. For the Adalimumab producing cell lines, CHO/STX17 K had the best specific productivity but in a similar range to CHO/STX7 C, which demonstrated neither an overexpression of recombinant product in the western blot experiments or a statistical difference in the octet measurement compared to the controls, whereas CHO/SNAP29 B had a similar specific productivity to the controls (host cell lines and eGFP expressing cell lines).

Growth profiles of the different cell lines were similar in both experiments, first a lag phase followed by an exponential phase until day 6 and then a stationary/decline phase. The untransfected cell line did not show any lag phase in both experiments indicating that the lag phase was probably a consequence of the electroporation. This was also associated by a reduction of viability at day 2 in all the electroporated cell lines compared to the untransfected control. The effect on cell line culture viability on the transfected cell lines was different across both experiments so it was not possible to determine if overexpression of the targets of interest influence electroporation recovery.

When the results from the different transient expression studies were compared (Table 4.1), it was observed that 3 cell lines had a constant positive increase in productivity over the control cell lines, these being cell line CHO/STX17 J, CHO/SNAP29 B and in to a smaller extent, CHO/STX18 F. While the CHO/STX17 J cell line did not have an extended longevity of culture as the CHO/STX17 K cell line, it had enhanced productivity under different

conditions and to a greater extent than the CHO/STX17 J cell line compared to the controls. The CHO/STX17 J cell line had a higher expression of the STX17-eGFP fusion protein compared to the CHO/STX17 K cell line, suggesting that the magnitude of expression was linked to the impact on productivity. STX17 plays a role in autophagy by facilitating the generation of autophagosomes (Hubert et al. 2016; Itakura and Mizushima 2013) but also plays a role in traffic between the smooth ER and ERGIC/Golgi compartment (Muppirala et al. 2011). Positive increase in titre in batch and fed-batch experiments suggests that not only the action of STX7 on autophagosomes is involved but also its function in the traffic between the smooth ER and ERGIC/Golgi.

The CHO/SNAP29 B cell line also had enhanced secretory recombinant protein production compared to the controls and prolonged culture viability. This effect was observed in the different batch experiments but not as such in the fed-batch transient expression experiment. During fed-batch, feed is added to the culture to compensate for the deprivation of nutrients in the media. Autophagy is triggered by nutrient deprivation (Glick, Barth, and Macleod 2010) and SNAP29 is involved in fusion between the autophagosome and the lysosome. Hence, when the cells are not deprived of nutrients they do not form autophagosomes so there is less need for maturation of the autophagosome and fusion with the lysosome. This could be an explanation as to why the effect on productivity of CHO/SNAP29 B was limited in fed-batch experiments and more pronounced under batch conditions. Moreover, it was possible to observe a difference between the CHO/SNAP29 A and B cell lines, suggesting that the level of expression of SNAP29 plays a role in determining an enhancement of secretory recombinant product production under batch conditions.

Table 4.1. Summary of the results of the different experiments for the characterisation of the monoclonal populations.

				Effect on Titre						Effect on specific productivity					
		Effect on growth		Etanercept			Adalimumab			Etanercept			Adalimumab		
Cell line	Relative level eGFP-protein expression	Viable cell number	Culture viability	96-DWP batch section 4.3.1.1	fed-batch section 4.3.2.2	large scale section 4.3.3.1	96-DWP batch section 4.3.1.2	fed-batch section 4.3.2.1	large scale section 4.3.3.2	96-DWP batch section 4.3.1.1	fed-batch section 4.3.2.2	large scale section 4.3.3.1	96-DWP batch section 4.3.1.2	fed-batch section 4.3.2.1	large scale section 4.3.3.2
CHO/MRXIP-GFP H	/	no difference	No difference	/	-	/	/	/	/		/	/		/	/
CHO/MRXIP-GFP L	/	no difference	No difference	/		/	/		/			/			/
CHO/STX7 A	***	no difference	No difference	+			/								
CHO/STX7 B	**	no difference	No difference	/	/	/	/	/	/		/	/		/	/
CHO/STX7 C	*	no difference	No difference	/	/	/	/	+	/		/	/		/	+
CHO/STX17 J	**	no difference	No difference	++	++	+	+	++	/		/	/		++	/
CHO/STX17 K	*	no difference	Extended culture time and increased viability	+	/	/	/	+	++		/	/		/	+
CHO/STX18 C	Not detected	no difference	No difference	/			/								
CHO/STX18 H	Not detected	no difference	No difference	+		/	/		/			/			/
CHO/STX18 F	*	no difference	No difference	++	/	/	+	+	+		/	/		++	/
CHO/SNAP29 A	***	no difference	No difference	/	/	/	/	/	/		/	/		/	/
CHO/SNAP29 B	*	no difference	Extended culture time and increased viability	+	-	+	+	+	+		/	/		/	/

Relative levels of expression of the eGFP fused proteins of different monoclonal cell lines is represented by (*) ((*) low, (**) medium and (***) high) based on the western blot and densitometry analyses realised in section 4.2.2. Regarding the effect on titre or specific productivity, (/) indicates no change compared to the host cell line, (+) indicates statistically higher titre/specific productivity of the recombinant protein compared to the host cell line, (++) indicates statistically higher titre/specific productivity compared to the host cell line and empty vector controls (CHO/MRXIP-GFP H/L) and (-) indicates a lower titre than the host cell line.

The STX18 expressing cell lines did not show any impact on the cell growth, however it is important to note that only the cell line CHO/STX18 F expressed a full-length fused protein. On different occasions, cell line CHO/STX18 F showed significantly higher product concentration than the host cell line (see section 4.3.3.2, 4.3.2.1 and 4.3.1). STX18 is a protein involved in the organisation of the different subdomains of the ER (Iinuma et al. 2009) and the retrograde traffic between the ER and the Golgi (Hatsuzawa et al. 2000). By overexpressing STX18, cells may gain the ability to extend their ER capacity which could lead to improved secretory productivity. Indeed, an increase in ER content had been documented as an approach to improve recombinant protein production (Tigges and Fussenegger 2006). By overexpressing STX18, cells might be able to expand their ER for improved ER capacity, this inherently leading to improvement in productivity. The enhancement of secretory product amounts from the CHO/STX18 F cell line compared to the control was less than the increase observed with STX17 or SNAP29 expressing cell lines and this might reflect the low expression of the eGFP-STX18 fusion protein in the cell line.

Finally, where enhancement of product yields was observed from an engineered cell line compared to the controls the effect was demonstrated for both Etanercept and Adalimumab, suggesting that the increase in secretory productivity is not related to the nature of the product. However, further investigations need to be performed to confirm this because even if the two model molecules are structurally different, they share a lot in common around the IgG1 constant heavy chain constant domains.

4.5. Conclusions

In this chapter, the different syntaxin/SNAP engineered CHO-S cell monoclonal populations overexpressing eGFP fused SNAREs were characterised with respect to their growth profiles and recombinant protein secretory capacity compared to control cell lines. The key findings of the work in this chapter is that the over-expression of a number of the SNAREs appeared to enhance recombinant protein secretory product yields and the extent of this increase was possibly defined by the extent of over-expression of the eGFP-syntaxin/SNAP protein. In particular, overexpression of STX17, STX18 and SNAP29 positively altered the productivity of the model recombinant proteins investigated compared to the host cell line. Further, investigation showed that the level of expression was associated with the

improvement observed and higher titres were obtained with cell lines overexpressing relatively higher amounts of eGFP-STX17 and lower amounts of eGFP-SNAP29. After demonstrating the possible titre improvement by the overexpression of key SNARE proteins at the laboratory scale, these proof-of-concept studies and targets were evaluated and validated under industrially relevant conditions. This work is reported in the next chapter.

CHAPTER 5: Industrial Scale Investigation and Validation of SNARE Engineering of CHO Cells on Secretory Recombinant Protein Production

5.1. Introduction

In the previous chapter (Chapter 4), CHO-S cells genetically engineered with a number of different syntaxin/SNAPs were shown to yield increased production of secreted recombinant protein compared to the original host cell line. Of the four SNARE targets investigated in detail (STX7, 17, 18 and SNAP29), STX17 and SNAP29 when over-expressed in CHO-S cells resulted in longer viable cell culture times under batch culture conditions and increased secretory recombinant protein productivity depending on the levels of expression of these SNARE. In this chapter, these two SNAREs were to be investigated in terms of the impact of their over-expression in an industrial host cell line and the effect in the industrial environment determined. Indeed, cell line engineering and the impact of this can be cell line dependent such as the overproduction of XBP1 (Tigges and Fussenegger 2006), while other approaches may be applied to a range of cell lines with similar effects (Jaluria et al. 2007; Peng et al. 2011). In this chapter, work was undertaken at Fujifilm Diosynth Biotechnologies (FDB) to assess the impact on the secretion of recombinant proteins of manipulation of SNARE proteins using a CHO-DG44 cell line and FDB methodology at their facilities.

FDB is a contract manufacturing company offering cell line development services and manufacturing for recombinant protein production. FDB has developed a CHO-DG44 derived cell line known as “Clone 27” for secretory recombinant protein production commercially. The CHO-DG44 host was generated in 1981 by Urlaub’s team by two mutagenesis steps to obtain a DHFR deficient cell line (Urlaub et al. 1983). The dihydrofolate reductase enzyme (DHFR) is responsible for the conversion of dihydrofolate into tetrahydrofolate, an important intermediate for the synthesis of purines and amino acids (Chen et al. 1984). Methotrexate (MTX) is a competitive inhibitor of DHFR (Goodsell 1999; Rajagopalan et al. 2002) and one manner to overcome its effects is by overexpressing DHFR. The DHFR/MTX combination has since been used as a metabolic selection system involving the transfection of a plasmid containing a *dhfr* gene and addition of MTX to the media. The host Clone 27 cell line was used to investigate the impact of syntaxin cell

engineering. A direct comparison of the impacts of syntaxin/SNAP engineering between the CHO-S cell line and the CHO-DG44 cell line which share a common ancestor could be seen as limited, but several reports have shown heterogeneity in-between and between different host cell lines derived from CHO cells (Kim et al. 2011; Lewis et al. 2013). Derouazi et al. (2006) also demonstrated the heterogeneity of monoclonal populations derived from the same parental cell line. It is therefore necessary to undertake appropriate experiments to unravel any cell line dependent effect of engineering the targets of interest.

This chapter is focused on determining if the findings described in Chapter 4 investigating transient expression of target biotherapeutic proteins are transferable to a different host CHO cell line in an industrial environment stably expressing the target biotherapeutic under fed-batch conditions. Initially, new genetic constructions in the pAVE vector system used at FDB are described. Following generation of the different vectors of interest, the process for mini-pool generation is described and the different selection steps documented. In parallel, transient transfection experiments were undertaken to analyse the impact of different promoters and the fusion of an eGFP tag to the syntaxin/SNAP proteins. A further co-transfection strategy was also used to generate stably expressing cell lines using vectors generated in Chapter 3. Once stably expressing syntaxin/SNAP and target recombinant protein cell lines were obtained, a fed-batch over grow method was used to determine any effect on the industrial relevant cell lines engineered with SNARE proteins on the production of recombinant protein. Finally, expression of the fused eGFP-syntaxin/SNAP proteins was evaluated in the stably expressing cell lines and levels of endogenous SNARE were compared between the industrial host, Clone 27, and the cell line used in the academic lab, CHO-S.

5.2. Generation of vectors for the engineering of syntaxin/SNAP and expression of model recombinant proteins in the FDB CHO-DG44 host cell line

For the different experiments that were undertaken at FDB, the eGFP-STX7, 17, 18 and SNAP29 fusions were selected as targets to engineer based upon the proof-of-concept work described in Chapter 4. The engineering of the CHO-S host with eGFP-STX17 and -SNAP29 gave interesting results in the proof-of-concept academic lab studies (see Chapter 4), whilst engineering of STX7 and STX18 was undertaken to determine if the observed

effect in CHO-S cells could be transferred to another industrial host grown under industrially relevant conditions. Fujifilm Diosynth Biotechnologies have developed a CHO-DG44 cell line, Clone 27, as part of an expression system, the Apollo™ platform, for the production of recombinant proteins. To be able to assess the potential of syntaxin/SNAP engineering in the Clone 27 host cell line, new genetic constructs needed to be generated. Indeed, Clone 27, being derived from a CHO-DG44 cell line uses metabolic DHFR overexpression and MTX supplementation to select for cells that have incorporated the DNA of interest. The platform uses a proprietary plasmid system, the pAVE system, which includes the different required elements for recombinant protein expression and selection of Clone 27 derived cell lines.

When the product of interest is an antibody, the pAVE system starts with the generation of two different plasmids, one containing the heavy chain gene and one containing the light chain gene, which are then ligated together to form a unique expression vector, the Double Gene Vector or DGV. To avoid a dual selection process with the co-transfection of two plasmids, one for the recombinant model protein and one for the SNARE protein, the targets of interest were cloned into the DGV. To do so, a gene present for hygromycin B resistance in the DGV but not used as a selection marker, was replaced by the gene coding for the different SNARE proteins. Some modifications to the vector were necessary for this strategy, notably a change of promoter and polyA tail of the resistance gene. The hygromycin resistance gene was under the control of a HSV mini-TK promoter and a HSV TK polyA tail which tend to result in low expression of genes compared to a CMV promoter (Ede et al. 2016). Information about the ectopic expression of the SNARE proteins under control of a promoter other than CMV was not available so it was decided to switch the promoter and polyA tail to a CMV promoter and a bGH polyA tail as used in the proof-of-concept studies described in Chapter 4. Two sets of recombinant gene containing constructs were also generated, one expressing Adalimumab and one expressing Blosozumab. Blosozumab, an IgG4 used for the treatment of osteoporosis (Mccolm et al. 2014), is the standard model molecule used at FDB for process evaluation. In order to further analyse the impact of the eGFP tag on the fused proteins, plasmids were designed to express the protein of interest with or without an eGFP tag. Plasmids were also generated with the gene of interest under the control of a TK promoter and TK polyA tail to determine any impact of promoters of different strengths. The details of the different genetic vectors generated in the work described in this chapter are detailed in Table 5.1.

To generate the pAVE HC ADA vector containing the coding sequence for the heavy chain (HC) of the Adalimumab antibody, the HC coding sequence was obtained by PCR using the Adalimumab plasmid as a template and ligated into the pAVE931 plasmid. Primers for PCR were designed to amplify the coding sequence of the HC gene of Adalimumab (1426 bp) with restriction sites AflII and BamHI (Figure 5.1A). For ligation into the pAVE931 vector, the PCR product and acceptor pAVE931 vector were digested using AflII and BamHI restriction enzymes. After digestion, two bands were obtained at the expected size of 7515 bp and 426 bp for the backbone as determined by agarose gel electrophoresis analysis (Figure 5.1A). The upper band containing the desired portion of pAVE931 was extracted from the gel and purified before being ligated with the purified and digested PCR product. Ligation was successful using a 3:1 ratio (insert: vector) and several colonies obtained were used to extract DNA. From analytical digestion with AflII and BamHI, two fragments at 7509 bp and 1426 bp were expected for successful ligations, one colony showed the required DNA pattern (Figure 5.1B). The region containing the Adalimumab heavy chain gene was then sequenced to check for any anomalies in the sequence, such as point mutations, and was found to be correct.

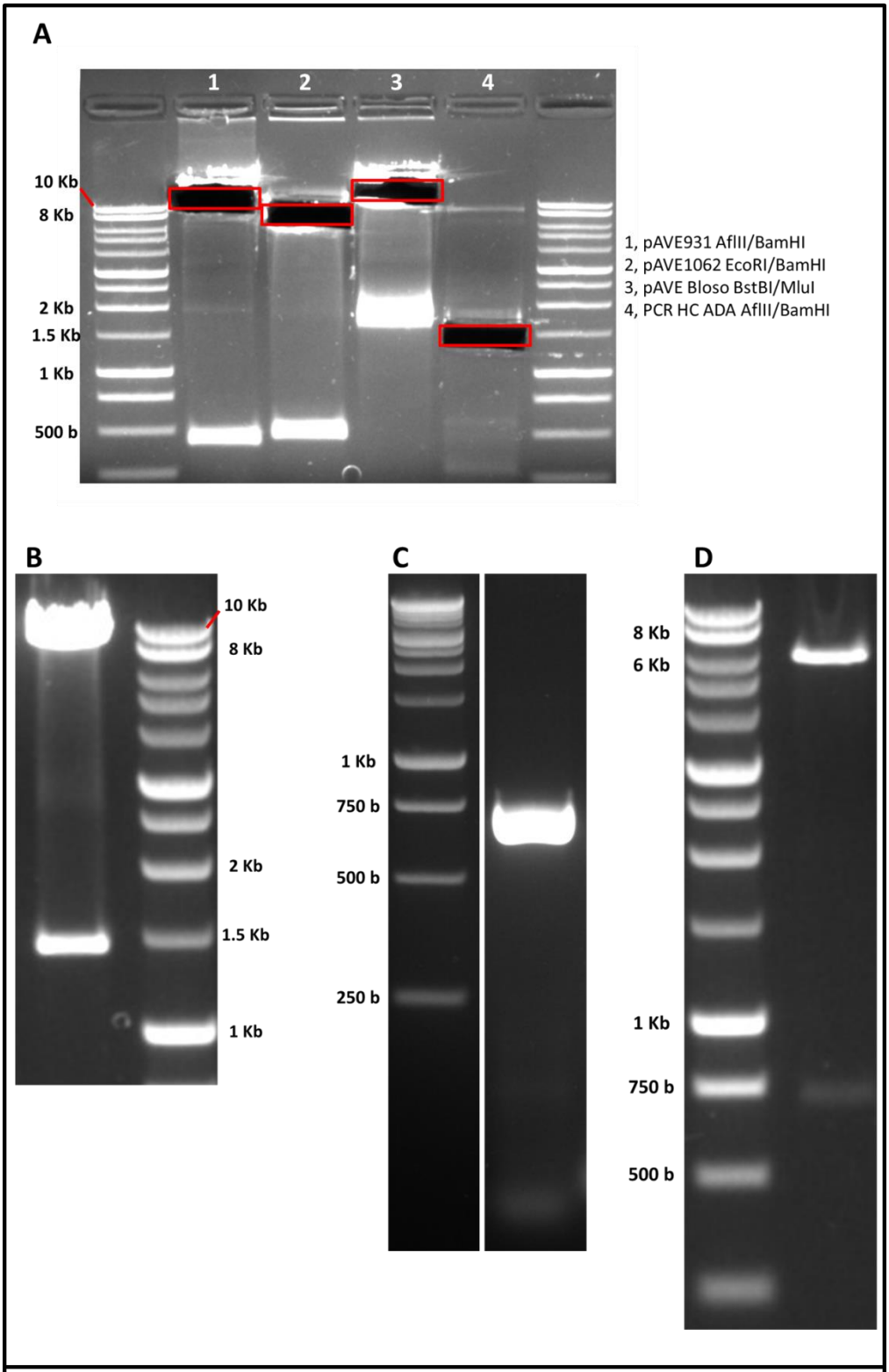

Figure 5.1. Agarose gel electrophoresis analysis of digested DNA. **A,** (*1*) Digestion of pAVE931 with AflII and BamHI to yield bands at 7515 bp and 426 bp, (*2*) Digestion of pAVE1062 with EcoRI and BamHI to yield bands at 6074 bp and 495 bp, (*3*) Digestion of pAVE Bloso with BstBI and MluI to yield bands at 10225 bp and 1658 bp, (*4*) Digestion of the HC Adalumimab PCR product with AflII and BamHI to yield a band at 1416 bp. **B,** Successful test digest of pAVE HC ADA with AflII and BamHI to yield bands at 7509 bp and 1426 bp. **C,** PCR of the LC Adalumimab fragment to yield a band at 717 bp. **D,** Successful test digest of pAVE LC ADA with EcoRI and BamHI to yield bands at 6074 bp and 717 bp. Red squares outline excised bands for ligation.

To generate the pAVE LC ADA vector containing the coding sequence for the light chain (LC) of the Adalimumab antibody, the coding sequence was again amplified by PCR using the Adalimumab plasmid as a template and the resulting product ligated into the pAVE1062 plasmid. PCR primers were designed to obtain the coding sequence of the light chain gene of Adalimumab (717 bp long) with EcoRI and BamHI restriction sites (Figure 5.1C). For ligation into the pAVE1062 vector, the PCR product and the acceptor plasmid were digested using EcoRI and BamHI restriction enzymes. After digestion of the pAVE1062 plasmid, two bands were obtained at the expected size of 6074 bp and 495 bp as determined by agarose gel electrophoresis analysis (Figure 5.1A). The upper band containing the desired portion of pAVE1062 was extracted from the gel and purified before being ligated to the digested and purified PCR product. Ligation was successful using a 3:1 ratio (insert:vector) and several colonies obtained were used to extract DNA. From analytical digestion with EcoRI and BamHI enzymes, two fragments at 6074 bp and 717 bp were expected for successful ligations, one colony showed the required DNA pattern (Figure 5.1D). Sequencing was performed on the region containing Adalimumab light chain gene to confirm presence of the correct sequence.

The DGV, pAVE ADA, was obtained by ligating together a fragment of pAVE HC ADA and pAVE LC ADA using BssHII and PmEI as restriction enzymes. After digestion of pAVE HC ADA, three fragments at the respective sizes of 5158 bp, 3752 bp and 10 bp were obtained as determined by agarose gel electrophoresis analysis. The upper band (5158 bp), containing the desired sequence, was excised from the gel and purified before ligation with pAVE LC ADA, referred to as the backbone, previously digested with the same enzymes. Ligation was successful using a 3:1 ratio (insert: vector) and several colonies obtained were used to extract DNA. When performing a test digest with BamHI, two fragments at 8818 bp and 3112 bp were expected for a successful ligation. One colony showed the corresponding pattern (Figure 5.2A).

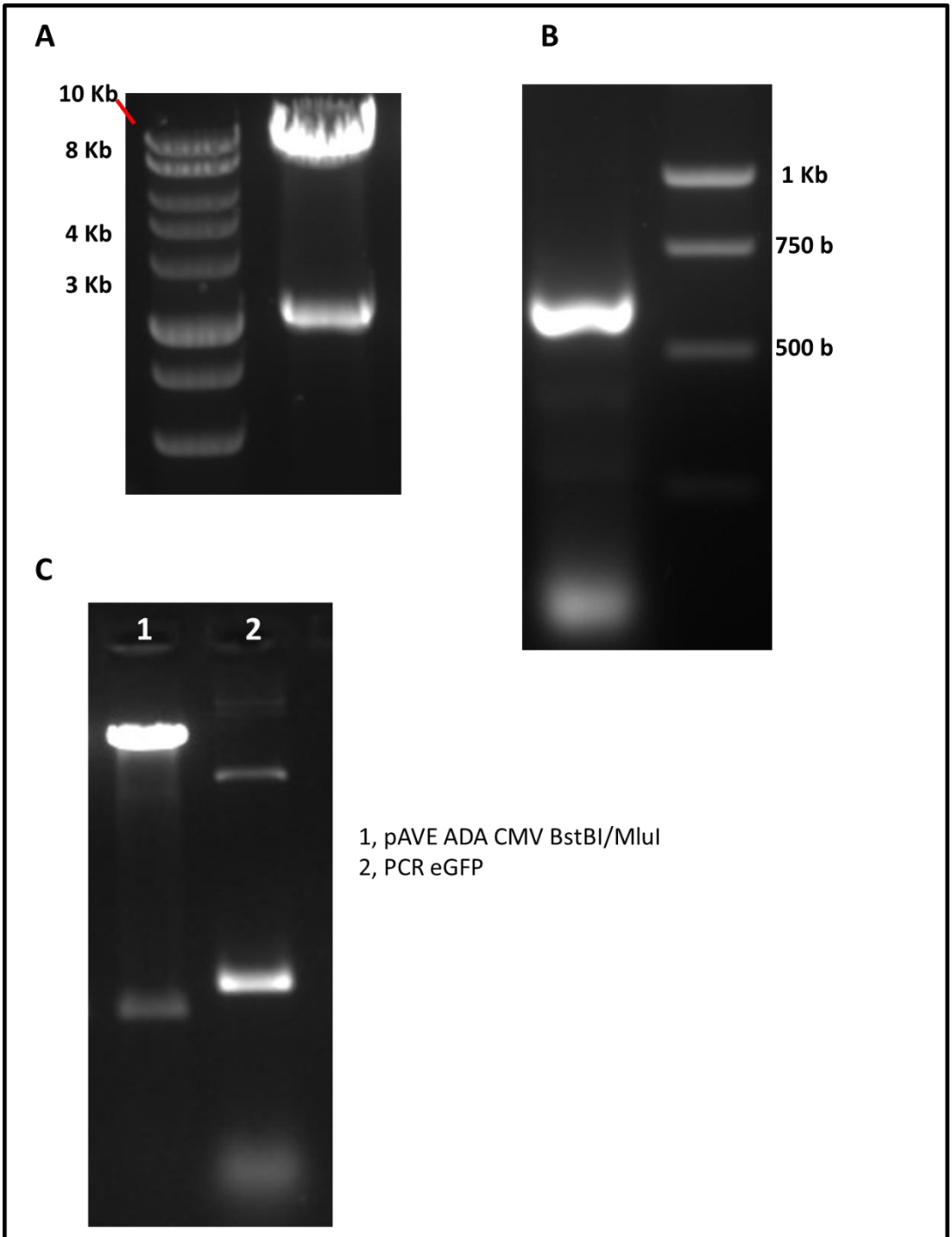

Figure 5.2. Agarose gel electrophoresis analysis of digested DNA. **A,** Successful test digest of pAVE ADA using BamHI restriction enzyme with two bands at 8818 bp and 3112 bp. **B,** PCR of the CMV promoter fragment to yield a band at 615 bp. **C,** (*1*) Successful test digestion of pAVE ADA CMV using BstBI and MluI enzymes with two expected bands at 10210 bp and 603 bp, (*2*) PCR of the eGFP fragment with an expected band at 741 bp.

Generation of the pAVE ADA CMV construct was performed by insertion of a CMV promoter to replace the promoter driving the hygromycin resistance cassette gene. The CMV promoter sequence with the desired restriction sites was obtained by PCR with appropriate primers using pcDNA3.1/Hygro(+) vector as a template. A 615 bp fragment was obtained (Figure 5.2B) with 5' BstBI and 3' MluI restriction sites as demonstrated by agarose gel electrophoresis analysis. A complementary PmlI site was also added at the 3' during this operation. The PCR product was digested using BstBI and MluI restriction enzymes, purified and then ligated to the backbone pAVE ADA previously digested with the same set of enzymes. Ligation was successful using a 3:1 ratio (insert: vector) and several colonies obtained were used to extract DNA. One colony showed the required DNA pattern as determined by agarose gel electrophoresis analysis, with two bands expected at 10210 bp and 615 bp after analytical digestion with BstBI and MluI (Figure 5.2C). The region containing the new CMV promoter was confirmed as correct by sequence analysis.

The pAVE ADA CMVbGH was created by introduction of a bGH polyA tail downstream of the introduced CMV promoter in pAVE ADA CMV. The bGH polyA tail was obtained by PCR using the pcDNA3.1/Hygro(+) vector as a template with designed primers. A fragment of 258 bp was expected as demonstrated by agarose gel electrophoresis analysis (Figure 5.3A). The primers for amplification contained the restriction sites, PmlI and NotI in 5' and MluI in 3'. The PCR fragment was digested using PmlI and MluI restriction enzymes, cut from the agarose gel and then ligated with pAVE ADA CMV previously digested with PmlI and MluI. Ligation was successful using a 3:1 ratio (insert: vector) and several colonies obtained were used to extract DNA. A successful ligation pattern when digesting with BstBI and NotI was two bands at 10442 bp and 604 bp as showed in Figure 5.3B. Successful ligation was confirmed by sequencing of the region of interest.

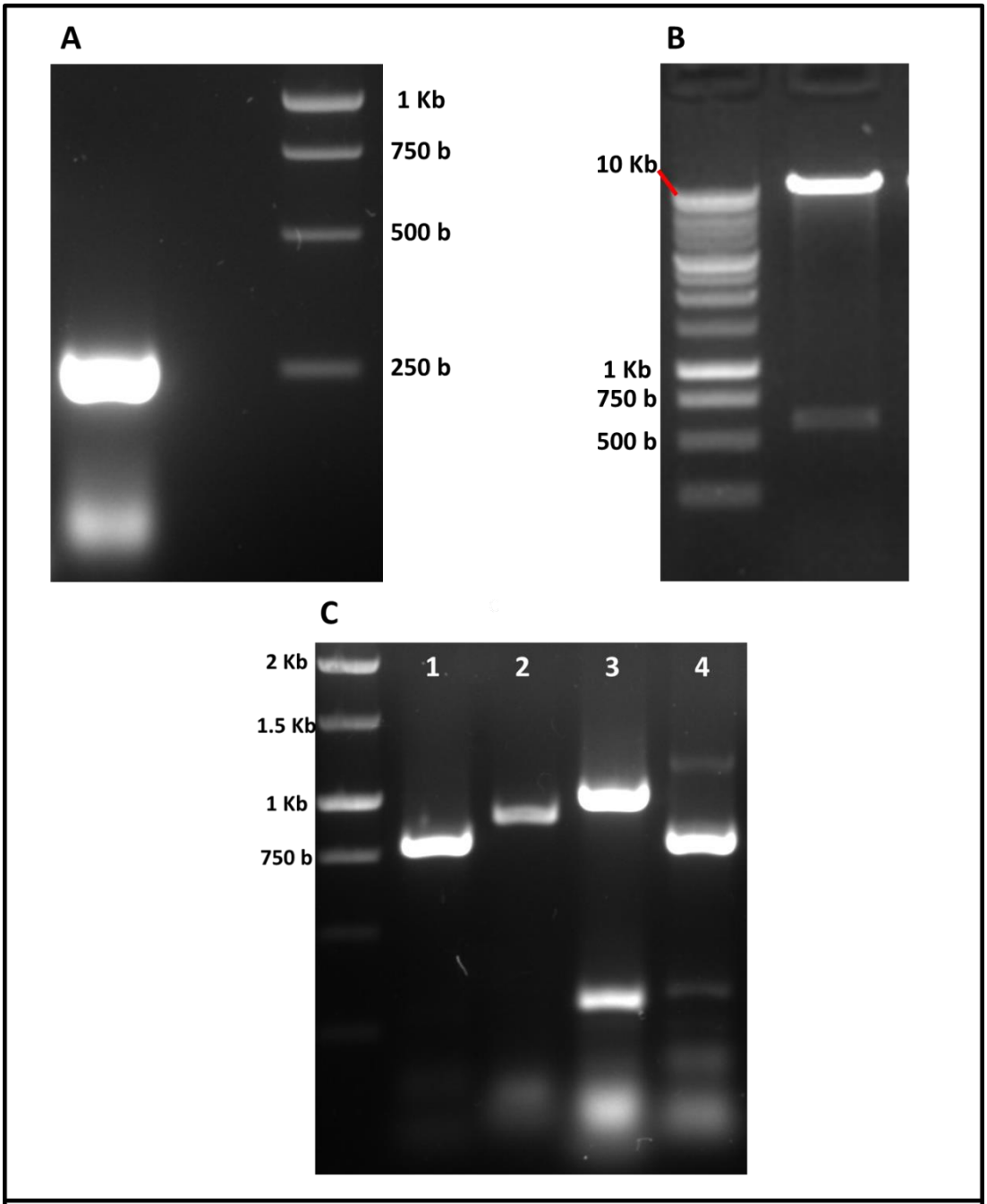

Figure 5.3. Analyses of digested DNA by agarose gel electrophoresis. **A,** PCR amplification of the bGH polyA tail to yield an expected fragment of 258 bp. **B,** Successful test digest of pAVE ADA CMVbGH with BstBI and NotI to yield two bands at 10442 bp and 604 bp. **C,** PCR amplification of the different syntaxin genes (*1*) STX7, (*2*) SXT17, (*3*) STX18 and (*4*) SNAP29 to yield expected bands at 807 bp, 930 bp, 1029 bp and 798 bp respectively.

Vectors pAVE ADA CMV STX7, pAVE ADA CMV STX17, pAVE ADA CMV STX18, pAVE ADA CMV SNAP29 and pAVE ADA CMV eGFP were generated in a similar manner, by inserting DNA fragments containing the gene of interest into the pAVE ADA CMVbGH. For the different SNARE genes, PCR primers were design to only amplify the syntaxin gene

(omitting the eGFP) and to add complementary restriction sites (PmlI in 5' and NotI in 3'). The plasmids pMRXIP-STX7, pMRXIP-STX17, pMRXIP-STX18 and pMRXIP-SNAP29 were used as templates to obtain the desired PCR fragments of 807 bp, 930 bp, 1029 bp and 798 bp for STX7, STX17, STX18 and SNAP29 genes as demonstrated by agarose gel analysis (Figure 5.3C). The eGFP gene was obtained by PCR amplification using pcDNA3.1Hygro/GFP as a template. A PCR product of 741 bp was expected as shown in Figure 5.2C. The different PCR products were digested using PmlI and NotI restriction enzymes, purified and then ligated into pAVE ADA CMVbGH plasmid previously digested with the same enzymes. Ligations were successful using a 3:1 ratio (insert: vector) and several colonies obtained were used to extract DNA. When test digested with PmlI and NotI the expected patterns were two bands at 11031 bp and 795 bp for pAVE ADA CMV STX7, 11031 bp and 918 bp for pAVE ADA CMV STX17, 11031 bp and 1017 bp for pAVE ADA CMV STX18, 11031 bp and 786 bp for pAVE ADA CMV SNAP29 and 11031 bp and 729 bp for pAVE ADA CMV GFP as highlighted by the successful ligations in Figure 5.4. The correct insertion of the different genes of interest was confirmed by sequencing analysis.

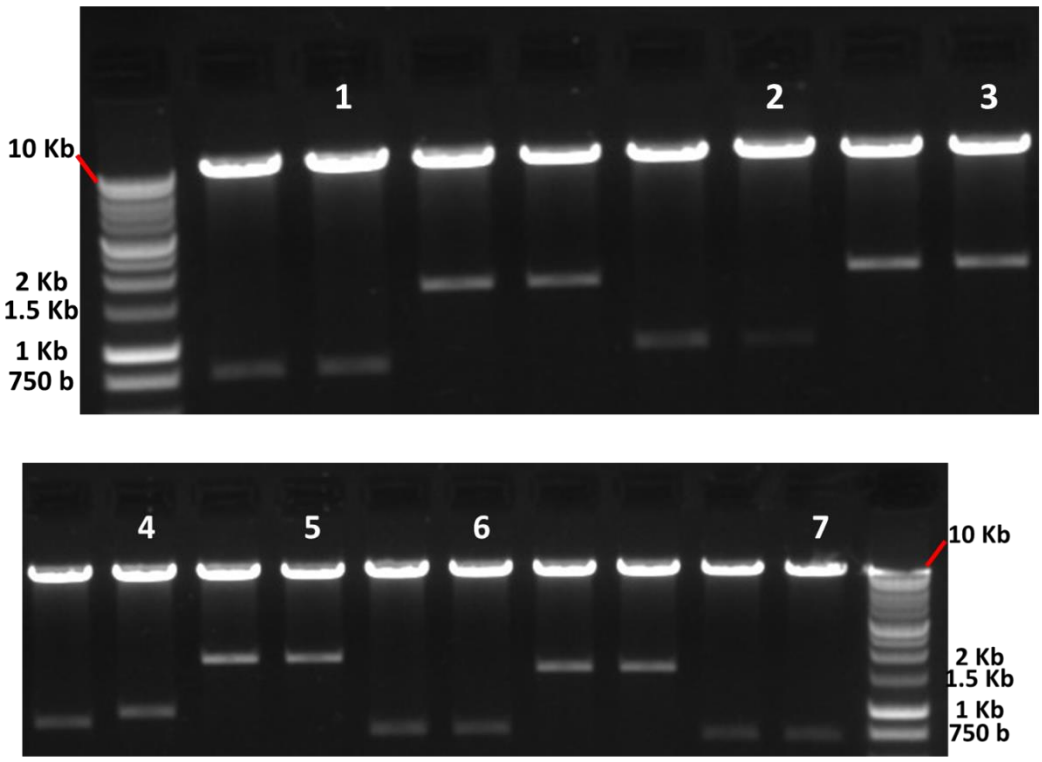

1, pAVE ADA CMV STX7 PmlI/NotI
2, pAVE ADA CMV STX17 PmlI/NotI
3, pAVE ADA CMV STX17GFP PmlI/NotI
4, pAVE ADA CMV STX18 PmlI/NotI
5, pAVE ADA CMV STX18GFP PmlI/NotI
6, pAVE ADA CMV SNAP29 PmlI/NotI
7, pAVE ADA CMV GFP PmlI/NotI

Figure 5.4. Agarose gel electrophoresis analysis of digested DNA. Successful test digestion using PmlI and NotI enzymes for pAVE ADA CMV STX7 (*1*), pAVE ADA CMV STX17 (*2*), pAVE ADA CMV STX17GFP (*3*), pAVE ADA CMV STX18 (*4*), pAVE ADA CMV STX18GFP (*5*), pAVE ADA CMV SNAP29 (*6*) and pAVE ADA CMV GFP (*7*).

Plasmid pAVE ADA CMV STX17GFP and pAVE ADA CMV STX18GFP were generated by digesting the sequence containing the fused protein from pMRXIP-STX17 and pMRXIP-STX18 using PmlI and NotI restriction enzymes. Three bands were obtained of 5687 bp, 1779 bp and 325 bp sizes for pMRXIP-STX17 or 5687 bp, 1878 bp and 325 bp for pMRXIP-STX18. The desired band (1779 bp for STX17 and 1878 bp for STX18), containing the gene of interest, was extracted from the agarose gel, purified and ligated into the pAVE ADA CMVbGH vector previously digested with PmlI and NotI. Ligations were successful using a 3:1 ratio (insert: vector) and several of the resulting colonies were used to extract DNA. One colony for each construct showed the required DNA pattern as determined by agarose gel electrophoresis analysis, with two bands expected at 11031 bp and 1783 bp for pAVE

ADA CMV STX17GFP or 11031 bp and 1882 bp for pAVE ADA CMV STX18GFP after analytical digestion with PmlI and NotI (Figure 5.4).

Plasmids with genes of interest (STX17 and STX18 with or without tag) with expression controlled by TK promoter and TK polyA tail were also generated to be able to compare against the CMV promoter. Indeed, the TK promoter is a weaker promoter than the CMV promoter. In order to integrate those into the DGV, sequences were designed and ordered from Twist Bioscience, USA.

The plasmid pAVE ADA TK STX17, pAVE ADA TK STX17GFP, pAVE ADA TK STX18, pAVE ADA TK STX18GFP were generated by digesting pTwist TK STX17 and pTwist TK STX18 with BstBI and PmlI restriction enzymes or digesting pTwist TK STX17GFP and pTwist STX18GFP with BstBI, PvuI and PmlI. Plasmids pTwist TK STX17GFP and pTwist STX18GFP had to be digested with 3 enzymes to obtain bands of different size able to be distinguished after agarose gel analysis. After digestion, the desired bands (1150 bp for STX17, 1250 bp for STX18, 1956 bp for STX17GFP and 2031 bp for STX18GFP) were excised from the gel, purified and ligated into pAVE ADA CMV previously digested with BstBI and PmlI. Ligations were successful using a 3:1 ratio (insert: vector) and several of the resulting colonies were used to extract DNA. After test digest with BstBI and PmlI restriction enzymes, a pattern for successful ligation were two bands at 10264 bp and 1150 bp for pAVE ADA TK STX17, 10264 bp and 1249 bp for pAVE ADA TK STX18, 10264 bp and 1954 bp for pAVE ADA TK STX17GFP and 10264 bp and 2029 bp for pAVE ADA TK STX18GFP as demonstrated by successful colonies in Figure 5.5.

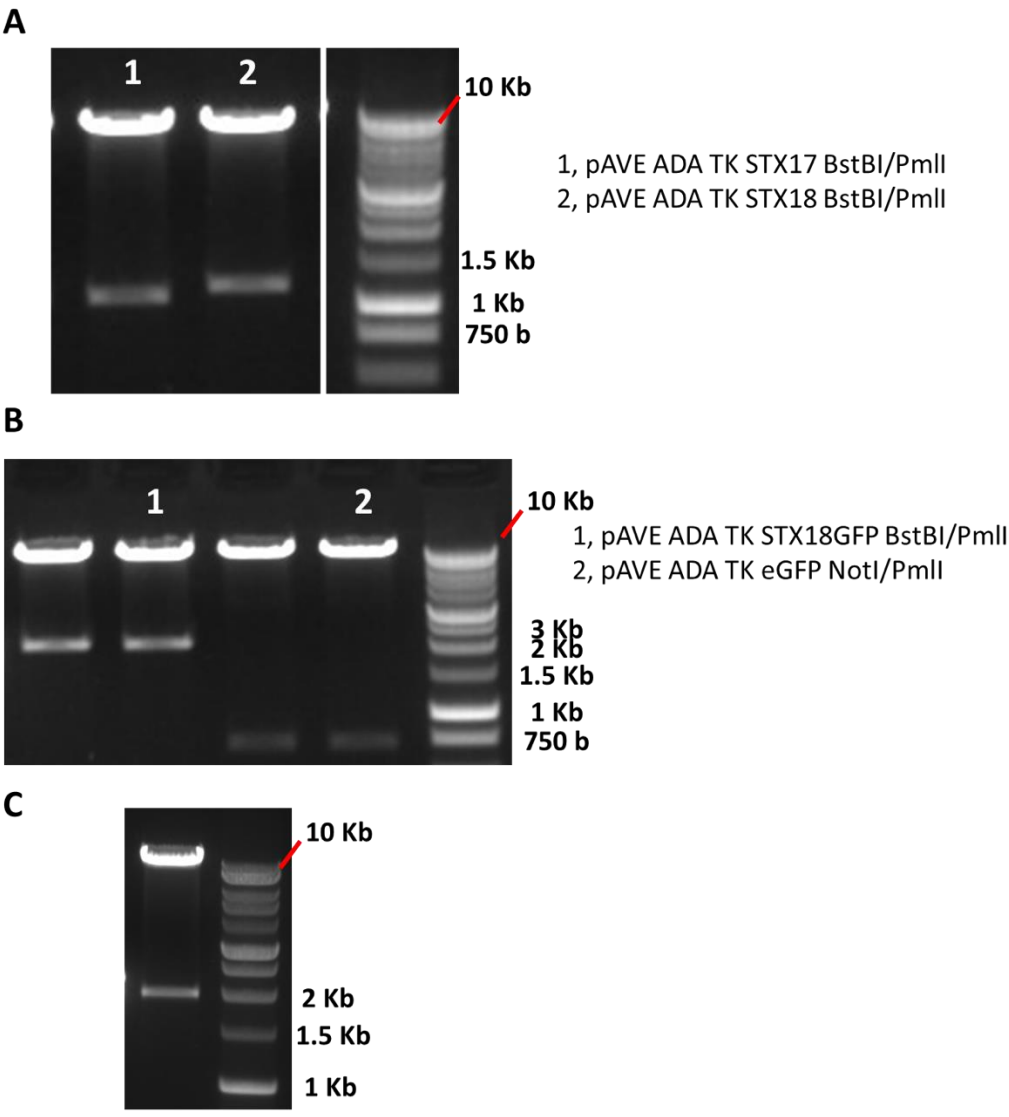

Figure 5.5. Agarose gel electrophoresis analysis of digested DNA. **A,** Successful test digest of pAVE ADA TK STX17 (*1*) and pAVE ADA TK STX18 (*2*) using BstBI and PmlI to yield two bands at 1150 or 1250 bp and 10224 bp. **B,** (*1*) Successful test digest of pAVE ADA TK STX18GFP using BstBI and PmlI to yield two bands at 10224 bp and 2029 bp, (*2*) successful test digest of pAVE ADA TK eGFP with NotI and PmlI to yield two bands at 10445 bp and 729 bp. **C,** Successful test digest of pAVE ADA TK STX17GFP using BstBI and PmlI to yield bands at 10224 bp and 1954 bp.

Generation of the control vector pAVE ADA TK GFP was achieved in two steps. First, generation of pAVE ADA TK D2GFP was undertaken by ligating TK D2GFP fragment into pAVE ADA. pTwist TK D2GFP was digested with MluI for extraction of a band of 1059 bp. The fragment containing the coding gene for D2GFP, a destabilised GFP, was purified and ligated into pAVE ADA previously digested with MluI. Ligation was successful using a 3:1 ratio (insert: vector) and several of the resulting colonies were used to extract DNA. Successful test digest with PmlI and BamHI restriction enzymes was a pattern of three

bands, 6985 bp, 3112 bp and 1234 as demonstrated by one colony. The newly generated pAVE ADA TK D2GFP was digested with PmlI and NotI restriction enzymes and ligated with a purified and digested PCR fragment obtained by amplification of the GFP gene using appropriate primers and pcDNA3.1Hygro/GFP as a template (Figure 5.2C). Ligation was successful using a 3:1 ratio (insert: vector) and several of the resulting colonies were used to extract DNA. Following test digest with NotI and PmlI, one colony was observed with the required successful pattern of two bands at 10445 bp and 729 bp (Figure 5.5C).

The equivalent vectors were generated from pAVE Bloso, a DGV expressing Blosozumab. The steps and enzymes were similar, only the sizes of the DNA fragments were different. All the plasmids used in this chapter are described in Table 5.1.

Table 5.1. List of the vectors generated and used in Chapter 5.

Name	Backbone	Gene of interest	Recombinant model protein	Promoter/polyA tail	Tag	restriction sites used for cloning	Mammalian selection	Origin
pAVE HC ADA	pAVE 931	/	heavy chain Adalimumab	/	/	AflII/BamHI	MTX	This work
pAVE LC ADA	pAVE 1062	/	Light chain Adalimumab	/	/	EcoRI/BamHI	MTX	This work
pAVE ADA	/	/	Adalimumab	/	/	BssHII/PmeI	MTX	This work
pAVE ADA CMV	pAVE ADA	/	Adalimumab	CMV/-	/	BstBI/MluI	MTX	This work
pAVE ADA CMVbGH	pAVE ADA CMV	/	Adalimumab	CMV/bGH	/	PmlI/MluI	MTX	This work
pAVE ADA CMV STX7	pAVE ADA CMVbGH	STX7	Adalimumab	CMV/bGH	/	PmlI/NotI	MTX	This work
pAVE ADA CMV STX17	pAVE ADA CMVbGH	STX17	Adalimumab	CMV/bGH	/	PmlI/NotI	MTX	This work
pAVE ADA CMV STX18	pAVE ADA CMVbGH	STX18	Adalimumab	CMV/bGH	/	PmlI/NotI	MTX	This work
pAVE ADA CMV SNAP29	pAVE ADA CMVbGH	SNAP29	Adalimumab	CMV/bGH	/	PmlI/NotI	MTX	This work
pAVE ADA CMV STX17GFP	pAVE ADA CMVbGH	STX17	Adalimumab	CMV/bGH	eGFP	PmlI/NotI	MTX	This work
pAVE ADA CMV STX18GFP	pAVE ADA CMVbGH	STX18	Adalimumab	CMV/bGH	eGFP	PmlI/NotI	MTX	This work
pAVE ADA CMV eGFP	pAVE ADA CMVbGH	eGFP	Adalimumab	CMV/bGH	/	PmlI/NotI	MTX	This work
pAVE ADA TK STX17	pAVE ADA CMV	STX17	Adalimumab	TK/TK	/	BstBI/PmlI	MTX	This work
pAVE ADA TK STX18	pAVE ADA	STX18	Adalimumab	TK/TK	/	BstBI/PmlI	MTX	This work
pAVE ADA TK STX17GFP	pAVE ADA	STX17	Adalimumab	TK/TK	eGFP	BstBI, PvuI and PmlI	MTX	This work
pAVE ADA TK STX18GFP	pAVE ADA	STX18	Adalimumab	TK/TK	eGFP	BstBI, PvuI and PmlI	MTX	This work
pAVE ADA TK eGFP	pAVE ADA	eGFP	Adalimumab	TK/TK	/	PmlI/NotI	MTX	This work
pAVE Bloso	/	/	Blosozumab	/	/	BssHII/PmeI	MTX	FDB
pAVE Bloso CMV	pAVE Bloso	/	Blosozumab	CMV/-	/	BstBI/MluI	MTX	This work
pAVE Bloso CMVbGH	pAVE Bloso CMV	/	Blosozumab	CMV/bGH	/	PmlI/MluI	MTX	This work
pAVE Bloso CMV STX7	pAVE Bloso CMVbGH	STX7	Blosozumab	CMV/bGH	/	PmlI/NotI	MTX	This work
pAVE Bloso CMV STX17	pAVE Bloso CMVbGH	STX17	Blosozumab	CMV/bGH	/	PmlI/NotI	MTX	This work
pAVE Bloso CMV STX18	pAVE Bloso CMVbGH	STX18	Blosozumab	CMV/bGH	/	PmlI/NotI	MTX	This work
pAVE Bloso CMV SNAP29	pAVE Bloso CMVbGH	SNAP29	Blosozumab	CMV/bGH	/	PmlI/NotI	MTX	This work
pAVE Bloso CMV STX17GFP	pAVE Bloso CMVbGH	STX17	Blosozumab	CMV/bGH	eGFP	PmlI/NotI	MTX	This work
pAVE Bloso CMV STX18GFP	pAVE Bloso CMVbGH	STX18	Blosozumab	CMV/bGH	eGFP	PmlI/NotI	MTX	This work
pAVE Bloso CMV eGFP	pAVE Bloso CMVbGH	eGFP	Blosozumab	CMV/bGH	/	PmlI/NotI	MTX	This work
pAVE Bloso TK STX17	pAVE Bloso CMV	STX17	Blosozumab	TK/TK	/	BstBI/PmlI	MTX	This work
pAVE Bloso TK STX18	pAVE Bloso	STX18	Blosozumab	TK/TK	/	BstBI/PmlI	MTX	This work
pAVE Bloso TK STX17GFP	pAVE Bloso	STX17	Blosozumab	TK/TK	eGFP	BstBI, PvuI and PmlI	MTX	This work
pAVE Bloso TK STX18GFP	pAVE Bloso	STX18	Blosozumab	TK/TK	eGFP	BstBI, PvuI and PmlI	MTX	This work
pAVE Bloso TK eGFP	pAVE Bloso	eGFP	Blosozumab	TK/TK	/	PmlI/NotI	MTX	This work

5.3. Generation of CHO-DG44 cell pools stably expressing the SNAREs and target model recombinant proteins

5.3.1. Generation of stably expressing mini-pools

Monoclonal cell lines are highly desired in industry in order to obtain homogenous cell line populations, but the generation of these monoclonal populations and validation of their monoclonality are expensive and time consuming processes. For bioprocess development approaches, industry therefore often uses mini-pools of recombinant cells as opposed to monoclonal cell lines. Mini-pools are recombinant cell pools generated from a small number of cells and are established based on the fact that the stable integration in the genome of DNA after transfection is a rare event. Hence, mini-pools may not be a homogenous population such as a monoclonal population but their heterogeneity is restrained by the small number of cells initially used to establish the pool and the rare event of stable integration. The establishment of mini-pools compared to monoclonal populations is more rapid and less work intensive giving the opportunity to generate and characterised cell pools with a set phenotype and obtain recombinant cells lines expressing the desired product much more quickly. Moreover, Fan et al. (2017) have shown that mini-pools and monoclonal cell lines derived from the same mini-pool shared the same phenotype.

The mini-pool generation process used at FDB is summarised in Figure 5.6. The process starts with transfection of cells with the desired vector for the expression of the recombinant protein of interest. Following transfection (electroporation), media with a selection agent is added to select for only stably expressing cell lines. Cells are then aliquoted into wells of a 96-well plate at 1000 cells/well and incubated over a period of 2-3 weeks to allow for recovery and cell out growth. Typically in a cell line development project, up to 10 x 96-well plates are processed for each cell line. During the recovery period, cells are monitored regularly to check for contamination and confluency. When confluency of most of the wells reaches over 50%, wells with a monoclonal profile (growth of one colony in the well) are selected for titre screening. Mini-pools reaching the desired titre are progressed from 96-well plates to spin tubes in several steps. Once in spin tubes, populations are ranked again by titre. Selected cell lines are then assessed in a fed-batch over grow experiment in shaken 24-DWPs. During this experiment, only titre is monitored

over a period of 14 days. The results of the experiment are used to set up another FOG at larger scale to monitor not only titre, but also cell growth and viability.

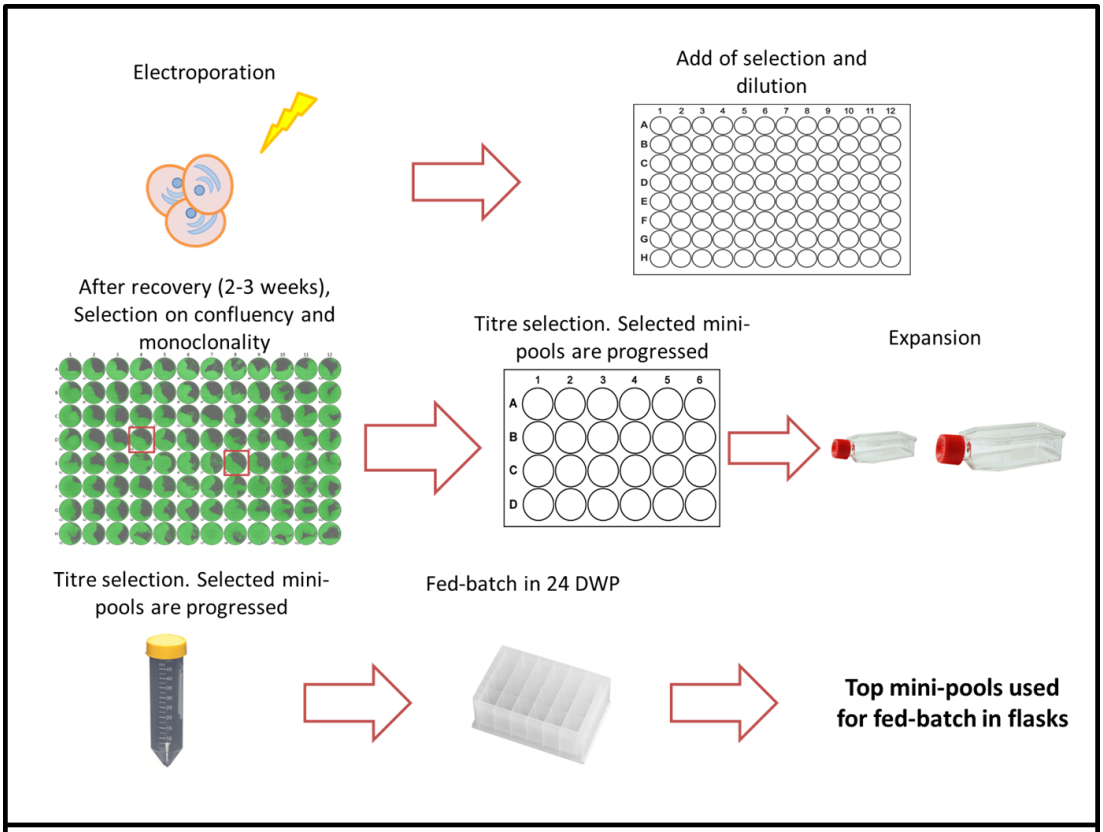

Figure 5.6. Graphical representation of the process to establish mini-pools at Fujifilm Dyosinth Biotechnologies. The day following transfection, cells are diluted to 1000 cells/well into 96-well plates. After 2-3 weeks recovery, cells are selected based on confluency (between 50 and 70%) and monoclonality to be expanded into 24-well plates. In 24 well plates, mini-pools are selected based on productivity. Selected mini-pools are expanded into spin tube cultures where another selection based on titre is performed. Chosen mini-pools are analysed by a FOG in 24-DWPs and the top mini-pools from that experiment are then assessed in a larger scale FOG experiment.

Generation of mini-pools was undertaken with the following constructs; pAVE ADA and pAVE ADA CMVbGH (both controls); pAVE ADA CMV STX7, pAVE ADA CMV STX17, pAVE ADA CMV STX18, pAVE ADA CMV SNAP29; pAVE Bloso, pAVE Bloso CMVbGH (both controls); pAVE Bloso CMV STX7, pAVE Bloso CMV STX17, pAVE Bloso CMV STX18 and pAVE Bloso CMV SNAP29. None of the different SNARE constructs contained an eGFP fused syntaxin/SNAP protein as in the proof-of-concept studies (i.e. the constructs contained the SNARE gene alone with no tag).

A variety of cell pools were generated with the same plasmids for different purposes. To indicate the origin of a cell pool and how it was generated, cell pools were named using “mp” (e.g. mpDG44/ADA STX7 3 for mini-pool number 3 of Clone 27 cell line stably

transfected with the plasmid pAVE ADA CMV STX7) for mini-pools or “pool” for pool cell lines (e.g. poolDG44/ADA STX18 for a pool cell line generated with the plasmid pAVE ADA CMV STX18). The promoter utilised to drive the expression of the gene of interest was only used in the naming of cell lines when the promoter was other than CMV. No mini-pool was generated for the construct pAVE ADA CMV STX18.

For each different construct, 5 x 96-well plates were processed. Following the 3 weeks recovery, confluency was determined using either a Cell Metric CLD (Solentim, UK) plate reader or visually. Figure 5.7 represents the output of the Cell Metric CLD plate reader for one plate. Criteria for selection were confluency between 50 and 70% and a high probability of monoclonality (presence of one colony in the well). Because the goal was to generate mini-pools, the monoclonality criterion was not stringent. From this first screen, 48 mini-pools for each transfection were selected and progressed into 24 well plates. After a week of growth in 24 well plates, titre measurement for each mini-pool was achieved by harvesting 200 µL of supernatant. Results for the highest and lowest expressing mini-pool are displayed in Table 5.2A for each construct. Surprisingly, for all the cell pools co-expressing a SNARE and a recombinant product, titre concentrations were too low to be measured. Low titres were expected at this stage due to the low number of cells and conditions of the screen, however it was expected that they would be measurable. Antibody titres were measurable for the cell lines transfected with the DGV expressing Adalimumab or Blosozumab alone. The lowest Blosozumab clone had a titre of 24.9 µg/mL whereas the best Adalimumab clone had a titre of 22.2 µg/mL suggesting higher titre for Blosozumab expressing cell pools. From this initial titre screen, 8 mini-pools for each construct (88 in total) were progressed into T25, T75 tissue culture flasks and finally into spin tubes.

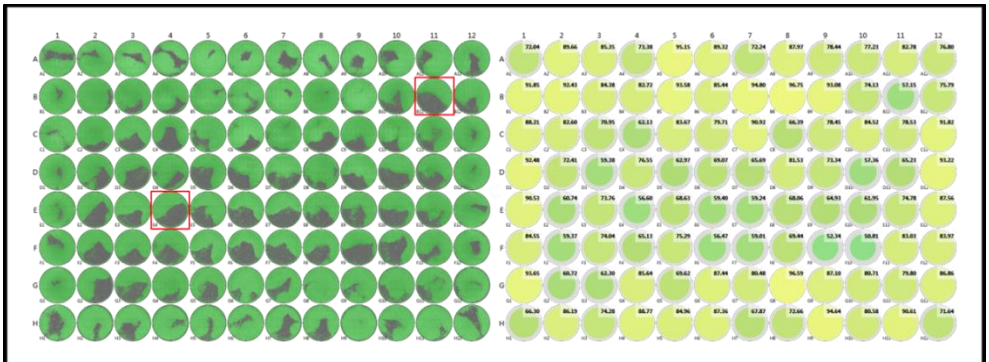

Figure 5.7. Output data obtained after using the Solentim plate reader to check confluency and monoclonality of 96-well plates. Left image represent the physical spread of the cells in the wells. Right image is the calculated confluency of the well. Wells outlined in red are examples of wells selected for progression.

At the spin tube stage, titre was again determined after 2-3 subcultures. The results for the highest 2 expressing mini-pools for each construct are reported in Table 5.2B for both Adalimumab and Blosozumab. An increase in titre in the spin tubes compared to the earlier well plate titres was observed for the all the constructs, with notably the highest expressing mpDG44/Bloso 6 pool having a titre of 70.6 µg/mL (2 times more than in 24-well plate) and the highest mpDG44/ADA 7 having a titre of 29.5 µg/mL. The cell pools engineering with the different SNAREs however, were still below reliable measurement. The SNARE engineered cell titres being so low, it was decided not to carry on with characterisation of these mini-pools. The top 2 mini-pools transfected with the DGV for both recombinant molecules were kept and cryopreserved for further experiments (see 5.5.2).

Table 5.2. Titre measurement using an Octet instrument of the mini-pool and cell pools transfected with pAVE vectors expressing a model recombinant protein and a syntaxin/SNAP gene.

A

Cell mini-pool	Binding rate	Product titre (µg/mL)
Bloso Max	0.0935	36.4
Bloso Min	0.0638	24.9
Bloso CMVbGH Max	0.0011	Too Low
Bloso CMVbGH Min	6.86E-04	Too Low
Bloso STX7 Max	0.0017	0.7358
Bloso STX7 Min	0.0013	Too Low
Bloso STX17 Max	0.0011	Too Low
Bloso STX17 Min	8.88E-04	Too Low
Bloso STX18 Max	0.0018	0.765
Bloso STX18 Min	0.0014	Too Low
Bloso SNAP29 Max	0.0012	Too Low
Bloso SNAP29 Min	7.73E-04	Too Low

Cell mini-pool	Binding rate	Product titre (µg/mL)
Ada Max	0.0796	22.2
Ada Min	0.0481	14.4
Ada CMVbGH Max	0.0026	0.8507
Ada CMVbGH Min	9.97E-04	Too Low
Ada STX7 Max	0.0024	0.746
Ada STX7 Min	0.0019	Too Low
Ada STX17 Max	0.0027	0.9425
Ada STX17 Min	0.0013	Too Low
Ada SNAP29 Max	0.0011	Too Low
Ada SNAP29 Min	7.26E-04	Too Low

B

Cell mini-pool	Binding rate	Product titre (µg/mL)
Bloso 6	0.1789	70.6
Bloso 3	0.0834	32.5
Bloso CMVbGH 1	6.87E-04	Too Low
Bloso CMVbGH 4	3.81E-04	Too Low
Bloso STX7 6	0.0037	1.67
Bloso STX7 1	0.0013	Too Low
Bloso STX17 7	0.0037	1.69
Bloso STX17 5	0.0011	Too Low
Bloso STX18 7	0.004	1.81
Bloso STX18 2	0.0017	0.7244
Bloso SNAP29 6	0.0022	0.9685
Bloso SNAP29 8	8.94E-04	Too Low

Cell mini-pool	Binding rate	Product titre (µg/mL)
Ada 7	0.1087	29.5
Ada 4	0.0585	16.9
Ada CMVbGH 1	0.0018	Too Low
Ada CMVbGH 5	6.30E-04	Too Low
Ada STX7 3	0.0034	1.32
Ada STX7 4	0.0021	Too Low
Ada STX17 3	0.0031	1.14
Ada STX17 8	7.74E-04	Too Low
Ada SNAP29 1	7.47E-04	Too Low
Ada SNAP29 8	4.72E-04	Too Low

C

Cell pool	Binding rate	Product titre (µg/mL)
Bloso pool	0.063	24.6
Bloso CMVbGH pool	6.65E-04	Too Low
Bloso STX7 pool	5.44E-04	Too Low
Bloso STX17 pool	5.54E-04	Too Low
Bloso STX18 pool	8.18E-04	Too Low
Bloso SNAP pool	6.94E-04	Too Low

Cell pool	Binding rate	Product titre (µg/mL)
Ada pool	0.0482	14.4
Ada CMVbGH pool	0.002	Too Low
Ada STX7 pool	0.0021	Too Low
Ada STX17 pool	0.0016	Too Low
Ada STX18 pool	0.0011	Too Low
Ada SNAP29 pool	3.56E-04	Too Low

A, titres at the first selection step for mini-pools. **B**, titres after 2-3 passages of the selected mini-pools in spin tubes. **C**, Titres for the pool cell lines generated after 2-3 passages in flasks. No replicates were performed for the different measurements.

5.3.2. Generation of stably expressing antibody and syntaxin/SNAP pools using the DG44 Clone 27 host cell line

Alongside the generation and selection of mini-pools, general cell pools were generated with the same vectors (pAVE ADA, pAVE ADA CMVbGH, pAVE ADA CMV STX7, pAVE ADA CMV STX17, pAVE ADA CMV STX18, pAVE ADA CMV SNAP29, pAVE Bloso, pAVE Bloso CMVbGH, pAVE Bloso CMV STX7, pAVE Bloso CMV STX17, pAVE Bloso CMV STX18 and pAVE Bloso CMV SNAP29). As described in 2.2.5.2, Clone 27 was electroporated with the desired constructs. The following day, selection reagent was added to the media for selection of stably expressing cells and cultures were left to recover for 2 weeks. Cultures were monitored regularly to check for contamination. After 2 weeks, and if the parameters were met (viability > 60% and cell concentration > 0.5 x 10^6 cells/mL), cells were progressed to spin tubes cultures. A titre measurement was processed on supernatant samples after 2-3 passages and the results are displayed in Table 5.2C. Similar to the results of the mini-pools (see 5.3.1), the cell pools engineering with SNAREs had low titre or were below the limit of quantification. Due to recurrent low titre with SNARE engineered cells, it was decided to not carry on experiments with the stably expressing cell pools. A different strategy was therefore investigated to try and overcome the problem as described in 5.5.2. The fact that appropriate titres were observed with the DGV transfected (24.6 and 14.4 µg/mL for poolDG44/Bloso and poolDG44/ADA respectively) confirmed that the cell pool generation process was not flawed and there was either a problem with the genetic constructs or that the syntaxin burden/over-expression prevented secretion of the target recombinant protein.

5.4. Transient transfection experiments to evaluate the impact of the use of different promoters and presence of the fluorescent tag on the expression of model recombinant protein

In parallel to the generation and recovery of stable mini-pools described under section 1.3 above, transient transfection experiments were undertaken. These experiments were undertaken to determine the impact of the promoter used to drive SNARE expression (using either the miniTK or CMV promoter) and of the presence of an eGFP tag when cells were overexpressing SNARE proteins. In the previous chapters, correct folding of the eGFP

tag and complete processing of the fused molecule was confirmed and control cell lines expressing only eGFP were generated to determine the effects due to the vector or the tag on cells. Here, a similar approach was undertaken with vectors generated in the pAVE system. Further analysis was also planned to determine the impact of the eGFP tag on the fusion protein and not only the cell line. SNAREs are membrane proteins so their conformation is important for their localisation and function. The addition of a tag may affect the folding and function of the protein (Miyawaki, Sawano, and Kogure 2003) as well as its localisation (Cui et al. 2016).By comparing overexpression of fused and non-fused syntaxin proteins, effects of the tag on the function of the protein might be detected. Moreover in Chapter 4, the impact of STX17 and SNAP29 over-expression on cells was dependent of their level of expression. Only relatively low expression (compared to the high expressing cells investigated) of SNAP29 had an effect on productivity while relatively high expression of STX17 had an effect on productivity and a low expression on cell survival. The comparison of promoters with different strength (CMV and miniTK promoter) was therefore undertaken to determine if promoters that should drive expression of the syntaxin genes at different amounts resulted in different impacts on the cell growth and productivity.

Transient transfections were undertaken in spin tubes with vented caps using NovaCHOice as a transfection agent. Cells were cultivated for 6 days with sampling every other day from day 2. On sampling days, cell growth and culture viability was measured using a Vi-CELL instrument. The experiments was performed with the following constructs; pAVE ADA, pAVE ADA CMVbGH, pAVE ADA CMV STX17, pAVE ADA CMV STX17GFP, pAVE ADA CMV STX18, pAVE ADA CMV STX18GFP, pAVE ADA CMV GFP, pAVE ADA TK STX17, pAVE ADA TK STX17GFP, pAVE ADA TK STX18, pAVE ADA TK STX18GFP, pAVE ADA TK GFP. The experiment was also performed with the equivalent plasmids containing the genes for the recombinant model IgG protein Blosozumab.

Figure 5.8 shows the Blosozumab and Adalimumab expression as determined by Octet on supernatant samples from day 6 when the Clone 27 cells were transfected with the different constructs. Surprisingly, all conditions had low titre or high variability, even with the transient transfection of the DGV containing no SNARE.

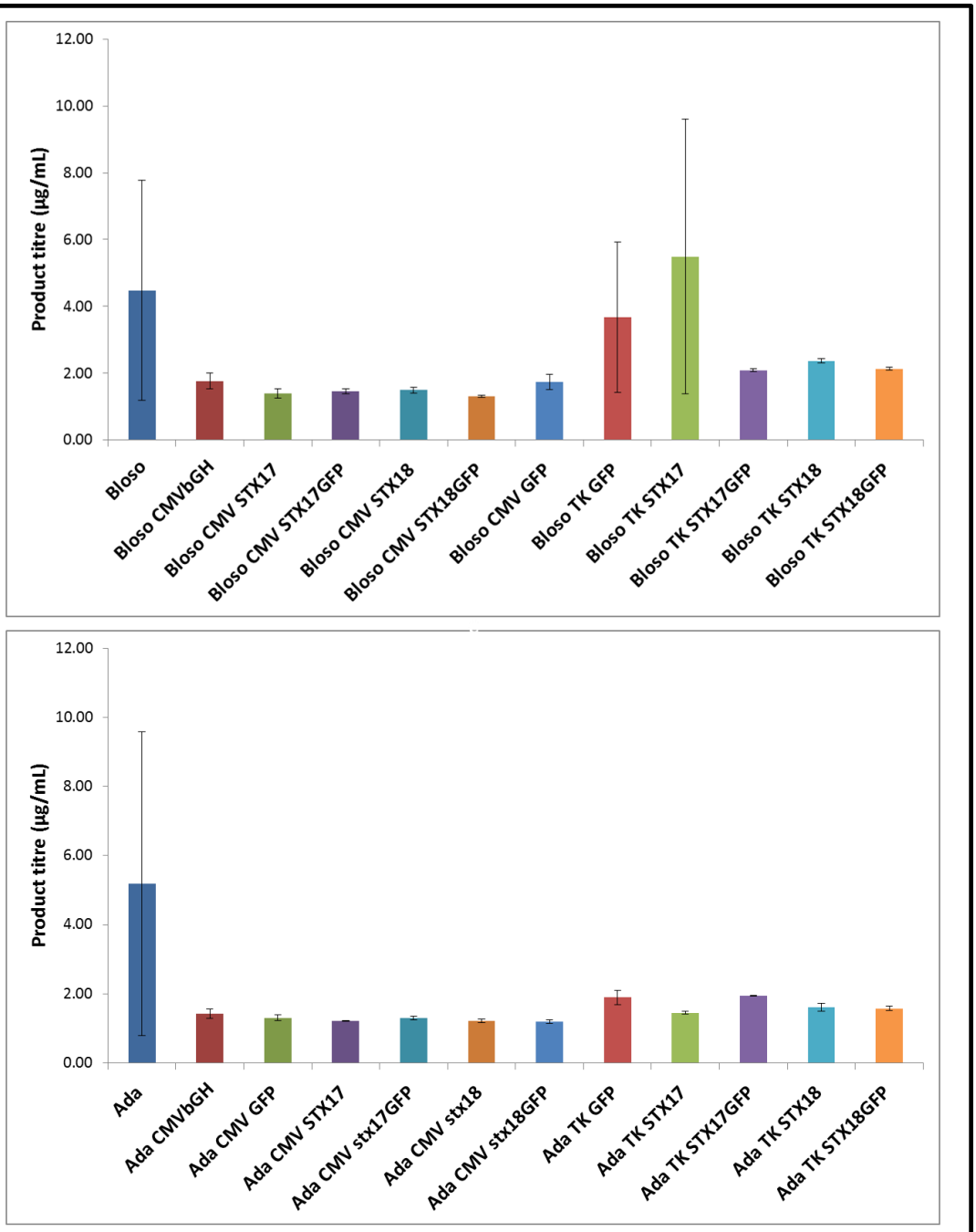

Figure 5.8. Blosozumab and Adalimumab titres in cell culture supernatant 6 days after transient transfection with the different plasmids using NovaCHOice reagent as described in the text. Error bars show the standard deviation from the mean (n=3).

The parameters used for the transient transfection were similar to the experiments described in section 4.3 except that the host cell line and media were different. For each host cell line a method adapted for one might not be appropriate for another. Moreover, NovaCHOice reagent is greatly affected by the addition of supplements in the media such as pluronic acid. An optimisation experiment was therefore performed with different methods (electroporation and NovaCHOice) and parameters (volume reagent, viable cell

concentration) to identify more favourable conditions for transfection with regard to recombinant protein expression from the Clone 27 host. To monitor transfection efficiency, a GFP expressing vector was transfected (pcDNA3.1Hygro/GFP or pmaxGFP) and fluorescence from the cells monitored using a Cellometer Vision CBA device (Nexcelom, USA). The Cellometer instrument is a device able to estimate the transfection efficiency by determining the fluorescent population of cells among the total population. The different conditions investigated are detailed in Figure 5.9. Fluorescent measurements were undertaken 48 h after transfection.

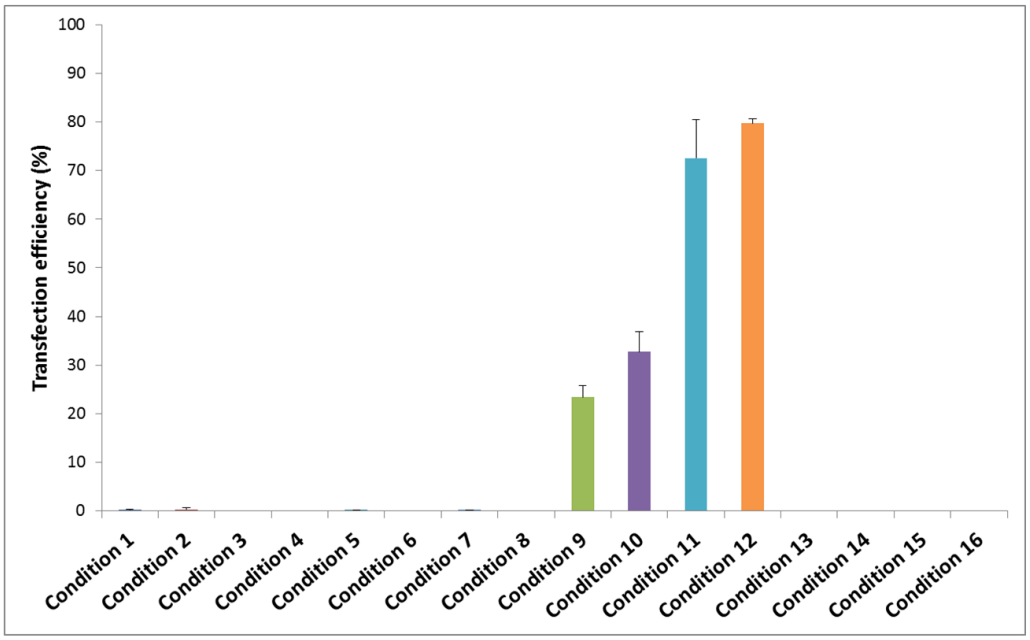

	Method of transfection	Parameters	Plasmid
Condition 1	NovaCHOice	0.5 cells/mL, 0.5 µg/mL DNA, Booster	pcDNA3.1Hygro/GFP
Condition 2	NovaCHOice	0.5 cells/mL, 0.5 µg/mL DNA, No Booster	pcDNA3.1Hygro/GFP
Condition 3	NovaCHOice	0.5 cells/mL, 1 µg/mL DNA, Booster	pcDNA3.1Hygro/GFP
Condition 4	NovaCHOice	0.5 cells/mL, 1 µg/mL DNA, No Booster	pcDNA3.1Hygro/GFP
Condition 5	NovaCHOice	1 cells/mL, 0.5 µg/mL DNA, Booster	pcDNA3.1Hygro/GFP
Condition 6	NovaCHOice	1 cells/mL, 0.5 µg/mL DNA, No Booster	pcDNA3.1Hygro/GFP
Condition 7	NovaCHOice	1 cells/mL, 1 µg/mL DNA, Booster	pcDNA3.1Hygro/GFP
Condition 8	NovaCHOice	1 cells/mL, 1 µg/mL DNA, No Booster	pcDNA3.1Hygro/GFP
Condition 9	Electroporation	8 µg DNA	pcDNA3.1Hygro/GFP
Condition 10	Electroporation	16 µg DNA	pcDNA3.1Hygro/GFP
Condition 11	Electroporation	8 µg DNA	pmaxGFP™ Vector
Condition 12	Electroporation	16 µg DNA	pmaxGFP™ Vector
Condition 13	Unstranfected	0.5 cells/mL	/
Condition 14	Unstranfected	1 cells/mL	/
Condition 15	NovaCHOice	1 cells/mL, No DNA, Booster	/
Condition 16	Electroporation	No DNA	/

Figure 5.9. Transient transfection experiment to determine improved conditions for transfection of the clone 27 host cell using the NovaCHOice reagent in 24-well plates. All the conditions investigated are detailed in the table in the figure. Fluorescence measurements were performed 48 h after transfection using a Cellometer device. Error bars show the standard deviation from the mean (n=3).

The transfection efficiency, as determined by the percentage of cells expressing GFP 48 h post-transfection, when using the NovaCHOice reagent was close to zero with the Clone 27 cell line for all the different conditions. In comparison, when using electroporation to transfect the cells, the transfection efficiency achieved was between 20 and 80%, depending on the parameters used and the GFP vector. The pmaxGFP plasmid is a plasmid provided by Lonza in the SF Cell line 4D-Nucleofector™ X Kit L as a control to check for transfection efficiency. The vector expressed a GFP under the control of a CMV promoter coupled to an intron. The difference in transfection efficiency between the two plasmids (2 times more efficiency when using pmaxGFP compared to the pcDNA3.1Hygro/GFP) suggested that the vector construction had an impact on the transfection as well as the method, with the major difference being the presence of the intron in the pmaxGFP vector.

It is noted that NovaCHOice transfection is a method heavily impacted by the composition of the media, notably the presence of pluronic. To check for the effect of the media on the efficiency of transfection when using the NovaCHOice reagent, an experiment with three different media was undertaken. The media compared were FDB-MAP and then CD-DG44 with or without 0.18% pluronic. All the media were supplemented with 200 mM L-glutamine and the plasmids pmaxGFP and pcDNA3.1Hygro/GFP were used for transfection. Transfection efficiency was determined using the Cellometer and the results are displayed in Figure 5.10 24 h post-transfection. Efficiency of transfection was determined to be 2 times higher when using the pMaxGFP plasmid compared to pcDNA3.1Hygro/GFP but the levels of transfection efficiency were very low, all below 8%. This approach was therefore considered inappropriate for transient expression analysis with the CHO-DG44 cell line Clone 27.

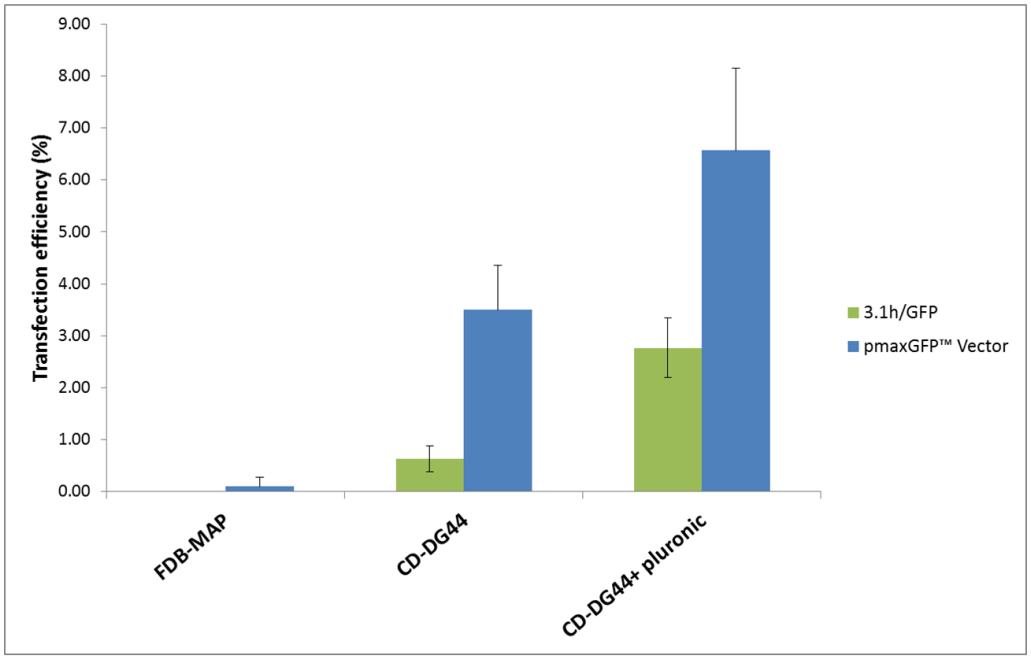

Figure 5.10. Determination of transient transfection efficiency using NovaCHOice reagent with different media's. Fluorescence in the cells and the percentage of cells expressing GFP was measured 24 h post-transfection using a Cellometer device. Error bars show the standard deviation from the mean (n=3).

5.5. Generation of stably expressing CHO-DG44 cell pools co-expressing a model protein and a syntaxin/SNAP protein by transfection of stably expressing recombinant biotherapeutic protein expressing cell pools with the different SNAREs

The attempts to generate mini-pools or pools of DG44 Clone 27 engineered cells co-expressing a recombinant model protein and one of the SNARE targets using a single vector containing both the recombinant protein of interest and the SNARE failed to generate cells expressing meaningful amounts of the target recombinant protein. The different results obtained suggested that the makeup of the vectors may be responsible for this (see discussion in this chapter). A new strategy to generate cell lines expressing both the SNARE and recombinant biotherapeutic of interest was therefore investigated involving transfection of the mini-pools generated with the DGV with constructs containing the target SNAREs. The 2 mini-pools expressing the highest amount of Adalimumab or Blosozumab were transfected with the pMRXIP-STX7, pMRXIP-STX17, pMRXIP-STX18, pMRXIP-SNAP29 and pMRXIP-STXGFP constructs that had been previously evaluated and shown to express the SNARE proteins in Chapters 3 and 4.

5.5.1. Titration of puromycin to determine the appropriate amount that kills the mini-pools expressing Adalimumab or Blosozumab for use in stable cell line generation

Genetic constructs in the pMRXIP GFP-Ci2 vector are selected for stable integration using the resistance gene for puromycin and addition of puromycin to the media. Appropriate amounts of puromycin need to be added to the media in order to obtain a stringent selection of stably expressing cells. A kill curve for puromycin was therefore realised with the cell line mpDG44/ADA 7 to determine the appropriate concentration of puromycin that would kill the cells in the absence of the selection marker. Cells were inoculated at 0.2 x 10^6 cells/mL in 1 mL of FDB-MAP with 8 mM L-glutamine with different concentrations (0, 7.5, 10 or 15 µg/mL) of puromycin in 24-well plates. Plates were incubated at 37˚C, 10% CO_2, 80% humidity for 5 days. At day 5, the viable cell concentration and culture viability were determined using a Vi-CELL instrument.

Figure 5.11 presents the viable cell concentration and culture viability after incubation in media containing the different concentrations of puromycin for 5 days. A concentration of 7.5 µg/mL of puromycin impacted the cell growth and culture viability compared to the control, however there was still many viable cells and the culture viability was over 80% at day 5. A concentration of 10 µg/mL did not kill the cells but prevented growth with a viable cell concentration of 0.25 x 10^6 cells/mL and a culture viability of 60% at day 5. The concentration that killed the most cells whilst allowing some to survive and rapidly decreased the culture viability was 15 µg/mL of puromycin which resulted in a decrease of the viable cell concentration to 0.08 x 10^6 cells/mL and a culture viability below 40%. The working concentration chosen was 10 µg/mL which prevented growth at day 5 and reduced culture viability.

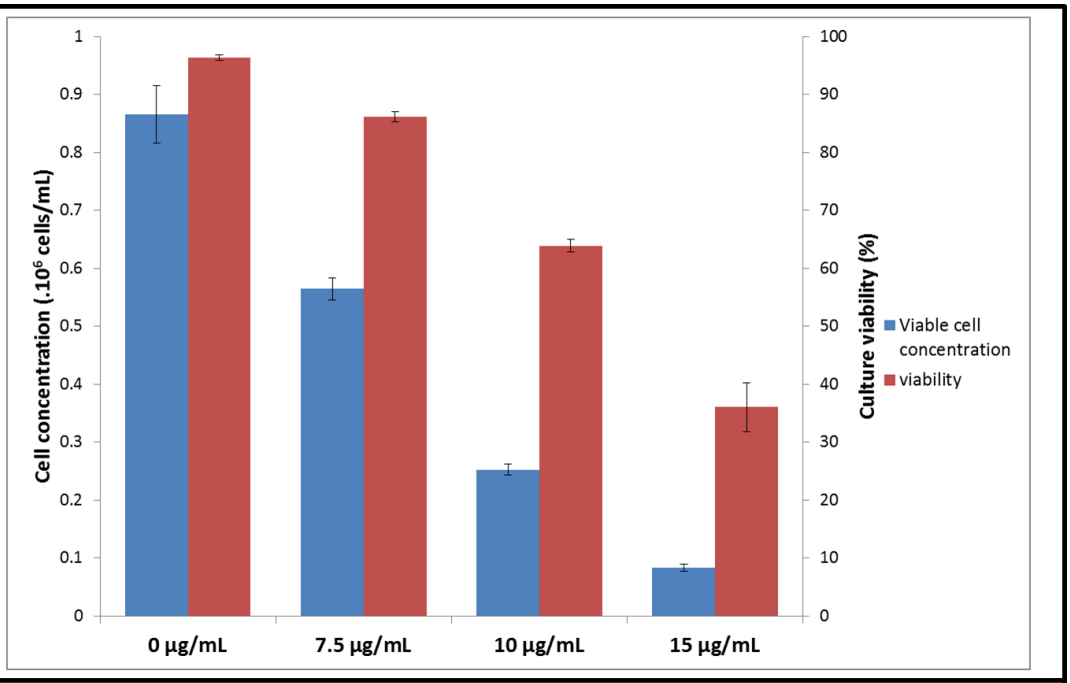

Figure 5.11. Viable cell concentration and culture viability of mpDG44/ADA 7 cell pools after 5 days of incubation using media with various concentration of puromycin. Cells were grown in 24-well plates and incubated for 5 days before the viable cell concentration and culture viability was measured using a Vi-CELL instrument Error bars show the standard deviation from the mean (n=3).

5.5.2. Transfection of mini-pools expressing model IgGs with pMRXIP plasmids for the generation of stably expressing cell lines expressing a model IgG recombinant protein and a target SNARE protein

The mini-pools mpDG44/ADA 7 and mpDG44/Bloso 6 were transfected with pMRXIP-STX7, pMRXIP-STX17, pMRXIP-STX18, pMRXIP-SNAP29 or pMRXIP-STXGFP following the protocol outlined in section 2.2.5.2. Generation of 2 distinct pools for each construct was performed. One day after electroporation, the selection agent puromycin was added to the fresh media at a final concentration of 10 µg/mL. Cultures were then allowed to recover for 2 weeks. Emerging cell pools were monitored from time to time to check for contamination. When cultures reached a viable cell concentration >0.5 x 10^6 cells/mL and culture viability >60%, cells were progressed into 125 mL Erlenmeyer flasks with vented caps. Cells transfected with the plasmid pMRXIP-STX18 never recovered. As such, the cell pools obtained were DG44/ADA+STX7, DG44/ADA+STX17, DG44/ADA+SNAP29 and DG44/ADA+GFP generated with the transfection of mpDG44/ADA 7 with the plasmids pMRXIP-STX7, pMRXIP-STX17, pMRXIP-STX18, pMRXIP-SNAP29 or pMRXIP-STXGFP respectively. Similar cell lines were generated with the transfection of mpDG44/Bloso 6; DG44/Bloso+STX7, DG44/Bloso+STX17, DG44/Bloso+SNAP29 and DG44/Bloso+GFP.

5.5.3. Determination of IgG titre and expression of the eGFP fused proteins in the SNARE engineered IgG expressing mini-pools

The previous experiment (see section 5.3) failed to generate cells expressing both molecules of interest, the recombinant IgG model protein and a SNARE. In order to assess expression of both at an early stage, and to be able to react rapidly to titre and transfection efficiency, these were monitored at early stages. In this case, fluorescence measurements were possible because the transfected plasmids were design for the expression of fused proteins with an eGFP tag.

Titre and transfection efficiency were initially monitored 5 days after transfection. The day following transfection, and before adding the selection agent, 1 mL of transfected cells was withdrawn and used to inoculate a 24-well plate. After incubation of the cultures for 5 days at 37˚C, 10% CO_2 and 80% humidity IgG titre and fluorescence were measured. Figure 5.12 presents the results for the transfection with each construct. No titre or fluorescence for the pool 1 of DG44/ADA+STX7 or DG44/Bloso+STX17 were obtained due to contamination of the wells. Values above the limit of quantification were obtained for the different cell lines. Higher titres were obtained for cell lines expressing the model protein Blosozumab compared to Adalimumab (2 times higher, Figure 5.12). Significantly higher values were observed for pools expressing SNAP29 and model recombinant protein, Adalimumab or Blosozumab, comparing to the eGFP expressing control. Similar results were observed for both DG44/ADA+STX18 pools, DG44/ADA+STX17 2, DG44/Bloso+STX17 2 and DG44/Bloso+STX18 2. Transfection efficiency was low for the different cell lines, below 15%. The absence of selection agent might explain the low efficiency obtained after 5 days when several divisions of the cells had diluted the plasmid non-integrated into the cells.

A

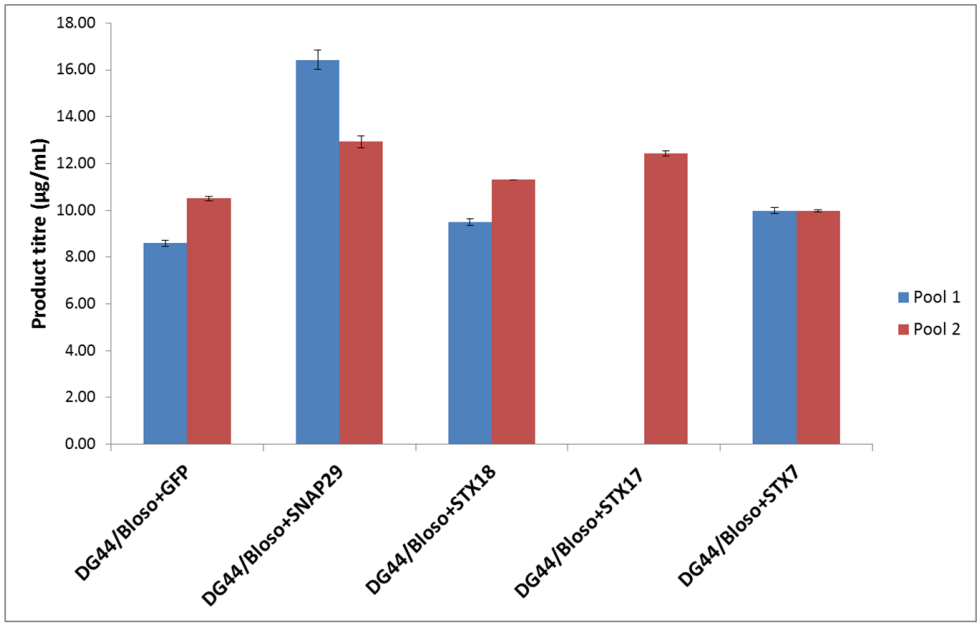

	Titre
DG44/Bloso+GFP 1	F
DG44/Bloso+GFP 2	D
DG44/Bloso+SNAP29 1	A
DG44/Bloso+SNAP29 2	B
DG44/Bloso+STX18 1	E
DG44/Bloso+STX18 2	C
DG44/Bloso+STX17 2	B
DG44/Bloso+STX7 1	D E
DG44/Bloso+STX7 2	E

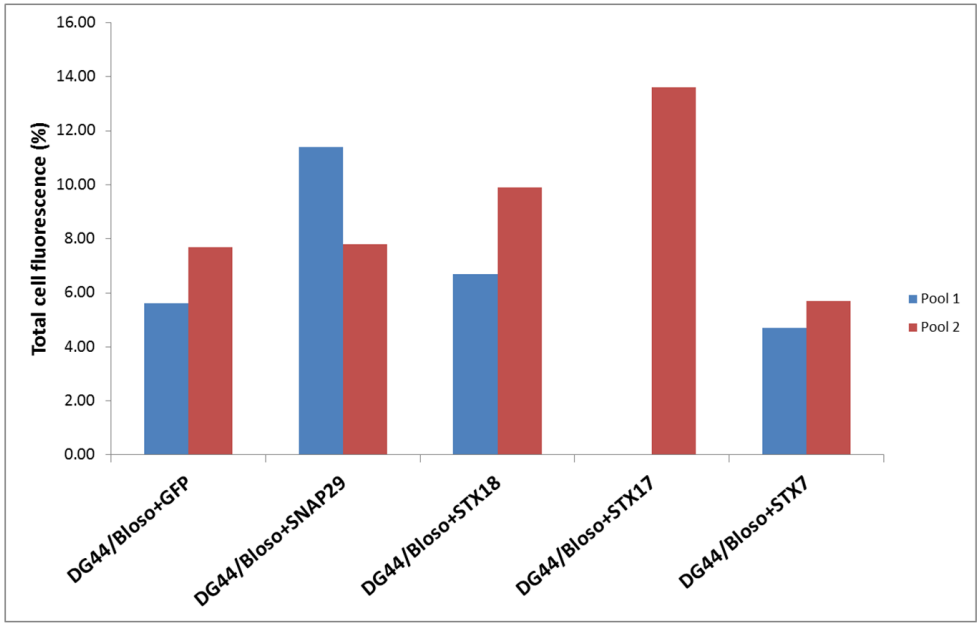

Figure 5.12. Titre and transfection efficiency measurement of pools generated by the transfection of pMRXIP plasmids into mpDG44/ADA 7 and mpDG44/Bloso 6 mini-pools. The day following transfection, 1 mL of culture was placed into a 24-well plate without selection agent and titre and fluorescence were measured after 5 days of incubation. **A**, Results for the cell pools expressing the model antibody Blosozumab. **B**, Results for the cell pools expressing the model protein Adalimumab. Missing measurements were due to well contamination. Error bars show the standard deviation from the mean (n=2). Tables represent one way ANOVA analysis followed by a Tukey test. Means that do not share a letter are statistically different.

B

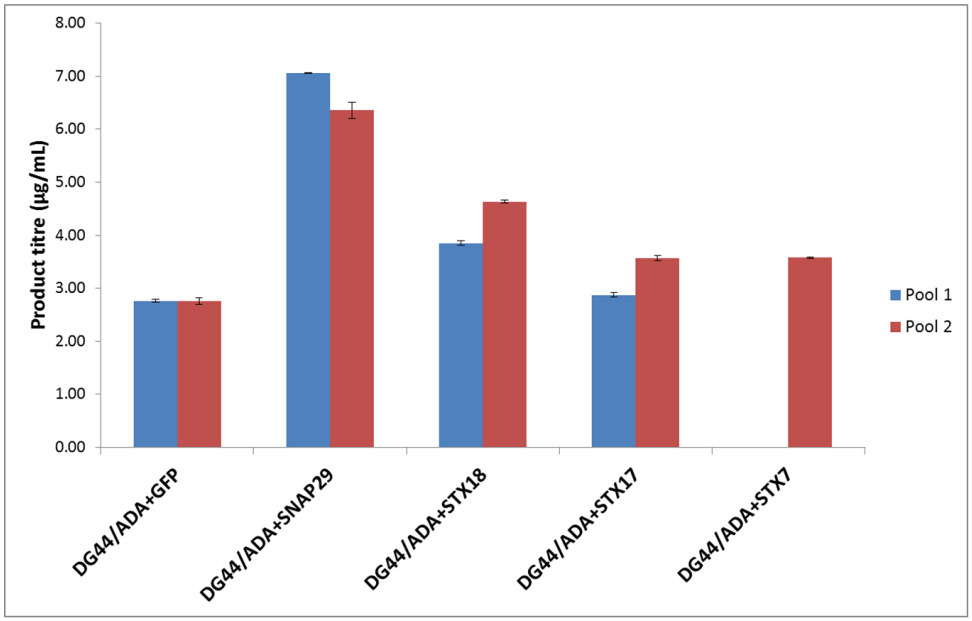

	Titre
DG44/ADA+GFP 1	F
DG44/ADA+GFP 2	F
DG44/ADA+SNAP29 1	A
DG44/ADA+SNAP29 2	B
DG44/ADA+STX18 1	D
DG44/ADA+STX18 2	C
DG44/ADA+STX17 1	F
DG44/ADA+STX17 2	E
DG44/ADA+STX7 2	E

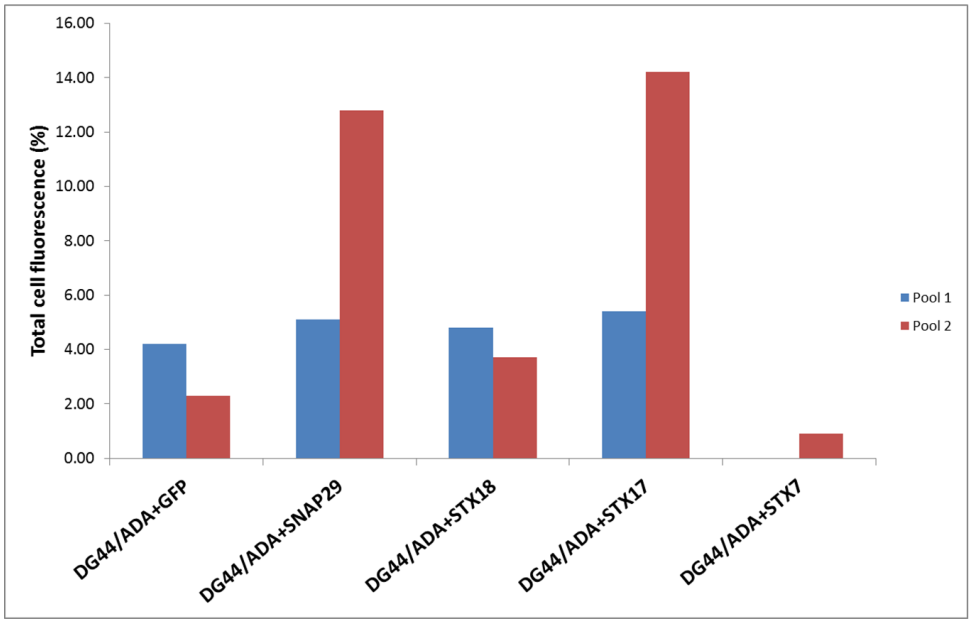

Figure 5.12 (cont.). Titre and transfection efficiency measurement of pools generated by the transfection of pMRXIP plasmids into mpDG44/ADA 7 and mpDG44/Bloso 6 mini-pools. The day following transfection, 1 mL of culture was placed into a 24-well plate without selection agent and titre and fluorescence were measured after 5 days incubation. **A**, Results for the cell pools expressing the model antibody Blosozumab. **B**, Results for the cell pools expressing the mode protein Adalimumab. Missing measurements were due to well contamination. Error bars show the standard deviation from the mean (n=2). Tables represent one way ANOVA analysis followed by a Tukey test. Means that do not share a letter are statistically different.

Another assessment for titre and transfection efficiency was performed after 2-3 passages of the stably expressing cell pools in 125 mL Erlenmeyer flasks. Figure 5.13 shows the results obtained for the different cell pools generated. No titre measurements were performed on both pools of DG44/Bloso+STX7 due to technical problems with the Octet instrument and no transfection efficiency was performed for DG44/Bloso+STX7 2 because the cell pool did not recover in time. Measurements in shaken flasks gave much higher titre that the measurement in a static environment a few days after transfection. Cell pools expressing Blosozumab had a higher titre than cell pools expressing Adalimumab again. The high transfection efficiency at over 70% for most cell pools suggested puromycin selection had been achieved and good expression of the fusion protein and stable integration of the pMRXIP plasmids in the majority of the cells.

The combination of the transient and stable pool data suggested that the transfection of mpDG44/ADA 7 and mpDG44/Bloso 6 with vectors for the expression of the SNARE proteins of interest was an appropriate strategy to assess the impact of SNARE engineering. Cell pools expressing the model IgG protein and high transfection efficiency were obtained. Detection of expression of the full size fusion protein was still required and performed to confirm expression of the fusion protein (see section 5.5.4).

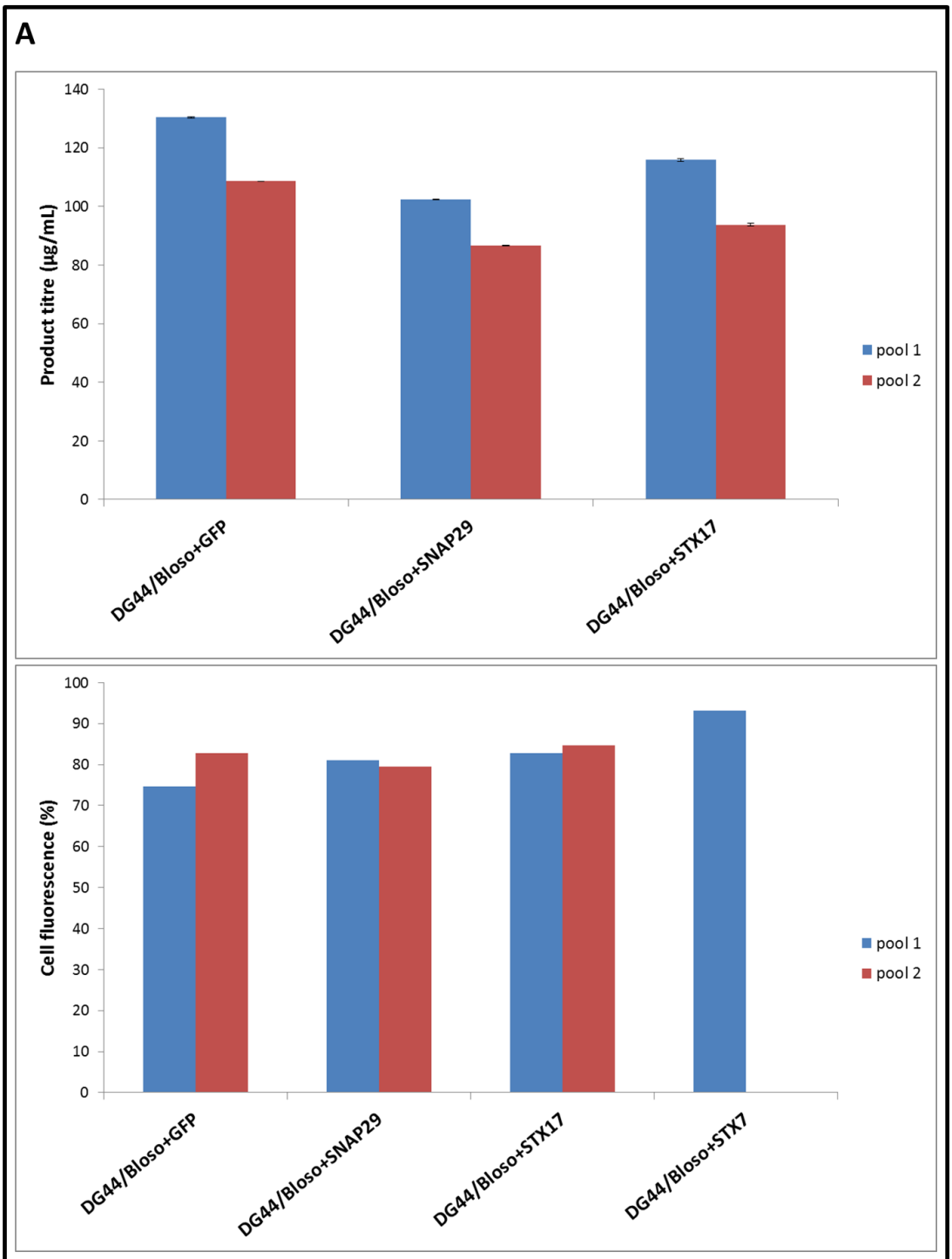

Figure 5.13. Titre and fluorescence measurement of pools generated by the transfection of pMRXIP plasmids into mpDG44/ADA 7 and mpDG44/Bloso 6 after recovery and 2-3 passages in Erlenmeyer flasks. Absence of data is due to delays in recovery for the cell pools. **A**, Results for the cell pools expressing the model antibody Blosozumab. **B**, Results for the cell pools expressing the mode protein Adalimumab. Missing measurements were due to well contamination. Error bars show the standard deviation from the mean (n=3).

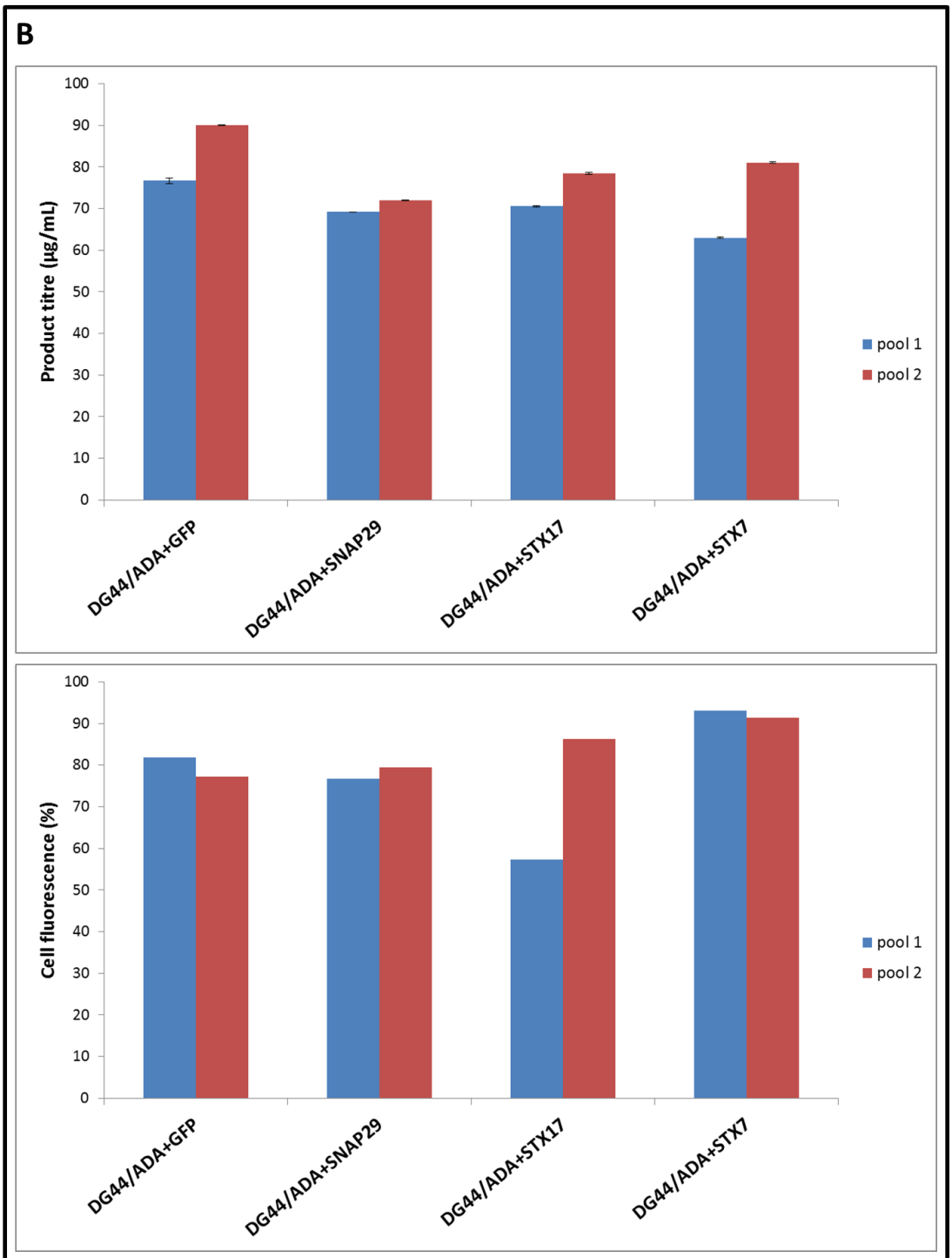

Figure 5.13 (cont.). Titre and fluorescence measurement of pools generated by the transfection of pMRXIP plasmids into mpDG44/ADA 7 and mpDG44/Bloso 6 after recovery 2-3 passages in Erlenmeyer flasks. Absence of measurement were due to delays in recovery for the cell pools. **A**, Results for the cell pools expressing the model antibody Blosozumab. **B**, Results for the cell pools expressing the mode protein Adalimumab. Missing measurements were due to well contamination. Error bars show the standard deviation from the mean (n=3).

5.5.4. Fed-batch over grow (FOG) assessment of the cell pools co-expressing a model IgG protein and a target eGFP-SNARE

The results reported in section 5.5.3 provided evidence about the expression of both the recombinant IgG model protein and SNARE of interest was achieved in the newly generated cell pools. Fed-batch over grow experiments were therefore performed with one of the generated pools of each engineered target. The selection of the pool to be assessed was based on the viability of cultures when setting up the experiment with the pool with the highest culture viability used to inoculate the FOG experiment. Fed-batch over grow is a fed-batch culture approach routinely used at FDB for early material production or screening of cell pools and lines. Here, experiments were designed to monitor cell growth and culture viability daily from day 2 of culture whilst IgG titre was measured every second day from day 4. The concentration of glucose, glutamine, lactate, glutamate and ammonia in the cell culture supernatant were monitored daily from day 3. The fed strategy consisted of daily addition of Hyclone Cell Boost 7A and 7B at 2% (v/v) and 0.2% (v/v) amounts of the initial volume. Hyclone Cell Boost 7A is composed of amino acids, vitamins, salts, trace elements and glucose whereas feed 7B contains a concentrated solution of amino acids. Glutamine and glucose were also fed to the culture when amounts fell below 0.22 g/L and 3 g/L respectively. Glutamine feed consisted of 0.5% (v/v) of 200 mM L-glutamine whereas the glucose feed to add was calculated using the equation detailed in 2.2.11. Cells were inoculated at 0.2 x 10^6 viable cells/mL in 60 mL of FDB-MAP containing 8 mM L-glutamine. Cultures were incubated at 37˚C, 125 rpm, 5% CO_2 and 80% humidity for a period of 14 days or until the culture viability declined to <70%. The cell pools assessed in this experiment were mpDG44/ADA 7, DG44/ADA+STX7, DG44/ADA+STX17, DG44/ADA+SNAP29, mpDG44/Bloso 6, DG44/Bloso+STX7, DG44/Bloso+STX17, DG44/Bloso+SNAP29. Cell pools DG44/ADA+GFP and DG44/Bloso+GFP were also assessed in this experiment as controls.

Figure 5.14 reports the viable cell concentrations and culture viability across the different fed-batch cultures. No large differences were observed in the growth characteristics between the cell pools engineered with the different SNARE proteins. A difference was observed between the growth characteristics of the cell pools expressing Adalimumab or Blosozumab, suggesting an effect of the IgG target product on the cell pool phenotypes. Blosozumab expressing cell pools grew faster and the culture viability decreased rapidly from day 7 compared to the Adalimumab expressing cell pools. The culture viability of cells

pools expressing Blosozumab declined below 70% culture viability on day 12, two days before cell pools expressing Adalimumab.

	Day 2	Day 3	Day 4	Day 5	Day 6	Day 7
DGV ADA	C	C D	C D	B C	B C	B C
GFP ADA	C	D	E	D	C	C
SNAP29 ADA	B C	C	C	C	A B C	B C
STX17 ADA	C	C D	D E	C D	C	C
STX7 ADA	C	C D	C	C D	B C	C
DGV BLOSO	A	A B	A	A	A	A
GFP BLOSO	A	A B	A	A	A	A
SNAP29 BLOSO	A	A	A	A	A	A
STX17 BLOSO	A B	A B	A	A	A	A
STX7 BLOSO	A B	B	B	A B	A B	A B

	Day 8	Day 9	Day 10	Day 11	Day 12	Day 13	Day 14
DGV ADA	D E	C	A B C	B	A	A	A B
GFP ADA	F	C	C	B	A	A	A B
SNAP29 ADA	C D E	A B	A B C	B	A	A	A B
STX17 ADA	F	B C	B C	B	A	A	A
STX7 ADA	E F	A B C	A B C	B	A	A	B
DGV BLOSO	A	A	A	A	A		
GFP BLOSO	A B C	A B C	A B	A B	A		
SNAP29 BLOSO	A B	A B C	A B	A B	A		
STX17 BLOSO	B C D	A B C	A B C	A B	A		
STX7 BLOSO	A B	A B C	A B	A B	A		

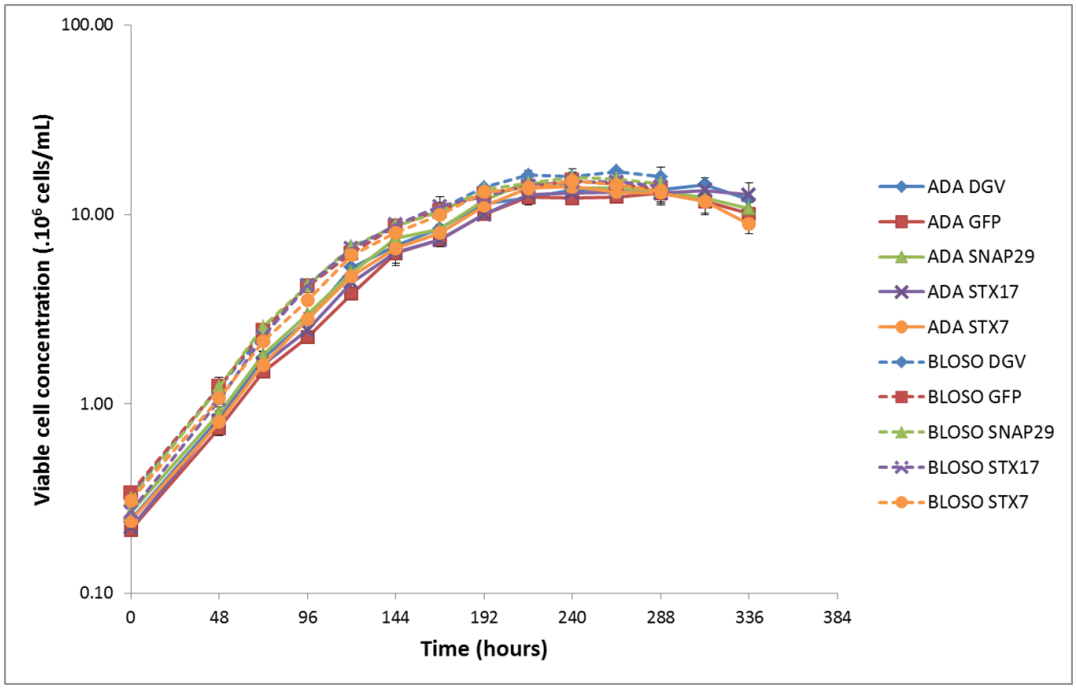

Figure 5.14. Growth curve characteristics of the different cell pools engineered with a syntaxin/SNAP target and expressing a model IgG molecule assessed during the FOG experiment. Viable cell concentration and culture viability were measured daily from day 2 using a Vi-CELL instrument. Dashed lines represent cell pools expressing Blosozumab recombinant protein and straight lines represent cell pools expressing Adalimumab recombinant protein. Error bars show the standard deviation from the mean (n=3). The tables show the outcome of one way ANOVA analysis followed by a Tukey test. Means that do not share a letter are statistically different.

	Day 2	Day 3	Day 4	Day 5	Day 6	Day 7	Day 8
DGV ADA	A	A	A	A	A B	A	A B
GFP ADA	B	A B	A B	B C	A B C	A	A B
SNAP29 ADA	A B	A B	A	A B	A B	A	A B
STX17 ADA	A B	A B	A	A B	A B	A	A
STX7 ADA	A B	A B	A	A	A	A	A B
DGV BLOSO	A	A B	A B	C	C D	A	A B
GFP BLOSO	A B	A B	A B	B C	B C D	A	B
SNAP29 BLOSO	A B	A B	A	A B	A B C	A	A B
STX17 BLOSO	A B	A B	A	A B C	A B C	A	B
STX7 BLOSO	A B	B	B	C	D	A	B

	Day 9	Day 10	Day 11	Day 12	Day 13	Day 14
DGV ADA	A	A	A	A B	A	A B
GFP ADA	A B C	A B	A	A B C D	A	A B
SNAP29 ADA	A B C	A	A	A B C	A	A B
STX17 ADA	A B	A	A	A	A	A
STX7 ADA	A B	A	A	A B C	A	B
DGV BLOSO	B C	C	B	B C D E		
GFP BLOSO	B C	C	B	D E		
SNAP29 BLOSO	A B C	B C	B	C D E		
STX17 BLOSO	B C	C	B	E		
STX7 BLOSO	C	C	B	E		

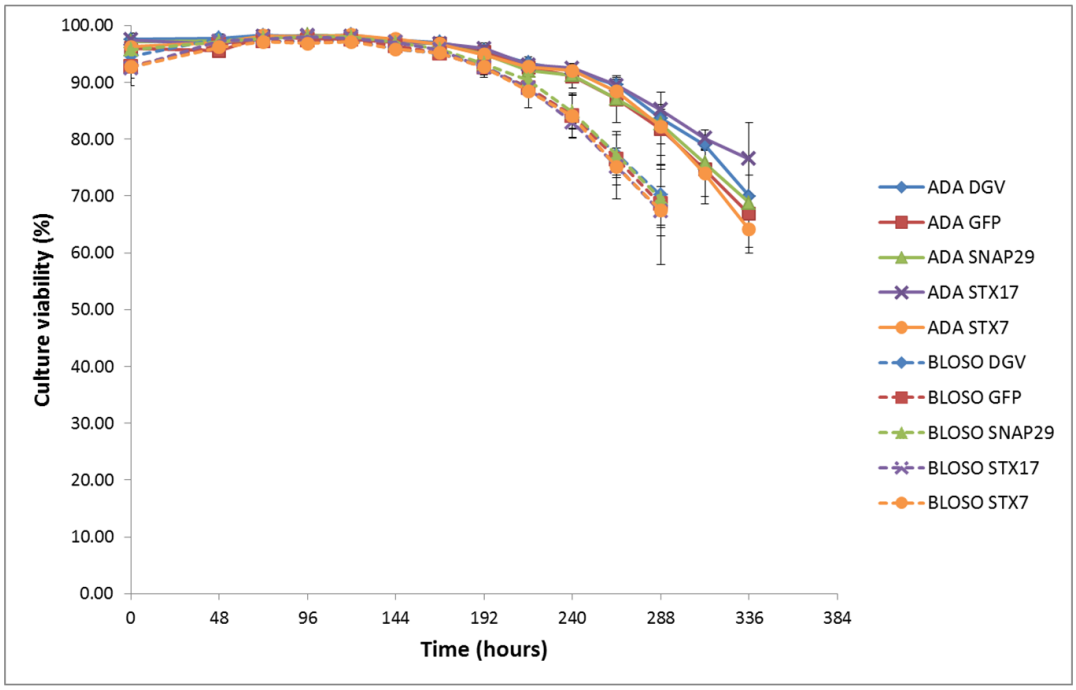

Figure 5.14 (cont.). Growth curve characteristics of the different cell pools engineered with a syntaxin/SNAP target and expressing a model IgG molecule assessed during the FOG experiment. Viable cell concentration and culture viability were measured daily from day 2 using a Vi-CELL instrument. Dashed lines represent cell pools expressing Blosozumab recombinant protein and straight lines represent cell pools expressing Adalimumab recombinant protein. Error bars show the standard deviation from the mean (n=3). Tables represent one way ANOVA analysis followed by a Tukey test. Means that do not share a letter are statistically different.

Figure 5.15 reports the IgG titre measurements for each sampling day (day 4, 6, 8, 10, 12, 14) for all the cell pools assessed. At day 12, no statistical difference was observed between the different cell pools when expressing the recombinant protein Blosozumab. All the cell pools achieved a titre over 1500 µg/mL with the highest titre at 1700 µg/m achieved by the

control cell pool co-expressing eGFP. No titre at day 14 was available for the different cell pools expressing Blosozumab because the FOG experiment was stopped at day 12 when they reached viabilities declined to <70%.

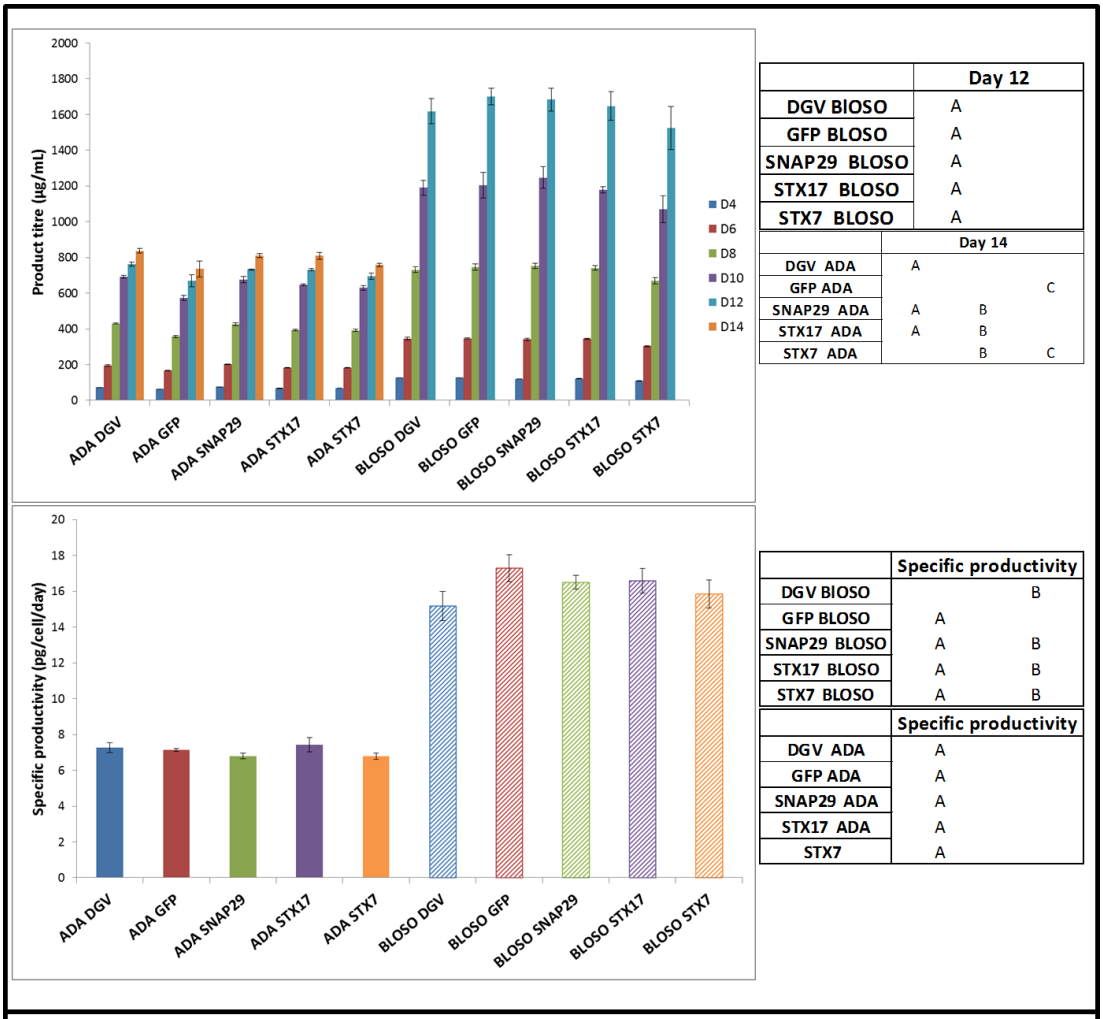

	Day 12
DGV BIOSO	A
GFP BLOSO	A
SNAP29 BLOSO	A
STX17 BLOSO	A
STX7 BLOSO	A

	Day 14		
DGV ADA	A		
GFP ADA			C
SNAP29 ADA	A	B	
STX17 ADA	A	B	
STX7 ADA		B	C

	Specific productivity	
DGV BIOSO		B
GFP BLOSO	A	
SNAP29 BLOSO	A	B
STX17 BLOSO	A	B
STX7 BLOSO	A	B

	Specific productivity
DGV ADA	A
GFP ADA	A
SNAP29 ADA	A
STX17 ADA	A
STX7	A

Figure 5.15. IgG titre and specific productivity measurement of the different cell pools engineered with a syntaxin/SNAP target and expressing a model IgG molecule assessed during the FOG experiment. Titre was measured every other day from day 4. Error bars show the standard deviation from the mean (n=3). Tables represent one way ANOVA analysis followed by a Tukey test. Means that do not share a letter are statistically different.

For the cell pools expressing Adalimumab, titre at day 14 was approximately half of that for the cell pools expressing Blosozumab at day 12 (around 800 µg/mL for Adalimumab cell pools and 1600 µg/mL for Blosozumab cell pools). Little difference in titre was observed between the cell pools except for cell lines DG44/ADA-STXGFP and DG44/ADA-STX7 which appeared to express slightly less than the other cell pools. It was observed that for the different cell pools the titre increased until day 10 after which there was a reduced increase in IgG yield between day 10 and 14. For example, the titre in the DG44/ADA cultures went

from 430 to 690 µg/mL from day 8 to 10 (increase if 260 µg/mL over 2 days) but then only increased to 837 µg/mL from day 10 to 14 (increase of 145 µg/mL). This phenomenon was not observed in the cell pools expressing Blosozumab where titre increased more-or-less constantly every 2 days. When comparing the different specific productivities, no statistical difference was observed between the control cells and when expressing the different syntaxin/SNAP proteins. The noticeable difference was IgG specific between the cell pools expressing Blosozumab or Adalimumab. Blosozumab expressing cell pools had specific productivities more than twice that of the cell pools expressing Adalimumab. Specific productivity calculations take into account the viable cell concentration, suggesting that not only did the Blosozumab expressing cell pools grow faster but they also produced more molecule of interest.

The metabolite consumption or production data are reported in Appendix 4. Cell pools expressing Blosozumab had a lower concentration of glutamine and glucose in the media compared to the cell lines expressing Adalimumab, suggesting that the cells used this more rapidly indicative of the faster growth. At the end of the experiments, cell pools expressing Adalimumab had a higher concentration of glutamate and ammonia in the media than pools expressing Blosozumab although the increased amount was not large. Amounts of lactate were similar between the different cell pools although cells producing Blosozumab tended to have a lower concentration of lactate from day 6.

5.5.5. Analysis of the expression of the syntaxin/SNAP fused proteins in the DG44 cell pools co-expressing a model IgG recombinant protein

When the IgG cell pools were engineered to co-express a target eGFP-SNARE fusion protein, no assessment was performed to determine if a full size fused syntaxin protein was expressed in these pools. Cellometer analysis was able to confirm fluorescence of the cells and hence the presence of a properly folded eGFP tag but no information on the SNARE part of the fused protein was accessible with the Cellometer results. Western blot analyses were therefore performed on total protein extracts from pellets harvested at day 4 and 10 of culture during the FOG experiment. Proteins were extracted from cell pellets of the different cell pools producing either Blosozumab or Adalimumab and samples prepared under reduced conditions. Results of the western blot analysis are showed in Figure 5.16. After incubation of the different membranes with anti-GFP antibody, signal was detected at the expected size for the cell pools expressing STX7, STX17, SNAP29 and GFP and co-expressing either blosozumab or Adalimumab on both days. No signal was detected for

mpDG44/ADA 7 or mpDG44/Bloso 6 (DGV controls) as expected as these were not engineered to express an eGFP fused protein or GFP. Comparison of the amounts of expression with β-acting gave an indication as to the relative level of expression in the different triplicates. No obvious difference in eGFP-SNARE fusion protein expression was observed between the different triplicates. A band corresponding to the eGFP tag alone was visible at day 10 for the cell pools expressing Blosozumab and SNAP29 implying cleavage of the tag. At day 10, cells expressing Blosozumab had a reduced culture viability indicating cell death. The signal for the eGFP tag alone might come from cells undergoing cell death and degrading their internal content in protein.

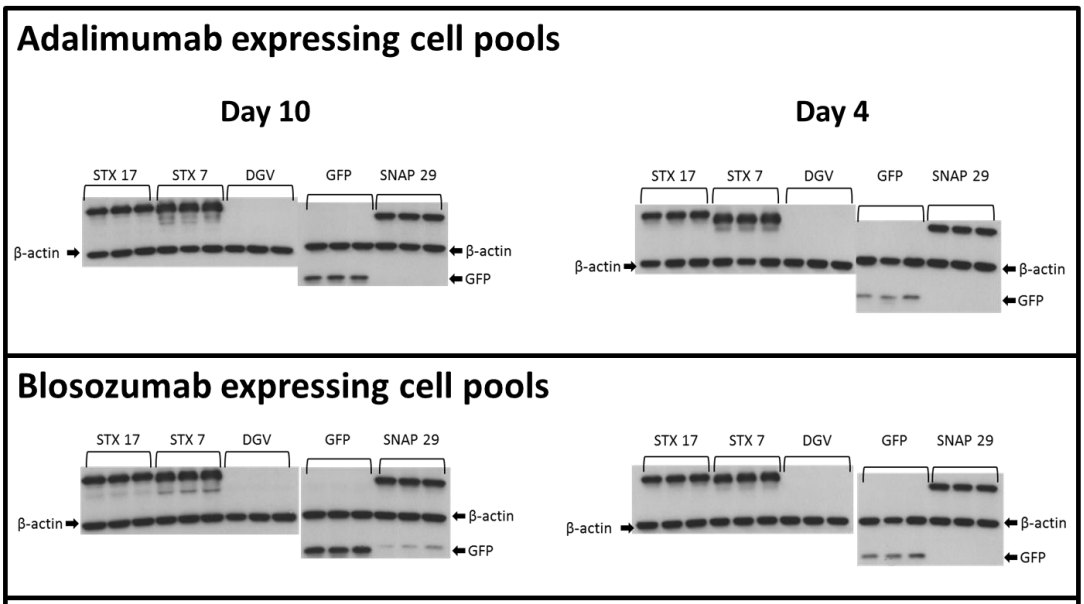

Figure 5.16. Western blot analysis for eGFP-syntaxin/SNAP fusion protein expression on protein extracts from the different cell pools assessed during the FOG experiment at day 4 and 8. Samples were prepared in a reducing sample buffer at a concentration of 1 µg protein/µL. Membranes were incubated with anti-GFP or anti-β-actin antibody diluted at 1:5000.

5.6. Comparison of the endogenous amounts of the target SNAREs in the two CHO host cell lines, Clone 27 and CHO-S

The CHO-S and CHO-DG44 host cell lines were derived from the same ancestor host cell line (Reinhart et al. 2018; Urlaub et al. 1983). However, as cell lines are originated from different sources, are under different selection pressures and grow in different media, they may not express the endogenous target engineered SNARE proteins at a similar amount. To compare the relative amounts of SNARE protein expressed between the two host cell lines examined in this study, western blot analysis was performed on pellets from Clone 27 cell

lines used at FDB and the CHO-S cell line used at the University of Kent. Specific antibodies against STX7, STX18 and SNAP29 were used. Two different protein extracts were analysed for each cell line. Figure 5.17 reports the different western blot analyses of these samples using specific antibodies for SNAP29, STX18 and STX7 on the protein extracts. When analysing for STX18 expression, a clear signal was obtained for both cell lines (band at 42 kDa). When performing densitometry to quantify the relative level of expression of STX18 in both cell lines, the analysis showed that the level of expression was similar. When probing with anti-STX7 and anti-SNAP29 antibodies a number of non-specific bands were observed (Figure 5.17), the expected sizes for STX7 and SNAP29 are 42 kDa and 29 kDa respectively. A faint band at the expected size was observed and densitometry performed on this band and the results are displayed in Figure 5.17. Expression levels of STX7 in Clone 27 and CHO-S cell lines were similar when normalised with the signal for the house keeping protein α-tubulin whereas higher levels of SNAP29 were detected in Clone 27 compared to that in the CHO-S host cell line.

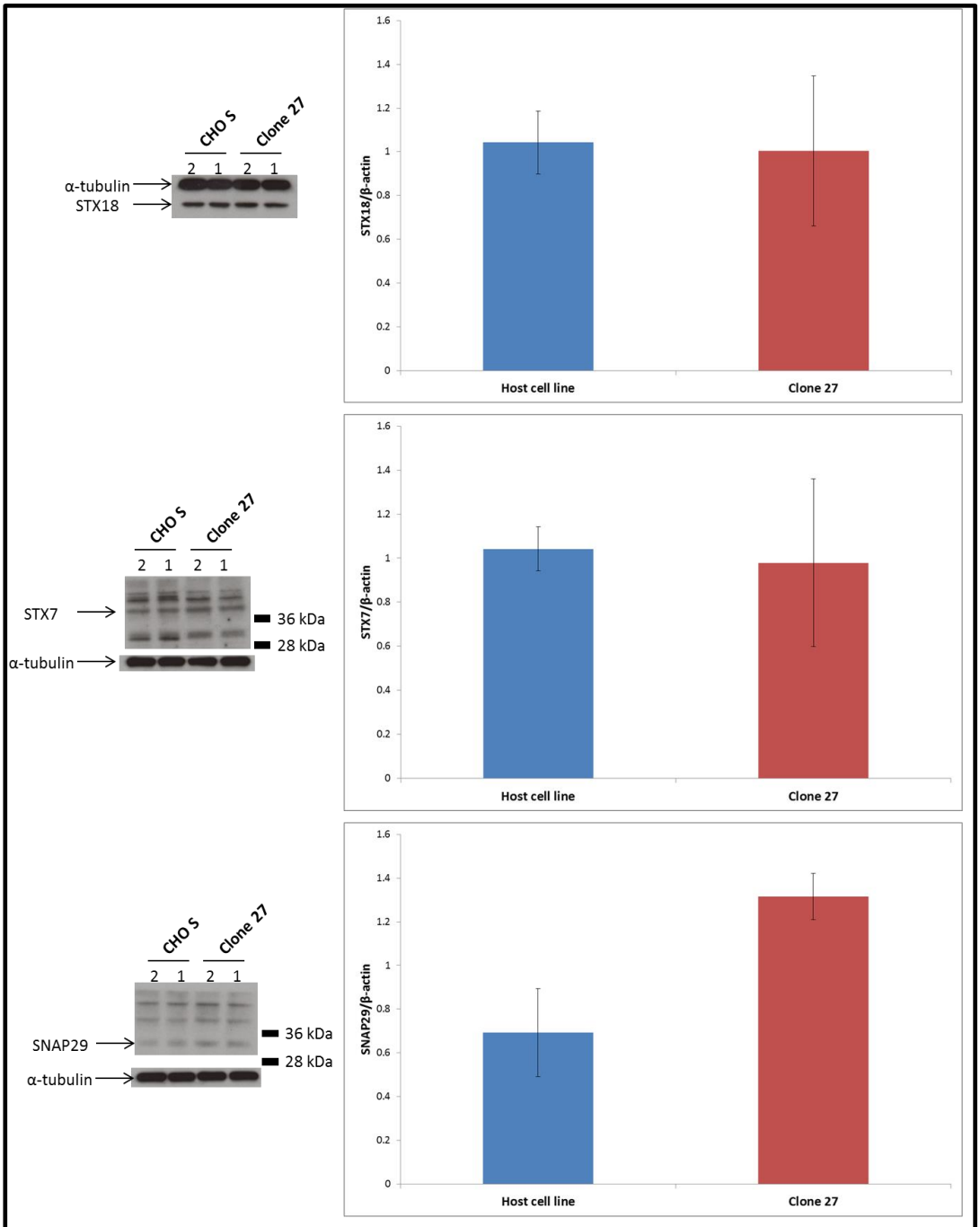

Figure 5.17. Western blot and densitometry analysis on protein extracts from Clone 27 and CHO-s host cells using syntaxin/SNAP specific antibodies. Samples were prepared in reducing conditions at 1 µg protein/µL. Antibodies anti-STX7, anti-STX18 and anti-SNAP29 were used at a dilution 1:1000. The expected band size was 42 kDa for STX18. For STX7 and SNAP29, the band size expected for the protein of interest is indicated by an arrow.

5.7. Discussion

This chapter reports on the implementation of the strategy validated in Chapter 4, for the enhancement of the secretory capacity of CHO cells by SNARE engineering, in an industrial environment. In collaboration with Fujifilm Diosynth Biotechnologies, an industrially optimised DG44 CHO host cell line known as “Clone 27” was engineering to overexpress SNARE proteins shown to have an effect on productivity and/or cell survival in the CHO-S host cell line (see Chapter 4). The experiments performed were carried out following procedures used at FDB in their own facilities. The aim was to determine whether the strategy validated in a CHO-S host cell line in the academic laboratory was reproducible and transferable to industry in another CHO host cell line.

To try and avoid using plasmids unoptimised for use in the FDB host cell and to avoid a dual system of selection (the pMRXIP plasmid selection used in Chapter 4 is based on puromycin), the different syntaxin/SNAP genes were cloned into the DGV. The different genes coding for the SNARE of interest used for the construction of the different pAVE vectors were not fused to an eGFP tag as in the previous studies. In order to reduce the burden placed on the engineered host to a minimum and move the potential for any negative impact on the target function of the presence of the GFP tag, the fluorescent tag was removed. For the detection of the protein of interest, specific antibodies to the protein were required. Alternatively, qPCR for mRNA detection could be undertaken to confirm that at the transcript level elevated expression had been achieved.

Two DGVs were used as backbones in the studies described in this chapter, one expressing the IgG Adalimumab and one expressing the IgG Blosozumab. As previously detailed, Adalimumab is an IgG1 molecule used to treat inflammatory arthritis. Adalimumab was kept as a model protein to be able to compare directly with the results previously reported in Chapter 4. Blosozumab is an IgG4 molecule developed for the treatment of osteoporosis by Eli Lilly (Reid 2017). Blosozumab is a standard molecule used by FDB to test new processes and strategies. Both molecules are type G immunoglobulins but from different classes, 1 and 4, with a principal difference in the number of disulphide bonds in the hinge region (Vidarsson, Dekkers, and Rispens 2014). Vectors for the expression of both molecules and the syntaxin proteins were generated.

Additional vectors for syntaxin STX17 and STX18 fused to an eGFP tag expression were generated to be able to investigate any impact of the presence of the tag on the effect of

expression of the protein. Previously (Chapter 4), only verification of the correct folding of the fluorescent tag and expression of the full length fusion protein were performed. SNAREs are membrane proteins and important components of the vesicle traffic system in the cells and hence their function and localisation is important and could be impaired by the presence of a tag. The presence of the eGFP might disturb their function or localisation generating unexpected effects on the observed cell phenotype (Cui et al. 2016). A comparison between constructs expressing GFP fused and non-fused SNARE proteins would give information about any potential effect(s) of the tag on the cell phenotype. Other vectors expressing syntaxin STX17 and STX18 under the control of the HSV miniTK promoter were also generated. Indeed, the work in Chapter 4 had shown that the effect of SNARE expression on the CHO-S cell was dependent on the level of expression. In the case of STX17 higher expression was related to higher productivity and lower expression resulted in prolonged culture viability under batch culture conditions. All the different constructs generated in this chapter are detailed in Table 5.1.

After generation of the vectors necessary for the different experiments, mini-pools stably expressing a model IgG protein and SNARE of interest were generated. Mini-pool generation is a strategy implemented in the industry as a first screening method for rapid generation of monoclonal like cell lines for phenotype studies. Generation of mini-pools is faster than the generation of monoclonal populations and gives phenotypes close to that of monoclonal populations. Mini-pools are therefore a rapid way to test strategies or obtain early material generation without the stringency of a monoclonal cell line generation process.

Mini-pools generated were subjected to 3 selection steps, one based on confluency and monoclonality and two based on product titre. After transfection, dilution in 96-well plates and recovery, wells with culture viability between 50 and 70% and a monoclonal profile were selected for expansion into 24-well plate. To ensure sufficient diversity, 48 mini-pools were selected. After a week of growth in 24-well plates, mini-pools were screened on their titre concentration using an Octet device. The results demonstrated titre below the limit of quantification for the different mini-pools engineered with the SNAREs or eGFP control whereas mini-pools stably transfected with the DGV yielded detectable titres. Low titres were expected at this stage due to the conditions of the screen. Indeed, suspension cells were grown in an adherent culture and cells might still be recovering from the selection process. Moreover, only a low number of cells might be present. Nonetheless, detectable

titres are the norm from FDB experience with this process. Blosozumab expressing mini-pools had higher titre levels than Adalimumab (24.9 µg/mL for the lowest Blosozumab expresser against 22.2 µg/mL for the best Adalimumab expresser). This trend was observed for all the different experiments suggesting that Blosozumab was an "easier to express" molecule compared to Adalimumab.

Because low titres were a possible outcome during the first selection step based on product titre, and that the process was different from the original FDB cell line development process, mini-pool selection was advanced further by the selection of the top 8 mini-pools for each condition and progression in T25 flasks and then spin tubes. After a few passages of the mini-pools in spin tubes, titre was analysed again. The results still showed low/undetectable titres for the different mini-pools engineered with SNARE proteins whereas cells stably transfected with DGVs showed increased titres. Low titres for cells engineered with SNARE proteins using pAVE vectors were also observed in an attempted to generate bulk cell pools (section 5.3.2). The observation of low titres with all vectors with the co-expression of a model IgG and a SNARE protein in two different processes suggested that the limitation was either around the SNARE vectors or that in the CHO-DG44 cells over-expression of the SNAREs somehow prevented secretion of the target IgG molecule.

Two possible events might explain the lack of expression of the model IgG protein from the constructs generated. When inserting the different SNARE genes and the elements for their expression (CMV promoter and bGH polyA tail) into the expression vector, options for cloning these in were limited in the DGV. Due to cloning constrains, two bGH polyA tails were present back to back with a relatively small distance between them, less than 100 bp (see Figure 5.18) in the final constructs generated. The two polyA tails were elements of the heavy chain and SNARE sequences. By their close proximity, and the single strand nature of the mRNA, possible hybridisation of the two tails could prevent translation of the mRNA into a protein. Another possibility is transcriptional interference. Transcriptional interference refers to direct negative impact of one transcriptional activity on another (Shearwin, Callen, and Egan 2005). Here, two promoters were convergent and in close proximity, the CMV promoter driving the expression of the syntaxin gene and the EF-1α promoter driving the expression of the heavy chain gene (Figure 5.18). Several reports suggest that the EF-1α promoter is more active than the CMV promoter in CHO cells (Kim et al. 2002; Wang et al. 2017). From the results observed when using the generated

constructs, no or little recombinant IgG model protein was expressed whilst no information was collected as to the expression of the SNARE protein. Undertaking qPCR to determine mRNA amounts of the IgG heavy chain in the presence/absence of the SNARE and associated polyA tail could be undertaken to confirm if there was transcriptional interference. Two different transcriptional interference mechanism could take place, collision where converging elongation complexes collide and "fall off" or roadblock when the converging elongation complex from the weaker promoter inhibits progression of the elongation complex from the strong promoter To determine if, and what kind of transcriptional interference might have been happening (collision or roadblock), further investigations about the transcriptional expression of the syntaxin gene would be required.

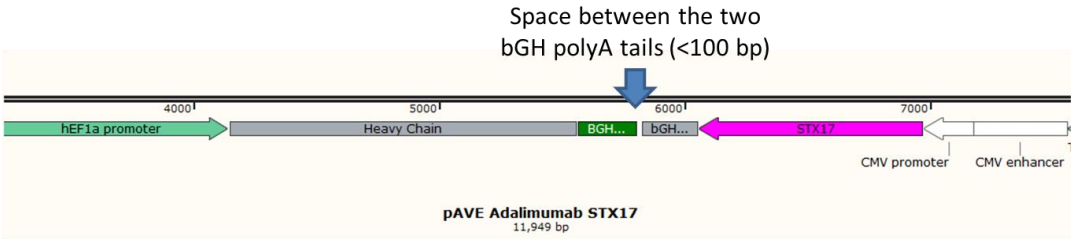

Figure 5.18. Physical position and orientation of the gene coding for the heavy chain of Adalumimab and the gene coding for syntaxin 17 showing the back-to-back bGH polyA tails.

Transient transfection performed to study the impact of the eGFP tag and of the use of different strength promoters gave unexpected results possibly linked to the vectors design. The experiments described in section 5.5.3 showed transient expression was possible in the CHO-DG44 cells and that the transient expression of the SNAREs in the stably expressing IgG mini-pools positively impacted on transient IgG yields (see Figure 5.12) but when the transient transfection was undertaken with a vector containing the IgG molecule and the syntaxin gene with the back-to-back polyA tails the IgG concentration observed was low. High variability was also observed for the conditions achieving higher product concentrations with the single vector transient expression. After the different experiments, no satisfactory transfection conditions were found for the transient transfection of Clone 27 cells with NovaCHOice reagent.

As the pAVE system vectors containing the SNARE genes did not give appropriate IgG yields, a different strategy was applied to obtain syntaxin/SNAP and IgG co-expressing cell lines. Mini-pools, which had the DGV integrated and were already expressing the IgG, were transfected with the plasmids used in Chapter 4, pMRXIP-STX7, pMRXIP-STX17, pMRXIP-

STX18, pMRXIP-SNAP29 and pMRXIP-STXGFP. When using these vectors, selection using puromycin was used to obtain stably expressing target syntaxin cell pools. To determine the adequate concentration of puromycin to use with these pools, Clone 27 was cultured in the presence of different amounts of puromycin and the cell number and culture viability monitored. The results showed that a concentration of 10 µg/mL was sufficient for selection of stably expressing cell pools after recovery. This concentration was higher than the one used for the generation of stably expressing cell lines with CHO-S but as discussed before, CHO derived cell lines have a large genetic heterogeneity.

Stably SNARE expressing cell pools were generated and early assessment of their productivity undertaken to detect any decrease in production compared to the parent pool of the recombinant model protein. Two pools were generated for each construct/SNARE. A first measurement of titre was assessed 5 days after transfection. The titres measured were low but detectable which was an improvement over the previous approach using a single vector containing the IgG and syntaxin/SNAP genes. Moreover, mini-pools transfected with SNAP29 notably demonstrated a positive effect on productivity over the eGFP expressing control when expressed transiently assenting with results from Chapter 4. When titre was measured again after 2-3 passages in shake flask (when stable cell lines for both the model recombinant molecule and the SNARE protein were established), no significant effect was observed .This observation might suggest a larger burden on the cells in transient conditions overcame by the overexpression of the eGFP-fused SNARE protein compared to stable expressing conditions. By measurement of cell fluorescence, low transfection efficiencies were also observed. Measurements were undertaken on cells 5 days after transfection in a media without selection agent (puromycin) and in a static environment. The absence of the selection agent and the short period of recovery since electroporation were probably the cause for low titre and observed transfection efficiency. Because no selection was added, the different cell lines did not integrate stably the plasmid into their genome diluting the expression of fluorescent protein by cell division and degradation of non-integrated plasmid. Moreover, cells were recovering from electroporation and probably directing their energy towards cell survival and division instead of recombinant protein production. Meanwhile, titres were detectable and cell pools were recovering in media containing selection agent to ensure the selection of cells where integration of the vectors into their genome had occurred. It is noted that no cells co-expressing eGFP-STX18 and the model IgGs recovered after electroporation. Previously, only low expressers and

cells expressing a truncated fused protein were generated (see 4.2) suggesting that high levels of STX18 might be detrimental to the cells.

After recovery of the cells and 2-3 passages in Erlenmeyer flasks, the titre and transfection efficiency were measured again. High titre and transfection efficiency were observed implying the success of the strategy, transfection of mini-pools expressing Adalimumab or Blosozumab with pMXRIP for expression of the target syntaxin/SNAP proteins. These results also provided further evidence that the design of the pAVE vectors was responsible for the lack of IgG expression when previously generating mini-pools and cell pools with the single pAVE vector approach. Fluorescence was assessed for the different cell pools demonstrating eGFP tag expression but no information was available about the expression of the full length fused SNARE protein from these data. In the previous experiments, no cleavage of the tag was observed except for the eGFP-STX18 fused protein giving confidence that it was likely the expression of the full length fused proteins occurred. Cells co-expressing the model IgG protein of choice and target SNARE proteins were therefore generated and used for further experiments, notably FOG experiments, to assess any impact on cell growth and productivity.

Fed-batch over growth or FOG is a fed-batch culture approach widely used in industry for the screening purposes or the generation of early material. For screening, FOGs are mainly undertaken at small scale such as 24-DWP and in spin tubes and small shake flasks while larger scales are reserved for early material generation. Due to the number of cell pools to test, and the need of regular sampling, the initial volume of the FOG was 60 mL in 250 mL Erlenmeyer flasks with vented caps in this study. During the FOG, viable cell concentration, culture viability, IgG titre and specific metabolites levels were monitored.

When the results for viable cell concentration, culture viability and titre were compared between the control and SNARE engineered mini-pools, any differences observed were between the model IgG proteins produced and not between the controls and mini-pools engineered with the different SNARE proteins. Thus, there was no impact of the overexpression of the SNARE proteins observed on growth, culture viability and IgG production when producing Adalimumab or Blosozumab. Faster growth, higher titre and cell specific productivity was observed for Blosozumab producing cell lines compared to cell pools producing Adalimumab. Adalimumab and Blosozumab are both antibodies but from two distinct subclasses, IgG1 and IgG4. Both IgG1 and IgG4 have similar structures but IgG4 have less secondary structure complexity with fewer inter heavy chain disulphide bonds in

the hinge region compared to IgG1 (Vidarsson et al. 2014). This reduced complexity might be the explanation for the greater yield of product from cells producing Blosozumab compared to Adalimumab. Indeed, the presence of fewer disulphide bonds makes the molecule easier and faster to assemble, producing less stress on the cells and notably on the ER. It was also observed that cell lines producing Adalimumab had a reduction of recombinant protein expression from day 10 compared to cell lines producing Blosozumab which maintained their productivity through time.

Metabolites levels between cell pools producing Adalimumab or Blosozumab can be linked to their different growth profiles. Cells producing Blosozumab grew faster and consumed more resources to maintain their division, this was linked to the lower concentrations of glucose, the main source of energy in the media, and glutamine, an important amino acid for protein production and also energy production, observed compared to the cells producing Adalimumab. The concentration of lactate diminished during the culture indicating an intake by the cells which happens when cells switch their metabolism in presence of low glucose concentration (Mulukutla, Gramer, and Hu 2012). A reduction of lactate reduction was more important in cells producing Blosozumab suggesting a higher consumption. Adalimumab expressing cell lines tended to have higher glutamate and ammonia concentrations in culture notably from day 10. Fast growing cells need more energy to divide, mainly provided by aerobic mitochondrial respiration. However, aerobic mitochondrial respiration is responsible for the generation of reactive oxygen species (ROS) (Cadenas and Davies 2000). To mitigate against the effects of ROS, cells have defence mechanisms, notably the production of reduced glutathione (Birben et al. 2012; Davies 2000; Pereira et al. 2018). Two amino acids are essential for glutathione synthesis, glutamate and cysteine. Cancer cells with high proliferation rates can recycle ammonia (Spinelli et al. 2017) which may also happen in CHO cells with high growth rates. Cell pools producing Blosozumab might produce higher levels of reduced glutathione necessary to counterpart elevated oxidative stress due to faster growth. For this production, glutamate and ammonia intake would be necessary, explaining the difference in ammonia and glutamate concentration between cell pools producing Blosozumab and Adalimumab at the end of the experiment. Moreover, elevated oxidative stress in the stationary phase might explain the reduced productivity of cells expressing Adalimumab. It has been demonstrated that high oxidative levels downregulates gene expression (Morel and Barouki 1999).

No differences in the productivity between the different cell pools stably engineered with the syntaxin/SNAP and the controls were observed which did not agree with the findings in Chapter 3 and 4. No control of the actual expression of the fused protein was performed with the cell pools generated and used in the FOG experiment, hence an absence of the full size fused protein could have explained the absence of effect. Total protein extractions were then performed on 2 different days to determine if the fused protein were correctly expressed and not cleaved. After western blot analysis, expression for the different cell lines of the fused protein was confirmed. Those results suggested that the eGFP tag wasn't cleaved and the full size fused protein was expressed but no confirmation of the correct folding and activity of the syntaxin protein was performed.

A major difference between the assessments in Chapter 3 and 4 and that in this chapter is in how the assessment was undertaken. In the earlier work all assessment involved the transient expression of the recombinant molecule of interest, largely transfected into CHO-S cell lines already engineered to over-express the SNARE protein of interest at a defined level. In this chapter, cell pools expressing the highest amounts of the target recombinant protein were selected and then the syntaxin/SNAP molecule over-expressed in these. This is a very different approach to the assessment. In the first approach, cells for engineering and assessment were selected based upon different exogenous syntaxin/SNAP expression and then assessed by their ability to transiently express a secretory recombinant protein. In this chapter, already high expressing pools of IgG were selected and then the SNARE was expressed in these cell pools with the result that there would be different amounts of syntaxin/SNAP expressed across the pool. As the amount of SNARE expressed in Chapter 4 suggested this was important in observing an impact, the difference expression across cells may mean that no net effect is observed when in a pool. Therefore, cloning of these pools to identify monoclonal cell lines with different SNARE expression and then assessment of the growth and titre impacts might elucidate an impact of different syntaxin/SNAP expression amounts. In retrospect, and in order to more closely mirror the earlier studies, it may have been a better approach to select the 2 or 3 SNAREs with the greatest impact on titre from Chapter 4 and then make new host DG44 cell lines over-expressing these to different amounts. These could then have subsequently been assessed for their ability to transiently and stably express target secretory recombinant proteins.

It is noted that the CHO-S and Clone 27 cell line hosts have a common ancestor but remain genetically different. Moreover, development of Clone 27 and the expression system and

bioprocess around this is the result of several years of cell line development to obtain a host suiting FDB needs. With that information in mind, the amount of endogenous syntaxin/SNAP could already be naturally upregulated in Clone 27 explaining the lack of effect. After western blot analysis and densitometry with specific antibodies on total protein extract of Clone 27 and host CHO-S cells, no significant difference was found in the expression of STX18 or STX7. A difference in the levels of SNAP29 was observed when measuring the expression levels by densitometry. Levels of expression were two times higher in Clone 27 cell line compared to CHO-S cell line. The bands used for the densitometry analysis were faint, implying a strong effect of the background signal on the values calculated. A hypothesis for the absence of effect in Clone 27 when engineered with SNARE proteins is the presence early on of a bottleneck in the secretory pathway such as in the ER capacity or transcriptional level.

5.8. Conclusions

This chapter reports on experiments undertaken to confirm the approach validated in Chapter 4 in an industrial environment and with a different host cell line. All experiments in this chapter were performed with Clone 27, a CHO-DG44 host cell line, at FDB facilities in order to be in conditions as close to an industrial cell line development process with the different targets identified in Chapter 4. After generating the different vectors using the pAVE platform, mini-pools and cell pools were transfected to obtain cells stably expressing a model protein, Adalimumab or Blosozumab, and a target SNARE, STX7, STX17, STX18 or SNAP29. Unfortunately the different cell pools generated using the pAVE plasmid set did not produce any recombinant protein when co-expressing a SNARE. By the close proximity and the convergence of a CMV promoter and an EF-1α promoter, transcriptional interference was thought to be reason for the absence of production. Further analyses were needed to confirm this hypothesis. Another strategy was implemented to generate co-expressing cell lines, the transfection of cell lines already producing Adalimumab or Blosozumab with vectors generated in Chapter 3. After validation of the expression of recombinant protein for the newly generated cell lines, FOG experiments were accomplished. Results showed no effect of the different overexpressed ectopic syntaxin target on the growth or productivity. Differences observed suggested that Blosozumab was an “easier” to produce molecule compared to Adalimumab with cells growing faster and producing more. Western blot analysis on pellets from the FOG experiment confirmed the

expression of a full size fused protein for the different SNARE targets and further analysis by western blot and densitometry on the host cell lines, Clone 27 and CHO-S, demonstrated no difference in the endogenous expression of the different SNAREs. The discussion of this chapter explains why this may be the case.

CHAPTER 6: Overall Discussion, Conclusions and Future Work

The work performed and reported in this thesis was focused around the investigation and manipulation of SNAREs, important proteins necessary for vesicle fusion, and the impact of their manipulation on the secretory capacity of CHO cells. To achieve this, vectors for the expression of eGFP fused SNARE proteins were designed and used to generate CHO-S cell lines stably expressing the different SNARE targets. The SNARE engineered cell lines were then characterised with respect to their growth characteristics and ability to secrete target recombinant proteins. To assess the later, transient transfection experiments were performed with model proteins, the IgG antibody Adalimumab and the Fc-TNFR fusion protein Etanercept, to determine SNARE manipulation effects on the secretory machinery. After initial validation of the strategy in the CHO-K1 derived CHO-S host cell line, a different industrial cell line, a CHO-DG44 derived cell line known as "Clone 27" developed by Fujifilm Diosynth Biotechnologies, was engineered with the same targets to investigate the transferability of the strategy across different host CHO cell lines. The main finding from the work was that expression of two SNAREs, STX17 and SNAP29, at particular amounts, extended culture longevity times and improved culture viability. An increase in the secretory productivity was also observed (up to 5-fold change for STX17 and 2.5-fold for SNAP29) in CHO-S cells engineered with STX17, SNAP29 and to a lesser extent STX18 when expressing model proteins in a transient manner. These results are in line with other studies using SNAREs to improve recombinant protein production (Peng et al. 2011; Peng and Fussenegger 2009) suggesting that SNARE engineering and more globally vesicle traffic and formation manipulation can enhance the secretory capacity of CHO cells.

When generating eGFP-SNARE engineered CHO-S monoclonal cell populations of the different targets of choice, it was observed that the cell lines expressing VAMP fusion proteins expressed at lower amounts compared to the STX/SNAP engineered cell lines as determined by the relative eGFP expression. Moreover, after monoclonal selection and adaptation of the monoclonal cell lines most of the selected monoclonal cell lines expressing a target VAMP protein lost the majority of their expression suggesting this was unstable or that overexpression was toxic to cells and only those with very low exogenous expression survived prolonged culture. An siRNA screen (Gordon et al. 2010) demonstrated that none of the VAMP proteins were essential for constitutive secretion in HeLa cells

suggesting that other R-SNAREs are able to rescue the lost function of VAMP proteins although siRNA only knocks down expression and does not completely delete it. Thus, a small amount of VAMP protein may remain even under siRNA knockdown conditions that may be sufficient to undertake the required VAMP role. Moreover, it has been observed that overexpression of VAMP4 in HeLa cells impacts the regulation of VAMP4 (Laufman et al. 2011), suggesting that overexpressing a VAMP could interfere with its role and control of the secretory pathway, impacting on crucial steps requiring tight regulation for cell survival such as membrane homeostasis. However, generation of cell pools expressing exogenous VAMP has been performed with and without a GFP tag (Laufman et al. 2011; Peng et al. 2011) suggesting that some level of exogenous expression of VAMP is possible but no high expressing VAMP cell lines were generated. To investigate and potentially overcome any possible toxicity of the expression of exogenous VAMP, the generation of an inducible system could be applied, notably in the case of VAMP7 for which no viable stably expressing cells were generated.

After generation of monoclonal cell populations expressing the eGFP-fused SNAREs at different amounts, growth profiles under batch culture conditions were generated to characterise any impact of the expression on the growth phenotype of the cells. The expression of the eGFP-SNAREs generally had no effect on the growth profiles in terms of the viable cell numbers achieved or the culture viability, except for cells engineered to express eGFP-STX17 or eGFP-SNAP29 in which case some of the cells showed an extended culture time and culture viability. In both cases these were cell lines that expressed the proteins of interest at a low level compared to other cell lines, suggesting that high levels of expression have detrimental effects. This could be linked to UPR overload leading to apoptosis but would need to be confirmed.

STX17 and SNAP29 are both part of a *trans*-SNARE complex involved in the autophagy process, specifically the fusion of autophagosomes with lysosome (Hubert et al. 2016; Itakura et al. 2012). Autophagy is a mechanism involved in the degradation and recycling of elements in the cell such as unwanted proteins, damaged mitochondria, intracellular pathogens and in some cases protein aggregates, which is triggered by starvation conditions and notably lack of critical amino acids such as arginine, leucine, lysine or methionine (Han et al. 2011; Levine and Yuan 2005). While apoptosis is termed programmed cell death I (PCDI), autophagy is considered as programmed cell death II (PCDII) even if autophagy is more of a pro-survival mechanism. Indeed, by degradation of

membranes and proteins autophagy generates essential nutrients (amino acids and fatty acids) that can be reused by mitochondria for ATP production or for protein synthesis in the ER (Levine and Yuan 2005).

The growth characterisation of the different monoclonal cell lines was performed under batch culture conditions where nutrient depleted conditions would be expected to be perceived by cells at the end of the culture (end of stationary phase). One hypothesis as to why specific amounts of over-expression of STX17 and SNAP29 might impact growth and productivity characteristics is that when tuned to particular amounts this may improve the cells recycling capacity by improving autophagy. As a result, more nutrients would be available to the cell which is able to maintain its integrity for longer. Whilst lower levels of STX17 and SNAP29 improve culture viability, higher levels may trigger too much autophagy leading to autophagy mediated apoptosis (Levine and Yuan 2005). This is in line with reported work on autophagy and apoptosis engineering, where overexpression of Bcl-2, an anti-apoptotic regulator, and Beclin-1, an autophagy inducer, led to increased culture period as well as higher viability during serum-free suspension culture but also protected the cells from cell death more efficiently when an insult was made to the cells. Collectively this supports the argument that 'controlled' autophagy induction is a strategy that can improve culture longevity and viability in batch mode. While strategies to inhibit PCD by regulation of apoptosis and autophagy have been performed (Hwang and Lee 2009; Kim et al. 2009), a certain level of autophagy in the cells might be desirable to remove damaged membranes and proteins in order to recycle nutrients and energy to the cell (Zustiak et al. 2008).

When monoclonal cell populations overexpressing fused eGFP SNAREs were transiently transfected with plasmids for the production of the recombinant proteins Adalimumab or Etanercept, cells overexpressing STX17 and SNAP29 showed an increase in productivity of the recombinant molecule. Those cells expressing the eGFP-STX18 fusion also showed an increase in recombinant protein productivity but to a lesser extent. As discussed above, only a specific expression profile had an impact on productivity, that being the relatively high expression of STX17 (compared to the other eGFP-STX17 expressing cell lines) and low expresser of SNAP29. There was no impact of cell lines expressing high levels of SNAP29 observed on productivity, suggesting that higher levels resulted in a cancelling out of the impact of a more moderate over-expression whilst lower levels of STX17 had less impact on productivity than higher levels of STX17, suggesting a tuning effect dependent on STX17

levels of expression. Again, collectively these data show that there is likely to be an 'optimum' amount of SNARE over-expression that helps tune the overall secretory capacity of the cell that is probably dependent upon the make up of the secretory capacity of a particular cell line. It should also be noted that although 3 different monoclonal cell lines were generally investigated, it is possible that a particular monoclonal cell lines happens to have an overall 'enhanced' secretory capacity that was not due to SNARE engineering.

Only monoclonal cells expressing low levels of eGFP-SNAP29 had an increase in secreted recombinant protein productivity with a reduced effect observed in fed-batch culture experiments, once again suggesting that the increase of productivity under batch conditions could be linked to autophagy activity as described for the effect on culture viability. Indeed, during fed-batch culture, media is supplemented with essential nutrients in order to support cell growth. Under those conditions, the cells are presumably not under starvation conditions, implying low levels of autophagy and hence overexpression of SNAP29, involved in the fusion of autophagosomes and lysosomes, would have less impact. By increasing the level of autophagy activity and hence the number of autophagosomes and their fusion with lysosomes, cells overexpressing SNAP29 might be expected to impact amino acid recycling in particular by increasing the fusion events between autophagosome and lysosome. High levels of SNAP29 however, could be detrimental to cells by over-activating degradation of proteins and cell components.

Impacting of recycling through autophagy might not be the only potential effect of SNAP29 over-expression. It is suggested that SNAP29 is a regulator of SNARE complex disassembly via its capacity to bind to a large range of syntaxins and thereby enhancing its binding to vesicles when interacting with a syntaxin. Low levels of SNAP29 might improve productivity by generally enhancing vesicle formation and disassembly steps where SNAP29 is involved. On-the-other-hand, high levels of SNAP29 might be detrimental by reducing the availability of STX to form complexes. Indeed, SNAP29 presence might increase the number of futile cycles where *trans*-SNARE complexes are formed but no fusion event is performed (Baker and Hughson 2016). Disassembly of *trans*-SNARE complexes necessitates the intervention of α-SNAP in an ATP dependent process, making the increase of futile cycles an energy expensive process for the cell (Hong and Lev 2014). To determine if the effect of SNAP29 on productivity is due to its interaction with other STX and ability to form complexes or its improvement of autophagy, it would be interesting to carry experiments with autophagy inhibitors such as Bafilomycin or 3-methyladenine (Zustiak et al. 2008) and observe

whether the effects on productivity are maintained. Immunofluorescence and co-immunoprecipitation to determine where and with what proteins SNAP29 interacts are also experiments that could be performed in order to help elucidate the mechanism of action. Electron microscopy experiments could also be performed to determine the number and the maturation of the autophagosomes in cell lines overexpressing SNAP29 compared to control cell lines in order to evaluate if the increase of the likelihood of fusion events reduce the number of autophagosomes.

Another SNARE protein whose over-expression as an eGFP-fusion to impact positively on the secretion of target recombinant proteins from the engineered cells compared to the control cells was syntaxin17. Relatively low expression of STX17 compared to other engineered cell lines resulted in extended culture longevity, whereas higher levels of STX17 had a positive effect on productivity. It is important to note that lower levels of STX17 also had a positive effect on secretory productivity, but to a lesser extent than higher expressing STX17 engineered cells, suggesting an effect dependent on the proportion of expression. STX17, as for SNAP29 is involved in autophagy, but it is also known to participate in mitochondria fission in nutrient rich conditions by interacting with Drp1.

Mitochondria are the central organelle for the generation of energy where ATP production is performed and are necessary for a wide range of cellular functions. Being an essential organelle, mitochondria possess their own mechanism for damage repair and recycling, fusion and fission. Indeed, impaired mitochondria can be toxic to the cell by producing excessive amounts of ROS, ATP consumption through reversal of ATP synthetase or interfering in other metabolic processes (Youle and van der Bliek 2012). Fusion promotes exchange of healthy material while fission separates damaged parts of mitochondria to ensure a healthy mitochondrial network is maintained and for regulation of morphology and to facilitate mitochondrial traffic. Damaged mitochondria resulting from fission can be directed to autophagosomes to perform mitophagy, a specific degradation of the mitochondrion (Ni, Williams, and Ding 2015).

Before a fission event, Drp1 is recruited by mitochondrial receptors such as Mff, MiD49 and MiD51/MIEF1 from the cytosol and oligomerises and folds around the mitochondria. GTP hydrolysis of Drp1 leads to constriction and separation of the mitochondrial membrane to yield two mitochondria by fission. GTP hydrolysis of Drp1 releases Drp1 from the mitochondria. STX17 promotes fission in nutrient rich conditions by directly interacting with Drp1 and also Rab32 to avoid Drp1 phosphorylation (Arasaki et al. 2015). Despite

being involved in the autophagy pathway, STX17 has not been demonstrated to be indispensable for mitophagy (Juhász 2016; McLelland et al. 2016) but only observed to be involved in complex with SNAP29 and VAMP7 in the degradation of mitochondria derived vesicles via fusion with lysosomes. Modification of mitochondrion dynamics, fusion and fission events, is assimilated with degeneration of the cells (Chen and Chan 2009; Knott and Bossy-Wetzel 2008) although some work has demonstrated that an increased fission leads to an increase in the lifespan of flies and proliferation in vascular smooth muscle cells (Marsboom et al. 2012; Rana et al. 2017), suggesting possible positive impact on enhancement of mitochondrial fission.

Promotion of mitochondrial fission in cells overexpressing STX17 might lead to the presence of more mitochondria in each cell, possibly providing a greater power house for the cell and the ability to produce more energy when required. Moreover, fission is closely linked to mitophagy (Twig et al. 2008), suggesting that increased fission in cells would also lead to increase mitophagic events which would result in improved recycling of damaged mitochondria and making more resources available for protein production. Increased mitophagy might also be linked to increased culture viability or cell growth. Indeed, during respiration mitochondria are damaged by the generation of ROS yet generation of ROS is more important in high proliferating or aging cells. Thus, increased mitophagy would improve recycling of damaged mitochondria and positively affect cell growth and culture viability.

As STX17 may have an influence on mitochondrial fission and autophagy in addition to SNARE activity, further experiments could be undertaken to determine which, if any of these, functions underpins the improvement in secretory recombinant protein productivity observed. Mutations of the hydrophobic C-terminal domain of STX17, which is used for its interaction with Drp1 (Arasaki et al. 2015), could give an indication as to a role in mitochondrial fission in the observed increase in productivity. To determine if the increase in productivity upon STX17 overexpression is as a result of augmentation of the energy supply of the cell or better recycling of damaged mitochondria, measuring the ATP production of cells overexpressing STX17 or specifically block mitophagy with inhibitors are suitable experiments to address these scientific questions. Determination of the number of mitochondria in cells overexpressing STX17 could also give information about the viability of engineering mitochondrial fission.

With regard to overexpression of STX17 and SNAP29 and their effect on culture time and culture viability, the fact this could be due to increased autophagy has been discussed above but this could also underpin the observed impact on productivity too. Indeed, work using rapamycin as an inducer of autophagy has demonstrated that this can result in an increased final antibody titre under batch condition but no difference under fed-batch culture conditions (Han et al. 2011), which mirrors the results reported in this work upon overexpression of STX17 and SNAP29.

To a lesser extent than SNAP29 and STX17, overexpression of STX18 also had a positive impact on productivity, notably when transiently producing the IgG Adalimumab. STX18 is a SNARE involved in the recycle traffic between the Golgi and the ER and has been suggested to be important for the organisation of the ER exit sites (ERES) (Iinuma et al. 2009). ERES are subdomains of the ER where COPII complexes form (Budnik and Stephens 2009) and as such are key for organisation of traffic leaving the ER. Overexpression of STX18 might have a positive effect on productivity by generating or accelerating the turnover at the ERES sites. It has been observed that in response to chronic protein overload, cells generate more ERES (Farhan et al. 2008). The same phenomenon may happen when overexpressing STX18 which would generate more ERES sites, increasing the formation of COPII complexes and hence the anterograde transport from the ER. To verify this hypothesis, confocal microscopy could be undertaken to determine the number of ERES sites in cells overexpressing STX18 and co-immunoprecipitation experiments to observe the partners of STX18.

Interestingly, overexpression of STX18 had a larger effect on secreted Adalimumab amounts than Etanercept production which might be linked to the nature of the protein. Indeed, Etanercept is a fusion protein which might be more difficult to express than Adalimumab generating a bottleneck in the folding and assembly steps rather than the secretion and trafficking. The nature of the impact of STX18 overexpression might explain the generation of only low STX overexpressing cells. Overexpression of high levels of STX18 would potentially lead to a high number of ERES being formed, disturbing the balance between antero- and retrograde traffic. Membranes might accumulate on one side slowly disturbing membrane balance until critical levels that result in cell death are achieved.

The last results chapter (Chapter 5) investigated transfer of the results observed in Chapter 4 in the CHO-S host cell line under batch culture conditions to a different host cell line in an industrial context at FDB. Mini-pools stably expressing a model recombinant protein were

transfected with the plasmids generated in Chapter 3 to create cell pools stably expressing an eGFP fused SNARE and a model recombinant protein, Blosozumab or Adalimumab. The resulting cell pools were assessed in standard FOG experiments used at FDB to assess cell performance. When analysing the growth or productivity of these, there was no impact of the different SNAREs being overexpressed compared to the controls. A possible explanation for this is the mode of culture for the assessment in Chapter 5, fed-batch over grow and the impact of this as opposed to batch culturing as described previously. As described above, STX17 and SNAP29 are suspected to have an impact on autophagy which might result in increased culture time and increase of productivity. Under batch culture, cells are likely to be under starvation conditions towards the end of the culture which would trigger autophagy. However, under fed-batch conditions when following the FDB feeding regime cells are more likely to stay in nutrient rich conditions, hence autophagy is not likely to be activated to the same extent as that under batch conditions. The effect of STX17 and SNAP29 in cells with little activated autophagy might therefore be little.

Another important parameter that could explain the difference in observation between the two cell lines and culture conditions is the strategy used. In Chapter 3, cells were first engineered to stably express an eGFP-SNARE protein and then selected depending on their expression levels before determining their secretory capacity by transient transfection of model proteins. On the other hand in Chapter 5, stably expressing eGFP-SNARE pools were generated using selected high secretory recombinant protein producing mini-pools. This implied that cells expressed different level of SNARE while we showed in Chapter 4 the importance of specific level of expression of the different SNARE proteins on the impact on the cells regarding culture viability and productivity. Moreover, the selected high producers may already have appropriate secretion and bottlenecks may be at a different place (e.g. ER located). CHO-S and Clone 27, even if having a common ancestor, are different host cell lines and could therefore contain different genetic and phenotypic characteristics. Determination of the expression of endogenous levels of some of the overexpressed SNAREs was performed. Only expression of SNAP29 might be considered as different between the two host cell lines, but more precise quantification would be required to determine if this was the case as Western analysis is semi-quantitative at best.

The use of a transient (Chapter 4) and a stable (Chapter 5) strategy might also provide some explanation as to the differences observed. Various studies have shown that differences of effect in cell engineering strategies are possible between transient and

stable expression of a model recombinant protein. This phenomenon has been observed when engineering CHO cells with XBP-1; overexpression of XBP-1 in CHO cells had only a positive impact on productivity upon transient expression of EPO (Ku et al. 2008). The authors suggested that XBP-1 demonstrates a positive effect only in EPO-saturated cells that occurs during transient expression when numerous copies of vector for expression of the model recombinant proteins are present in the cell leading to protein overload in the ER. These observations are similar to the results observed in Chapter 4 but also the observation of a possible positive effect of SNARE overexpression, notably SNAP29, when transiently transfected in CHO-DG44 mini-pools expressing a model protein. Under these conditions, cells might be under more stress for protein production that in stable expression, so the effect of the overexpressed SNARE is observed under such conditions. In order to obtain directly comparable results between those of Chapter 4 and 5 with the two different host cell lines, CHO-DG44 cell lines overexpressing the desired SNARE should have been generated and selected regarding their level of SNARE expression before testing their performance when transiently transfecting model recombinant proteins.

Future Work

Although there is some promising findings from the work reported here, more work needs to be performed to confirm the localisation and function of the different eGFP-tagged fusion proteins. Use of specific sub-localisation stains for the different compartment and microscopy analysis would allow determination of the correct localisation of the different fusion proteins. Different *in vitro* or *in vivo* assays with the fusion proteins should be performed to determine that they can perform their role in the *trans*-SNARE complex and complete fusion of vesicles membranes.

To determine if the effects on productivity and culture viability are linked to the overexpression of the different SNAREs and not due to the selection of cell lines with inherent enhanced secretory characteristics, knock down/out experiments of the integrated SNARE gene by siRNA or CRISPR could be performed. Indeed, the limiting dilution procedure could result in the selection of cell lines with enhanced recombinant protein production capacity that is improved by mechanisms other than enhanced secretory pathway capacity. Return to the parental phenotype after knock out of the

SNARE gene in the engineered cell lines would confirm the effect of the overexpression on the enhancement of recombinant protein production.

Manipulation of *trans*-SNARE complexes instead of single SNAREs by multiple over-expression could also be an interesting approach. Overexpression of the different elements of a *trans*-SNARE complex would allow determination as to whether a specific vesicle fusion step could be improved without limiting the effect of individual SNAREs. Nonetheless, this approach needs to be conducted with care as the overexpression of multiple proteins might trigger the UPR leading to apoptosis of the cells.

Overall Conclusions

The work described in this thesis outlines the successful manipulation of SNARE proteins as an approach for the engineering of the secretory capacity of mammalian cells, specifically CHO cells. The outcomes demonstrate that under batch culture conditions, an enhancement of culture longevity and prolonged culture viability is observed by the overexpression of STX17 and SNAP29, potentially by acting on autophagy activity. Most industrial processes are fed-batch processes for biotherapeutic production in order to improve the maximum viable cell concentration and secreted recombinant protein productivity. Specific engineering of the autophagy pathway to improve the recycling of amino acids within the cells without leading to autophagy related apoptosis would be an interesting strategy to alter or reduce the feed used. With further study of the mechanistic details that underpin how SNARE engineering can deliver enhanced phenotypes in CHO cells for recombinant protein production, it might also be possible to improve productivity further. The different experiments detailed here reveal the importance of fine tuning expression of engineered cells in order to deliver the desired impact on the cell. Indeed, only specific levels of the target SNARE had the desired effects, suggesting a different approach regarding the use of strong promoters for high levels of overexpression of exogenous proteins in cells. Engineering of cell lines already at their full capacity or with non-targeted bottleneck will probably result in failure of any engineering strategy. Regarding the secretory pathway, high throughput microscopy approaches combining automated microscopy and screening could be seen as particularly powerful methods to detect bottlenecks (Mathias et al. 2018; Simpson 2009) and if this work is to be taken

further forward such an approach would be very beneficial in identifying and delivering enhanced secretion via SNARE engineering.

References

Achuthan, Adrian et al. 2008. “Regulation of the Endosomal SNARE Protein Syntaxin 7 by Colony-Stimulating Factor 1 in Macrophages.” *Molecular and Cellular Biology* 28(20):6149–59.

Adams, Jerry M. and Suzanne Cory. 2001. “Life-or-Death Decisions by the Bcl-2 Protein Family.” *Trends in Biochemical Sciences* 26(1):61–66.

Advani, Raj J. et al. 1998. “Seven Novel Mammalian SNARE Proteins Localize to Distinct Membrane Compartments.” *Journal of Biological Chemistry* 273(17):10317–24.

Agathos, S. N. 1991. “Production Scale Insect Cell Culture.” *Biotechnology Advances* 9(1):51–68.

Akopian, David, Kuang Shen, Xin Zhang, and Shu-ou Shan. 2013. “Signal Recognition Particle: An Essential Protein-Targeting Machine.” *Annual Review of Biochemistry* 82(1):693–721.

Amann, Thomas et al. 2018. “CRISPR/Cas9-Multiplexed Editing of Chinese Hamster Ovary B4Gal-T1, 2, 3 and 4 Tailors N-Glycan Profiles of Therapeutics and Secreted Host Cell Proteins.” *Biotechnology Journal* 1800111.

Antonin, W., C. Holroyd, R. Tikkanen, S. Höning, and R. Jahn. 2000. “The R-SNARE Endobrevin/VAMP-8 Mediates Homotypic Fusion of Early Endosomes and Late Endosomes.” *Molecular Biology of the Cell* 11(10):3289–98.

Aoyagi, Kyota et al. 2016. “VAMP7 Regulates Autophagy to Maintain Mitochondrial Homeostasis and to Control Insulin Secretion in Pancreatic β-Cells.” *Diabetes* 65(6):1648–59.

Appenzeller-Herzog, Christian and Lars Ellgaard. 2008. “The Human PDI Family: Versatility Packed into a Single Fold.” *Biochimica et Biophysica Acta - Molecular Cell Research* 1783(4):535–48.

Araki, Kazutaka and Kazuhiro Nagata. 2012. “Protein Folding and Quality Control in the ER.” *Cold Spring Harbor Perspectives in Biology* 4(8):a015438–a015438.

Arasaki, Kohei et al. 2015. “A Role for the Ancient SNARE Syntaxin 17 in Regulating Mitochondrial Division.” *Developmental Cell* 32(3):304–17.

Arasaki, Kohei, May Taniguchi, Katsuko Tani, and Tagaya Mitsuo. 2006. “RINT-1 Regulates the Localization and Entry of ZW10 to the Syntaxin 18 Complex.” *Molecular Biology of the Cell* 125(2):351–69.

Archbold, Julia K., Andrew E. Whitten, Shu-Hong Hu, Brett M. Collins, and Jennifer L. Martin. 2014. “SNARE-Ing the Structures of Sec1/Munc18 Proteins.” *Current Opinion in Structural Biology* 29:44–51.

Arden, Nilou and Michael J. Betenbaugh. 2004. “Life and Death in Mammalian Cell Culture: Strategies for Apoptosis Inhibition.” *Trends in Biotechnology* 22(4):174–80.

Ashkenazi, Avi, Wayne J. Fairbrother, Joel D. Leverson, and Andrew J. Souers. 2017. “From Basic Apoptosis Discoveries to Advanced Selective BCL-2 Family Inhibitors.” *Nature Reviews. Drug Discovery* 16(4):273–84.

Baker, Richard W. and Frederick M. Hughson. 2016. “Chaperoning SNARE Assembly and Disassembly.” *Nature Reviews Molecular Cell Biology* 17(8):465–79.

Barlowe, Charles. 2002. “COPII-Dependent Transport from the Endoplasmic Reticulum.” *Current Opinion in Cell Biology* 14(4):417–22.

Becker, E., L. Florin, K. Pfizenmaier, and H. Kaufmann. 2008. “An XBP-1 Dependent Bottle-Neck in Production of IgG Subtype Antibodies in Chemically Defined Serum-Free Chinese Hamster

Ovary (CHO) Fed-Batch Processes." *Journal of Biotechnology* 135(2):217–23.

Berting, Andreas, Maria R. Farcet, and Thomas R. Kreil. 2010. "Virus Susceptibility of Chinese Hamster Ovary (CHO) Cells and Detection of Viral Contaminations by Adventitious Agent Testing." *Biotechnology and Bioengineering* 106(4):598–607.

Bhide, Gaurang P. and Karen J. Colley. 2017. "Sialylation of N-Glycans: Mechanism, Cellular Compartmentalization and Function." *Histochemistry and Cell Biology* 147(2):149–74.

Birben, Esra, Umit Murat Sahiner, Cansin Sackesen, Serpil Erzurum, and Omer Kalayci. 2012. "Oxidative Stress and Antioxidant Defense." *World Allergy Organization Journal* 5(1):9–19.

Böhm, Ernst et al. 2004. "Screening for Improved Cell Performance: Selection of Subclones with Altered Production Kinetics or Improved Stability by Cell Sorting." *Biotechnology and Bioengineering* 88(6):699–706.

Bonifacino, Juan S. and Benjamin S. Glick. 2004. "The Mechanisms of Vesicle Budding and Fusion." *Cell* 116(2):153–66.

Borth, Nicole, Diethard Mattanovich, Renate Kunert, and Hermann Katinger. 2005. "Effect of Increased Expression of Protein Disulfide Isomerase and Heavy Chain Binding Protein on Antibody Secretion in a Recombinant CHO Cell Line." *Biotechnology Progress* 21(1):106–11.

Budnik, Annika and David J. Stephens. 2009. "ER Exit Sites--Localization and Control of COPII Vesicle Formation." *FEBS Letters* 583(23):3796–3803.

Burgo, Andrea et al. 2012. "A Molecular Network for the Transport of the TI-VAMP/VAMP7 Vesicles from Cell Center to Periphery" edited by H. R. B. Pelham. *Developmental Cell* 23(1):166–80.

Burmester, Gerd R., Remo Panaccione, Kenneth B. Gordon, Melissa J. McIlraith, and Ana P. M. Lacerda. 2013. "Adalimumab: Long-Term Safety in 23 458 Patients from Global Clinical Trials in Rheumatoid Arthritis, Juvenile Idiopathic Arthritis, Ankylosing Spondylitis, Psoriatic Arthritis, Psoriasis and Crohn's Disease." *Annals of the Rheumatic Diseases* 72(4):517–24.

Butler, Michael and Maureen Spearman. 2014. "The Choice of Mammalian Cell Host and Possibilities for Glycosylation Engineering." *Current Opinion in Biotechnology* 30:107–12.

Cadenas, Enrique and Kelvin J. a. Davies. 2000. "Mitochondrial Free Radical Generation, Oxidative Stress, and Aging11This Article Is Dedicated to the Memory of Our Dear Friend, Colleague, and Mentor Lars Ernster (1920–1998), in Gratitude for All He Gave to Us." *Free Radical Biology and Medicine* 29(3–4):222–30.

Caramelo, Julio J. and Armando J. Parodi. 2015. "A Sweet Code for Glycoprotein Folding." *FEBS Letters* 589(22):3379–87.

Chaineau, Mathilde, Lydia Danglot, and Thierry Galli. 2009. "Multiple Roles of the Vesicular-SNARE TI-VAMP in Post-Golgi and Endosomal Trafficking." *FEBS Letters* 583(23):3817–26.

Chakrabarti, Anirikh, Aaron W. Chen, and Jeffrey D. Varner. 2011. "A Review of the Mammalian Unfolded Protein Response." *Biotechnology and Bioengineering* 108(12):2777–93.

Chen, Fei et al. 2012. "Insight into the Roles of Hypoxanthine and Thydimine on Cultivating Antibody-Producing CHO Cells: Cell Growth, Antibody Production and Long-Term Stability." *Applied Microbiology and Biotechnology* 93(1):169–78.

Chen, Hsiuchen and David C. Chan. 2009. "Mitochondrial Dynamics--Fusion, Fission, Movement, and Mitophagy--in Neurodegenerative Diseases." *Human Molecular Genetics* 18(R2):R169-76.

Chen, M. J. et al. 1984. "The Functional Human Dihydrofolate Reductase Gene." *The Journal of Biological Chemistry* 259(6):3933–43.

Chiang, Gisela G. and William P. Sisk. 2005. “Bcl-XL Mediates Increased Production of Humanized Monoclonal Antibodies in Chinese Hamster Ovary Cells.” *Biotechnology and Bioengineering* 91(7):779–92.

Chong, William P. K. et al. 2010. “Metabolomics-Driven Approach for the Improvement of Chinese Hamster Ovary Cell Growth: Overexpression of Malate Dehydrogenase II.” *Journal of Biotechnology* 147(2):116–21.

Chung, Bevan Kai-Sheng, Faraaz N. K. Yusufi, Mariati, Yuansheng Yang, and Dong-Yup Lee. 2013. “Enhanced Expression of Codon Optimized Interferon Gamma in CHO Cells.” *Journal of Biotechnology* 167(3):326–33.

Chung, Joo Young, Seung Wook Lim, Yeon Joo Hong, Sun Ok Hwang, and Gyun Min Lee. 2004. “Effect of Doxycycline-Regulated Calnexin and Calreticulin Expression on Specific Thrombopoietin Productivity of Recombinant Chinese Hamster Ovary Cells.” *Biotechnology and Bioengineering* 85(5):539–46.

Clincke, Marie-Françoise et al. 2013. “Very High Density of CHO Cells in Perfusion by ATF or TFF in WAVE Bioreactor™. Part I. Effect of the Cell Density on the Process.” *Biotechnology Progress* 29(3):754–67.

Cocucci, E., G. Racchetti, M. Rupnik, and J. Meldolesi. 2008. “The Regulated Exocytosis of Enlargeosomes Is Mediated by a SNARE Machinery That Includes VAMP4.” *Journal of Cell Science* 121(18):2983–91.

Collins, Richard F., Alan D. Schreiber, Sergio Grinstein, and William S. Trimble. 2002. “Syntaxins 13 and 7 Function at Distinct Steps During Phagocytosis.” *The Journal of Immunology* 169(6):3250–56.

Connolly, T., P. Rapiejko, and R. Gilmore. 1991. “Requirement of GTP Hydrolysis for Dissociation of the Signal Recognition Particle from Its Receptor.” *Science* 252(5009):1171–73.

Cost, Gregory J. et al. 2010. “BAK and BAX Deletion Using Zinc-Finger Nucleases Yields Apoptosis-Resistant CHO Cells.” *Biotechnology and Bioengineering* 105(2):330–40.

Cui, Yong, Caiji Gao, Qiong Zhao, and Liwen Jiang. 2016. “Using Fluorescent Protein Fusions to Study Protein Subcellular Localization and Dynamics in Plant Cells.” Pp. 113–23 in Vol. 1474, *Methods in Molecular Biology*, edited by S. D. Schwartzbach, O. Skalli, and T. Schikorski. New York, NY: Springer New York.

Daste, F., T. Galli, and D. Tareste. 2015. “Structure and Function of Longin SNAREs.” *Journal of Cell Science* 128(23):4263–72.

Davami, Fatemeh. 2016. “Utilization of Site-Specific Recombination in Biopharmaceutical Production.” 20(April):68–76.

Davies, Kelvin J. A. 2000. “An Overview of Oxidative Stress.” *IUBMB Life* 50(4):241–44.

Demain, Arnold L. and Preeti Vaishnav. 2009. “Production of Recombinant Proteins by Microbes and Higher Organisms.” *Biotechnology Advances* 27(3):297–306.

Derouazi, M. et al. 2006. “Genetic Characterization of CHO Production Host DG44 and Derivative Recombinant Cell Lines.” *Biochemical and Biophysical Research Communications* 340(4):1069–77.

Dierks, T. et al. 1996. “A Microsomal ATP-Binding Protein Involved in Efficient Protein Transport into the Mammalian Endoplasmic Reticulum.” *The EMBO Journal* 15(24):6931–42.

Doolan, Padraig et al. 2010. “Microarray and Proteomics Expression Profiling Identifies Several Candidates, Including the Valosin-Containing Protein (VCP), Involved in Regulating High

Cellular Growth Rate in Production CHO Cell Lines." *Biotechnology and Bioengineering* 106(1):42–56.

Dumont, Jennifer, Don Euwart, Baisong Mei, Scott Estes, and Rashmi Kshirsagar. 2016. "Human Cell Lines for Biopharmaceutical Manufacturing: History, Status, and Future Perspectives." *Critical Reviews in Biotechnology* 36(6):1110–22.

Ecker, Dawn M., Susan Dana Jones, and Howard L. Levine. 2015. "The Therapeutic Monoclonal Antibody Market." *MAbs* 7(1):9–14.

Ede, Christopher, Ximin Chen, Meng-Yin Lin, and Yvonne Y. Chen. 2016. "Quantitative Analyses of Core Promoters Enable Precise Engineering of Regulated Gene Expression in Mammalian Cells." *ACS Synthetic Biology* 5(5):395–404.

Fader, Claudio Marcelo, Milton Osmar Aguilera, and María Isabel Colombo. 2012. "ATP Is Released from Autophagic Vesicles to the Extracellular Space in a VAMP7-Dependent Manner." *Autophagy* 8(12):1741–56.

Fan, Lianchun et al. 2012. "Improving the Efficiency of CHO Cell Line Generation Using Glutamine Synthetase Gene Knockout Cells." *Biotechnology and Bioengineering* 109(4):1007–15.

Fan, Lianchun et al. 2017. "Comparative Study of Therapeutic Antibody Candidates Derived from Mini-Pool and Clonal Cell Lines." *Biotechnology Progress* 33(6):1456–62.

Farhan, Hesso, Matthias Weiss, Katsuko Tani, Randal J. Kaufman, and Hans-Peter Hauri. 2008. "Adaptation of Endoplasmic Reticulum Exit Sites to Acute and Chronic Increases in Cargo Load." *The EMBO Journal* 27(15):2043–54.

Fernández, Francisco J. and M. Cristina Vega. 2016. "Choose a Suitable Expression Host: A Survey of Available Protein Production Platforms." Pp. 15–24 in.

Fischer, Simon, René Handrick, and Kerstin Otte. 2015. "The Art of CHO Cell Engineering: A Comprehensive Retrospect and Future Perspectives." *Biotechnology Advances* 33(8):1878–96.

Le Fourn, Valérie, Pierre-alain Girod, Montse Buceta, Alexandre Regamey, and Nicolas Mermod. 2014. "CHO Cell Engineering to Prevent Polypeptide Aggregation and Improve Therapeutic Protein Secretion." *Metabolic Engineering* 21:91–102.

Fu, Ruoqiu et al. 2018. "A Novel Autophagy Inhibitor Berbamine Blocks SNARE-Mediated Autophagosome-Lysosome Fusion through Upregulation of BNIP3." *Cell Death and Disease* 9(2).

Galli, Thierry et al. 1994. "Tetanus Toxin-Mediated Cleavage of Cellubrevin Impairs Exocytosis of Transferrin Receptor-Containing Vesicles in CHO Cells." *The Journal of Cell Biology* 125(5):1015–24.

Geisse, Sabine. 2009. "Reflections on More than 10 Years of TGE Approaches." *Protein Expression and Purification* 64(2):99–107.

Gerst, J. E. 1999. "SNAREs and SNARE Regulators in Membrane Fusion and Exocytosis." *Cellular and Molecular Life Sciences* 55(5):707–34.

Gleeson, Paul A., John G. Lock, Michael R. Luke, and Jennifer L. Stow. 2004. "Domains of the TGN: Coats, Tethers and G Proteins." *Traffic* 5(5):315–26.

Glick, Benjamin S. and Alberto Luini. 2011. "Models for Golgi Traffic: A Critical Assessment." *Cold Spring Harbor Perspectives in Biology* 3(11):a005215–a005215.

Glick, Danielle, Sandra Barth, and Kay F. Macleod. 2010. "Autophagy : Cellular and Molecular Mechanisms" edited by J. Padmanabhan. *Journal of Pathology The* 221(1):3–12.

Godi, Anna et al. 2004. “FAPPS Control Golgi-to-Cell-Surface Membrane Traffic by Binding to ARF and PtdIns(4)P.” *Nature Cell Biology* 6(5):393–404.

Goodsell, David S. 1999. “The Molecular Perspective: Methotrexate.” *Stem Cells* 17(5):314–15.

Gordon, David E. et al. 2017. “VAMP3/Syb and YKT6 Are Required for the Fusion of Constitutive Secretory Carriers with the Plasma Membrane” edited by G. P. Copenhaver. *PLoS Genetics* 13(4):e1006698.

Gordon, David E., Lisa M. Bond, Daniela a. Sahlender, and Andrew a. Peden. 2010. “A Targeted SiRNA Screen to Identify SNAREs Required for Constitutive Secretion in Mammalian Cells.” *Traffic* 11(9):1191–1204.

Grav, Lise Marie et al. 2015. “One-Step Generation of Triple Knockout CHO Cell Lines Using CRISPR/Cas9 and Fluorescent Enrichment.” *Biotechnology Journal* 10(9):1446–56.

Gulis, Galina, Kelly Cristina Simi, Renata de Toledo, Andrea Maranhao, and Marcelo Brigido. 2014. “Optimization of Heterologous Protein Production in Chinese Hamster Ovary Cells under Overexpression of Spliced Form of Human X-Box Binding Protein.” *BMC Biotechnology* 14(1):26.

Guo, Bin et al. 2014. “O-GlcNAc-Modification of SNAP-29 Regulates Autophagosome Maturation.” *Nature Cell Biology* 16(12):1215–26.

Hamasaki, Maho, Nobumichi Furuta, et al. 2013. “Autophagosomes Form at ER-Mitochondria Contact Sites.” *Nature* 495(7441):389–93.

Hamasaki, Maho, Shusaku T. Shibutani, and Tamotsu Yoshimori. 2013. “Up-to-Date Membrane Biogenesis in the Autophagosome Formation.” *Current Opinion in Cell Biology* 25(4):455–60.

Hamman, Brian D., Linda M. Hendershot, and Arthur E. Johnson. 1998. “BiP Maintains the Permeability Barrier of the ER Membrane by Sealing the Lumenal End of the Translocon Pore before and Early in Translocation.” *Cell* 92(6):747–58.

Han, Young Kue, Tae Kwang Ha, So Jeong Lee, Jae Seong Lee, and Gyun Min Lee. 2011. “Autophagy and Apoptosis of Recombinant Chinese Hamster Ovary Cells during Fed-Batch Culture: Effect of Nutrient Supplementation.” *Biotechnology and Bioengineering* 108(9):2182–92.

Handlogten, Michael W. et al. 2018. “Intracellular Response to Process Optimization and Impact on Productivity and Product Aggregates for a High-Titer CHO Cell Process.” *Biotechnology and Bioengineering* 115(1):126–38.

Hansen, Henning Gram et al. 2015. “Versatile Microscale Screening Platform for Improving Recombinant Protein Productivity in Chinese Hamster Ovary Cells.” *Scientific Reports* 5:18016.

Hansen, Henning Gram, Nuša Pristovšek, Helene Faustrup Kildegaard, and Gyun Min Lee. 2017. “Improving the Secretory Capacity of Chinese Hamster Ovary Cells by Ectopic Expression of Effector Genes: Lessons Learned and Future Directions.” *Biotechnology Advances* 35(1):64–76.

Hartl, F. Ulrich. 1996. “Molecular Chaperones in Cellular Protein Folding.” *Nature* 381(6583):571–80.

Hassell, T., S. Gleave, and M. Butler. 1991. “Growth Inhibition in Animal Cell Culture.” *Applied Biochemistry and Biotechnology* 30(1):29–41.

Hatsuzawa, Kiyotaka et al. 2000. “Syntaxin 18, a SNAP Receptor That Functions in the Endoplasmic Reticulum, Intermediate Compartment, and Cis-Golgi Vesicle Trafficking.” *Journal of Biological Chemistry* 275(18):13713–20.

Hatsuzawa, Kiyotaka et al. 2006. “Involvement of Syntaxin 18, an Endoplasmic Reticulum (ER)-Localized SNARE Protein, in ER-Mediated Phagocytosis.” *Molecular Biology of the Cell*

17(9):3964–77.

Hausmann, Ruth, Ivana Chudobová, Holger Spiegel, and Stefan Schillberg. 2018. “Proteomic Analysis of CHO Cell Lines Producing High and Low Quantities of a Recombinant Antibody before and after Selection with Methotrexate.” *Journal of Biotechnology* 265(November 2017):65–69.

Hayes, N. V. L., C. M. Smales, and P. Klappa. 2010. “Protein Disulfide Isomerase Does Not Control Recombinant IgG4 Productivity in Mammalian Cell Lines.” *Biotechnology and Bioengineering* 105(4):770–79.

He, C. and D. J. Klionsky. 2009. “Regulation Mechanisms and Signalling Pathways of Autophagy.” *Annual Review of Genetics* 43(68):67.

He, Yuhong and Maurine E. Linder. 2009. “Differential Palmitoylation of the Endosomal SNAREs Syntaxin 7 and Syntaxin 8.” *Journal of Lipid Research* 50(3):398–404.

Hebert, Daniel N. and Maurizio Molinari. 2007. “In and Out of the ER: Protein Folding, Quality Control, Degradation, and Related Human Diseases.” *Physiological Reviews* 87(4):1377–1408.

Hegedus, Krisztina, Szabolcs Takats, Attila L. Kovacs, and Gabor Juhasz. 2013. “Evolutionarily Conserved Role and Physiological Relevance of a STX17/Syx17 (Syntaxin 17)-Containing SNARE Complex in Autophagosome Fusion with Endosomes and Lysosomes.” *Autophagy* 9(10):1642–46.

von Heijne, Gunnar. 1985. “Signal Sequences.” *Journal of Molecular Biology* 184(1):99–105.

Von Heijne, Gunnar. 1983. “Patterns of Amino Acids near Signal-Sequence Cleavage Sites.” *European Journal of Biochemistry* 133(1):17–21.

Hesse, Friedemann and Roland Wagner. 2000. “Developments and Improvements in the Manufacturing of Human Therapeutics with Mammalian Cell Cultures.” *Trends in Biotechnology* 18(4):173–80.

Hetz, Claudio. 2012. “The Unfolded Protein Response: Controlling Cell Fate Decisions under ER Stress and Beyond.” *Nature Reviews Molecular Cell Biology* 13(2):89–102.

Hetz, Claudio and Feroz R. Papa. 2018. “The Unfolded Protein Response and Cell Fate Control.” *Molecular Cell* 69(2):169–81.

Hinners, I. 2003. “Changing Directions: Clathrin-Mediated Transport between the Golgi and Endosomes.” *Journal of Cell Science* 116(5):763–71.

Hirata, T. et al. 2015. “Post-Golgi Anterograde Transport Requires GARP-Dependent Endosome-to-TGN Retrograde Transport.” *Molecular Biology of the Cell* 26(17):3071–84.

Hohenstein, Anita C. and Paul A. Roche. 2001. “SNAP-29 Is a Promiscuous Syntaxin-Binding SNARE.” *Biochemical and Biophysical Research Communications* 285(2):167–71.

Hong, Wan Jin and Sima Lev. 2014. “Tethering the Assembly of SNARE Complexes.” *Trends in Cell Biology* 24(1):35–43.

Hong, Wanjin. 2005. “SNAREs and Traffic.” *Biochimica et Biophysica Acta - Molecular Cell Research* 1744(2):120–44.

Hooks, Michael A., Catherine S. Wade, and William J. Millikan. 1991. “Muromonab CD-3: A Review of Its Pharmacology, Pharmacokinetics, and Clinical Use in Transplantation.” *Pharmacotherapy* 11(1):26–37.

Hu, Chuan, Deborah Hardee, and Fred Minnear. 2007. “Membrane Fusion by VAMP3 and Plasma Membrane T-SNAREs.” *Experimental Cell Research* 313(15):3198–3209.

Huang, Yao-Ming et al. 2010. “Maximizing Productivity of CHO Cell-Based Fed-Batch Culture Using Chemically Defined Media Conditions and Typical Manufacturing Equipment.” *Biotechnology Progress* 26(5):1400–1410.

Hubert, Virginie et al. 2016. “LAMP-2 Is Required for Incorporating Syntaxin-17 into Autophagosomes and for Their Fusion with Lysosomes.” *Biology Open* 5(10):1516–29.

Hwang, C., a J. Sinskey, and H. F. Lodish. 1992. “Oxidized Redox State of Glutathione in the Endoplasmic Reticulum.” *Science (New York, N.Y.)* 257(5076):1496–1502.

Hwang, S. O., J. Y. Chung, and G. M. Lee. 2003. “Effect of Doxycycline-Regulated ERp57 Expression on Specific Thrombopoietin Productivity of Recombinant CHO Cells.” *Biotechnology Progress* 19(1):179–84.

Hwang, Sun Ok and Gyun Min Lee. 2009. “Effect of Akt Overexpression on Programmed Cell Death in Antibody-Producing Chinese Hamster Ovary Cells.” *Journal of Biotechnology* 139(1):89–94.

Iinuma, Takayuki et al. 2009. “Role of Syntaxin 18 in the Organization of Endoplasmic Reticulum Subdomains.” *Journal of Cell Science* 122(Pt 10):1680–90.

Irani, Zahra Azimzadeh, Eduard J. Kerkhoven, Seyed Abbas Shojaosadati, and Jens Nielsen. 2016. “Genome-Scale Metabolic Model of Pichia Pastoris with Native and Humanized Glycosylation of Recombinant Proteins.” *Biotechnology and Bioengineering* 113(5):961–69.

Itakura, Eisuke, Chieko Kishi-Itakura, and Noboru Mizushima. 2012. “The Hairpin-Type Tail-Anchored SNARE Syntaxin 17 Targets to Autophagosomes for Fusion with Endosomes/Lysosomes.” *Cell* 151(6):1256–69.

Itakura, Eisuke and Noboru Mizushima. 2013. “Syntaxin 17.” *Autophagy* 9(6):917–19.

Jahn, Reinhard, Thorsten Lang, and Thomas C. Südhof. 2003. “Membrane Fusion.” *Cell* 112(4):519–33.

Jahn, Reinhard and Richard H. Scheller. 2006. “SNAREs--Engines for Membrane Fusion.” *Nature Reviews. Molecular Cell Biology* 7(9):631–43.

Jaluria, Pratik, Michael Betenbaugh, Konstantinos Konstantopoulos, and Joseph Shiloach. 2007. “Enhancement of Cell Proliferation in Various Mammalian Cell Lines by Gene Insertion of a Cyclin-Dependent Kinase Homolog.” *BMC Biotechnology* 7:1–11.

Jarvis, Donald L. 2003. “Developing Baculovirus-Insect Cell Expression Systems for Humanized Recombinant Glycoprotein Production.” *Virology* 310(1):1–7.

Jovi, M. et al. 2014. “Endosomal Sorting of VAMP3 Is Regulated by PI4K2A.” *Journal of Cell Science* 127(17):3745–56.

Juhász, Gábor. 2016. “A Mitochondrial-Derived Vesicle HOPS to Endolysosomes Using Syntaxin-17.” *The Journal of Cell Biology* 214(3):241–43.

Kaneko, Yoshihiro, Ryuji Sato, and Hideki Aoyagi. 2010. “Changes in the Quality of Antibodies Produced by Chinese Hamster Ovary Cells during the Death Phase of Cell Culture.” *Journal of Bioscience and Bioengineering* 109(3):281–87.

Kapoor, Mili et al. 2003. “Interactions of Substrate with Calreticulin, an Endoplasmic Reticulum Chaperone.” *The Journal of Biological Chemistry* 278(8):6194–6200.

Kaufmann, Hitto, Xenia Mazur, Martin Fussenegger, and James E. Bailey. 1999. “Influence of Low Temperature on Productivity, Proteome and Protein Phosphorylation of CHO Cells.” *Biotechnology and Bioengineering* 63(5):573–82.

Ke, Na and Mehmet Berkmen. 2014. “Production of Disulfide-Bonded Proteins in Escherichia Coli.” P. 16.1B.1-16.1B.21 in *Current Protocols in Molecular Biology*. Vol. 108. Hoboken, NJ, USA: John Wiley & Sons, Inc.

Kim, Eun Jeong and Tai Hyun Park. 2003. “Anti-Apoptosis Engineering.” *Biotechnology and Bioprocess Engineering* 8(2):76–82.

Kim, Minsoo, Peter M. O’Callaghan, Kurt A. Droms, and David C. James. 2011. “A Mechanistic Understanding of Production Instability in CHO Cell Lines Expressing Recombinant Monoclonal Antibodies.” *Biotechnology and Bioengineering* 108(10):2434–46.

Kim, No Soo and Gyun Min Lee. 2000. “Overexpression of Bcl-2 Inhibits Sodium Butyrate-Induced Apoptosis in Chinese Hamster Ovary Cells Resulting in Enhanced Humanized Antibody Production.” *Biotechnology and Bioengineering* 71(3):184–93.

Kim, Seon-Young, Jae-Ho Lee, Hyun-Seock Shin, Hye-Ja Kang, and Yeon-Soo Kim. 2002. “The Human Elongation Factor 1 Alpha (EF-1α) First Intron Highly Enhances Expression of Foreign Genes from the Murine Cytomegalovirus Promoter.” *Journal of Biotechnology* 93(2):183–87.

Kim, Sung Hyun and Gyun Min Lee. 2007. “Down-Regulation of Lactate Dehydrogenase-A by SiRNAs for Reduced Lactic Acid Formation of Chinese Hamster Ovary Cells Producing Thrombopoietin.” *Applied Microbiology and Biotechnology* 74(1):152–59.

Kim, Tae Kyung and James H. Eberwine. 2010. “Mammalian Cell Transfection: The Present and the Future.” *Analytical and Bioanalytical Chemistry* 397(8):3173–78.

Kim, Yeon-Gu, Jee Yon Kim, Chaya Mohan, and Gyun Min Lee. 2009. “Effect of Bcl-XL Overexpression on Apoptosis and Autophagy in Recombinant Chinese Hamster Ovary Cells under Nutrient-Deprived Condition.” *Biotechnology and Bioengineering* 103(4):757–66.

Kingston, Robert E., Randal J. Kaufman, C. R. Bebbington, and M. R. Rolfe. 2002. “Amplification Using CHO Cell Expression Vectors.” P. Unit 16.23 in *Current Protocols in Molecular Biology*. Vol. Chapter 16. Hoboken, NJ, USA: John Wiley & Sons, Inc.

Knappskog, Stian et al. 2007. “The Level of Synthesis and Secretion of Gaussia Princeps Luciferase in Transfected CHO Cells Is Heavily Dependent on the Choice of Signal Peptide.” *Journal of Biotechnology* 128(4):705–15.

Knott, Andrew B. and Ella Bossy-Wetzel. 2008. “Impairing the Mitochondrial Fission and Fusion Balance: A New Mechanism of Neurodegeneration.” *Annals of the New York Academy of Sciences* 1147(407):283–92.

Kober, Lars, Christoph Zehe, and Juergen Bode. 2013. “Optimized Signal Peptides for the Development of High Expressing CHO Cell Lines.” *Biotechnology and Bioengineering* 110(4):1164–73.

Koenig, Paul-Albert and Hidde L. Ploegh. 2014. “Protein Quality Control in the Endoplasmic Reticulum.” *F1000prime Reports* 6(July):49.

Koterba, Kristen L., Trissa Borgschulte, and Michael W. Laird. 2012. “Thioredoxin 1 Is Responsible for Antibody Disulfide Reduction in CHO Cell Culture.” *Journal of Biotechnology* 157(1):261–67.

Krampe, Britta and Mohamed Al-Rubeai. 2010. “Cell Death in Mammalian Cell Culture: Molecular Mechanisms and Cell Line Engineering Strategies.” *Cytotechnology* 62(3):175–88.

Krzewski, Konrad, Aleksandra Gil-Krzewska, James Watts, Joel N. H. Stern, and Jack L. Strominger. 2011. “VAMP4- and VAMP7-Expressing Vesicles Are Both Required for Cytotoxic Granule Exocytosis in NK Cells.” *European Journal of Immunology* 41(11):3323–29.

Ku, Sebastian C. Y., Daphne T. W. Ng, Miranda G. S. Yap, and Sheng-hao Chao. 2008. “Effects of

Overexpression of X-Box Binding Protein 1 on Recombinant Protein Production in Chinese Hamster Ovary and NS0 Myeloma Cells." *Biotechnology and Bioengineering* 99(1):155–64.

Kumar, Suresh et al. 2018. "Mechanism of Stx17 Recruitment to Autophagosomes via IRGM and Mammalian Atg8 Proteins." *The Journal of Cell Biology* jcb.201708039.

Kuster, Aurelia et al. 2015. "The Q-Soluble-N-Ethylmaleimide-Sensitive Factor Attachment Protein Receptor (Q-SNARE) SNAP-47 Regulates Trafficking of Selected Vesicle-Associated Membrane Proteins (VAMPs)." *Journal of Biological Chemistry* 290(47):jbc.M115.666362.

Kuystermans, Darrin and Mohamed Al-Rubeai. 2009. "CMyc Increases Cell Number through Uncoupling of Cell Division from Cell Size in CHO Cells." *BMC Biotechnology* 9(1):76.

Lalonde, Marie-Eve and Yves Durocher. 2017. "Therapeutic Glycoprotein Production in Mammalian Cells." *Journal of Biotechnology* 251(April):128–40.

Lao, M. S. and D. Toth. 1997. "Effects of Ammonium and Lactate on Growth and Metabolism of a Recombinant Chinese Hamster Ovary Cell Culture." *Biotechnology Progress* 13(5):688–91.

Laufman, Orly, WanJin Hong, and Sima Lev. 2011. "The COG Complex Interacts Directly with Syntaxin 6 and Positively Regulates Endosome-to-TGN Retrograde Transport." *Journal of Cell Biology* 194(3):459–72.

Lee, Jae Seong, Tae Kwang Ha, Jin Hyoung Park, and Gyun Min Lee. 2013. "Anti-Cell Death Engineering of CHO Cells: Co-Overexpression of Bcl-2 for Apoptosis Inhibition, Beclin-1 for Autophagy Induction." *Biotechnology and Bioengineering* 110(8):2195–2207.

Lee, Jae Seong and Gyun Min Lee. 2012. "Rapamycin Treatment Inhibits CHO Cell Death in a Serum-Free Suspension Culture by Autophagy Induction." *Biotechnology and Bioengineering* 109(12):3093–3102.

Lee, Yih Yean et al. 2009. "Overexpression of Heat Shock Proteins (HSPs) in CHO Cells for Extended Culture Viability and Improved Recombinant Protein Production." *Journal of Biotechnology* 143(1):34–43.

Levine, Beth and Junying Yuan. 2005. "Autophagy in Cell Death: An Innocent Convict?" *The Journal of Clinical Investigation* 115(10):2679–88.

Lewis, Nathan E. et al. 2013. "Genomic Landscapes of Chinese Hamster Ovary Cell Lines as Revealed by the Cricetulus Griseus Draft Genome." *Nature Biotechnology* 31(8):759–65.

Lewy, Tyler G., Jeffrey M. Grabowski, and Marshall E. Bloom. 2017. "BiP: Master Regulator of the Unfolded Protein Response and Crucial Factor in Flavivirus Biology ." *The Yale Journal of Biology and Medicine* 90(2):291–300.

Li, Hongwen et al. 2016. "Genetic Analysis of the Clonal Stability of Chinese Hamster Ovary Cells for Recombinant Protein Production." *Molecular BioSystems* 12(1):102–9.

Li, J. and J. Yuan. 2008. "Caspases in Apoptosis and Beyond." *Oncogene* 27(48):6194–6206.

Liew, Jane C. J., Wen Siang Tan, Noorjahan Banu Mohamed Alitheen, Eng Seng Chan, and Beng Ti Tey. 2010. "Over-Expression of the X-Linked Inhibitor of Apoptosis Protein (XIAP) Delays Serum Deprivation-Induced Apoptosis in CHO-K1 Cells." *Journal of Bioscience and Bioengineering* 110(3):338–44.

Lin, Nan et al. 2015. "Chinese Hamster Ovary (CHO) Host Cell Engineering to Increase Sialylation of Recombinant Therapeutic Proteins by Modulating Sialyltransferase Expression." *Biotechnology Progress* 31(2):334–46.

Low, Seng Hui et al. 2003. "Syntaxin 2 and Endobrevin Are Required for the Terminal Step of

Cytokinesis in Mammalian Cells." *Developmental Cell* 4(5):753–59.

Luftman, Kevin, Nazarul Hasan, Paul Day, Deborah Hardee, and Chuan Hu. 2009. "Silencing of VAMP3 Inhibits Cell Migration and Integrin-Mediated Adhesion." *Biochemical and Biophysical Research Communications* 380(1):65–70.

Mabashi-Asazuma, Hideaki and Donald L. Jarvis. 2017. "CRISPR-Cas9 Vectors for Genome Editing and Host Engineering in the Baculovirus–insect Cell System." *Proceedings of the National Academy of Sciences* 114(34):201705836.

Majors, Brian S. et al. 2008. "E2F-1 Overexpression Increases Viable Cell Density in Batch Cultures of Chinese Hamster Ovary Cells." *Journal of Biotechnology* 138(3–4):103–6.

Makrides, S. C. 1999. "Components of Vectors for Gene Transfer and Expression in Mammalian Cells." *Protein Expression and Purification* 17(2):183–202.

Mallard, Frédéric et al. 2002. "Early/Recycling Endosomes-to-TGN Transport Involves Two SNARE Complexes and a Rab6 Isoform." *Journal of Cell Biology* 156(4):653–64.

Malphettes, Laetitia et al. 2010. "Highly Efficient Deletion of FUT8 in CHO Cell Lines Using Zinc-Finger Nucleases Yields Cells That Produce Completely Nonfucosylated Antibodies." *Biotechnology and Bioengineering* 106(5):774–83.

Mancias, Joseph D. and Jonathan Goldberg. 2008. "Structural Basis of Cargo Membrane Protein Discrimination by the Human COPII Coat Machinery." *The EMBO Journal* 27(21):2918–28.

de Marco, Ario. 2009. "Strategies for Successful Recombinant Expression of Disulfide Bond-Dependent Proteins in Escherichia Coli." *Microbial Cell Factories* 8:26.

Marsboom, Glenn et al. 2012. "Dynamin-Related Protein 1-Mediated Mitochondrial Mitotic Fission Permits Hyperproliferation of Vascular Smooth Muscle Cells and Offers a Novel Therapeutic Target in Pulmonary Hypertension." *Circulation Research* 110(11):1484–97.

Martinez-Arca, Sonia, Philipp Alberts, Ahmed Zahraoui, Daniel Louvard, and Thierry Galli. 2000. "Role of Tetanus Neurotoxin Insensitive Vesicle-Associated Membrane Protein (TI-VAMP) in Vesicular Transport Mediating Neurite Outgrowth." *Journal of Cell Biology* 149(4):889–99.

Martoglio, Bruno and Bernhard Dobberstein. 1998. "Signal Sequences: More than Just Greasy Peptides." *Trends in Cell Biology* 8(10):410–15.

Mathias, Sven et al. 2018. "Visualisation of Intracellular Production Bottlenecks in Suspension-Adapted CHO Cells Producing Complex Biopharmaceuticals Using Fluorescence Microscopy." *Journal of Biotechnology* 271:47–55.

Matsuoka, Ken et al. 1998. "COPII-Coated Vesicle Formation Reconstituted with Purified Coat Proteins and Chemically Defined Liposomes." *Cell* 93(2):263–75.

De Matteis, Maria Antonietta and Alberto Luini. 2008. "Exiting the Golgi Complex." *Nature Reviews Molecular Cell Biology* 9(4):273–84.

Mccolm, Juliet, Leijun Hu, Theresa Womack, Cheng Cai Tang, and Alan Y. Chiang. 2014. "Single- and Multiple-Dose Randomized Studies of Blosozumab, a Monoclonal Antibody against Sclerostin, in Healthy Postmenopausal Women." *Journal of Bone and Mineral Research* 29(4):935–43.

McLelland, Gian-Luca, Sydney A. Lee, Heidi M. McBride, and Edward A. Fon. 2016. "Syntaxin-17 Delivers PINK1/Parkin-Dependent Mitochondrial Vesicles to the Endolysosomal System." *The Journal of Cell Biology* 214(3):275–91.

McMahon, Harvey T. et al. 1993. "Cellubrevin Is a Ubiquitous Tetanus-Toxin Substrate Homologous to a Putative Synaptic Vesicle Fusion Protein." *Nature* 364(6435):346–49.

McNiven, Mark A., Hong Cao, Kelly R. Pitts, and Yisang Yoon. 2000. “The Dynamin Family of Mechanoenzymes: Pinching in New Places.” *Trends in Biochemical Sciences* 25(3):115–20.

Mead, Emma J. et al. 2012. “Experimental and in Silico Modelling Analyses of the Gene Expression Pathway for Recombinant Antibody and By-Product Production in NS0 Cell Lines.” *PloS One* 7(10):e47422.

Mellman, Ira and Graham Warren. 2000. “The Road Taken: Past and Future Foundations of Membrane Traffic.” *Cell* 100(1):99–112.

Mergulhão, F. J. M., D. K. Summers, and G. A. Monteiro. 2005. “Recombinant Protein Secretion in Escherichia Coli.” *Biotechnology Advances* 23(3):177–202.

Miyawaki, Atsushi, Asako Sawano, and Takako Kogure. 2003. “Lighting up Cells: Labelling Proteins with Fluorophores.” *Nature Cell Biology* Suppl(1):S1-7.

Mohan, Chaya, Yeon-Gu Kim, Jane Koo, and Gyun Min Lee. 2008. “Assessment of Cell Engineering Strategies for Improved Therapeutic Protein Production in CHO Cells.” *Biotechnology Journal* 3(5):624–30.

Mohan, Chaya and Gyun Min Lee. 2010. “Effect of Inducible Co-Overexpression of Protein Disulfide Isomerase and Endoplasmic Reticulum Oxidoreductase on the Specific Antibody Productivity of Recombinant Chinese Hamster Ovary Cells.” *Biotechnology and Bioengineering* 107(2):337–46.

Molino, Diana et al. 2015. “Role of Tetanus Neurotoxin Insensitive Vesicle-Associated Membrane Protein in Membrane Domains Transport and Homeostasis.” *Cellular Logistics* 5(1):e1025182.

Moreau, Kevin and David C. Rubinsztein. 2012. “The Plasma Membrane as a Control Center for Autophagy.” *Autophagy* 8(5):861–63.

Morel, Y. and R. Barouki. 1999. “Repression of Gene Expression by Oxidative Stress.” *The Biochemical Journal* 342 Pt 3:481–96.

Morelli, Elena et al. 2014. “Multiple Functions of the SNARE Protein Snap29 in Autophagy, Endocytic, and Exocytic Trafficking during Epithelial Formation in Drosophila.” *Autophagy* 10(12):2251–68.

Morelli, Elena et al. 2016. “An Essential Step of Kinetochore Formation Controlled by the SNARE Protein Snap29.” *The EMBO Journal* 1270(9):321–46.

Morrison, Chris and Riku Lähteenmäki. 2018. “Public Biotech in 2017 - The Numbers.” *Nature Biotechnology* 36(7):576–84.

Mossessova, Elena, Lincoln C. Bickford, and Jonathan Goldberg. 2003. “SNARE Selectivity of the COPII Coat.” *Cell* 114(4):483–95.

Mulukutla, Bhanu Chandra, Michael Gramer, and Wei Shou Hu. 2012. “On Metabolic Shift to Lactate Consumption in Fed-Batch Culture of Mammalian Cells.” *Metabolic Engineering* 14(2):138–49.

Muppirala, Madhavi, Vijay Gupta, and Ghanshyam Swarup. 2011. “Syntaxin 17 Cycles between the ER and ERGIC and Is Required to Maintain the Architecture of ERGIC and Golgi.” *Biology of the Cell* 103(7):333–50.

Muppirala, Madhavi, Vijay Gupta, and Ghanshyam Swarup. 2012. “Tyrosine Phosphorylation of a SNARE Protein, Syntaxin 17: Implications for Membrane Trafficking in the Early Secretory Pathway.” *Biochimica et Biophysica Acta - Molecular Cell Research* 1823(12):2109–19.

Murray, Rachael Z., Fiona G. Wylie, Tatiana Khromykh, David A. Hume, and Jennifer L. Stow. 2005. “Syntaxin 6 and Vti1b Form a Novel SNARE Complex, Which Is Up-Regulated in Activated Macrophages to Facilitate Exocytosis of Tumor Necrosis Factor-α.” *Journal of Biological*

Chemistry 280(11):10478–83.

Nakamura, Norihiro, Akitsugu Yamamoto, Yoh Wada, and Masamitsu Futai. 2000. "Syntaxin 7 Mediates Endocytic Trafficking to Late Endosomes." *Journal of Biological Chemistry* 275(9):6523–29.

Neubrand, Veronika E. et al. 2005. "γ-BAR, a Novel AP-1-Interacting Protein Involved in Post-Golgi Trafficking." *EMBO Journal* 24(6):1122–33.

Ni, Hong-Min, Jessica A. Williams, and Wen-Xing Ding. 2015. "Mitochondrial Dynamics and Mitochondrial Quality Control." *Redox Biology* 4:6–13.

Nicchitta, Christopher V. and Günter Blobel. 1993. "Lumenal Proteins of the Mammalian Endoplasmic Reticulum Are Required to Complete Protein Translocation." *Cell* 73(5):989–98.

Nicholson-Fish, Jessica C., Alexandros C. Kokotos, Thomas H. Gillingwater, Karen J. Smillie, and Michael A. Cousin. 2015. "VAMP4 Is an Essential Cargo Molecule for Activity-Dependent Bulk Endocytosis." *Neuron* 88(5):973–84.

Nogueira, Cristina et al. 2014. "SLY1 and Syntaxin 18 Specify a Distinct Pathway for Procollagen VII Export from the Endoplasmic Reticulum." *ELife* 2014(3):e02784.

Noh, Soo Min, Seunghyeon Shin, and Gyun Min Lee. 2018. "Comprehensive Characterization of Glutamine Synthetase-Mediated Selection for the Establishment of Recombinant CHO Cells Producing Monoclonal Antibodies." *Scientific Reports* 8(1):5361.

Nozawa, Takashi, Atsuko Minowa-Nozawa, Chihiro Aikawa, and Ichiro Nakagawa. 2017. "The STX6-VTI1B-VAMP3 Complex Facilitates Xenophagy by Regulating the Fusion between Recycling Endosomes and Autophagosomes." *Autophagy* 13(1):57–69.

Oishi, Yohei et al. 2006. "Role of VAMP-2, VAMP-7, and VAMP-8 in Constitutive Exocytosis from HSY Cells." *Histochemistry and Cell Biology* 125(3):273–81.

Okayama, Miki et al. 2012. "SNARE Proteins Are Not Excessive for the Formation of Post-Golgi SNARE Complexes in HeLa Cells." *Molecular and Cellular Biochemistry* 366(1–2):159–68.

Park, Hyo-Soon, Ik-Hwan Kim, Ick-Young Kim, Ki-Ho Kim, and Hong-Jin Kim. 2000. "Expression of Carbamoyl Phosphate Synthetase I and Ornithine Transcarbamoylase Genes in Chinese Hamster Ovary Dhfr -Cells Decreases Accumulation of Ammonium Ion in Culture Media." *Journal of Biotechnology* 81(2–3):129–40.

Parodi, Armando J., Nicolas H. Behrens, Luis F. Leloir, and Hector Carminatti. 1972. "The Role of Polyprenol-Bound Saccharides as Intermediates in Glycoprotein Synthesis in Liver." *Proceedings of the National Academy of Sciences of the United States of America* 69(11):3268–72.

Parrish, Amanda B., Christopher D. Freel, and Sally Kornbluth. 2013. "Cellular Mechanisms Controlling Caspase Activation and Function." *Cold Spring Harbor Perspectives in Biology* 5(6):a008672.

Paumet, F. et al. 2000. "Soluble NSF Attachment Protein Receptors (SNAREs) in RBL-2H3 Mast Cells: Functional Role of Syntaxin 4 in Exocytosis and Identification of a Vesicle-Associated Membrane Protein 8-Containing Secretory Compartment." *The Journal of Immunology* 164(11):5850–57.

Peng, Ren-Wang, Eric Abellan, and Martin Fussenegger. 2011. "Differential Effect of Exocytic SNAREs on the Production of Recombinant Proteins in Mammalian Cells." *Biotechnology and Bioengineering* 108(3):611–20.

Peng, Ren-Wang and Martin Fussenegger. 2009. "Molecular Engineering of Exocytic Vesicle Traffic

Enhances the Productivity of Chinese Hamster Ovary Cells." *Biotechnology and Bioengineering* 102(4):1170–81.

Peng, Ren-Wang, Claudio Guetg, Eric Abellan, and Martin Fussenegger. 2010. "Munc18b Regulates Core SNARE Complex Assembly and Constitutive Exocytosis by Interacting with the N-Peptide and the Closed-Conformation C-Terminus of Syntaxin 3." *The Biochemical Journal* 431(3):353–61.

Peng, Ren-Wang, Claudio Guetg, Marcel Tigges, and Martin Fussenegger. 2010. "The Vesicle-Trafficking Protein Munc18b Increases the Secretory Capacity of Mammalian Cells." *Metabolic Engineering* 12(1):18–25.

Peng, Renwang and Dieter Gallwitz. 2002. "Sly1 Protein Bound to Golgi Syntaxin Sed5p Allows Assembly and Contributes to Specificity of SNARE Fusion Complexes." *The Journal of Cell Biology* 157(4):645–55.

Pennock, G. D., C. Shoemaker, and L. K. Miller. 1984. "Strong and Regulated Expression of Escherichia Coli Beta-Galactosidase in Insect Cells with a Baculovirus Vector." *Molecular and Cellular Biology* 4(3):399–406.

Pereira, Sara, Helene Faustrup Kildegaard, and Mikael Rørdam Andersen. 2018. "Impact of CHO Metabolism on Cell Growth and Protein Production: An Overview of Toxic and Inhibiting Metabolites and Nutrients." *Biotechnology Journal* 13(3):1700499.

Polishchuk, Elena V., Alessio Di Pentima, Alberto Luini, and Roman S. Polishchuk. 2003. "Mechanism of Constitutive Export from the Golgi: Bulk Flow via the Formation, Protrusion, and En Bloc Cleavage of Large Trans -Golgi Network Tubular Domains." *Molecular Biology of the Cell* 14(11):4470–85.

Pols, Maaike S. et al. 2013. "HVps41 and VAMP7 Function in Direct TGN to Late Endosome Transport of Lysosomal Membrane Proteins." *Nature Communications* 4(May 2012):1312–61.

Prekeris, R., B. Yang, V. Oorschot, J. Klumperman, and R. H. Scheller. 1999. "Differential Roles of Syntaxin 7 and Syntaxin 8 in Endosomal Trafficking." *Molecular Biology of the Cell* 10(11):3891–3908.

Pryor, Paul R. et al. 2004. "Combinatorial SNARE Complexes with VAMP7 or VAMP8 Define Different Late Endocytic Fusion Events." *EMBO Reports* 5(6):590–95.

Puck, T. T. 1958. "GENETICS OF SOMATIC MAMMALIAN CELLS: III. LONG-TERM CULTIVATION OF EUPLOID CELLS FROM HUMAN AND ANIMAL SUBJECTS." *Journal of Experimental Medicine* 108(6):945–56.

Raetz, Christian R. H. and Chris Whitfield. 2002. "Lipopolysaccharide Endotoxins." *Annual Review of Biochemistry* 71:635–700.

Rajagopalan, P. T. Ravi et al. 2002. "Interaction of Dihydrofolate Reductase with Methotrexate: Ensemble and Single-Molecule Kinetics." *Proceedings of the National Academy of Sciences* 99(21):13481–86.

Ramirez, Denise M. O. and Ege T. Kavalali. 2012. "The Role of Non-Canonical SNAREs in Synaptic Vesicle Recycling." *Cellular Logistics* 2(1):20–27.

Rana, Anil et al. 2017. "Promoting Drp1-Mediated Mitochondrial Fission in Midlife Prolongs Healthy Lifespan of Drosophila Melanogaster." *Nature Communications* 8(1).

Rao, Swathi K., Chau Huynh, Veronique Proux-Gillardeaux, Thierry Galli, and Norma W. Andrews. 2004. "Identification of SNAREs Involved in Synaptotagmin VII-Regulated Lysosomal Exocytosis." *Journal of Biological Chemistry* 279(19):20471–79.

Rapaport, Debora, Yevgenia Lugassy, Eli Sprecher, and Mia Horowitz. 2010. “Loss of SNAP29 Impairs Endocytic Recycling and Cell Motility” edited by N. A. Hotchin. *PLoS ONE* 5(3):e9759.

Reid, Ian R. 2017. “Targeting Sclerostin in Postmenopausal Osteoporosis: Focus on Romosozumab and Blosozumab.” *BioDrugs* 31(4):289–97.

Rein, Ulrike, Uwe Andag, Rainer Duden, Hans Dieter Schmitt, and Anne Spang. 2002. “ARF-GAP–mediated Interaction between the ER-Golgi v-SNAREs and the COPI Coat.” *The Journal of Cell Biology* 157(3):395–404.

Reinhart, David et al. 2018. “Bioprocessing of Recombinant CHO-K1, CHO-DG44, and CHO-S: CHO Expression Hosts Favor Either MAb Production or Biomass Synthesis.” *Biotechnology Journal* 1700686:1700686.

Reinhart, David, Lukas Damjanovic, Christian Kaisermayer, and Renate Kunert. 2015. “Benchmarking of Commercially Available CHO Cell Culture Media for Antibody Production.” *Applied Microbiology and Biotechnology* 99(11):4645–57.

Riethoven, Jean-Jack M. 2010. “Regulatory Regions in DNA: Promoters, Enhancers, Silencers, and Insulators.” Pp. 33–42 in.

Ritacco, Frank V., Yongqi Wu, and Anurag Khetan. 2018. “Cell Culture Media for Recombinant Protein Expression in Chinese Hamster Ovary (CHO) Cells: History, Key Components, and Optimization Strategies.” *Biotechnology Progress*.

Rizo, Josep and Thomas C. Südhof. 2002. “Snares and Munc18 in Synaptic Vesicle Fusion.” *Nature Reviews Neuroscience* 3(8):641–53.

Rüdiger, S., A. Buchberger, and B. Bukau. 1997. “Interaction of Hsp70 Chaperones with Substrates.” *Nature Structural Biology* 4(5):342–49.

RunningDeer, J. and DS Allison. 2004. “High-Level Expression of Proteins in Mammalian Cells Using Transcription Regulatory Sequences from the Chinese Hamster EF-1α Gene.” *Biotechnology Progress* 20(3):880–89.

Schröder, Martin and Randal J. Kaufman. 2005. “THE MAMMALIAN UNFOLDED PROTEIN RESPONSE.” *Annual Review of Biochemistry* 74(1):739–89.

Scott, Lesley J. 2014. “Etanercept: A Review of Its Use in Autoimmune Inflammatory Diseases.” *Drugs* 74(12):1379–1410.

Shaffer, A. L. et al. 2004. “XBP1, Downstream of Blimp-1, Expands the Secretory Apparatus and Other Organelles, and Increases Protein Synthesis in Plasma Cell Differentiation.” *Immunity* 21(1):81–93.

Shearwin, K., B. Callen, and J. Egan. 2005. “Transcriptional Interference – a Crash Course.” *Trends in Genetics* 21(6):339–45.

Shibutani, Shusaku T. and Tamotsu Yoshimori. 2014. “A Current Perspective of Autophagosome Biogenesis.” *Cell Research* 24(1):58–68.

Shitara, Akiko et al. 2013. “VAMP4 Is Required to Maintain the Ribbon Structure of the Golgi Apparatus.” *Molecular and Cellular Biochemistry* 380(1–2):11–21.

Shridhar, Smriti et al. 2017. “Transcriptomic Changes in CHO Cells after Adaptation to Suspension Growth in Protein-Free Medium Analysed by a Species-Specific Microarray.” *Journal of Biotechnology* 257:13–21.

Simpson, Jeremy C. 2009. “Screening the Secretion Machinery: High Throughput Imaging Approaches to Elucidate the Secretory Pathway.” *Seminars in Cell & Developmental Biology*

20(8):903–9.

Singh, Anupam, Vaibhav Upadhyay, Arun Kumar Upadhyay, Surinder Mohan Singh, and Amulya Kumar Panda. 2015. “Protein Recovery from Inclusion Bodies of Escherichia Coli Using Mild Solubilization Process.” *Microbial Cell Factories* 14(1):41.

Skalski, Michael and Marc G. Coppolino. 2005. “SNARE-Mediated Trafficking of A5β1 Integrin Is Required for Spreading in CHO Cells.” *Biochemical and Biophysical Research Communications* 335(4):1199–1210.

Spinelli, Jessica B. et al. 2017. “Metabolic Recycling of Ammonia via Glutamate Dehydrogenase Supports Breast Cancer Biomass.” *Science* 358(6365):941–46.

Sprecher, Eli et al. 2005. “A Mutation in SNAP29, Coding for a SNARE Protein Involved in Intracellular Trafficking, Causes a Novel Neurocutaneous Syndrome Characterized by Cerebral Dysgenesis, Neuropathy, Ichthyosis, and Palmoplantar Keratoderma.” *The American Journal of Human Genetics* 77(2):242–51.

Steegmaier, M. et al. 1998. “Three Novel Proteins of the Syntaxin/SNAP-25 Family.” *The Journal of Biological Chemistry* 273(51):34171–79.

Steegmaier, M., Viola Oorschot, Judith Klumperman, and Richard H. Scheller. 2000. “Syntaxin 17 Is Abundant in Steroidogenic Cells and Implicated in Smooth Endoplasmic Reticulum Membrane Dynamics” edited by R. W. Schekman. *Molecular Biology of the Cell* 11(8):2719–31.

Stepanenko, Aleksei A. and Henry H. Heng. 2017. “Transient and Stable Vector Transfection: Pitfalls, off-Target Effects, Artifacts.” *Mutation Research - Reviews in Mutation Research* 773:91–103.

Su, Q., S. Mochida, J. H. Tian, R. Mehta, and Z. H. Sheng. 2001. “SNAP-29: A General SNARE Protein That Inhibits SNARE Disassembly and Is Implicated in Synaptic Transmission.” *Proceedings of the National Academy of Sciences* 98(24):14038–43.

Sung, Yun Hee, Jae Seong Lee, Soon Hye Park, Jane Koo, and Gyun Min Lee. 2007. “Influence of Co-down-Regulation of Caspase-3 and Caspase-7 by SiRNAs on Sodium Butyrate-Induced Apoptotic Cell Death of Chinese Hamster Ovary Cells Producing Thrombopoietin.” *Metabolic Engineering* 9(5–6):452–64.

Szul, Tomasz and Elizabeth Sztul. 2011. “COPII and COPI Traffic at the ER-Golgi Interface.” *Physiology* 26(5):348–64.

Tabuchi, Hisahiro, Tomoya Sugiyama, Saeko Tanaka, and Satoshi Tainaka. 2010. “Overexpression of Taurine Transporter in Chinese Hamster Ovary Cells Can Enhance Cell Viability and Product Yield, While Promoting Glutamine Consumption.” *Biotechnology and Bioengineering* 107(6):998–1003.

Takáts, Szabolcs et al. 2018. “Non-Canonical Role of the SNARE Protein Ykt6 in Autophagosome-Lysosome Fusion.” *PLoS Genetics* 14(4):1–23.

Takáts, Szabolcs and Gábor Juhász. 2013. “A Genetic Model with Specifically Impaired Autophagosome-Lysosome Fusion.” *Autophagy* 9(8):1251–52.

Teh, Ser Huy, Mun Yik Fong, and Zulqarnain Mohamed. 2011. “Expression and Analysis of the Glycosylation Properties of Recombinant Human Erythropoietin Expressed in Pichia Pastoris.” *Genetics and Molecular Biology* 34(3):464–70.

Tey, B. T., R. P. Singh, Lucia Piredda, M. Piacentini, and M. Al-Rubeai. 2000. “Influence of Bcl-2 on Cell Death during the Cultivation of a Chinese Hamster Ovary Cell Line Expressing a Chimeric Antibody.” *Biotechnology and Bioengineering* 68(1):31–43.

Thorn, Peter and Herbert Gaisano. 2012. “Molecular Control of Compound Exocytosis: A Key Role for

VAMP8." *Communicative & Integrative Biology* 5(1):61–63.

Tigges, Marcel and Martin Fussenegger. 2006. "Xbp1-Based Engineering of Secretory Capacity Enhances the Productivity of Chinese Hamster Ovary Cells." *Metabolic Engineering* 8(3):264–72.

Tran, T. H. T., Q. Zeng, and W. Hong. 2007. "VAMP4 Cycles from the Cell Surface to the Trans-Golgi Network via Sorting and Recycling Endosomes." *Journal of Cell Science* 120(6):1028–41.

Trexler-Schmidt, Melody et al. 2010. "Identification and Prevention of Antibody Disulfide Bond Reduction during Cell Culture Manufacturing." *Biotechnology and Bioengineering* 106(3):452–61.

Tsien, Roger Y. 1998. "The Green Fluorescent." *Proteins* 67(11):509–44.

Twig, Gilad et al. 2008. "Fission and Selective Fusion Govern Mitochondrial Segregation and Elimination by Autophagy." *EMBO Journal* 27(2):433–46.

Urlaub, Gail, Emmanuel Käs, Adelaide M. Carothers, and Lawerence A. Chasin. 1983. "Deletion of the Diploid Dihydrofolate Reductase Locus from Cultured Mammalian Cells." *Cell* 33(2):405–12.

Vidarsson, Gestur, Gillian Dekkers, and Theo Rispens. 2014. "IgG Subclasses and Allotypes: From Structure to Effector Functions." *Frontiers in Immunology* 5(OCT):1–17.

Walsh, Gary. 2014. "Biopharmaceutical Benchmarks 2014." *Nature Biotechnology* 32(10).

Walsh, Gary and Roy Jefferis. 2006. "Post-Translational Modifications in the Context of Therapeutic Proteins." *Nature Biotechnology* 24(10):1241–52.

Walter, Peter and Günter Blobel. 1982. "Signal Recognition Particle Contains a 7S RNA Essential for Protein Translocation across the Endoplasmic Reticulum." *Nature* 299(5885):691–98.

Wang, Cheng-Chun et al. 2007. "VAMP8/Endobrevin as a General Vesicular SNARE for Regulated Exocytosis of the Exocrine System" edited by V. Malhotra. *Molecular Biology of the Cell* 18(3):1056–63.

Wang, Cheng Chun et al. 2004. "A Role of VAMP8/Endobrevin in Regulated Exocytosis of Pancreatic Acinar Cells." *Developmental Cell* 7(3):359–71.

Wang, Xiaoyin et al. 2017. "The EF-1α Promoter Maintains High-Level Transgene Expression from Episomal Vectors in Transfected CHO-K1 Cells." *Journal of Cellular and Molecular Medicine* 21(11):3044–54.

Wang, Yun, Irina Dulubova, Josep Rizo, and Thomas C. Südhof. 2001. "Functional Analysis of Conserved Structural Elements in Yeast Syntaxin Vam3p." *Journal of Biological Chemistry* 276(30):28598–605.

Ward, D. M., J. Pevsner, M. A. Scullion, M. Vaughn, and J. Kaplan. 2000. "Syntaxin 7 and VAMP-7 Are Soluble N-Ethylmaleimide-Sensitive Factor Attachment Protein Receptors Required for Late Endosome-Lysosome and Homotypic Lysosome Fusion in Alveolar Macrophages." *Molecular Biology of the Cell* 11(7):2327–33.

Westers, Lidia, Helga Westers, and Wim J. Quax. 2004. "Bacillus Subtilis as Cell Factory for Pharmaceutical Proteins: A Biotechnological Approach to Optimize the Host Organism." *Biochimica et Biophysica Acta - Molecular Cell Research* 1694(1–3 SPEC.ISS.):299–310.

Westoby, Matthew, James Chrostowski, Philippe de Vilmorin, John Paul Smelko, and Jonathan K. Romero. 2011. "Effects of Solution Environment on Mammalian Cell Fermentation Broth Properties: Enhanced Impurity Removal and Clarification Performance." *Biotechnology and Bioengineering* 108(1):50–58.

Wickner, William and Randy Schekman. 2005. “Protein Translocation across Biological Membranes.” *Science (New York, N.Y.)* 310(5753):1452–56.

Wildt, Stefan and Tilllman U. Gerngross. 2005. “The Humanization of N-Glycosylation Pathways in Yeast.” *Nature Reviews Microbiology* 3(2):119–28.

Williams, C. M. et al. 2016. “Identification of Roles for the SNARE-Associated Protein, SNAP29, in Mouse Platelets.” *Platelets* 27(4):286–94.

Wong, S. H. et al. 1998. “Endobrevin, a Novel Synaptobrevin/VAMP-like Protein Preferentially Associated with the Early Endosome.” *Molecular Biology of the Cell* 9(June):1549–63.

Wong, Siew Heng, Yue Xu, Tao Zhang, and Wanjin Hong. 1998. “Syntaxin 7, a Novel Syntaxin Member Associated with the Early Endosomal Compartment.” *Journal of Biological Chemistry* 273(1):375–80.

Wurm, Florian M. 2004. “Production of Recombinant Protein Therapeutics in Cultivated Mammalian Cells.” *Nature Biotechnology* 22(11):1393–98.

Xia, Wei et al. 2006. “High Levels of Protein Expression Using Different Mammalian CMV Promoters in Several Cell Lines.” *Protein Expression and Purification* 45(1):115–24.

Xie, Liangzhi, Weichang Zhou, and David Robinson. 2003. “Gene Transfer and Expression in Mammalian Cells.” *New Comprehensive Biochemistry* 38:605–23.

Xu, Chunyan, Beatrice Bailly-Maitre, and John C. Reed. 2005. “Endoplasmic Reticulum Stress: Cell Life and Death Decisions.” *The Journal of Clinical Investigation* 115(10):2656–64.

Yamane-Ohnuki, Naoko et al. 2004. “Establishment of FUT8 Knockout Chinese Hamster Ovary Cells: An Ideal Host Cell Line for Producing Completely Defucosylated Antibodies with Enhanced Antibody-Dependent Cellular Cytotoxicity.” *Biotechnology and Bioengineering* 87(5):614–22.

Yamane-Ohnuki, Naoko and Mitsuo Satoh. 2009. “Production of Therapeutic Antibodies with Controlled Fucosylation.” *MAbs* 1(3):230–36.

Yang, Zhang et al. 2015. “Engineered CHO Cells for Production of Diverse, Homogeneous Glycoproteins.” *Nature Biotechnology* 33(8):842–44.

Yeaman, Charles et al. 1997. “The O-Glycosylated Stalk Domain Is Required for Apical Sorting of Neurotrophin Receptors in Polarized MDCK Cells.” *Journal of Cell Biology* 139(4):929–40.

Yip, Shirley S. M. et al. 2014. “Complete Knockout of the Lactate Dehydrogenase A Gene Is Lethal in Pyruvate Dehydrogenase Kinase 1, 2, 3 down-Regulated CHO Cells.” *Molecular Biotechnology* 56(9):833–38.

Yoshida, Hiderou, Toshie Matsui, Akira Yamamoto, Tetsuya Okada, and Kazutoshi Mori. 2001. “XBP1 MRNA Is Induced by ATF6 and Spliced by IRE1 in Response to ER Stress to Produce a Highly Active Transcription Factor.” *Cell* 107(7):881–91.

Youle, Richard J. and Alexander M. van der Bliek. 2012. “Mitochondrial Fission, Fusion, and Stress.” *Science (New York, N.Y.)* 337(6098):1062–65.

Yu, Kai, Chengcheng Liu, Byung Gee Kim, and Dong Yup Lee. 2015. “Synthetic Fusion Protein Design and Applications.” *Biotechnology Advances* 33(1):155–64.

Yun, Chee Yong et al. 2007. “Specific Inhibition of Caspase-8 and -9 in CHO Cells Enhances Cell Viability in Batch and Fed-Batch Cultures.” *Metabolic Engineering* 9(5–6):406–18.

Zeng, Qi, Thi Ton Hoai Tran, Hui Xian Tan, and Wanjin Hong. 2003. “The Cytoplasmic Domain of Vamp4 and Vamp5 Is Responsible for Their Correct Subcellular Targeting: The N-Terminal

Extension of Vamp4 Contains a Dominant Autonomous Targeting Signal for the Trans-Golgi Network." *Journal of Biological Chemistry* 278(25):23046–54.

Zhang, Fang, Xiangming Sun, Xiaoping Yi, and Yuanxing Zhang. 2006. "Metabolic Characteristics of Recombinant Chinese Hamster Ovary Cells Expressing Glutamine Synthetase in Presence and Absence of Glutamine." *Cytotechnology* 51(1):21–28.

Zhang, Lei, Qixin Leng, and A. James Mixson. 2005. "Alteration in the IL-2 Signal Peptide Affects Secretion of Proteinsin Vitro Andin Vivo." *The Journal of Gene Medicine* 7(3):354–65.

Zhang, Qian, Jiang Li, Michael Deavers, James L. Abbruzzese, and Linus Ho. 2005. "The Subcellular Localization of Syntaxin 17 Varies among Different Cell Types and Is Altered in Some Malignant Cells." *Journal of Histochemistry and Cytochemistry* 53(11):1371–82.

Zimmermann, Richard, Susanne Eyrisch, Mazen Ahmad, and Volkhard Helms. 2011. "Protein Translocation across the ER Membrane." *Biochimica et Biophysica Acta (BBA) - Biomembranes* 1808(3):912–24.

Zustiak, Matthew P., Judith K. Pollack, Mark R. Marten, and Michael J. Betenbaugh. 2008. "Feast or Famine: Autophagy Control and Engineering in Eukaryotic Cell Culture." *Current Opinion in Biotechnology* 19(5):518–26.

Appendices

Appendix 1. PCR primers

Name	Sequence	length of amplified fragment(bp)	Fragment details	Tm (^{0}C)
Forward HC Adalimumab	ATA CTTAAG ATGGAGTTTGGGCTGAGCTGGG (spacer, AflII)	1424	Adalimumab heavy chain gene	61.9
Backward HC Adalimumab	TAT GGATCC TCAGCCGGGGCT (spacer, BamHI)			62.7
Forward LC Adalimumab	ATA GAATTC ATG GAC ATG AGG GTC CCT GCT CAG (spacer, EcoRI)	730	Adalimumab light chain gene	62.5
Backward LC Adalimumab	TAT GGATCC TCAGCACTCGCCCCGGTT (spacer, BamHI)			62.5
Forward CMV	ATA TTCGAA GACATTGATTATTGACTAGTTATTAATAGTAATCAATTACGGGG (spacer, BstBI)	615	CMV promoter sequence	58.4
Backward CMV	TAT ACGCGT TATATA CACGTG AGCTCTGCTTATATAGACCTCCCACC (spacer, PmlI, MluI)			59.2
Forward bGH	ATA CACGTG TATATA GCGGCCGC CTGTGCCTTCTAGTTGCCAGCC (spacer, PmlI, NotI)	258	bGH poly A seuqnce	60.5
Backward bGH	TAT ACGCGT CCATAGAGCCCACCGCATCC (spacer, MluI)			60.5
Forward STX7	ATA CACGTG ATGTCTTACACTCCAGGAGTTGGTGG (spacer, PmlI)	807	STX7 gene sequence	60
Backward STX7	TAT GCGGCCGC TCAGTGGTTCAATCCCCATATGATGAGACT (spacer, NotI)			60.5
Forward STX17	ATA CACGTG ATGTCTGAAGATGAAGAAAAAGTGAAATTACGCCG (spacer, PmlI)	930	STX17 gene sequence	60.4
Backward STX17	TAT GCGGCCG CTTAACTGCATTTCTTGTCAGTTTGGCTGG (spacer, NotI)			61.4
Forward STX18	ATA CACGTG ATGGCGGTGGACATCACGC (spacer, PmlI)	1029	STX18 gene sequence	61
Backward STX18	TAT GCGGCCGC CTAGCTGTCGTACCAGTCGAGGAAG (spacer, NotI)			60
Forward SNAP29	ATA CACGTG ATGTCAGCTTACCCTAAAAGCTACAATCCG (spacer, PmlI)	798	SNAP29 gene sequence	60
Backward SNAP29	TAT GCGGCCGC TCAGAGTTGTCGAACTTTTCTTTCTGTGCT (spacer, NotI)			59.9
Forward GFP	ATA CACGTG ATGGTGAGCAAGGGCGAGGA (spacer, PmlI)	741	eGFP gene sequence	61.4
Backward GFP	TAT GCGGCCGC TTACTTGTACAGCTCGTCCATGCCG (spacer, NotI)			60.7

Appendix 2. Vectors maps

For the different inserted sequences, several elements are highlighted; yellow for the restriction sites used, green for the eGFP sequence, purple for the linker sequence of the different fusion proteins and blue for the sequence of interest (gene, promoter or polyA tail).

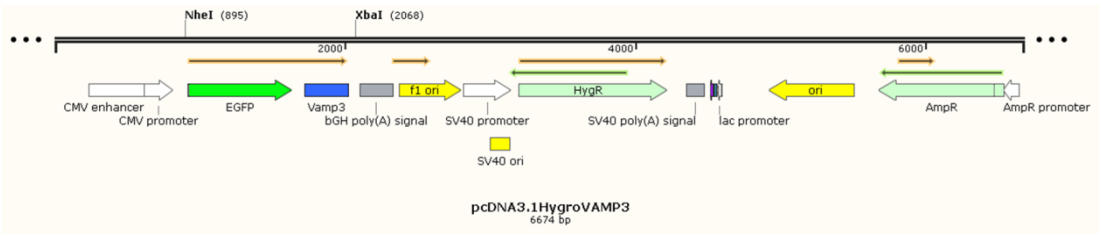

Sequence inserted pcDNA3.1Hygro/VAMP3 using NheI and XbaI restriction sites

Gctagcgctaccggtcgccaccatggtgagcaagggcgaggagctgttcaccggggtggtgcccatcctggtcgagctggacggcgacgtaaa
cggccacaagttcagcgtgtccggcgagggcgagggcgatgccacctacggcaagctgaccctgaagttcatctgcaccaccggcaagctgcc
cgtgccctggcccaccctcgtgaccaccctgacctacggcgtgcagtgcttcagccgctaccccgaccacatgaagcagcacgacttcttcaagt
ccgccatgcccgaaggctacgtccaggagcgcaccatcttcttcaaggacgacggcaactacaagacccgcgccgaggtgaagttcgagggcg
acaccctggtgaaccgcatcgagctgaagggcatcgacttcaaggaggacggcaacatcctggggcacaagctggagtacaactacaacagc
cacaacgtctatatcatggccgacaagcagaagaacggcatcaaggtgaacttcaagatccgccacaacatcgaggacggcagcgtgcagctc
gccgaccactaccagcagaacaccccatcggcgacggccccgtgctgctgcccgacaaccactacctgagcacccagtccgccctgagcaaa
gaccccaacgagaagcgcgatcacatggtcctgctggagttcgtgaccgccgccgggatcactctcggcatggacgagctgtacaagtactcag
atctcgagctcaagcttcgaattctgcagtcgacggtaccgagctcggatccactagtccagtgtggtggaattgcccttatgtctacaggtccaa
ctgctgccactggcagtaatcgaagacttcagcagacacaaaatcaagtagatgaggtggtggacataatgcgagttaacgtggacaaggttct
ggaaagagaccagaagctctctgagttagacgaccgtgcagacgcactgcaggcaggcgcttctcaatttgaaacgagcgcagccaagttgaa
gaggaaatattggtggaagaattgcaagatgtgggcaatcgggattactgttctggttatcttcatcatcatcatcatcgtgtgggttgtctcttcat
gaaagggcaattctgcagatatccagcacagtggcggccgctcgagttctaga

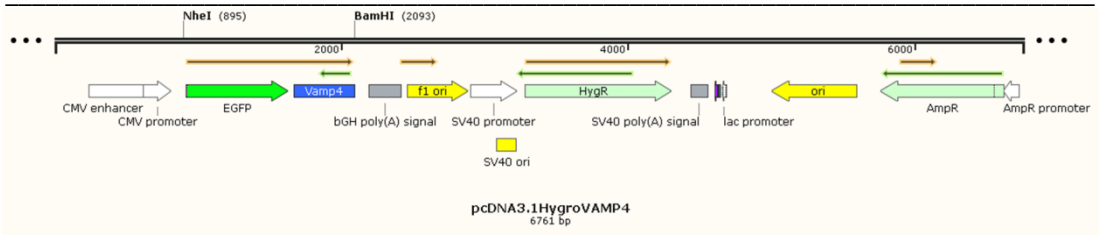

Sequence inserted in pcDNA3.1Hygro/VAMP4 using NheI and BamHI restriction sites

Gctagcgctaccggtcgccaccatggtgagcaagggcgaggagctgttcaccggggtggtgcccatcctggtcgagctggacggcgacgtaaa
cggccacaagttcagcgtgtccggcgagggcgagggcgatgccacctacggcaagctgaccctgaagttcatctgcaccaccggcaagctgcc
cgtgccctggcccaccctcgtgaccaccctgacctacggcgtgcagtgcttcagccgctaccccgaccacatgaagcagcacgacttcttcaagt
ccgccatgcccgaaggctacgtccaggagcgcaccatcttcttcaaggacgacggcaactacaagacccgcgccgaggtgaagttcgagggcg
acaccctggtgaaccgcatcgagctgaagggcatcgacttcaaggaggacggcaacatcctggggcacaagctggagtacaactacaacagc
cacaacgtctatatcatggccgacaagcagaagaacggcatcaaggtgaacttcaagatccgccacaacatcgaggacggcagcgtgcagctc
gccgaccactaccagcagaacaccccatcggcgacggccccgtgctgctgcccgacaaccactacctgagcacccagtccgccctgagcaaa
gaccccaacgagaagcgcgatcacatggtcctgctggagttcgtgaccgccgccgggatcactctcggcatggacgagctgtacaagtactcag
atctcgagctcaagcttcgaattctgatgcctcccaagtttaagcgccacctcaatgatgatgatgtcacaggttctgtgaaaagtgaaaggaga
aatcttttggaagatgattcagatgaagaagaggacttttttctaaggggaccatctggaccaagatttggacctagaaatgataaaattaagca
tgttcagaatcaagtggatgaagttattgatgtcatgcaagaaaatattacaaaggtaattgagagaggggagagactagatgaactacagga
caaatcagaaagcttatcggataatgcaacagcttttagcaacagatccaaacaacttcgaaggcaaatgtggtggcgtggatgcaaaataaa
agccatcatggctttggttgctgctatccttttgctagtgattatcattcttatagtcatgaaataccgtacttgaggatcc

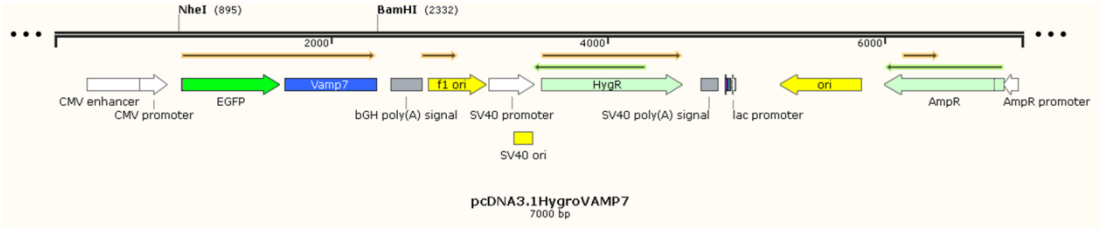

Sequence inserted in pcDNA3.1Hygro/VAMP7 using NheI and BamHI

gctagcgctaccggtcgccaccatggtgagcaagggcgaggagctgttcaccggggtggtgcccatcctggtcgagctggacggcgacgtaaa
cggccacaagttcagcgtgtccggcgagggcgagggcgatgccacctacggcaagctgaccctgaagttcatctgcaccaccggcaagctgcc
cgtgccctggcccaccctcgtgaccaccctgacctacggcgtgcagtgcttcagccgctaccccgaccacatgaagcagcacgacttcttcaagt
ccgccatgcccgaaggctacgtccaggagcgcaccatcttcttcaaggacgacggcaactacaagacccgcgccgaggtgaagttcgagggcg
acaccctggtgaaccgcatcgagctgaagggcatcgacttcaaggaggacggcaacatcctggggcacaagctggagtacaactacaacagc
cacaacgtctatatcatggccgacaagcagaagaacggcatcaaggtgaacttcaagatccgccacaacatcgaggacggcagcgtgcagctc
gccgaccactaccagcagaacaccccatcggcgacggccccgtgctgctgcccgacaaccactacctgagcacccagtccgccctgagcaaa
gaccccaacgagaagcgcgatcacatggtcctgctggagttcgtgaccgccgccgggatcactctcggcatggacgagctgtacaagtactcag
atctcgagctcaagcttcgaattctgatggcgattcttttgctgttgttgccaggggaccactatccttgccaaacatgcttggtgtggaggaaa
cttcctggaggtgacagagcagattctggctaagataccttctgaaaataacaaactaacgtactcacatggcaattatttgtttcattacatctgc
caagacaggattgtatatctttgtatcactgatgatgattttgaacgttcccgagccttaattttctgaatgagataaagaagaggttccagacta
cttacggttcaagagcacagacagcacttccatatgccatgaatagcgagttctcaagtgtcttagctgcacagctgaagcatcactctgagaat
aagggcctagacaaagtgatggagactcaagcccaagtggatgaactgaaaggaatcatggtcagaaacatagatctggtagctcagcgagg
agaaagattggaattattgattgacaaaacagaaaatcttgtggattcttctgtcaccttcaaaactaccagcagaaatcttgctcgagccatgtg
tatgaagaacctcaagctcactattatcatcatcatcgtatcaattgtgttcatctatatcattgtttcacctctctgtggtggatttacatggccaag
ctgtgtgaagaaatagcgggatcc

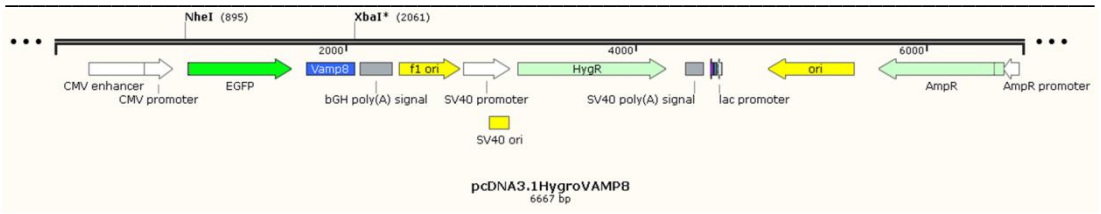

Sequence inserted in pcDNA3.1Hygro/VAMP8 using NheI and XbaI restriction sites

gctagcgctaccggtcgccaccatggtgagcaagggcgaggagctgttcaccggggtggtgcccatcctggtcgagctggacggcgacgtaaa
cggccacaagttcagcgtgtccggcgagggcgagggcgatgccacctacggcaagctgaccctgaagttcatctgcaccaccggcaagctgcc
cgtgccctggcccaccctcgtgaccaccctgacctacggcgtgcagtgcttcagccgctaccccgaccacatgaagcagcacgacttcttcaagt
ccgccatgcccgaaggctacgtccaggagcgcaccatcttcttcaaggacgacggcaactacaagacccgcgccgaggtgaagttcgagggcg
acaccctggtgaaccgcatcgagctgaagggcatcgacttcaaggaggacggcaacatcctggggcacaagctggagtacaactacaacagc
cacaacgtctatatcatggccgacaagcagaagaacggcatcaaggtgaacttcaagatccgccacaacatcgaggacggcagcgtgcagctc
gccgaccactaccagcagaacaccccatcggcgacggccccgtgctgctgcccgacaaccactacctgagcacccagtccgccctgagcaaa
gaccccaacgagaagcgcgatcacatggtcctgctggagttcgtgaccgccgccgggatcactctcggcatggacgagctgtacaagtactcag
atctcgagctcaagcttcgaattctgcagtcgacggtaccgagctcggatccactagtaacggccgccagtgtgctggaattcgcccttatggag
gaagccagtgaaggtggaggaaatgatcgtgtgcggaacctgcaaagtgaggtggagggagttaagaatattatgacccagaatgtggagcg
gatcctggcccgggggaaaacttggaacatctccgcaacaagacagaggatctggaagccacatctgagcacttcaagacgacatcgcaga
aggtggctcgaaaattctggtggaagaacgtgaagatgattgtccttatctgcgtgattgtttttatcatcatcctcttcattgtgctctttgccactg
gtgccttctcaagggcgaattctgcagatgggatccaccggatctaga

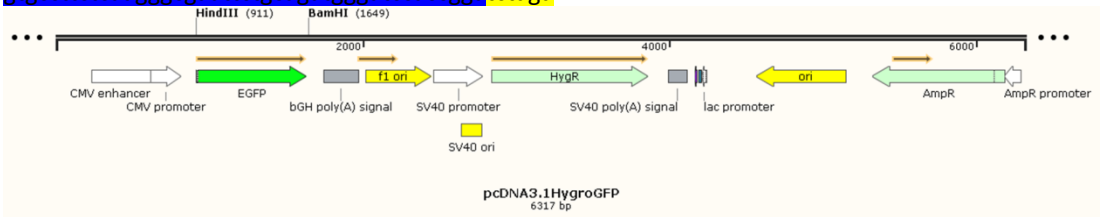

Sequence inserted in pcDNA3.1Hygro/GFP using HindIII and BamHI restriction sites

Aagcttatggtgagcaagggcgaggagctgttcaccggggtggtgcccatcctggtcgagctggacggcgacgtaaacggccacaagttcagc
gtgtccggcgagggcgagggcgatgccacctacggcaagctgaccctgaagttcatctgcaccaccggcaagctgcccgtgccctggcccaccc
tcgtgaccaccctgacctacggcgtgcagtgcttcagccgctaccccgaccacatgaagcagcacgacttcttcaagtccgccatgcccgaaggc
tacgtccaggagcgcaccatcttcttcaaggacgacggcaactacaagacccgcgccgaggtgaagttcgagggcgacaccctggtgaaccgc

atcgagctgaagggcatcgacttcaaggaggacggcaacatcctggggcacaagctggagtacaactacaacagccacaacgtctatatcatg
gccgacaagcagaagaacggcatcaaggtgaacttcaagatccgccataacatcgaggacggcagcgtgcagctcgccgaccactaccagca
gaacacccccatcggcgacggccccgtgctgctgcccgacaaccactacctgagcacccagtccgccctgagcaaagaccccaacgagaagcg
cgatcacatggtcctgctggagttcgtgaccgccgccgggatcactctcggcatggacgagctgtacaagtaaggtaccgagctcggatcc

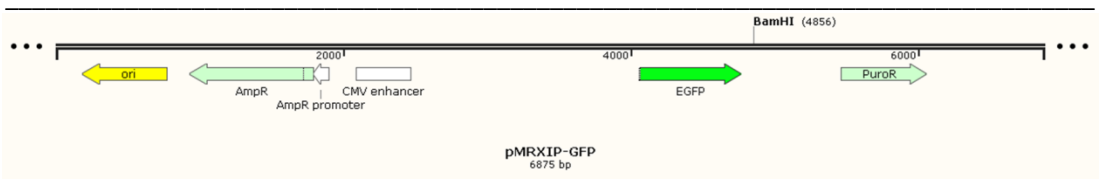

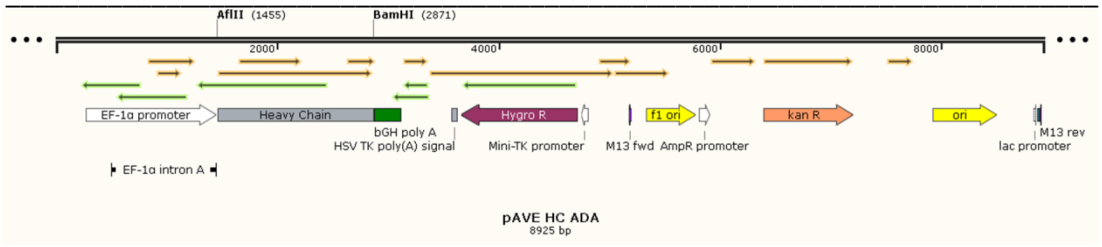

Sequence inserted in pAVE HC ADA using AflII and BamHI restriction sites

cttaagatggagtttgggctgagctgggttttcctcgttgctcttttagaggtgtccagtgtgaagtgcagctggtggaatccggcggaggcctgg
tgcagcctggcagatctctgagactgtcctgtgccgcctccggcttcaccttcgacgactacgctatgcactgggtgcgacaggccctggcaag
ggactggaatgggtgtccgccatcacctggaactccggccacatcgactacgccgactctgtggaaggccggttcaccatctctcgggacaacg
ccaagaactccctgtacctgcagatgaacagcctgcgggccgaggacaccgccgtgtactactgtgccaaggtgtcctacctgtccaccgcctcc
tccctggattattggggccagggcaccctcgtgaccgtgtcctctgcttctaccaagggcccctccgtgttccctctggccccttccagcaagtcta
cctctggcggaaccgccgctctgggctgcctcgtgaaggactacttccccgagcccgtgacagtgtcttggaactctggcgccctgacctccggcg
tgcacaccttttccagctgtgctgcagtcctccggcctgtactccctgtcctccgtcgtgactgtgccctccagctctctgggcacccagacctacatc
tgcaacgtgaaccacaagccctccaacaccaaggtggacaagaaggtggaacccaagtcctgcgacaagacccacacctgtccccttgtcct
gcccctgaactgctgggcggacccagcgtgttcctgttcccccaaagcccaaggacaccctgatgatctccccggacccccgaagtgacctgcgt
ggtggtggatgtgtcccacgaggaccctgaagtgaagttcaattggtacgtggacggcgtggaagtgcacaatgccaagaccaagcctagaga
ggaacagtacaactccacctaccgggtggtgtccgtgctgaccgtgctgcatcaggactggctgaacggcaaagagtacaagtgcaaagtgtcc
aacaaggccctgcctgcccccatcgaaaagaccatctccaaggccaagggccagccccgggaaccccaggtgtacacactgcccccctagcagg
gacgagctgaccaagaaccaggtgtccctgacatgcctcgtgaaaggcttctacccctccgatatcgccgtggaatgggagagcaacggccag
cccgagaacaactacaagaccacccccctgtgctggactccgacggctcattcttcctgtacagcaagctgacagtggacaagtcccggtggc
agcagggcaacgtgttctcctgctccgtgatgcacgaggccctgcacaaccactacacccagaagtccctgtccctgagccccggctgaggatcc

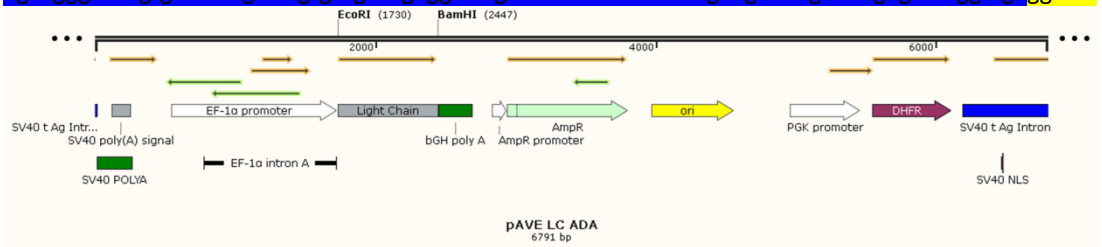

Sequence inserted in pAVE LC ADA using EcoRI and BamHI restriction sites

Gaattcatggacatgagggtccctgctcagctcctggggctcctgctgctctggctctcaggtgccagatgtgacatccagatgacccagtccccc
tccagcctgtctgcctctgtgggcgacagagtgaccatcacctgtcgggcctcccagggcatcagaaactacctggcctggtatcagcagaagcc
cggcaaggccccaagctgctgatctacgctgcctccacactgcagtccggcgtgccctctagattctccggctctggctctggcaccgactttac
cctgaccatcagctccctgcagcccgaggatgtggccacctactactgccagcggtacaacagagccccctacacctttggccagggcaccaag
gtggaaatcaagcggaccgtggccgctccctccgtgttcatcttcccaccttccgacgagcagctgaagtccggcaccgcttctgtcgtgtgcctg
ctgaacaacttctacccccgcgaggccaaggtgcagtggaaggtggacaacgccctgcagagcggcaactcccaggaatccgtgaccgagca
ggactccaaggacagcacctactccctgtcctccaccctgaccctgtccaaggccgactacgagaagcacaaggtgtacgcctgcgaagtgacc
caccagggcctgtctagccccgtgaccaagtctttcaaccggggcgagtgctgaggatcc

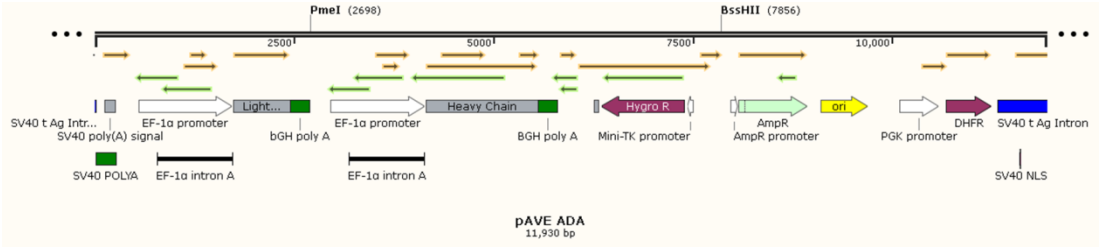

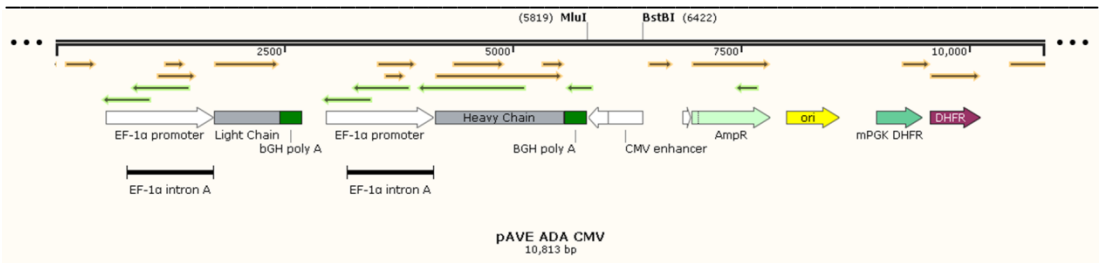

Sequence inserted in pAVE ADA CMV using MluI and BstBI restriction sites

acgcgttatatacacgtgagctctgcttatatagacctcccaccgtacacgcctaccgcccatttgcgtcaatggggcggagttgttacgacatttt
ggaaagtcccgttgattttggtgccaaaacaaactcccattgacgtcaatggggtggagacttggaaatccccgtgagtcaaaccgctatccacg
cccattgatgtactgccaaaaccgcatcaccatggtaatagcgatgactaatacgtagatgtactgccaagtaggaaagtcccataaggtcatgt
actgggcataatgccaggcgggccatttaccgtcattgacgtcaataggggcgtacttggcatatgatacacttgatgtactgccaagtgggca
gtttaccgtaaatactccacccattgacgtcaatggaaagtccctattggcgttactatgggaacatacgtcattattgacgtcaatgggcgggggg
tcgttgggcggtcagccaggcgggccatttaccgtaagttatgtaacgcggaactccatatatgggctatgaactaatgaccccgtaattgattac
tattaataactagtcaataatcaatgtcttcgaa

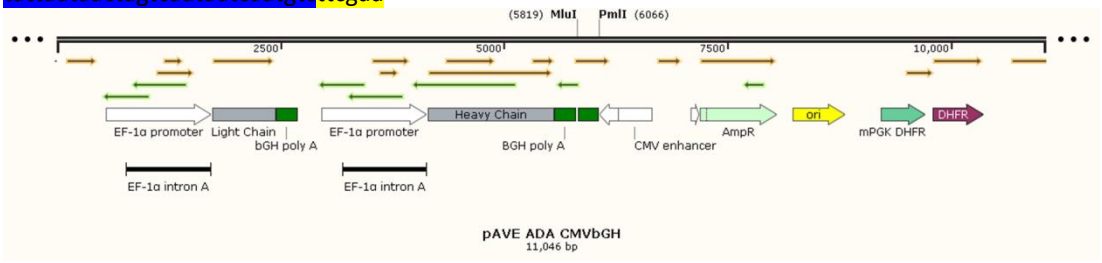

Sequence inserted in pAVE ADA CMVbGH using MluI and PmlI restriction sites

Acgcgtccatagagcccaccgcatccccagcatgcctgctattgtcttcccaatcctcccccttgctgtcctgccccaccccaccccccagaatag
aatgacacctactcagacaatgcgatgcaatttcctcattttattaggaaaggacagtgggagtggcaccttccagggtcaaggaaggcacggg
ggaggggcaaacaacagatggctggcaactagaaggcacaggcggccgctatatacacgtg

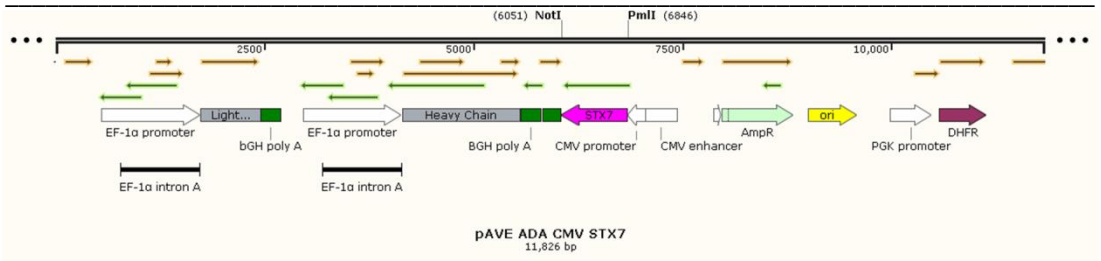

Sequence inserted in pAVE ADA CMV STX7 using NotI and PmlI restriction sites

Cggccgctcagtggttcaatccccatatgatgagactgataatcgcaactccaatgacaaggataagaatgatgatgcacagggtttttctggat
ttgcgctgataatctgctgcccttgacagctgctgatttgcttgctgaacgtgcacctctgcattttccacattggcttctatgctatctattacatctc
cttgttcatgaatcatcattcccaaatctttaaatatttcattaatatccataatatcagcttcaagttgcctgatagaagattctctctcatgaataa
gacggaggtcatcctctgtaatttcttcatcctgcacctgcacttgaggttgagtttggctttcccaggatacaagattcctttctttttgagctgtcct
caggaaaactgccagacactctggaactggctcttactcgagcaacaaactctttctctcgctcagcagcctgcctctggaccttctggaagtttg
tcagtgatgttgtgaactctgccactaagcgatccttctgtattttcctttgacgctgttcactgggggtggtgggcagagatccaaactctttaatg
tacttatctgtttctttggcaagctggttagtatactgctgcttctgttgcaactgttgcctcaattcaggtgaatcttgaggtgttccaagttgattca
gagttctttgtatttccacagaacactgtgtgatcttctggatgttagaagagatcctctgggccaactgggcggggtcaccaccaactcctggag
tgtaagacatcacgtg

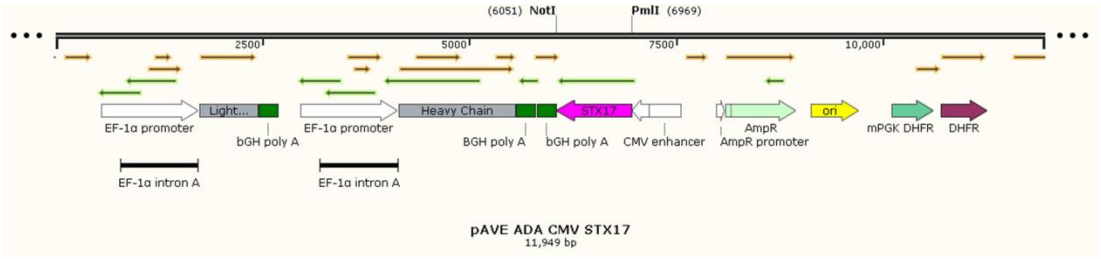

Sequence inserted in pAVE ADA CMV STX17 using NotI and PmlI restriction sites

Cggccgcttaactgcatttcttgtcagtttggctgggaagatctggacagctggaagtgagcttctccatcattttctgtttctttctttgtatcaattt
tccacctgtgaagcccaacaccccaccaccaagtgcagctgcaattcctgccactttgaagcctgcaaggaggccaataggacccccctaccattc
ccccgatgagtgcacctgccacaggcagagctgccagcttgtattttgcagccttccctaagttttggttccctcttcaacattcacagcagcact
gttgacatggtctgcaatgctgtcaatcttctcctgctgagaattcactaggagagagaagtcagtgaccagttggctaagttcaattaagtccgc
ttctaaggtttcccacgattctgcagcattttgatcttgaggaatttcaggtaaggcatatatctgagtcaaactctgagaactagcttcagcttca
gtagtatgaaatgctccaccaacagtcatggatctggtcaaaggaggctgtagcaaagtttcttcatcattaaattgcttcttaagttcttctacag
attccaaatggagttggagaaattctgctgttgctgctgatgcttcttctttaacaggatctatcattctcttcagaagtactaggtcatcctttcgga
ctttcaaacaaagtttctcaatttctcggatattggatcggagttgctgaactgtacgtcctgcattgatatgctcttcatgcaacttgtcccagattc
tgcacctttgatacttctcaatatttatctggtgctttcttaacctttccaggtctgttgggattactatcttaatgaatttctggatagctggttcaag
acggcgtaatttcacttttcttcatcttcagacatcacgtg

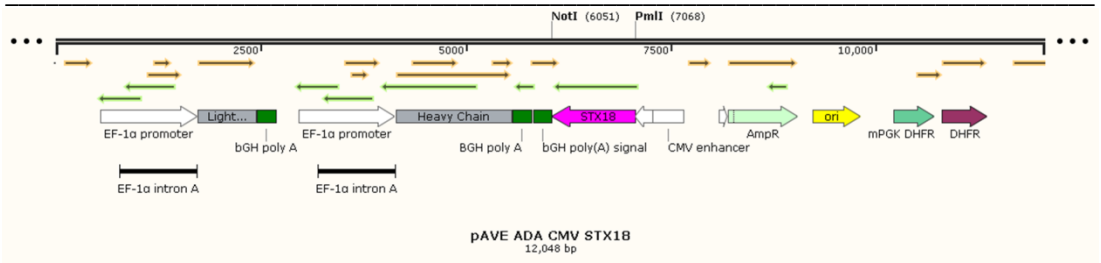

Sequence inserted in pAVE ADA CMV STX18 using NotI and PmlI restriction sites

Cggccgcctagctgtcgtaccagtcgaggaagagcaaggagaaggagcacatcacgaggaagaagaggatccacacgcggaagccagcgtt
gtttttaatggcctctcttatgtcttcgttgccttccttgatattttcagttgccccacaactaactggtgaatgctgtcaatctcagcttcctgttgca
aaaccttttccgtgaatatctcttggagtctggaaatctcaaccactctcccttcgatttgcctcacttcatcaaacaagctgttcatttcaccaatta
gtcgctgattttcctgttcaaacatttgtatttcttctggggataactcatcttcgcctttgccatctccccacgttcccaattcaggttgtgtttcagc
caaaatttttctggacgttcttcagtggcagggttttcttcagagtctttgaaggactctgtgaaactttctcagaagatgtggattctcttgtctt
gtatttggttctggttccagcttagataatcttttcttatccaccactcttttaactcggatggctctctgttctgagtaaagtttacatactcttttcaa
gtaatcttcaatgaaatccaaaacagcggtcctgtgctccttcacttgctgggaatgtatctccttgtgagcttctgttcgtagttgctgaattgcttc
tgaacaggtcctcatgaatatctgggcatcctggtctatctggtctcgttctgtgtctgtcatcctcccatattcagacatggtatggctataagcat
taatataatctttcctgtgttccagaagaaaatctctcagtttgccaatgtgagaaatcacttcgcgggcccggctggagaagtcgcccttgggcc
gggggctccggcggaacagctcgtcccggctgccatcgaccccgccgcccaccgccactcccagcgccttgttccgcgtcttcacggtcttgacg
ctggcccggaatagcagcgtgatgtccaccgccatcacgtg

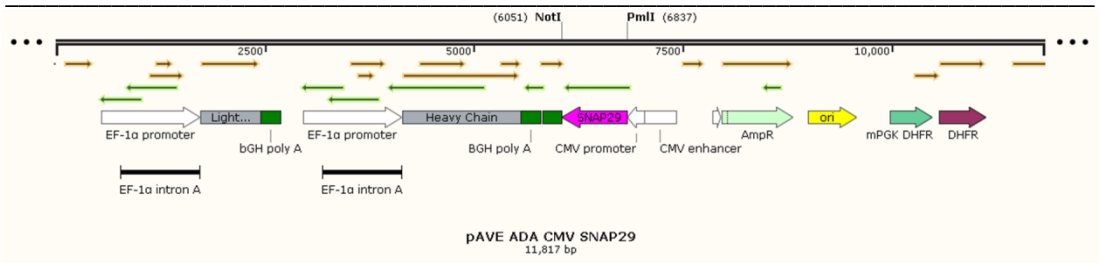

Sequence inserted in pAVE ADA CMV SNAP29 using NotI and PmlI restriction sites

cggccgcctcagagttgtcgaacttttctttctgtgcttttttatgttgacatctaacttgtccacttttggttgtcagccggtcaagaatgtcatcttgctc
ctcaatttctgtctgcatccccagggctatgtccttcagacgacccagtcccatggacagctcatctaggttgctgtcgatcttctggtgataggctc
gaaggtgtgggttctttgggtaagcatcagtactcatggcagaaccagcccctctggggacagggtctgtatcatccagctttctaaggtttgggt
ggctggcctggtactttgcttcctgttctttacttgtacttatagcttctttcaatctgttgttgggctgggaggtgagggtgccattctgttcaggtgg
ggtctctactggtttggatttgaagtaattgaccagccccccaaacacgctcttaatgctattgatgtgtttctggctgatcttcaaatcttggtccat
cttgtccaccatcttctctgtgcgctccaggactcctcgctgacgggcgagctcctcggaagaggcgaccccaaccttctcggactcgtacatgag
ggccagggacctgctggtgctggcggccgtggcctcagccctgcggaggacctcctgccgcaagtactgctgcctgtccgcgggcgcgtcgggc

ccgtcggggaggtctcgggcgtccctccaaggggccggccgggcgccttcgtcctccccgtcgtcgtcgaacggattgtagcttttagggtaagct
gacatcacgtg

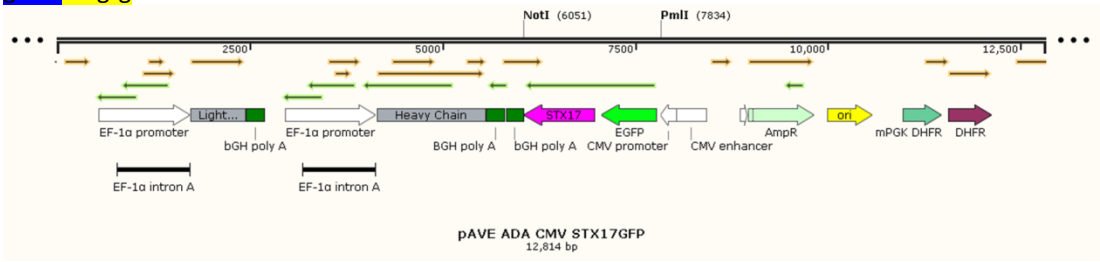

Sequence inserted in pAVE ADA CMV STX17GFP using NotI and PmlI restriction sites

cggccgctcgagggatcctaactgcatttcttgtcagtttggctgggaagatctggacagctggaagtgagcttctccatcattttctgtttctttct
ttgtatcaattttccacctgtgaagcccaacaccccaccaccaagtgcagctgcaattcctgccactttgaagcctgcaaggaggccaataggac
cccctaccattcccccgatgagtgcacctgccacaggcagagctgccagcttgtattttgcagccttccctaagttttggttccctcttcaacattc
acagcagcactgttgacatggtctgcaatgctgtcaatcttctcctgctgagaattcactaggagagagaagtcagtgaccagttggctaagttc
aattaagtccgcttctaaggtttcccacgattctgcagcattttgatcttgaggaatttcaggtaaggcatatatctgagtcaaactctgagaacta
gcttcagcttcagtagtatgaaatgctccaccaacagtcatggatctggtcaaaggaggctgtagcaaagtttcttcatcattaaattgcttcttaa
gttcttctacagattccaaatggagttggagaaattctgctgttgctgctgatgcttcttctttaacaggatctatcattctcttcagaagtactaggt
catcctttcggactttcaaacaaagtttctcaatttctcggatattggatcggagttgctgaactgtacgtcctgcattgatatgctcttcatgcaact
tgtcccagattctgcacctttgatacttctcaatatttatctggtgctttcttaacctttccaggtctgttgggattactatcttaatgaatttctggata
gctggttcaagacggcgtaatttcacttttcttcatcttcagacatcggatccgttaactcgcgaacgcgtgaattcaattcatcgatagatccgc
cgccacccgacccaccaccgcccgagccaccgccacccttgtacagctcgtccatgccgagagtgatcccggcggcggtcacgaactccagcag
gaccatgtgatcgcgcttctcgttggggtctttgctcagggcggactgggtgctcaggtagtggttgtcgggcagcagcacggggccgtcgccga
tgggggtgttctgctggtagtggtcggcgagctgcacgctgccgtcctcgatgttgtggcggatcttgaagttcaccttgatgccgttcttctgcttg
tcggccatgatatagacgttgtggctgttgtagttgtactccagcttgtgccccaggatgttgccgtcctccttgaagtcgatgcccttcagctcgat
gcggttcaccagggtgtcgccctcgaacttcacctcggcgcgggtcttgtagttgccgtcgtccttgaagaagatggtgcgctcctggacgtagcc
ttcgggcatggcggacttgaagaagtcgtgctgcttcatgtggtcggggtagcggctgaagcactgcacgccgtaggtcagggtggtcacgagg
gtgggccagggcacgggcagcttgccggtggtgcagatgaacttcagggtcagcttgccgtaggtggcatcgccctcgccctcgccggacacgc
tgaacttgtggccgtttacgtcgccgtccagctcgaccaggatgggcaccaccccggtgaacagctcctcgcccttgctcaccatggcagatccg
gcagtctagaggatggtccacccccggggtcggcagccttcacgtg

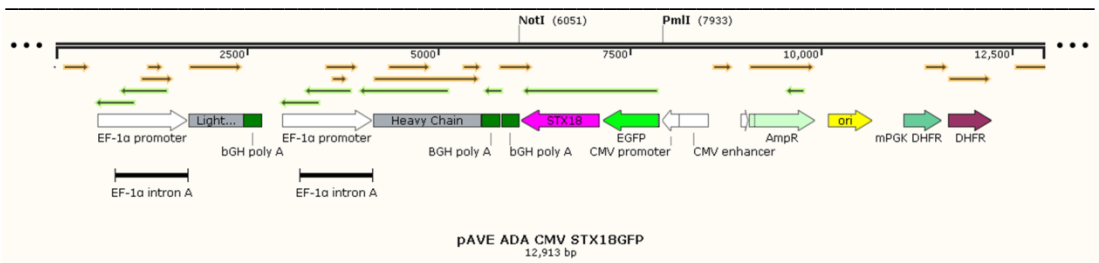

Sequence inserted in pAVE ADA CMV STX18GFP using NotI and PmlI restriction sites

cggccgctcgagggatccgttaactcgcgaacgcgtgaattcctagctgtcgtaccagtcgaggaagagcaaggagaaggagcacatcacgag
gaagaagaggatccacacgcggaagccagcgttgtttttaatggcctctcttatgtcttcgttgccttccttgatattttcagttgccccacaacta
actggtgaatgctgtcaatctcagcttcctgttgcaaaaccttttccgtgaatatctcttggagtctggaaatctcaaccactctcccttcgatttgcc
tcacttcatcaaacaagctgttcatttcaccaattagtcgctgattttcctgttcaaacatttgtatttcttctggggataactcatcttcgcctttgcc
atctccccacgttcccaattcaggttgtgtttcagccaaaatttttttctggacgttcttcagtggcagggttttcttcagagtctttgaaggactctgt
gaaacttttctcagaagatgtggattctcttgtctttgtatttggttctggttccagcttagataatcttttcttatccaccactctttttaactcggatgg
ctctctgttctgagtaaagtttacatactcttttcaagtaatcttcaatgaaatccaaaacagcggtcctgtgctccttcacttgctgggaatgtatct
ccttgtgagcttctgttcgtagttgctgaattgcttctgaacaggtcctcatgaatatctgggcatcctggtctatctggtctcgttctgtgtctgtcat
cctcccatattcagacatggtatggctataagcattaatataatctttcctgtgttccagaagaaaatctctcagtttgccaatgtgagaaatcact
tcgcgggcccggctggagaagtcgcccttgggccgggggctccggcggaacagctcgtcccggctgccatcgaccccgccgcccaccgccactc
ccagcgccttgttccgcgtcttcacggtcttgacgctggcccggaatagcagcgtgatgtccaccgccatagaattcaattcatcgatagatccgc
cgccacccgacccaccaccgcccgagccaccgccacccttgtacagctcgtccatgccgagagtgatcccggcggcggtcacgaactccagcag
gaccatgtgatcgcgcttctcgttggggtctttgctcagggcggactgggtgctcaggtagtggttgtcgggcagcagcacggggccgtcgccga
tgggggtgttctgctggtagtggtcggcgagctgcacgctgccgtcctcgatgttgtggcggatcttgaagttcaccttgatgccgttcttctgcttg
tcggccatgatatagacgttgtggctgttgtagttgtactccagcttgtgccccaggatgttgccgtcctccttgaagtcgatgcccttcagctcgat
gcggttcaccagggtgtcgccctcgaacttcacctcggcgcgggtcttgtagttgccgtcgtccttgaagaagatggtgcgctcctggacgtagcc
ttcgggcatggcggacttgaagaagtcgtgctgcttcatgtggtcggggtagcggctgaagcactgcacgccgtaggtcagggtggtcacgagg

gtgggccagggcacgggcagcttgccggtggtgcagatgaacttcagggtcagcttgccgtaggtggcatcgccctcgccctcgccggacacgc
tgaacttgtggccgtttacgtcgccgtccagctcgaccaggatgggcaccaccccggtgaacagctcctcgcccttgctcaccatggcagatccg
gcagtctagaggatggtccacccccggggtcggcagccttcacgtg

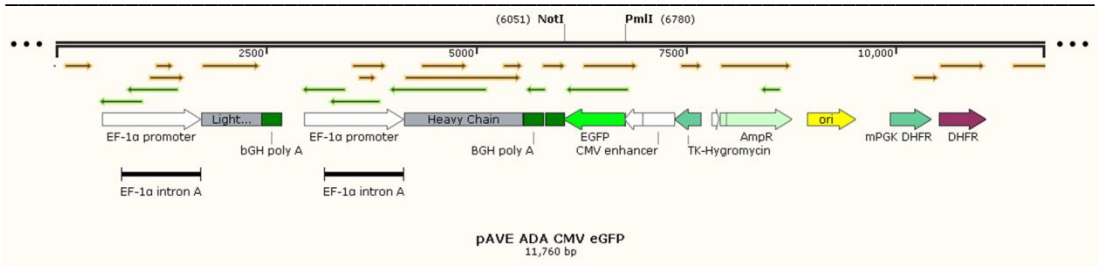

Sequence inserted in pAVE ADA CMV eGFP using NotI and PmlI restriction sites

Cggccgcttacttgtacagctcgtccatgccgagagtgatcccggcggcggtcacgaactccagcaggaccatgtgatcgcgcttctcgttgggg
tctttgctcagggcggactgggtgctcaggtagtggttgtcgggcagcagcacggggccgtcgccgatgggggtgttctgctggtagtggtcggc
gagctgcacgctgccgtcctcgatgttatggcggatcttgaagttcaccttgatgccgttcttctgcttgtcggccatgatatagacgttgtggctgt
tgtagttgtactccagcttgtgccccaggatgttgccgtcctccttgaagtcgatgcccttcagctcgatgcggttcaccagggtgtcgccctcgaa
cttcacctcggcgcgggtcttgtagttgccgtcgtccttgaagaagatggtgcgctcctggacgtagccttcgggcatggcggacttgaagaagtc
gtgctgcttcatgtggtcggggtagcggctgaagcactgcacgccgtaggtcagggtggtcacgagggtgggccagggcacgggcagcttgccg
gtggtgcagatgaacttcagggtcagcttgccgtaggtggcatcgccctcgccctcgccggacacgctgaacttgtggccgtttacgtcgccgtcc
agctcgaccaggatgggcaccaccccggtgaacagctcctcgcccttgctcaccatcacgtg

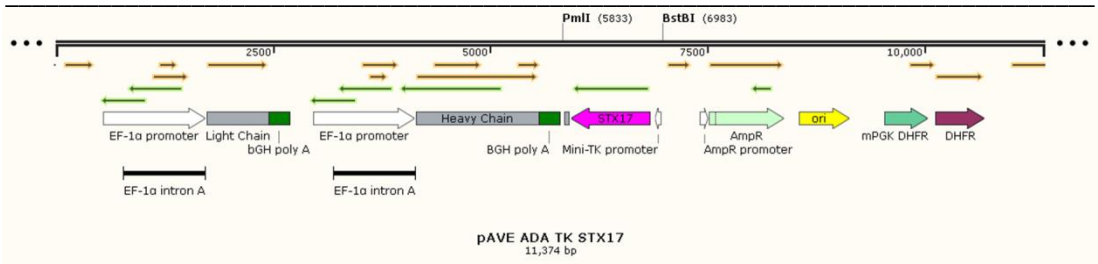

Sequence inserted in pAVE ADA TK STX17 using PmlI and BstBI restriction sites

cacgtgtatatagcggccgctatgaacaaacgacccaacacccgtgcgttttattctgtcttttattgccgtcgaggctgatcagcgggtttaaac
gggcccttaactgcatttcttgtcagtttggctgggaagatctggacagctggaagtgagcttctccatcattttctgtttctttctttgtatcaattt
tccacctgtgaagcccaacaccccaccaccaagtgcagctgcaattcctgccactttgaagcctgcaaggaggccaataggacccccctaccattc
ccccgatgagtgcacctgccacaggcagagctgccagcttgtattttgcagccttccctaagttttggttccctcttcaacattcacagcagcact
gttgacatggtctgcaatgctgtcaatcttctcctgctgagaattcactaggagagagaagtcagtgaccagttggctaagttcaattaagtccgc
ttctaaggtttcccacgattctgcagcattttgatcttgaggaatttcaggtaaggcatatatctgagtcaaactctgagaactagcttcagcttca
gtagtatgaaatgctccaccaacagtcatggatctggtcaaaggaggctgtagcaaagtttcttcatcattaaattgcttcttaagttcttctacag
attccaaatggagttggagaaattctgctgttgctgctgatgcttcttctttaacaggatctatcattctcttcagaagtactaggtcatcctttcgga
ctttcaaacaaagtttctcaatttctcggatattggatcggagttgctgaactgtacgtcctgcattgatatgctcttcatgcaacttgtcccagattc
tgcacctttgatacttctcaatatttatctggtgctttcttaacctttccaggtctgttgggattactatcttaatgaatttctggatagctggttcaag
acggcgtaatttcacttttcttcatcttcagacatatagtgagtcgtattaatttcgataagccagtaagcagtgggttctctagttagccagagtt
aagcgggtcgctgcagggtcgctcggtgttcgaggccacacgcgtcaccttaatatgcgaaatagatatcatatattcgaa

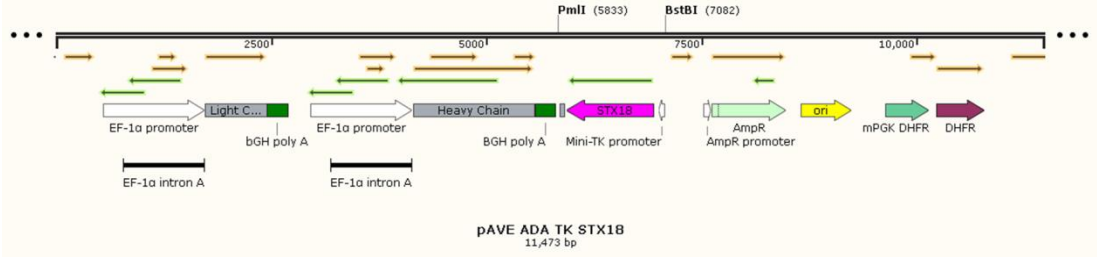

Sequence inserted in pAVE ADA TK STX18 using PmlI and BstBI restriction sites

cacgtgtatatagcggccgctatgaacaaacgacccaacacccgtgcgttttattctgtcttttattgccgtcgaggctgatcagcgggtttaaac
gggccctctagctgtcgtaccagtcgaggaagagcaaggagaaggagcacatcacgaggaagaagaggatccacacgcggaagccagcgtt
gtttttaatggcctctcttatgtcttcgttgccttccttgatattttcagttgccccacaactaactggtgaatgctgtcaatctcagcttcctgttgca
aaaccttttccgtgaatatctcttggagtctggaaatctcaaccactctcccttcgatttgcctcacttcatcaaacaagctgttcatttcaccaatta
gtcgctgattttcctgttcaaacatttgtatttcttctggggataactcatcttcgcctttgccatctccccacgttcccaattcaggttgtgtttcagc

caaaatttttttctggacgttcttcagtggcagggtttttcttcagagtcttttgaaggactctgtgaaactttctcagaagatgtggattctcttgtctttgtatttggttctggttccagcttagataatcttttcttatccaccactcttttaactcggatggctctctgttctgagtaaagtttacatactcttttcaagtaatcttcaatgaaatccaaaacagcggtcctgtgctccttcacttgctgggaatgtatctccttgtgagcttctgttcgtagttgctgaattgcttctgaacaggtcctcatgaatatctgggcatcctggtctatctggtctcgttctgtgtctgtcatcctcccatattcagacatggtatggctataagcattaatataatctttcctgtgttccagaagaaaatctctcagtttgccaatgtgagaaatcacttcgcgggcccggctggagaagtcgcccttgggccgggggctccggcggaacagctcgtcccggctgccatcgaccccgccgcccaccgccactcccagcgccttgttccgcgtcttcacggtcttgacgctggcccggaatagcagcgtgatgtccaccgccatatagtgagtcgtattaatttcgataagccagtaagcagtgggttctctagttagccagagttaagcgggtcgctgcagggtcgctcggtgttcgaggccacacgcgtcaccttaatatgcgaaatagatatcatatatttcgaa

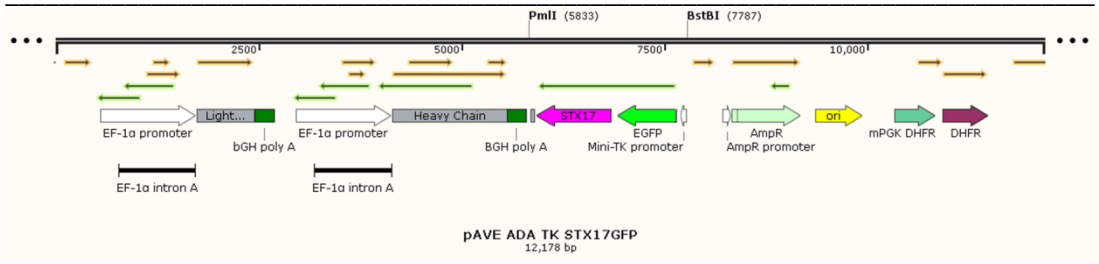

Sequence inserted in pAVE ADA TK STX17GFP using PmlI and BstBI restriction sites

cacgtgtatatagcggccgctatgaacaaacgacccaacacccgtgcgttttattctgtcttttattgccgtcgaggctgatcagcgggtttaaacgggcccttaactgcatttcttgtcagtttggctgggaagatctggacagctggaagtgagcttctccatcattttctgtttctttctttgtatcaatttctccacctgtgaagcccaacaccccaccaccaagtgcagctgcaattcctgccactttgaagcctgcaaggaggccaataggacccccctaccattccccgatgagtgcacctgccacaggcagagctgccagcttgtattttgcagccttccctaagtttttggttccctcttcaacattcacagcagcactgttgacatggtctgcaatgctgtcaatcttctcctgctgagaattcactaggagagagaagtcagtgaccagttggctaagttcaattaagtccgcttctaaggtttcccacgattctgcagcattttgatcttgaggaatttcaggtaaggcatatatctgagtcaaactctgagaactagcttcagcttcagtagtatgaaatgctccaccaacagtcatggatctggtcaaaggaggctgtagcaaagtttcttcatcattaaattgcttcttaagttcttctacagattccaaatggagttggagaaattctgctgttgctgctgatgcttcttctttaacaggatctatcattctcttcagaagtactaggtcatcctttcggactttcaaacaaagtttctcaatttctcggatattggatcggagttgctgaactgtacgtcctgcattgatatgctcttcatgcaacttgtcccagattctgcaccttgatacttctcaatatttatctggtgctttcttaacctttccaggtctgttgggattactatcttaatgaatttctggatagctggttcaagacggcgtaatttcacttttttcttcatcttcagacatcggatccgttaactcgcgaacgcgtgaattcaattcatcgatagatccgccgccacccgaccccaccaccgcccgagccaccgccacccttgtacagctcgtccatgccgagagtgatcccggcggcggtcacgaactccagcaggaccatgtgatcgcgcttctcgttggggtctttgctcagggcggactgggtgctcaggtagtggttgtcgggcagcagcacggggccgtcgccgatgggggtgttctgctggtagtggtcggcgagctgcacgctgccgtcctcgatgttgtggcggatcttgaagttcaccttgatgccgttcttctgcttgtcggccatgatatagacgttgtggctgttgtagttgtactccagcttgtgccccaggatgttgccgtcctccttgaagtcgatgcccttcagctcgatgcggttcaccaggtgtcgccctcgaacttcacctcggcgcgggtcttgtagttgccgtcgtccttgaagaagatggtgcgctcctggacgtagccttcgggcatggcggacttgaagaagtcgtgctgcttcatgtggtcggggtagcggctgaagcactgcacgccgtaggtcagggtggtcacgagggtgggccagggcacgggcagcttgccggtggtgcagatgaacttcagggtcagcttgccgtaggtggcatcgccctcgccctcgccggacacgctgaacttgtggccgtttacgtcgccgtccagctcgaccaggatgggcaccaccccggtgaacagctcctcgcccttgctcaccatatagtgagtcgtattaatttcgataagccagtaagcagtgggttctctagttagccagagttaagcgggtcgctgcagggtcgctcggtgttcgaggccacacgcgtcaccttaatatgcgaaatagatatcatatattcgaa

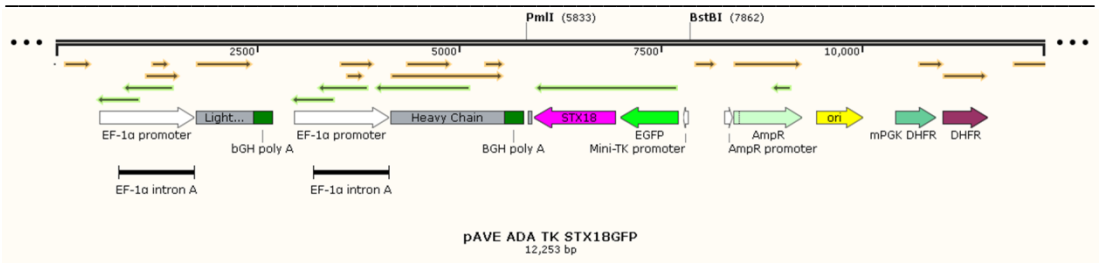

Sequence inserted in pAVE ADA TK STX18GFP using PmlI and BstBI restriction sites

cacgtgtatatagcggccgctatgaacaaacgacccaacacccgtgcgttttattctgtcttttattgccgtcgaggctgatcagcgggtttaaacgggccctctagctgtcgtaccagtcgaggaagagcaaggagaaggagcacatcacgaggaagaagaggatccacacgcggaagccagcgtt gtttttaatggcctctcttatgtcttcgttgccttccttgatattttcagttgccccacaactaactggtgaatgctgtcaatctcagcttcctgttgcaaaaccttttccgtgaatatctcttggagtctggaaatctcaaccactctcccttcgatttgcctcacttcatcaaacaagctgttcatttcaccaattagtcgctgattttcctgttcaaacatttgtatttcttctggggataactcatcttcgcctttgccatctccccacgttcccaattcaggttgtgtttcagccaaaatttttttctggacgttcttcagtggcagggtttttcttcagagtcttttgaaggactctgtgaaactttctcagaagatgtggattctcttgtctttgtatttggttctggttccagcttagataatcttttcttatccaccactcttttaactcggatggctctctgttctgagtaaagtttacatactcttttcaagtaatcttcaatgaaatccaaaacagcggtcctgtgctccttcacttgctgggaatgtatctccttgtgagcttctgttcgtagttgctgaattgcttc

tgaacaggtcctcatgaatatctgggcatcctggtctatctggtctcgttctgtgtctgtcatcctcccatattcagacatggtatggctataagcat
taatataatctttcctgtgttccagaagaaaatctctcagtttgccaatgtgagaaatcacttcgcgggcccggctggagaagtcgcccttgggcc
gggggctccggcggaacagctcgtcccggctgccatcgaccccgccgcccaccgccactcccagcgccttgttccgcgtcttcacggtcttgacg
ctggcccggaatagcagcgtgatgtccaccgccatagaattcaattcatcgatagatccgccgccacccgacccaccaccgcccgagccaccgc
acccttgtacagctcgtccatgccgagagtgatcccggcggcggtcacgaactccagcaggaccatgtgatcgcgcttctcgttggggtctttgc
tcagggcggactgggtgctcaggtagtggttgtcgggcagcagcacggggccgtcgccgatgggggtgttctgctggtagtggtcggcgagctg
cacgctgccgtcctcgatgttgtggcggatcttgaagttcaccttgatgccgttcttctgcttgtcggccatgatatagacgttgtggctgttgtagtt
gtactccagcttgtgccccaggatgttgccgtcctccttgaagtcgatgcccttcagctcgatgcggttcaccagggtgtcgccctcgaacttcacc
tcggcgcgggtcttgtagttgccgtcgtccttgaagaagatggtgcgctcctggacgtagccttcgggcatggcggacttgaagaagtcgtgctgc
ttcatgtggtcggggtagcggctgaagcactgcacgccgtaggtcagggtggtcacgagggtgggccagggcacgggcagcttgccggtggtg
cagatgaacttcagggtcagcttgccgtaggtggcatcgccctcgccctcgccggacacgctgaacttgtggccgtttacgtcgccgtccagctcg
accaggatgggcaccaccccggtgaacagctcctcgcccttgctcaccatatagtgagtcgtattaatttcgataagccagtaagcagtgggttct
ctagttagccagagttaagcgggtcgctgcagggtcgctcggtgttcgaggccacacgcgtcaccttaatatgcgaaatagatatcatatattcg
aa

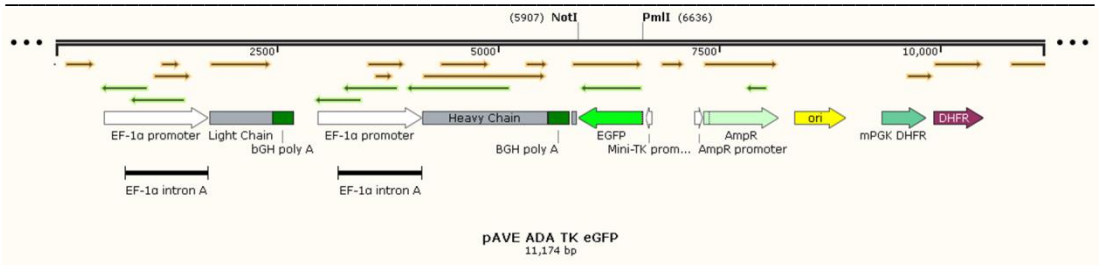

Sequence inserted in pAVE ADA TK eGFP using NotI and PmlI restriction sites

gcggccgcttacttgtacagctcgtccatgccgagagtgatcccggcggcggtcacgaactccagcaggaccatgtgatcgcgcttctcgttggg
gtctttgctcagggcggactgggtgctcaggtagtggttgtcgggcagcagcacggggccgtcgccgatgggggtgttctgctggtagtggtcgg
cgagctgcacgctgccgtcctcgatgttatggcggatcttgaagttcaccttgatgccgttcttctgcttgtcggccatgatatagacgttgtggctg
ttgtagttgtactccagcttgtgccccaggatgttgccgtcctccttgaagtcgatgcccttcagctcgatgcggttcaccagggtgtcgccctcga
acttcacctcggcgcgggtcttgtagttgccgtcgtccttgaagaagatggtgcgctcctggacgtagccttcgggcatggcggacttgaagaagt
cgtgctgcttcatgtggtcggggtagcggctgaagcactgcacgccgtaggtcagggtggtcacgagggtgggccagggcacgggcagcttgcc
ggtggtgcagatgaacttcagggtcagcttgccgtaggtggcatcgccctcgccctcgccggacacgctgaacttgtggccgtttacgtcgccgtc
cagctcgaccaggatgggcaccaccccggtgaacagctcctcgcccttgctcaccatcacgtg

Appendix 3. List of generated cell lines.

	Plasmid	selection	Host	type	Product of interest	Recombinant antibody	comments	section
CHO/V3	pcDNA3.1Hygro/VAMP3	Hygromycin	CHO-S	Pool	eGFP-VAMP3			Chapter 3
CHO/V4	pcDNA3.1Hygro/VAMP4	Hygromycin	CHO-S	Pool	eGFP-VAMP4			Chapter 3
CHO/V7	pcDNA3.1Hygro/VAMP7	Hygromycin	CHO-S	Pool	eGFP-VAMP7			Chapter 3
CHO/V8	pcDNA3.1Hygro/VAMP8	Hygromycin	CHO-S	Pool	eGFP-VAMP8			Chapter 3
CHO/3.1HGFP	pcDNA3.1Hygro/GFP	Hygromycin	CHO-S	Pool	eGFP		Control vector	Chapter 3
CHO/STX7	pMRXIP-STX7	Puromycin	CHO-S	Pool	eGFP-STX7			Chapter 3
CHO/STX17	pMRXIP-STX17	Puromycin	CHO-S	Pool	eGFP-STX17			Chapter 3
CHO/STX18	pMRXIP-STX18	Puromycin	CHO-S	Pool	eGFP-STX18			Chapter 3
CHO/SNAP29	pMRXIP-SNAP29	Puromycin	CHO-S	Pool	eGFP-SNAP29			Chapter 3
CHO/MRXIP-GFP	pMRXIP-GFP	Puromycin	CHO-S	Pool	eGFP		Control vector	Chapter 3
CHO/STX7 A	pMRXIP-STX7	Puromycin	CHO-S	Monoclonal	eGFP-STX7			Chapter 3, 4
CHO/STX7 B	pMRXIP-STX7	Puromycin	CHO-S	Monoclonal	eGFP-STX7			Chapter 3, 4
CHO/STX7 C	pMRXIP-STX7	Puromycin	CHO-S	Monoclonal	eGFP-STX7			Chapter 3, 4
CHO/STX17 J	pMRXIP-STX17	Puromycin	CHO-S	Monoclonal	eGFP-STX17			Chapter 3, 4
CHO/STX17 K	pMRXIP-STX17	Puromycin	CHO-S	Monoclonal	eGFP-STX17			Chapter 3, 4
CHO/STX18 C	pMRXIP-STX18	Puromycin	CHO-S	Monoclonal	eGFP-STX18			Chapter 3, 4
CHO/STX18 H	pMRXIP-STX18	Puromycin	CHO-S	Monoclonal	eGFP-STX18			Chapter 3, 4
CHO/STX18 F	pMRXIP-STX18	Puromycin	CHO-S	Monoclonal	eGFP-STX18			Chapter 3, 4
CHO/SNAP29 A	pMRXIP-SNAP29	Puromycin	CHO-S	Monoclonal	eGFP-SNAP29			Chapter 3, 4
CHO/SNAP29 B	pMRXIP-SNAP29	Puromycin	CHO-S	Monoclonal	eGFP-SNAP29			Chapter 3, 4
CHO/MRXIP-GFP H	pMRXIP-GFP	Puromycin	CHO-S	Monoclonal	eGFP			Chapter 3, 4
CHO/MRXIP-GFP L	pMRXIP-GFP	Puromycin	CHO-S	Monoclonal	eGFP			Chapter 3, 4
mpDG44/ADA	pAVE ADA	MTX	Clone 27/CHO-DG44	Mini pool		Adalimumab		Chapter 5
mpDG44/ADA CMVbGH	pAVE ADA CMVbGH	MTX	Clone 27/CHO-DG44	Mini pool		Adalimumab	control vector	Chapter 5
mpDG44/ADA STX7	pAVE ADA CMV STX7	MTX	Clone 27/CHO-DG44	Mini pool	eGFP-STX7	Adalimumab		Chapter 5
mpDG44/ADA STX17	pAVE ADA CMV STX17	MTX	Clone 27/CHO-DG44	Mini pool	eGFP-STX17	Adalimumab		Chapter 5
mpDG44/ADA SNAP29	pAVE ADA CMV SNAP29	MTX	Clone 27/CHO-DG44	Mini pool	eGFP-SNAP29	Adalimumab		Chapter 5
mpDG44/BLOSO	pAVE BLOSO	MTX	Clone 27/CHO-DG44	Mini pool		Blosozumab		Chapter 5
mpDG44/BLOSO CMVbGH	pAVE BLOSO CMVbGH	MTX	Clone 27/CHO-DG44	Mini pool		Blosozumab	control vector	Chapter 5
mpDG44/BLOSO STX7	pAVE BLOSO CMV STX7	MTX	Clone 27/CHO-DG44	Mini pool	eGFP-STX7	Blosozumab		Chapter 5
mpDG44/BLOSO STX17	pAVE BLOSO CMV STX17	MTX	Clone 27/CHO-DG44	Mini pool	eGFP-STX17	Blosozumab		Chapter 5
mpDG44/BLOSO STX18	pAVE BLOSO CMV STX18	MTX	Clone 27/CHO-DG44	Mini pool	eGFP-STX18	Blosozumab		Chapter 5
mpDG44/BLOSO SNAP29	pAVE BLOSO CMV SNAP29	MTX	Clone 27/CHO-DG44	Mini pool	eGFP-SNAP29	Blosozumab		Chapter 5
poolDG44/ADA	pAVE ADA	MTX	Clone 27/CHO-DG44	Pool		Adalimumab		Chapter 5
poolDG44/ADA CMVbGH	pAVE ADA CMVbGH	MTX	Clone 27/CHO-DG44	Pool		Adalimumab	control vector	Chapter 5
poolDG44/ADA STX7	pAVE ADA CMV STX7	MTX	Clone 27/CHO-DG44	Pool	eGFP-STX7	Adalimumab		Chapter 5
poolDG44/ADA STX17	pAVE ADA CMV STX17	MTX	Clone 27/CHO-DG44	Pool	eGFP-STX17	Adalimumab		Chapter 5
poolDG44/ADA STX18	pAVE ADA CMV STX18	MTX	Clone 27/CHO-DG44	Pool	eGFP-STX18	Adalimumab		Chapter 5
poolDG44/ADA SNAP29	pAVE ADA CMV SNAP29	MTX	Clone 27/CHO-DG44	Pool	eGFP-SNAP29	Adalimumab		Chapter 5
poolDG44/BLOSO	pAVE BLOSO	MTX	Clone 27/CHO-DG44	Pool		Blosozumab		Chapter 5
poolDG44/BLOSO CMVbGH	pAVE BLOSO CMVbGH	MTX	Clone 27/CHO-DG44	Pool		Blosozumab	control vector	Chapter 5
poolDG44/BLOSO STX7	pAVE BLOSO CMV STX7	MTX	Clone 27/CHO-DG44	Pool	eGFP-STX7	Blosozumab		Chapter 5
poolDG44/BLOSO STX17	pAVE BLOSO CMV STX17	MTX	Clone 27/CHO-DG44	Pool	eGFP-STX17	Blosozumab		Chapter 5
poolDG44/BLOSO STX18	pAVE BLOSO CMV STX18	MTX	Clone 27/CHO-DG44	Pool	eGFP-STX18	Blosozumab		Chapter 5
poolDG44/BLOSO SNAP29	pAVE BLOSO CMV SNAP29	MTX	Clone 27/CHO-DG44	Pool	eGFP-SNAP29	Blosozumab		Chapter 5
DG44/ADA+STX7	pMRXIP-STX7	MTX+Puromycin	mpDG44/ADA 7	Pool	eGFP-STX7	Adalimumab		Chapter 5
DG44/ADA+STX17	pMRXIP-STX17	MTX+Puromycin	mpDG44/ADA 7	Pool	eGFP-STX17	Adalimumab		Chapter 5
DG44/ADA+SNAP29	pMRXIP-SNAP29	MTX+Puromycin	mpDG44/ADA 7	Pool	eGFP-SNAP29	Adalimumab		Chapter 5
DG44/ADA+GFP	pMRXIP-GFP	MTX+Puromycin	mpDG44/ADA 7	Pool	eGFP	Adalimumab	control vector	Chapter 5
DG44/BLOSO+STX7	pMRXIP-STX7	MTX+Puromycin	mpDG44/BLOSO 6	Pool	eGFP-STX7	Blosozumab		Chapter 5
DG44/BLOSO+STX17	pMRXIP-STX17	MTX+Puromycin	mpDG44/BLOSO 6	Pool	eGFP-STX17	Blosozumab		Chapter 5
DG44/BLOSO+SNAP29	pMRXIP-SNAP29	MTX+Puromycin	mpDG44/BLOSO 6	Pool	eGFP-SNAP29	Blosozumab		Chapter 5
DG44/BLOSO+GFP	pMRXIP-GFP	MTX+Puromycin	mpDG44/BLOSO 6	Pool	eGFP	Blosozumab	control vector	Chapter 5

Appendix 4. Metabolites results from the FOG experiment.

During the FOG experiment, metabolites were analysed daily from day 3. Error bars represent the standard deviation. Error bars show the standard deviation from the mean (n=3).

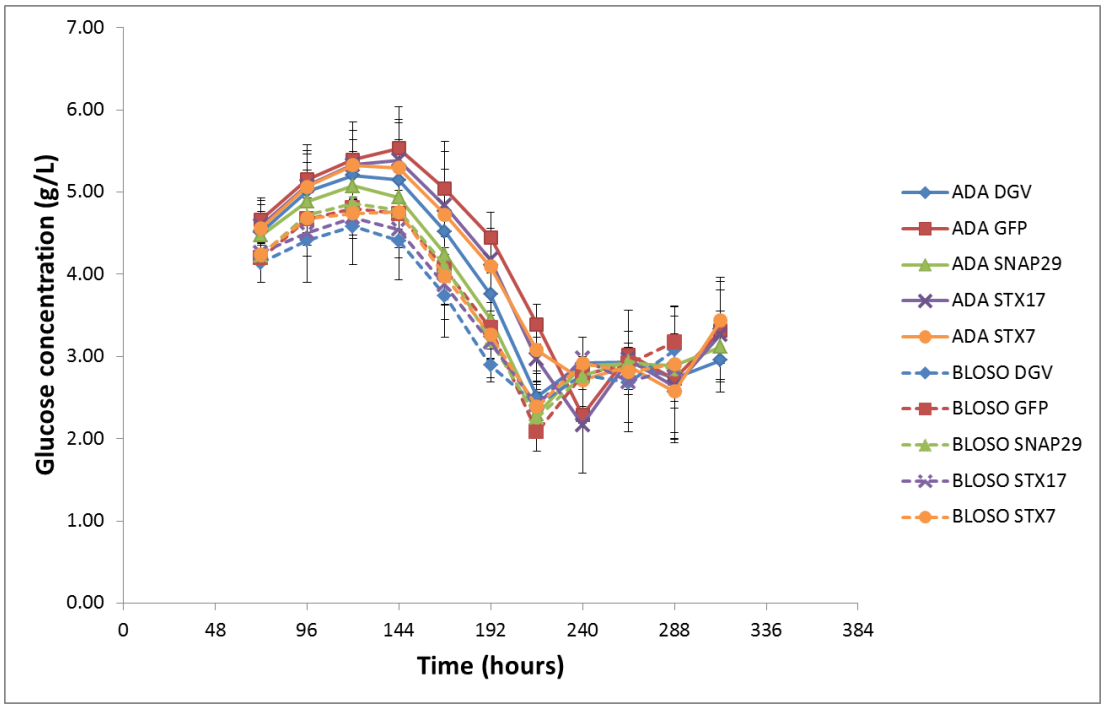

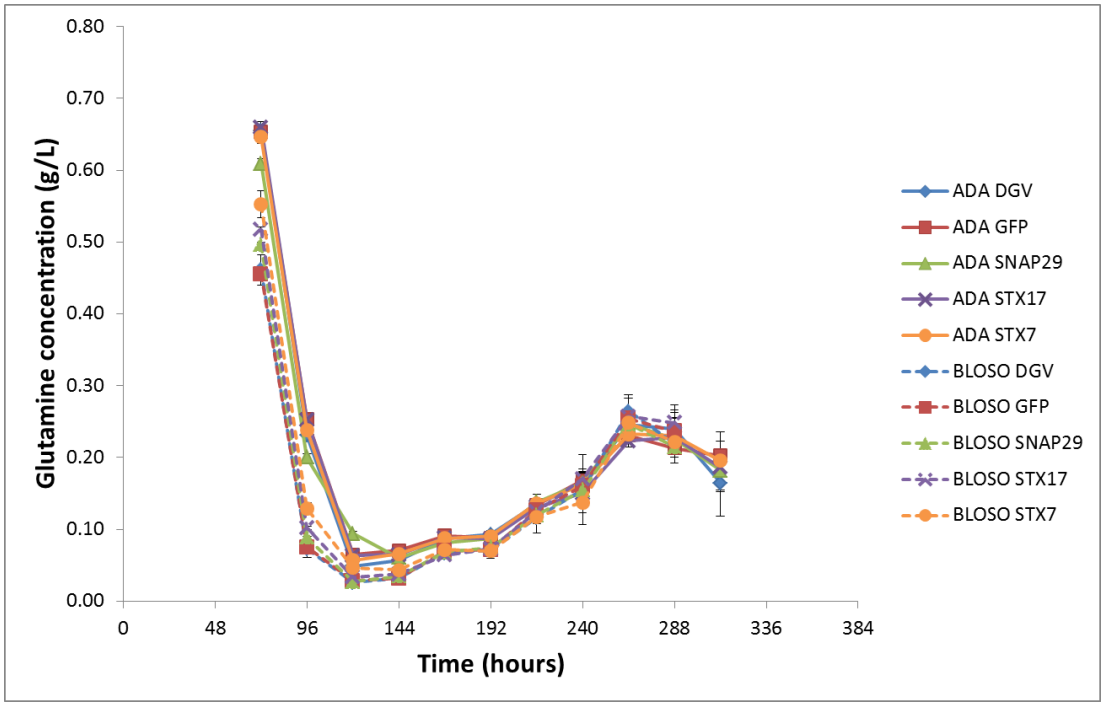

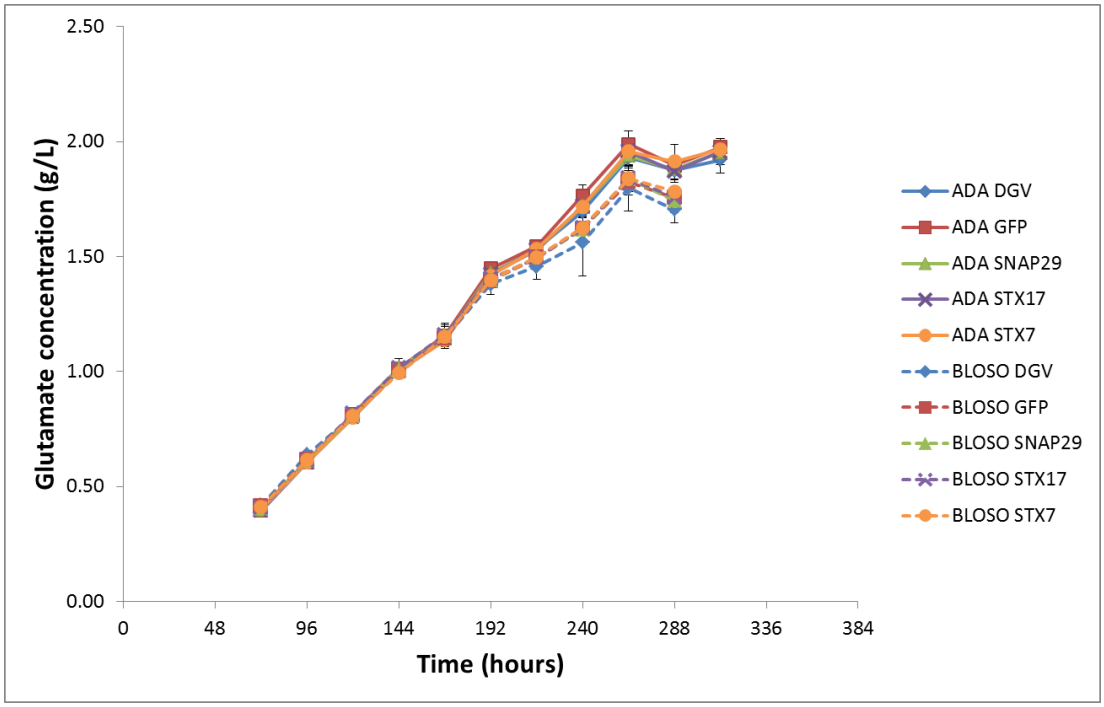
Glutamate concentration (g/L)
2.50
2.00
1.50
1.00
0.50
0.00
0
48
96
144
192
240
288
336
384
Time (hours)
ADA DGV
ADA GFP
ADA SNAP29
ADA STX17
ADA STX7
BLOSO DGV
BLOSO GFP
BLOSO SNAP29
BLOSO STX17
BLOSO STX7

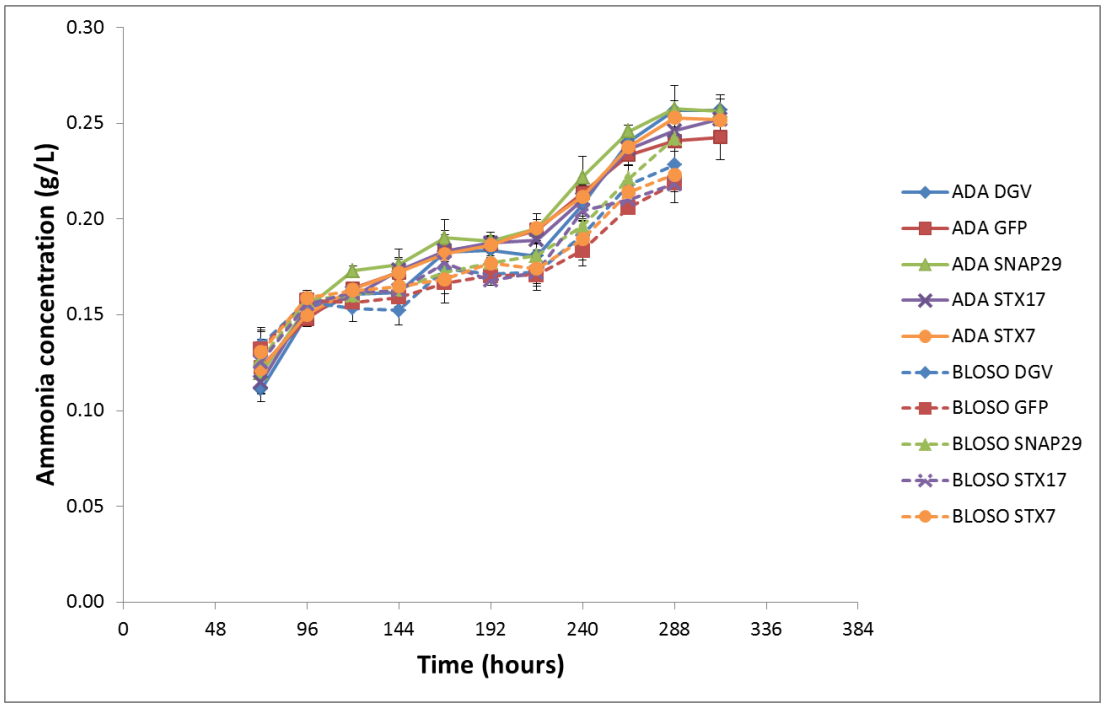
Ammonia concentration (g/L)
0.30
0.25
0.20
0.15
0.10
0.05
0.00
0
48
96
144
192
240
288
336
384
Time (hours)
ADA DGV
ADA GFP
ADA SNAP29
ADA STX17
ADA STX7
BLOSO DGV
BLOSO GFP
BLOSO SNAP29
BLOSO STX17
BLOSO STX7

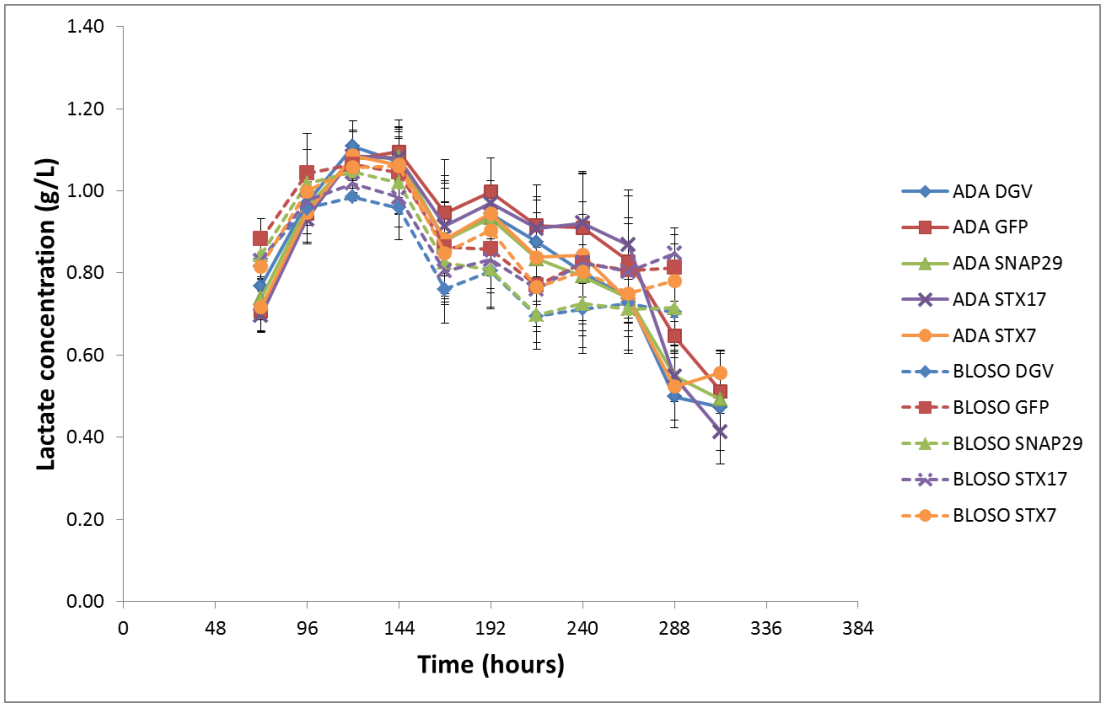
1.40
1.20
1.00
0.80
0.60
0.40
0.20
0.00
Lactate concentration (g/L)
0
48
96
144
192
240
288
336
384
Time (hours)
ADA DGV
ADA GFP
ADA SNAP29
ADA STX17
ADA STX7
BLOSO DGV
BLOSO GFP
BLOSO SNAP29
BLOSO STX17
BLOSO STX7